

2019

# Integer-forcing architectures: cloud-radio access networks, time-variation and interference alignment

---

<https://hdl.handle.net/2144/36140>

*"Downloaded from OpenBU. Boston University's institutional repository."*

BOSTON UNIVERSITY  
COLLEGE OF ENGINEERING

Dissertation

**INTEGER-FORCING ARCHITECTURES:  
CLOUD-RADIO ACCESS NETWORKS,  
TIME-VARIATION AND INTERFERENCE ALIGNMENT**

by

**ISLAM EL BAKOURY**

B.S., Alexandria University, 2010

M.S., Alexandria University, 2013

Submitted in partial fulfillment of the

requirements for the degree of

Doctor of Philosophy

2019

© 2019 by  
ISLAM EL BAKOURY  
All rights reserved

## Approved by

First Reader

---

Bobak Nazer, Ph.D.  
Associate Professor of Electrical and Computer Engineering

Second Reader

---

David Castañón, Ph.D.  
Professor of Electrical and Computer Engineering  
Professor of Systems Engineering

Third Reader

---

Ioannis Ch. Paschalidis , Ph.D.  
Professor of Electrical and Computer Engineering  
Professor of Systems Engineering  
Professor of Biomedical Engineering

Fourth Reader

---

Prakash Ishwar, Ph.D.  
Professor of Electrical and Computer Engineering  
Professor of Systems Engineering

## Acknowledgments

First and foremost, praise and thanks is due to Allah, the All-Knowing, and the Most-Generous. I express my sincere gratitude to Allah for his uncountable blessings. His grace provided me with strength, purpose, and patience to reach this stage of my life.

I owe my deepest gratitude to my adviser, Professor Bobak Nazer for his support, patience and guidance throughout the Ph.D. journey. On an academic level, I learned from him how to tackle interesting research problems, how to present ideas in a simple yet self-contained fashion whether in an oral presentation or on a written document and how to be precise when making an argument. On a personal level, his door was always open to me to discuss any ideas or problems that I had without showing any sign of boredom.

I would also like to thank Professors: David Castanon, Ioannis Paschalidis and Prakash Ishwar for being in my dissertation committee and for their insightful discussions.

I would like to thank the faculty of both; the Department of Electrical Engineering and the Department of Mathematics for creating a productive and positive environment through courses and invited talks. I would like also to thank Professor Ahmed Sultan who stimulated my love for research and for being there to answer my questions along this journey.

I would like also to thank my friends Maysara Sabry, Hussain El Kotby, Kareem Said, Ghada Saleh, Ahmed Abozaid, Ahmed Hindy, Mohammed Nafea, Omar Mehanna and Ahmed El Shafie for their support. I would like also to thank my colleagues who were there for me: Dr. Wenbo He, Dr. Corina Ionita, Dr. Michael Farag, Dr. Huanyu Ding, Waleed Tahir, Muhammad Usman Ghani, Parisa Babaheidarian, Furkan Eris and Hatice Kubra Cilingir.

I must express my gratitude to my family. Their constant support is endless.

Their endurance of my absence was a true sacrifice that I cannot repay and I could not reach this stage of my career without their guidance and prayers.

I would like to thank my wife, my colleague and my best friend Iman, who has been with me, side by side, throughout all the ups and downs of the last seven years and for her unique creativity and bright character who kept me motivated and without which I could not have achieved any of my goals. She never lost faith in me even in my darkest hours. I am truly blessed with my children; Zain and Talya, who made me realize how lucky I am to have them in my daily life.

Finally, I would like to thank all the ECE and CISE staff members for creating such a wonderful and professional environment.

**INTEGER-FORCING ARCHITECTURES:  
CLOUD-RADIO ACCESS NETWORKS,  
TIME-VARIATION AND INTERFERENCE ALIGNMENT**

**ISLAM EL BAKOURY**

Boston University, College of Engineering, 2019

Major Professor: Bobak Nazer, PhD  
Associate Professor of Electrical and Computer  
Engineering

ABSTRACT

Next-generation wireless communication systems will need to contend with many active mobile devices, each of which will require a very high data rate. To cope with this growing demand, network deployments are becoming denser, leading to higher interference between active users. Conventional architectures aim to mitigate this interference through careful design of signaling and scheduling protocols. Unfortunately, these methods become less effective as the device density increases. One promising option is to enable cellular basestations (i.e., cell towers) to jointly process their received signals for decoding users data packets as well as to jointly encode their data packets to the users. This joint processing architecture is often enabled by a cloud radio access network that links the basestations to a central processing unit via dedicated connections.

One of the main contributions of this thesis is a novel end-to-end communications architecture for cloud radio access networks as well as a detailed comparison to prior approaches, both via theoretical bounds and numerical simulations. Recent work has

that the following high-level approach has numerous advantages: each basestation quantizes its observed signal and sends it to the central processing unit for decoding, which in turn generates signals for the basestations to transmit, and sends them quantized versions. This thesis follows an integer-forcing approach that uses the fact that, if codewords are drawn from a linear codebook, then their integer-linear combinations are themselves codewords. Overall, this architecture requires integer-forcing channel coding from the users to the central processing unit and back, which handles interference between the users codewords, as well as integer-forcing source coding from the basestations to the central processing unit and back, which handles correlations between the basestations analog signals. Prior work on integer-forcing has proposed and analyzed channel coding strategies as well as a source coding strategy for the basestations to the central processing unit, and this thesis proposes a source coding strategy for the other direction. Iterative algorithms are developed to optimize the parameters of the proposed architecture, which involve real-valued beamforming and equalization matrices and integer-valued coefficient matrices in a quadratic objective.

Beyond the cloud radio setting, it is argued that the integer-forcing approach is a promising framework for interference alignment between multiple transmitter-receiver pairs. In this scenario, the goal is to align the interfering data streams so that, from the perspective of each receiver, there seems to be only a signal receiver. Integer-forcing interference alignment accomplishes this objective by having each receiver recover two linear combinations that can then be solved for the desired signal and the sum of the interference. Finally, this thesis investigates the impact of channel coherence on the integer-forcing strategy via numerical simulations.

# Contents

<b>1</b>	<b>Introduction</b>	<b>1</b>
1.1	Motivation . . . . .	1
1.2	Integer-Forcing Background . . . . .	3
1.2.1	Integer-Forcing Channel Coding . . . . .	3
1.2.2	Integer-Forcing Source Coding . . . . .	4
1.3	Related Work . . . . .	5
1.3.1	Compression-Based Schemes for C-RAN . . . . .	6
1.4	Contributions . . . . .	9
1.4.1	Integer-Forcing for Uplink C-RAN . . . . .	9
1.4.2	Integer-Forcing for Downlink C-RAN . . . . .	10
1.4.3	Integer-Forcing Interference Alignment . . . . .	11
1.4.4	Time-Varying Integer-Forcing Linear Receivers . . . . .	11
1.5	Notation . . . . .	12
1.6	Outline . . . . .	12
<b>2</b>	<b>Preliminaries</b>	<b>14</b>
<b>3</b>	<b>Distributed Lossy Compression</b>	<b>17</b>
3.1	Problem Formuation . . . . .	17
3.2	Conventional Distributed Compression Techniques . . . . .	19
3.2.1	“Single-User” Compression . . . . .	19
3.2.2	Wyner-Ziv Compression . . . . .	20
3.2.3	Symmetric Berger-Tung Compression . . . . .	21

3.3	Lattice Distributed Compression . . . . .	21
3.3.1	Lattice-Based Single-User Compression . . . . .	21
3.3.2	Symmetric Integer-Forcing Source Coding . . . . .	23
3.3.3	Asymmetric Integer-Forcing Source Coding . . . . .	26
3.3.4	Symmetric Integer-Forcing Source Coding with Outage . . . . .	30
3.3.5	Opportunistic Integer-Forcing Source Coding with Outage . . . . .	31
<b>4</b>	<b>Uplink Cloud-Radio Access Networks</b>	<b>35</b>
4.1	System Model . . . . .	35
4.1.1	The End-to-End Channel Coding Problem . . . . .	36
4.1.2	The Distributed Lossy Compression Sub-problem . . . . .	37
4.2	Conventional Receivers for Uplink C-RAN . . . . .	39
4.2.1	“Single-User” Decoding . . . . .	39
4.2.2	Successive Decoding . . . . .	40
4.2.3	Joint Decoding . . . . .	42
4.3	Integer-Forcing C-RAN Architecture . . . . .	43
4.3.1	Architecture . . . . .	43
4.3.2	Optimization Algorithms . . . . .	46
4.4	IF Outage Upper Bound . . . . .	48
4.5	Numerical Results . . . . .	53
4.5.1	Global CSIR . . . . .	53
4.5.2	Local CSIR . . . . .	54
<b>5</b>	<b>Distributed Lossy Decompression</b>	<b>58</b>
5.1	Problem Formulation . . . . .	58
5.2	Conventional Compression Schemes . . . . .	59
5.2.1	Single-User Compression . . . . .	59
5.2.2	Multivariate Compression . . . . .	60

5.3	The Reverse Integer-Forcing Source Coding . . . . .	60
5.3.1	Parallel Reverse Integer-Forcing Source Coding . . . . .	61
5.3.2	Successive Reverse Integer-Forcing Compression . . . . .	64
<b>6</b>	<b>Downlink Cloud-Radio Access Networks</b>	<b>71</b>
6.1	System Model . . . . .	72
6.1.1	The End-to-End Broadcast Channel . . . . .	72
6.1.2	Compression-Based Strategies for Downlink C-RAN . . . . .	73
6.2	Conventional Receivers for Downlink C-RAN . . . . .	73
6.3	Integer-Forcing C-RAN Architecture . . . . .	74
6.3.1	Channel Encoding . . . . .	75
6.3.2	Backhaul Compression . . . . .	76
6.3.3	Channel Decoding . . . . .	78
<b>7</b>	<b>Uplink-Downlink Integer-Forcing Duality through Algebraic Successive Decoding</b>	<b>80</b>
7.1	Uplink C-RAN . . . . .	81
7.1.1	Uplink C-RAN Channel . . . . .	81
7.1.2	Integer-Forcing for Uplink C-RAN . . . . .	82
7.2	Downlink C-RAN . . . . .	85
7.2.1	Downlink C-RAN Channel . . . . .	85
7.2.2	Integer-Forcing for Downlink C-RAN . . . . .	86
7.3	Duality . . . . .	89
7.4	Downlink C-RAN Optimization Algorithm Based on Duality . . . . .	91
7.5	Numerical Results . . . . .	93
<b>8</b>	<b>Integer-Forcing Interference Alignment</b>	<b>96</b>
8.0.1	Notation . . . . .	96
8.0.2	System Model . . . . .	96

8.1	Signal Space Alignment and Max-SINR Algorithm . . . . .	98
8.1.1	Objective and Optimization Problem . . . . .	98
8.1.2	Max-SINR Algorithm . . . . .	100
8.2	Integer-Forcing Interference Alignment . . . . .	101
8.2.1	Achievable Rates . . . . .	101
8.2.2	Integer Matrix $\mathbf{A}^{[k]}$ structure . . . . .	105
8.2.3	Objective and Optimization Problem . . . . .	106
8.2.4	Problem Relaxation . . . . .	108
8.3	Aligned LLL . . . . .	109
8.4	Beamforming and Equalization . . . . .	114
8.4.1	CVX-IFIA . . . . .	115
8.4.2	Dual-IFIA . . . . .	116
8.5	Simulation Results . . . . .	118
<b>9</b>	<b>Time-Varying Integer-Forcing Receivers</b>	<b>122</b>
9.1	Channel Models . . . . .	122
9.1.1	Static Channels . . . . .	123
9.1.2	Block Fading Channels . . . . .	123
9.2	Problem Formulation . . . . .	124
9.3	Conventional Block Fading Receivers . . . . .	124
9.3.1	Joint ML Receiver . . . . .	125
9.3.2	MMSE Linear Receiver . . . . .	125
9.4	Block Fading IF Receiver . . . . .	127
9.5	Simulation Results . . . . .	129
<b>10</b>	<b>Conclusion and Future Work</b>	<b>131</b>
10.1	Summary . . . . .	131
10.2	Future Work . . . . .	132

<b>A</b>	<b>Arithmetic Mean and Geometric Mean Decoders</b>	<b>134</b>
A.1	AM Decoder . . . . .	134
A.2	GM Decoder . . . . .	136
<b>B</b>	<b>Existence of L and C in UL C-RAN</b>	<b>141</b>
<b>C</b>	<b>Bounding <math>d^*</math></b>	<b>142</b>
<b>D</b>	<b>Existence of L and C in DL C-RAN</b>	<b>144</b>
<b>E</b>	<b>Matrix F Properties</b>	<b>146</b>
<b>F</b>	<b>Uplink Downlink Duality Appendix</b>	<b>147</b>
F.1	Proof of Lemma 18 . . . . .	147
F.2	Proof of Lemma 20 . . . . .	148
F.3	Proof of Lemma 19 . . . . .	148
<b>G</b>	<b>Aligned LLL for general <math>M^{[k]}</math></b>	<b>150</b>
G.0.1	Choosing the interference function $\mathbf{g}^{[k]}$ . . . . .	150
G.0.2	Finding the best two integer-combinations in $\mathbf{g}^{[k]}$ and $\mathbf{s}^{[k]}$ . . . . .	151
G.1	Generalized Aligned LLL Algorithm . . . . .	152
	<b>References</b>	<b>154</b>
	<b>Curriculum Vitae</b>	<b>159</b>
G.2	EDUCATION . . . . .	159
G.3	PROGRAMMING SKILLS . . . . .	159
G.4	COURSEWORK . . . . .	159
G.5	EXPERIENCE . . . . .	159
G.6	PUBLICATIONS . . . . .	160
G.7	RESEARCH INTEREST . . . . .	161

# List of Figures

3-1	The distributed lossy compression problem. . . . .	17
3-2	Integer-Forcing Source Coding, where the green arrows denotes algebraic successive cancellation. . . . .	24
4-1	Uplink C-RAN architecture with $K$ users and $L$ BSs. . . . .	36
4-2	Integer-forcing architecture for C-RAN with symmetric distortion. . .	43
4-3	5% outage rate for global CSIR with $K = 6$ , $L = 3$ and SNR = 25 dB.	56
4-4	2% outage rate for global CSIR with $K = 3$ , $L = 6$ and SNR = 25 dB.	56
4-5	10% outage rate for local CSIR Scenario with $K = 3$ , $L = 6$ and SNR = 25 dB. . . . .	56
4-6	10% outage rate for local CSIR Scenario with $K = 3$ , $L = 6$ and $C = 3$ bits/sec/Hz. . . . .	56
4-7	10% outage rate for local CSIR Scenario with $K = 6$ , $L = 3$ and SNR = 25 dB. . . . .	57
4-8	10% outage rate for local CSIR Scenario with $K = 6$ , $L = 3$ and $C = 6$ bits/sec/Hz. . . . .	57
4-9	10% outage rate for local CSIR Scenario with $K = L = 6$ and SNR = 25 dB. . . . .	57
4-10	10% outage rate for local CSIR Scenario with $K = L = 6$ and $C = 6$ bits/sec/Hz. . . . .	57
5-1	The distributed decompression problem. . . . .	58
5-2	Reverse Integer-Forcing Source Coding. . . . .	64

6.1	The downlink C-RAN channel model. . . . .	71
6.2	Integer-forcing architecture for Downlink C-RAN with symmetric distortion. . . . .	75
7.1	The Uplink and downlink C-RAN channel models. . . . .	81
7.2	The average sum-rate for $K = 4$ and $\text{SNR} = 30\text{dB}$ . . . . .	94
7.3	The average sum-rate for $K = 4$ and $C_{\text{sym}} = 20$ Bits/Sec/Hz. . . . .	95
8.1	The structure of the $\ell^{\text{th}}$ Tx. and the $k^{\text{th}}$ Rx. for IFIA scheme . . . . .	102
8.2	Example 1 . . . . .	107
8.3	$K = 3, N_{\text{Tx}}^{[k]} = N_{\text{Rx}}^{[k]} = 2, M^{[k]} = 2, \forall k.$ . . . . .	120
8.4	$K = 4, N_{\text{Tx}}^{[k]} = N_{\text{Rx}}^{[k]} = 2, M^{[k]} = 2, \forall k.$ . . . . .	121
9.1	MIMO MAC channel with $K$ users . . . . .	122
9.2	The block fading model. . . . .	123
9.3	Outage rates at $\rho = 0.1, N = 8, K = 2$ and $N_{\text{Rx}} = 2.$ . . . . .	129
9.4	Outage rates at $\rho = 0.1, N = 8, K = 3$ and $N_{\text{Rx}} = 3.$ . . . . .	129

## List of Abbreviations

BC	.....	Broadcast Channel
C-RAN	.....	Cloud-Radio Access Network
CSI	.....	Channel State Information
CSIR	.....	Channel State Information at Receiver
CSIT	.....	Channel State Information at Transmitter
IF	.....	Integer-Forcing
IFCC	.....	Integer-Forcing Channel Coding
IFSC	.....	Integer-Forcing Source Coding
MAC	.....	Multiple Access Channel
MIMO	.....	Multiple-Input-Multiple-Output
MMSE	.....	Minimum Mean Square Error
OFDM	.....	Orthogonal Frequency-Division Multiplexing
SINR	.....	Signal-to-Interference-and-Noise Ratio
SNR	.....	Signal-to-Noise Ratio

## Chapter 1

# Introduction

### 1.1 Motivation

Next-generation wireless communication systems are facing a growth in number of mobile devices and a sharply-increased demand for higher data rate, which highlights the need for techniques to mitigate interference between different users. Many of the proposed systems and architectures for next-generation wireless will have to contend with interference between devices. Conventional architectures aim to mitigate this interference through careful design of signaling and scheduling protocols which become less effective as the device density increases. Recently, Cloud radio access networks (C-RANs) have emerged as a promising framework that enable us to use advanced signal processing techniques to jointly process the received signals at different cellular basestations for decoding users data packets as well as to jointly encode their data packets to the users. This joint processing architecture is often enabled by using dedicated links between the basestations and a central processing unit.

This has been extensively analyzed via simultaneous joint typicality encoding and decoding, which is unfortunately not suitable for practical implementation. Practical architectures have been proposed that rely on sequential encoding and decoding, and substantial effort has gone into the design of algorithms to optimize the associated parameters. Alongside these efforts, a new wireless architecture, namely the *integer-forcing* receiver [Zhan et al., 2014], was proposed and has been analyzed for several basic communication building blocks, including MAC, broadcast, and dis-

tributed source coding.

The integer-forcing receiver builds upon the *compute-and-forward* framework [Nazer and Gastpar, 2011] proposed for the relay channel (i.e., the decoding is distributed across the relays, not centralized in one receiver as in the MAC). In the compute-and-forward strategy, the relay decodes integer-linear combinations of the desired codeword along with the interference codewords, then forwards it to the destination. Decoding integer-linear combinations is possible if all the users' codewords were generated using the same lattice codebook due to the closure under addition property of lattices.

For the MAC, the integer-forcing receiver first removes the noise by decoding integer-linear combinations of the codewords. Then it removes the interference by solving these combinations for the codewords themselves. This is unlike the conventional linear receiver approach which uses equalization to eliminate the interference between data streams before decoding, hence results in a poor performance due to noise amplification or residual interference.

Integer-forcing decoders have been also introduced for the distributed source coding [Ordentlich and Erez, 2013]. The integer-forcing source decoder first recovers integer-linear combinations of noisy sources' observations, then solves these combinations for the noisy sources' observations. Since the sources are correlated, the combinations of the noisy sources' observations can be chosen to have lower variances, hence lower compression rates.

Here, we build on these efforts and propose several architectures for next-generation wireless network topologies, such as C-RANs. The basic architecture of a C-RAN consists of many users that communicate to several base stations (BSs) over a shared wireless channel. Each BS has a finite-capacity fronthaul link to a central processor (CP), which can employ joint encoding and decoding strategies to improve the overall

rates. Part of the appeal of C-RANs is that in the uplink scenario the BSs do not need to know the users' codebooks, and can instead just forward their quantized channel observations to the CP [Sanderovich et al., 2009]. Similarly, in the downlink scenario the BSs decompress and transmit the recovered channel codewords to the users [Park et al., 2013]. The CP can then employ sophisticated encoding/decoding procedures to encode/decode the users' messages. We extend integer-forcing to the uplink and downlink C-RAN scenarios and develop algorithms to optimize the associated parameters. In the case when we are free to allocate the total transmitting power across different transmitters and the fronthaul total capacity across different fronthaul links, we established a sum-rate duality between the integer-forcing for uplink and downlink C-RAN.

## 1.2 Integer-Forcing Background

In this section, we briefly review the IF schemes proposed in the literature for both channel and source coding.

### 1.2.1 Integer-Forcing Channel Coding

Integer-forcing channel coding (IFCC), proposed in [Zhan et al., 2014] for the Gaussian MIMO multiple access channel (MAC), shows a promising performance that approaches the joint decoding performance on average when there is no channel state information available at the transmitter (CSIT). However, the work in [Ordentlich and Erez, 2015] showed that for some channel realizations, the sum-rate of IF can be far from the sum-rate of joint decoding. As a workaround to achieve a constant gap from the Gaussian MIMO capacity (i.e., centralized encoding), the authors proposed using a universal (i.e., independent of the channel realization) space-time precoder at the transmitter. Later, [Ordentlich et al., 2013] proposed successive integer-forcing decoding in which the decoder uses previously decoded integer-linear combinations

as side information to help reducing the effective noise variance affecting subsequent decoding steps at the expense of using different lattice codebooks at the transmitters. Alongside these contributions, [Hong and Caire, 2011] proposed a reverse compute-and-forward scheme for the broadcast channel (BC) (i.e., distributed antenna systems). In the reverse compute-and-forward, the encoder precodes the messages in the digital domain before performing channel encoding. This allows the distributed decoders after decoding integer-linear combinations of the codewords to map each combination to the desired message.

The work in [Zhan et al., 2014, Ordentlich and Erez, 2015, Ordentlich et al., 2013, Hong and Caire, 2011] assumed that all transmitters have the same power constraint, hence the nested lattice codebooks used had a single coarse lattice that enforces the power constraints. Later, [Nazer et al., 2016] generalized the compute-and-forward building block used in the aforementioned IF schemes to include asymmetric power allocation across transmitters by using nested lattice codebooks with multiple nested coarse lattices. Recently, the work in [He et al., 2018] extended the reverse compute-and-forward scheme to the asymmetric power allocation case using a digital version of dirty-paper precoding on the digital messages. This allowed the authors to establish an uplink-downlink IF sum-rate duality under a total power constraint. The uplink-downlink IF duality result helped the authors to develop an iterative algorithm to optimize the downlink channel parameters.

### 1.2.2 Integer-Forcing Source Coding

Recently, the distributed lossy compression for jointly Gaussian random variables, under quadratic distortion measure, has been studied extensively in [Pradhan and Ramchandran, 2003, Wagner et al., 2008, Krithivasan and Pradhan, 2009, Zamir et al., 2002]. For the scalar sources, [Wagner et al., 2008] proved that the Berger-Tung (BT) quantize-and-bin strategy [Berger, 1977] is optimal. In the BT scheme, we first quan-

tize the sources, realizations using i.i.d. codebook, then use a binning scheme similar to Slepian-Wolf binning to exploit the correlation between the sources. At the receiver, BT uses a joint typicality decoder which has implementation complexity that scales exponentially with the number of sources, thus preventing it from being realized in practice. Another way to exploit the correlation between the sources is to use Wyner-Ziv scheme [Wyner and Ziv, 1976] by successively decompressing the sources, using previously recovered sources as side information. Recently, integer-forcing source coding (IFSC) [Ordentlich and Erez, 2017] was proposed to extend the idea of IFCC to the distributed lossy compression problem with symmetric distortion. The underlying idea of IFSC is to use single-user decoders to decode integer-linear combinations of noisy realizations of the sources, then solve for these noisy observations. Decoding integer-linear combinations of the sources is possible when using the same lattice quantizer at the distributed sources. The combinations can be selected to have smaller variances than the sources, hence, for a fixed distortion, the encoders can use codebooks with lower compression rates.

Later, [He and Nazer, 2016] extended the IFSC scheme to the asymmetric distortion case by using nested lattice codebooks as quantizers at the encoders and algebraic successive decoding for the combinations at the decoder. Both IFSC schemes are promising candidates for the uplink C-RAN, where distributed BSs can use simple lattice quantizers to quantize their observations. The CP can then use IFSC to recover the BSs observations.

### 1.3 Related Work

In an uplink C-RAN, each BS can choose between decoding some users messages [Kramer et al., 2005] (probably the users closest to it), compressing its observation [Cover and El Gamal, 1979] or computing integer-linear combinations of the users

messages [Nazer and Gastpar, 2011]. The BS then forwards the result to the CP. On the other hand, several cooperation techniques were proposed for the downlink C-RAN including data sharing [Simeone et al., 2009], reverse compute-and-forward [Hong and Caire, 2011] and compress-and-forward (e.g., multivariate compression [Park et al., 2014]). In the data-sharing scheme, the digital messages (or a subset of the messages) are shared with each BS using the fronthaul links which creates a cooperation opportunity that helps eliminate the interference at the user end. On the other hand, in a reverse compute-and-forward scheme, the digital messages are initially precoded at the CP, then forwarded through the fronthaul links to the BSs. The users recover integer-linear combinations of the codewords transmitted from the BSs where each combination at the user side can be mapped back to the originally desired message at this user. Recent work [Ganguly and Kim, 2017] has proven that, in a cloud-radio access network (C-RAN) set-up, compressing the relay’s signal and forwarding it to the destination achieves the capacity within a constant gap in both uplink and downlink scenarios. However, the achievability scheme in [Ganguly and Kim, 2017] requires joint encoding/decoding at the CP which has implementation complexity that scales exponentially with the number of users. Hence, recent papers have developed strategies and optimization algorithms with lower implementation complexity, like Wyner-Ziv-based compression [Gesbert et al., 2010, Park et al., 2014, Zhou and Yu, 2014, Zhou and Yu, 2016] for the uplink scenario and multivariate compression using successive compression [Park et al., 2013] for the downlink scenario.

### 1.3.1 Compression-Based Schemes for C-RAN

In compression-based uplink C-RAN, each BS compresses its observation and forwards it to the CP which first recovers the BSs’ observations with some quantization noise, then use them to recover the users messages. In [Zhou and Yu, 2014], the authors proposed a successive decoding scheme for both phases, in which the CP first

successively recovers the BSs observations (i.e., Wyner-Ziv compression), then uses it to successively decode the users messages. In [Zhou et al., 2016], the authors generalized the successive decoding to include all permutations between recovering both the BSs' observations and the users messages and proved that, under some conditions, it recovers the performance of joint decoding.

Similarly to the uplink case, in a compression-based strategy the CP encodes the digital messages to channel codewords, performs a linear precoding, compresses each codeword and forwards it to a BS through the fronthaul links. Since the fronthaul links have finite capacity, the BSs recover the codewords with some quantization noise. The quantization noise from each BS is going to be combined at the users and introducing a correlation between them can be beneficial [Park et al., 2014].

In this thesis, we will focus on developing low implementation complexity architectures that use single-user encoders/decoders instead for joint encoders/decoders for compression-based uplink and downlink C-RAN.

### **Wyner-Ziv compression for uplink C-RAN**

The simplest way to compress and decompress the BSs observations is to do it independently discarding the correlation between these observations. However, discarding some of the information yields a significant loss in performance. One can opt rather to use previously decompressed observations at the CP as side information to help reduce the compression rate under fixed distortion measure (or reduce the distortion measure under fixed rate constraint) for subsequent recovered observations. This can be done by Wyner-Ziv compression and successive decompression as suggested by [Zhou and Yu, 2014]. In order to optimize their scheme, the authors developed a successive convex approximation (SCA) algorithm to jointly choose the covariance matrix of the quantization noise along with the channel precoding matrix (assuming that the channel is known at the transmitter side). Furthermore, they proposed a

heuristic approach for the decompression order which is essential to limit the SCA algorithm's complexity. Other than error propagation, the Wyner-Ziv compression technique used in [Zhou and Yu, 2014] faces two drawbacks. The first is that the optimization problem is non-convex and the proposed successive convex approximation algorithm is not guaranteed to converge (or may converge very slowly). The second is that taking all possible decompression orders into consideration may render it impractical and using the heuristic ordering suggested in [Zhou and Yu, 2014] may result in a considerable loss in performance. Hence, a lower complexity scheme that takes into consideration the correlation between BSs observations and is easy to optimize is needed. For that reason, we propose using IFSC with parallel or successive single-user decoders as the compression scheme of the end-to-end IF uplink C-RAN. One advantage for IFSC over Wyner-Ziv successive decompression is that IFSC could be done using parallel single-user decoders instead of successive single-user decoders which exhibit delay and error propagation. Furthermore, the structure of the single-user decoders used in IFSC has lower implementation complexity than the single-user decoders used in Wyner-Ziv decompression.

### **Multivariate compression for downlink C-RAN**

In order to minimize the distortions affecting the reconstructed codewords at the BSs in a downlink compression-based C-RAN, we should independently compress (decompress) the codewords at the CP (BSs), respectively. This can be performed efficiently using a rate-distortion code. However, since the quantization noise impacting the recovered codewords at the BSs will be combined later at the user's end, [Park et al., 2013] proposed a multivariate compression scheme that allows us to create correlated quantization noise at the BSs, which ultimately lowers the effective variances of the combined noise seen at the users. The multivariate compression, which demonstrated a promising performance in [Park et al., 2013], is done using joint compression. As

a lower complexity alternative, the authors also proposed successive single-user compression to create the correlation between the quantization noise at the BSs. In order to optimize the associated parameters, the authors proposed a successive convex optimization algorithm for a given compression order. Similar to the Wyner-Ziv compression for the uplink C-RAN, the optimization algorithm of this successive compression strategy suffers from the same implementation drawbacks (i.e., convergence issues and optimizing the compression order). This shows the need for an alternative to multivariate compression or successive compression that has a lower implementation complexity and is easier to be optimized which we can use to create a correlation between the quantization noise at different BSs. In this thesis, we propose a new integer-forcing compression scheme, namely the *reverse integer-forcing source coding*, that only uses parallel single-user encoders to create such a correlation. Furthermore, this reverse IFSC scheme is easy to be optimized using the sum-rate duality that we establish between both uplink and downlink IF architectures. Specifically, instead of optimizing the reverse IFSC in the downlink, we optimize the IFSC in the uplink then use the duality to get a solution for the reverse IFSC parameters that achieve the same sum-rate as in the uplink.

## 1.4 Contributions

### 1.4.1 Integer-Forcing for Uplink C-RAN

For the uplink C-RAN channel, where the BSs are connected to a CP through fronthaul links with limited capacity, we

- Start by providing a simpler and complete achievability proof for IFSC with algebraic successive cancellation proposed in [He and Nazer, 2016].
- Propose an end-to-end integer-forcing framework for compression-based uplink cloud radio access network with lower implementation complexity and compa-

rable performance over the state-of-the-art Wyner-Ziv-based compression with successive interference cancellation.

- Prove that, when the channel state information is only known at the receiver (CSIR), the IF outage probability is a constant gap from the optimal outage probability.
- Develop an opportunistic IF compression scheme that combines both the IFSC and single-user compression, for the important case when only local CSI is available at the BSs (i.e., each BS only knows the channel from all users to itself).

#### 1.4.2 Integer-Forcing for Downlink C-RAN

In [Park et al., 2013], a multivariate compression coupled with dirty paper channel coding is proposed which demonstrated a good performance despite its high implementation complexity. For that, we

- Introduce a novel *reverse integer-forcing source coding*, which uses only parallel single-user encoders, instead of the joint or successive encoders used in the multivariate compression, to create correlation between the quantization noise at the BSs.
- Extend this compression technique to include algebraic successive encoding, which can create quantization noise with a wider class of covariance matrices, hence resulting in higher performance at the expense of using different lattice codebook at each BS.
- Use the reverse IFSC to propose an end-to-end integer-forcing framework for the downlink C-RAN with lower complexity than multivariate compression and dirty paper coding.

- Under total power constraint and total fronthaul rate constraint, we establish a duality between the achievable end-to-end sum-rates using the proposed IF schemes for uplink and downlink C-RAN.

### 1.4.3 Integer-Forcing Interference Alignment

Finally, we study the K-user MIMO interference channel, where some form of interference alignment [Gomadam et al., 2011, Ntranos et al., 2013] is often needed to attain the highest possible rates. For the important special case of linear alignment strategies, many iterative optimization algorithms have been proposed that aim to maximize the signal-to-interference-and-noise ratio (SINR) at each receiver. We propose a class of iterative optimization algorithms for integer-forcing interference alignment (IFIA) proposed in [Ntranos et al., 2013]. There are two main components: an aligned lattice reduction algorithm and an equalization/beamforming optimization algorithm that utilizes either uplink-downlink duality [He et al., 2018] or convexity. We also demonstrate, via simulations, the rate gains of IFIA over the Max-SINR algorithm especially in the low/moderate SNR regime. These gains are most pronounced in scenarios that are not feasible [Yetis et al., 2010] for linear strategies in a degrees-of-freedom sense.

### 1.4.4 Time-Varying Integer-Forcing Linear Receivers

In many important scenarios, the channel may vary significantly within the span of a single codeword (i.e., the coherence time of the channel is longer than the codeword duration). For example, in orthogonal frequency division multiplexing (OFDM) systems, channel variation will occur across OFDM symbols if the channel is frequency selective. Hence, the tacit assumption that the channel is fixed through the block length that we assumed throughout this thesis work is not always true. Since relay channels (e.g., C-RAN) is sophisticated to study in nature, we start first by assuming a simple multiple access channel and extend the integer-forcing receivers for MAC to

include time-varying channels and comparing its performance to conventional linear receivers. The underlying idea of IF equalization is to approximate the channel to integers while decoding. Even if the channel is changing within the codeword duration, the integer coefficients in the combination should be held fixed so that the lattice closure property remains intact. We show that in the block-fading model, where the channel is assumed to be fixed within a subblock but changes from subblock to another, the IF performance still retains advantage over conventional linear receivers. For the C-RAN, it remains an open question whether the proposed IF architectures in this thesis still retain advantage over conventional decompression and decoding strategies (e.g., Wyner-Ziv compression and successive MMSE decoding) or not.

## 1.5 Notation

In this work, we denote column vectors by boldface lowercase (e.g.,  $\mathbf{x}$ ) and matrices by boldface uppercase (e.g.,  $\mathbf{X}$ ). Let  $\mathbf{X}^\dagger$  denote the transpose of a matrix  $\mathbf{X}$  and let  $\mathbf{X}_{\mathcal{A},\mathcal{B}}$  be the matrix composed of the rows and columns of  $\mathbf{X}$  with indices in the sets  $\mathcal{A}$  and  $\mathcal{B}$ , respectively. When  $\mathcal{A} = \mathcal{B}$ , we write  $\mathbf{X}_{\mathcal{A},\mathcal{B}}$  as  $\mathbf{X}_{\mathcal{A}}$ . Define  $\log^+(x) \triangleq \max(0, \log(x))$ . For simplicity, we focus on real-valued channels.<sup>1</sup> We use the superscripts ‘ul’ and ‘dl’ to denote symbols defined for the uplink and downlink channels, respectively. It is worth noting that throughout this dissertation, we calculate the outage and average rates for a certain scheme by computing its CDF numerically using the closed form expression for the achievable rate under that scheme.

## 1.6 Outline

The remainder of this dissertation is organized as follows. We first review some basic lattice definitions in Chapter 2. In Chapter 3, we study the distributed lossy

---

<sup>1</sup>Note that complex-valued channels can be handled via their real-valued decompositions [Zhan et al., 2014].

compression problem and introduce a simpler proof for the successive integer-forcing source coding with asymmetric distortion. Next, in Chapter 4, we study the uplink C-RAN and propose an end-to-end IF scheme based on the integer-forcing channel and source coding. In Chapter 5, we propose a low-complexity scheme for multivariate compression based on lattice coding. In Chapter 6, we study the downlink C-RAN and propose a low complexity end-to-end IF scheme, then establish an uplink-downlink IF duality in Chapter 7. We propose an algorithm to optimize the parameters of the integer-forcing interference alignment (IFIA) scheme in Chapter 8. In Chapter 9, we extend the integer-forcing receiver to the time-varying channel and finally conclude our work in Chapter 10.

## Chapter 2

# Preliminaries

We start with definitions and coding theorems for lattices that will be useful in our strategies.

**Definition 1.** *Lattice:* A lattice is a discrete additive subgroup of  $\mathbb{R}^T$  that is closed under addition and reflection. Given  $m$  linearly independent vectors (i.e., basis)  $\mathbf{g}_1, \dots, \mathbf{g}_m \in \mathbb{R}^T$ , the generated lattice is defined as

$$\Lambda(\mathbf{G}) = \left\{ \sum_{i=1}^m \mathbf{g}_i z_i : z_i \in \mathbb{Z} \right\} = \mathbf{G}\mathbb{Z}^m$$

where  $\mathbf{G} \triangleq [\mathbf{g}_1, \dots, \mathbf{g}_m]$  is called the generator matrix of  $\Lambda(\mathbf{G})$ . For a full-rank lattice  $\Lambda$  (i.e.,  $m=T$ ), we define its *dual lattice* as  $\Lambda^* \triangleq \{\mathbf{G}^{-\dagger} \mathbf{z} : \mathbf{z} \in \mathbb{Z}^T\}$ .

The lattice quantizer maps any point in  $\mathbb{R}^T$  to the nearest point in  $\Lambda$  (breaking ties in a systematic way),

$$\mathcal{Q}_\Lambda(\mathbf{x}) \triangleq \arg \min_{\boldsymbol{\lambda} \in \Lambda} \|\mathbf{x} - \boldsymbol{\lambda}\|^2,$$

which in turns defines the Voronoi region  $\mathcal{V}(\Lambda)$  as the set of points in  $\mathbb{R}^T$  that quantize to the zero vector. The mod  $\Lambda$  operator returns the lattice quantization error

$$[\mathbf{x}] \bmod \Lambda \triangleq \mathbf{x} - \mathcal{Q}_\Lambda(\mathbf{x}).$$

The second moment of a lattice is

$$\sigma^2(\Lambda) \triangleq \frac{1}{T} \mathbb{E} \|\mathbf{x}\|^2$$

for  $\mathbf{x} \sim \text{Unif}(\mathcal{V}(\Lambda))$ .

**Lemma 1** (Crypto Lemma). *For a vector  $\mathbf{y} \in \mathbb{R}^T$  and a dither  $\mathbf{u} \sim \text{Unif}(\mathcal{V}(\Lambda))$  independent of  $\mathbf{y}$ , we have that  $\mathbf{q} = [\mathbf{y} + \mathbf{u}] \bmod \Lambda$  is independent of  $\mathbf{y}$  and  $\mathbf{q} \sim \text{Unif}(\mathcal{V}(\Lambda))$ . See [Zamir, 2014] for a proof.*

We say that the lattice  $\Lambda_C$  is nested in the lattice  $\Lambda_F$  if  $\Lambda_C \subset \Lambda_F$ . A nested lattice codebook  $\Lambda_F \cap \mathcal{V}(\Lambda_C)$  consists of all of the fine lattice points inside the fundamental Voronoi region of the coarse lattice. Note that nested lattices  $\Lambda_C \subset \Lambda_F$  satisfy a distributive law, i.e., for any  $\mathbf{x}, \mathbf{y} \in \mathbb{R}^T$  and integers  $a, b \in \mathbb{Z}$ ,

$$[a [\mathbf{x}] \bmod \Lambda_C + b [\mathbf{y}] \bmod \Lambda_C] \bmod \Lambda_F \tag{2.1}$$

$$= [a\mathbf{x} + b\mathbf{y}] \bmod \Lambda_F. \tag{2.2}$$

The following theorem encapsulates some of the nested lattice existence results from [Ordentlich and Erez, 2016] in a form suitable for establishing our integer-forcing source coding results.

**Lemma 2** ([Ordentlich and Erez, 2016, Theorem 2]). *For  $\theta_1, \dots, \theta_K \in \mathbb{R}, \epsilon > 0$ , and  $T$  large enough, there exist a nested lattice chain  $\Lambda_K \subseteq \dots \subseteq \Lambda_1$  (generated using Construction A from a  $p$ -ary linear code for a large enough prime  $p$ ) such that for  $m = 1, \dots, L$ ,*

1. *The second moment satisfies  $\theta_m \leq \sigma^2(\Lambda_m) < \theta_m + \epsilon$ .*

2. *A mixture of Gaussian and lattice quantization noise will remain in the Voronoi cell w.h.p. if its second moment is below  $\theta_m$ . Specifically, if  $\mathbf{z}_{\text{eff}} = \beta_0 \mathbf{z}_0 + \sum_{k=1}^K \beta_k \mathbf{z}_k$  where  $\beta_0, \dots, \beta_K \in \mathbb{R}$ ,  $\mathbf{z}_0 \sim \mathcal{N}(\mathbf{0}, \mathbf{I})$ ,  $\mathbf{z}_k \sim \text{Unif}(\mathcal{V}(\Lambda_k))$  and if  $\beta_0^2 + \sum_{k=1}^K \beta_k^2 \theta_k < \theta_m$ , then  $\Pr([\mathbf{z}_{\text{eff}}] \bmod \Lambda_m \neq \mathbf{z}_{\text{eff}}) \leq \epsilon$ .*

3. The rate of the codebook formed by intersecting  $\Lambda_m$  with  $\mathcal{V}(\Lambda_\ell)$  satisfies

$$\frac{1}{2} \log \left( \frac{\theta_\ell}{\theta_m} \right) \leq \frac{1}{T} \log |\Lambda_m \cap \mathcal{V}(\Lambda_\ell)| < \frac{1}{2} \log \left( \frac{\theta_\ell}{\theta_m} \right) + \epsilon.$$

The  $m^{\text{th}}$  successive minimum of the full-rank lattice  $\Lambda(\mathbf{G})$ , defined by the basis  $\mathbf{G} \in \mathbb{R}^{T \times T}$ , is defined as

$$\lambda_m(\mathbf{G}) = \inf \{ r : \dim(\text{span}(\Lambda(\mathbf{G}) \cap \mathcal{B}(\mathbf{0}, r))) \geq m \} \quad (2.3)$$

where  $\mathcal{B}(\mathbf{0}, r)$  is a  $T$ -dimensional ball centered at the origin and has a radius  $r$ . In other words, the  $m^{\text{th}}$  successive minima is the radius of the smallest ball that contains  $m$  linearly independent lattice points. The following transference theorem due to Banaszczyk allows us to connect the successive minima of a lattice to those of its dual.

**Theorem 1** ([Banaszczyk, 1993, Theorem 2.1]). *For  $m = 1, \dots, T$ , we have that  $\lambda_m(\mathbf{G})\lambda_{T-m+1}(\mathbf{G}^{-\dagger}) \leq T$ .*

The successive minima are connected to the combinatorial  $L$  shortest independent vectors problem (SIVP) [Bremner, 2012] by the following representation

$$\lambda_m(\mathbf{G}) = \min_{\mathbf{a}_m \in \mathbb{Z}^T : \text{rank}([\mathbf{a}_1 \dots \mathbf{a}_m]) = m} \|\mathbf{G}\mathbf{a}_m\|^2, \quad m = 1, \dots, T. \quad (2.4)$$

Despite the fact that the SIVP is an NP-hard problem, a good approximation for the minimizers  $\mathbf{a}_1, \dots, \mathbf{a}_T$  can be obtained using polynomial-time lattice reduction algorithms as LLL [Lenstra et al., 1982].

**Definition 2.** *Algebraic Inverse:* For a prime  $p$ , we define the algebraic inverse of integer matrix  $\mathbf{A} \in \mathbb{Z}^{K \times K}$  over  $\mathbb{Z}_p$  as any integer matrix  $\mathbf{A}^{\text{inv}} \in \mathbb{Z}_p^{K \times K}$  that satisfies

$$[\mathbf{A}^{\text{inv}} \mathbf{A}] \bmod p = \mathbf{I}. \quad (2.5)$$

## Chapter 3

# Distributed Lossy Compression

In this chapter, we study the classical distributed lossy compression problem which plays an important role in compression-based C-RAN strategies which is one of the main topics in this work. We first recall the problem set-up, recall some conventional compression schemes, then finally study recently proposed low-complexity compression schemes based on lattice codes.

### 3.1 Problem Formulation

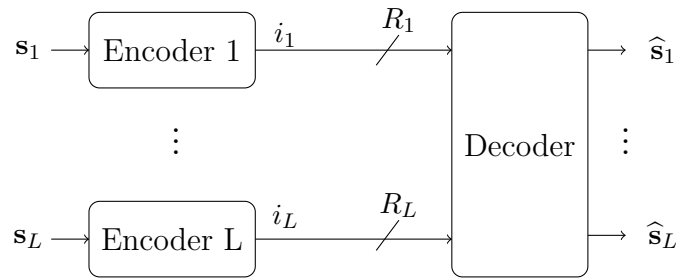


**Figure 3.1:** The distributed lossy compression problem.

Consider the distributed compression problem in Fig. 3.1, where we have  $L$  distributed correlated sources that generate  $T$  i.i.d. realizations  $\mathbf{s}(1) \cdots \mathbf{s}(T)$  of a Gaussian distribution with zero-mean and covariance matrix  $\mathbf{K}_{SS}$  and a single decoder. The  $\ell^{\text{th}}$  source is equipped with an encoder  $\mathcal{E}_\ell : \mathbb{R}^T \rightarrow \{1, \dots, 2^{TR_\ell}\}$  that maps  $\mathbf{s}_\ell \triangleq [s_\ell(1) \cdots s_\ell(T)]$  to an index  $i_\ell \triangleq \mathcal{E}_\ell(\mathbf{s}_\ell)$  with rate  $R_\ell$ . The decoder has a function  $\mathcal{D} : \{1, \dots, 2^{TR_1}\} \times \cdots \times \{1, \dots, 2^{TR_L}\} \rightarrow \mathbb{R}^T \times \cdots \times \mathbb{R}^T$  that uses all received

indices  $i_1, \dots, i_L$  to recover  $(\widehat{\mathbf{s}}_1, \dots, \widehat{\mathbf{s}}_L) = \mathcal{D}(i_1, \dots, i_L)$  where  $\widehat{\mathbf{s}}_\ell \triangleq \mathbf{s}_\ell + \mathbf{q}_\ell$  is a noisy version of  $\mathbf{s}_\ell$  with quantization noise  $\mathbf{q}_\ell$  that is characterized by its mean-square error  $\frac{1}{T}\mathbb{E}\|\mathbf{q}_\ell\|^2$ . We assume that the estimates  $\widehat{\mathbf{s}}_\ell$  are unbiased estimates of  $\mathbf{s}_\ell$  (i.e.,  $\mathbb{E}[\mathbf{q}_\ell] = 0$ ) for  $\ell = 1, \dots, L$ . This allows us to assume that the quantization noise  $\mathbf{q}_\ell$  is uncorrelated with the sources  $\mathbf{s}_1, \dots, \mathbf{s}_L$ , which is a desirable property for our C-RAN application as we will see later in Chapter 4.

The compression rates  $R_{\text{scheme},\ell}(\mathbf{K}_{SS}, d_1, \dots, d_L)$  for  $\ell \in \mathcal{L}$  are said to be achievable, via a particular scheme, for distortion levels  $d_1, \dots, d_L$ , if there exist encoders (with rates  $R_{\text{Scheme},\ell}(\mathbf{K}_{SS}, d_1, \dots, d_L)$ ) and a decoder such that for any  $\epsilon > 0$  and  $T$  large enough we have

$$\frac{1}{T}\mathbb{E}\left[\sum_{t=1}^T q_{\ell,t}^2\right] \leq d_\ell + \epsilon, \quad \ell = 1, \dots, L.$$

**Remark 1.** *Similarly, for fixed rates  $R_1, \dots, R_L$ , the distortion levels  $d_{\text{scheme},\ell}(\mathbf{K}_{SS}, R_1, \dots, R_L)$  for  $\ell \in \mathcal{L}$  are said to be achievable, via a particular scheme, if there exist encoders (with rates  $R_1, \dots, R_L$ ) and a decoder such that for any  $\epsilon > 0$  and  $T$  large enough we have*

$$\frac{1}{T}\mathbb{E}\left[\sum_{t=1}^T q_{\ell,t}^2\right] \leq d_{\text{scheme},\ell}(\mathbf{K}_{SS}, R_1, \dots, R_L) + \epsilon, \quad \ell = 1, \dots, L.$$

In some applications (e.g., compression-based C-RAN),  $\mathbf{K}_{SS}$  is not fixed and can be assumed to be drawn from some distribution. In general, each compression rate depends on  $\mathbf{K}_{SS}$  and all rates should be set jointly according to the realization of  $\mathbf{K}_{SS}$ . However, if the realization of  $\mathbf{K}_{SS}$  is only fully known to the decoder and partially known to the encoders (i.e., the  $\ell^{\text{th}}$  encoder knows only  $K_{SS,\ell,\ell}$ ), we can not set the rates jointly. In this case, each encoder can only set its compression rate separately, depending only on its source's variance. Hence, we can only use “single-user” compression so that the quantized observation from the  $\ell^{\text{th}}$  encoder can be

reconstructed directly from the index  $i_\ell$ . Unfortunately, this compression scheme does not exploit the correlation between sources observations. We propose a workaround, in which the sources fix the compression rates (along with the fixed distortion levels) regardless of the value of  $\mathbf{K}_{SS}$ , so that the decoder can recover  $\widehat{\mathbf{s}}_1, \dots, \widehat{\mathbf{s}}_L$  with some positive probability (w.r.t. the distribution of  $\mathbf{K}_{SS}$ ). Specifically, define the *compression outage probability*, for a target symmetric distortion level  $d_t$  and target symmetric compression rate  $R_t$ , to be

$$p_{\text{outage}}(R_t, d_t) \triangleq \mathbb{P} \left( \max_{\ell} R_{\text{scheme}, \ell}(\mathbf{K}_{SS}, d_t) > R_t \right) \quad (3.1)$$

where the probability is taken with respect to the covariance matrix  $\mathbf{K}_{SS}$ . Note that we opt to use a symmetric distortion level  $d_t$  when  $\mathbf{K}_{SS}$  is not fully known to the encoders, since it is not clear how to best choose  $d_{t,1}, \dots, d_{t,L}$  to obtain a given outage probability.

## 3.2 Conventional Distributed Compression Techniques

### 3.2.1 “Single-User” Compression

The simplest compression strategy is to ignore any correlations between  $\mathbf{s}_1, \dots, \mathbf{s}_L$  and use i.i.d. Gaussian codebooks to compress each source independently. At the decoder, we use single-user decoders to recover each source (i.e.,  $\widehat{\mathbf{s}}_\ell = \mathcal{D}_\ell(i_\ell)$  for  $\ell = 1, \dots, L$ ).

**Lemma 3** ([Zhou and Yu, 2016, Equation (8)]). *The achievable compression rates for single-user (SU) compression are*

$$R_{SU, \ell}(K_{SS, \ell, \ell}, d_\ell) = \frac{1}{2} \log \left( 1 + \frac{K_{SS, \ell, \ell}}{d_\ell} \right), \quad \forall \ell \in \mathcal{L} \quad (3.2)$$

where  $K_{SS, \ell, \ell}$  denotes the variance of the  $\ell^{\text{th}}$  source and  $d_\ell$  is the  $\ell^{\text{th}}$  distortion level.

Note that the “1 +” appears inside the logarithm since we insist upon unbiased estimates.

**Remark 2.** *Since the SU compression does not exploit the correlation between the sources, the  $\ell^{\text{th}}$  achievable rate only depends on the  $\ell^{\text{th}}$  variance  $K_{SS,\ell,\ell}$ .*

### 3.2.2 Wyner-Ziv Compression

Since the sources  $\mathbf{s}_1, \dots, \mathbf{s}_L$  are correlated, we can use a Wyner-Ziv (WZ) compression strategy [Wyner and Ziv, 1976] to exploit this correlation using successive decompression. Assume the decompression order is specified by a permutation  $\pi_s : \mathcal{L} \rightarrow \mathcal{L}$ . The basic idea behind WZ strategy is for the decoder to use previously decompressed signals  $\widehat{\mathbf{s}}_{\pi_s(1)}, \dots, \widehat{\mathbf{s}}_{\pi_s(\ell-1)}$  as side information while recovering  $\widehat{\mathbf{s}}_{\pi_s(\ell)}$  to obtain a finer reconstruction.

**Lemma 4** ([Zhou and Yu, 2016, Equation (28)]). *The achievable compression rates under Wyner-Ziv compression are given by*

$$R_{WZ,\pi_s(\ell)}(\mathbf{K}_{SS}, \mathbf{D}_{\mathcal{T}_\ell}) = \frac{1}{2} \log \left( \frac{|\mathbf{K}_{SS,\mathcal{T}_\ell,\mathcal{T}_\ell} + \mathbf{D}_{\mathcal{T}_\ell}|}{|\mathbf{K}_{SS,\mathcal{T}_{\ell-1},\mathcal{T}_{\ell-1}} + \mathbf{D}_{\mathcal{T}_{\ell-1}}|} \right) - \frac{1}{2} \log(d_{\pi_s(\ell)}), \quad \forall \ell \in \mathcal{L} \quad (3.3)$$

where  $\mathcal{T}_\ell \triangleq \{\pi_s(1), \dots, \pi_s(\ell)\}$  and  $\mathbf{D} \triangleq \text{diag}(d_1, \dots, d_L)$ .

See [Zhou and Yu, 2016] for a proof.

**Remark 3.** *Unlike SU compression, all achievable rates via WZ compression do depend on  $\mathbf{K}_{SS}$ . Hence, to find the achievable distortion levels subject to some rate constraints, as we will see in Chapter 4 in our C-RAN application, we need the knowledge of  $\mathbf{K}_{SS}$  at all encoders.*

Note that WZ compression can be also extended to the case where  $\mathbf{K}_{SS}$  is only available to the decoder and not to the encoders by setting a predetermined distortion levels and tolerate some outage probability that one (or more) of these values falls below the achievable distortion levels for WZ compression.

### 3.2.3 Symmetric Berger-Tung Compression

The rate region for distributed Gaussian source coding remains an open problem. However, the Berger-Tung (BT) quantize-and-bin strategy [Berger, 1977] is known to be optimal for two (scalar) sources [Wagner et al., 2008]. Here, following the example of [Ordentlich and Erez, 2017, Sec. II], we take the BT rate region, evaluated for Gaussian test channels and with a symmetric distortion constraint, as a benchmark for our compression schemes. This strategy relies upon joint typicality decoding, which has substantially higher implementation complexity than the successive decoding used for WZ compression.

**Lemma 5** ([Ordentlich and Erez, 2017, equation (6)]). *The achievable symmetric compression rate using the BT compression scheme is*

$$R_{BT}(\mathbf{K}_{SS}, d_{BT}) = \frac{1}{2L} \log \left| \mathbf{I} + \frac{1}{d_{BT}} \mathbf{K}_{SS} \right| \quad (3.4)$$

where  $\mathbf{K}_{SS}$  is the covariance matrix of the sources and  $d_{BT}$  is the symmetric distortion level.

## 3.3 Lattice Distributed Compression

### 3.3.1 Lattice-Based Single-User Compression

Lattice codes can be used to achieve the same rate and target distortion for the single-user compression strategy presented in Section 3.2.1.

For clarity, define permutations  $\pi_F$  and  $\pi_C$  such that the target distortion levels and the sources variances satisfy

$$d_{\pi_F(L)} \leq \cdots \leq d_{\pi_F(1)}$$

$$K_{SS, \pi_C(1), \pi_C(1)} \leq \cdots \leq K_{SS, \pi_C(L), \pi_C(L)}.$$

## Codebook

Generate nested lattice codebooks  $\mathcal{C}_\ell \triangleq \Lambda_{F,\ell} \cap \mathcal{V}(\Lambda_{C,\ell})$  with rates  $R_\ell = \frac{1}{2} \log \left( \frac{\theta_{C,\ell}}{\theta_{F,\ell}} \right)$  using nested lattices  $\Lambda_{C,\pi_C(L)} \subseteq \cdots \subseteq \Lambda_{C,\pi_C(1)} \subseteq \Lambda_{F,\pi_F(1)} \subseteq \cdots \subseteq \Lambda_{F,\pi_F(L)}$  selected using Lemma 2 with parameters  $\theta_{F,\ell} = d_\ell$  and  $\theta_{C,\ell}$  (to be chosen later), where  $d_\ell$  is the  $\ell^{\text{th}}$  distortion level.

## Compression

The  $\ell^{\text{th}}$  encoder adds a random dither  $\mathbf{u}_\ell \sim \text{Unif}(\mathcal{V}(\Lambda_{F,\ell}))$  to its realization  $\mathbf{s}_\ell$ , then takes modulo with respect to the coarse lattice  $\Lambda_{C,\ell}$  to obtain its codeword

$$\boldsymbol{\lambda}_\ell = [\mathcal{Q}_{\Lambda_{F,\ell}}(\mathbf{y}_\ell + \mathbf{u}_\ell)] \bmod \Lambda_{C,\ell} \quad (3.5)$$

where  $\boldsymbol{\lambda}_\ell \in \mathcal{C}_\ell$ . Note that the dithers  $\mathbf{u}_1, \dots, \mathbf{u}_L$  are independent and known to the decoder<sup>1</sup>. The  $\ell^{\text{th}}$  encoder then sends the index  $i_\ell \in \{1, \dots, 2^{TR_\ell}\}$  that corresponds to the codeword  $\boldsymbol{\lambda}_\ell$  to the decoder.

## Decompression

The decoder recovers the codewords  $\boldsymbol{\lambda}_1, \dots, \boldsymbol{\lambda}_L$  from the indices  $i_1, \dots, i_L$ , then recovers

$$\begin{aligned} \widehat{\mathbf{s}}_\ell &= [\boldsymbol{\lambda}_\ell - \mathbf{u}_\ell] \bmod \Lambda_{C,\ell} \\ &\stackrel{(a)}{=} [[\mathbf{s}_\ell + \mathbf{u}_\ell + \mathbf{q}_\ell] \bmod \Lambda_{C,\ell} - \mathbf{u}_\ell] \bmod \Lambda_{C,\ell} \\ &\stackrel{(b)}{=} [\mathbf{s}_\ell + \mathbf{q}_\ell] \bmod \Lambda_{C,\ell} \\ &\stackrel{(c)}{=} \mathbf{s}_\ell + \mathbf{q}_\ell \end{aligned} \quad (3.6)$$

---

<sup>1</sup>The availability of random dithers at the transmitters and receivers is a standard assumption made to streamline achievability proofs for nested lattice codes. It is straightforward to show that the same rates are achievable by replacing these random dithers with deterministic ones. See, for instance, [Nazer and Gastpar, 2011, App. C] for more details.

where  $\mathbf{q}_\ell = -[\mathbf{s}_\ell + \mathbf{u}_\ell] \bmod \Lambda_{F,\ell}$  is a quantization noise independent of  $\mathbf{s}_\ell$  and uniformly distributed over  $\mathcal{V}(\Lambda_{F,\ell})$  due to Lemma 1, (a) follows from the definition of the mod operator, (b) follows from the distributive law, (c) follows with high probability by the second property of Lemma 2 if the effective variance satisfies

$$\frac{1}{T} \mathbb{E} \|\mathbf{s}_\ell + \mathbf{q}_\ell\|^2 = K_{SS,\ell,\ell} + d_\ell < \theta_{C,\ell}, \quad \forall \ell \in \mathcal{L}. \quad (3.7)$$

This is guaranteed if we choose  $\theta_{C,\ell}$  such that

$$\theta_C = K_{SS,\ell,\ell} + d_\ell - \epsilon \quad (3.8)$$

where  $\epsilon$  goes to zero as the blocklength goes to infinity.

**Lemma 6.** *For a target distortion levels  $d_1, \dots, d_L$  and covariance matrix  $\mathbf{K}_{SS}$ , the achievable rates for lattice-based single-user compression are*

$$R_{SU\text{-lattice},\ell} = \frac{1}{2} \log \left( \frac{K_{SS,\ell,\ell} + d_\ell}{d_\ell} \right) \quad \forall \ell \in \mathcal{L} \quad (3.9)$$

which matches the performance of the i.i.d. Gaussian codebooks from (3.2).

### 3.3.2 Symmetric Integer-Forcing Source Coding

For this section, let us assume symmetric distortion levels  $d_1 = \dots = d_L = d$  and symmetric compression rate  $R_1 = \dots = R_L = R$ . In order to successfully recover the sources' realizations, we need to “break out” of the mod  $\Lambda_{C,\ell}$  operation as in (3.6). The distributive law (2.2) allows us to take integer-linear combinations of the sources prior to removing the mod  $\Lambda_C$  operation. Since the sources are correlated, we can select the integer coefficients to reduce the variance, thus relaxing the requirements on the second moment of the coarse lattice and decreasing the compression rate. If

we recover  $L$  linearly independent integer combinations

$$\mathbf{v}_m \triangleq \sum_{\ell=1}^L a_{m,\ell} \widehat{\mathbf{s}}_\ell, \quad a_{m,\ell} \in \mathbb{Z}, \quad m = 1, \dots, L, \quad (3.10)$$

then we can solve these for the quantized sources  $\widehat{\mathbf{s}}_1, \dots, \widehat{\mathbf{s}}_L$ . This is the main idea behind integer-forcing source coding (IFSC).

Let  $\mathbf{A}$  be the  $L \times L$  integer matrix whose  $(m, \ell)^{\text{th}}$  entry is  $a_{m,\ell}$  and note that we can solve for the quantized sources if  $\mathbf{A}$  is full-rank.

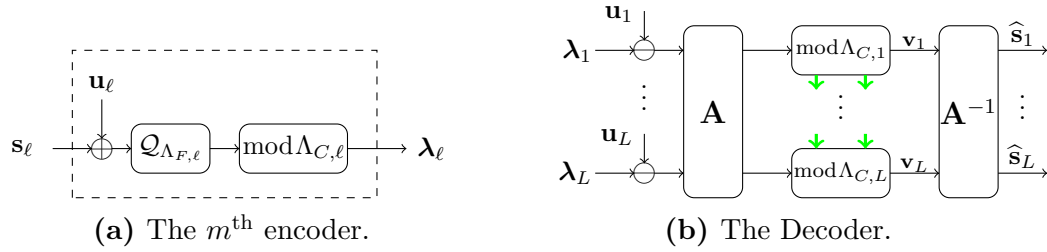


**Figure 3-2:** Integer-Forcing Source Coding, where the green arrows denotes algebraic successive cancellation.

## Codebook

Select a nested lattice pair  $\Lambda_F \subseteq \Lambda_C$  using Lemma 2 with parameters  $\theta_F = d$  and  $\theta_C$ , where  $d$  is the symmetric distortion. The nested lattice pair forms the lattice codebook  $\mathcal{C} \triangleq \Lambda_F \cap \mathcal{V}(\Lambda_C)$  with rate  $R = \frac{1}{2} \log \left( \frac{\theta_C}{\theta_F} \right)$ .

## Compression

As in the lattice-based single-user compression, the  $\ell^{\text{th}}$  encoder first quantizes its observation  $\mathbf{s}_\ell$  using  $\Lambda_F$  to obtain the lattice point

$$\mathbf{t}_\ell = \mathcal{Q}_{\Lambda_F}(\mathbf{s}_\ell + \mathbf{u}_\ell) \quad (3.11)$$

where  $\mathbf{u}_\ell$  is a random dither uniformly distributed over  $\mathcal{V}(\Lambda_F)$  and independent of  $\mathbf{s}_\ell$ .

Next, the  $\ell^{\text{th}}$  encoder takes  $\text{mod } \Lambda_C$  to obtain the lattice codeword  $\boldsymbol{\lambda}_\ell \in \mathcal{C}$  as follows:

$$\boldsymbol{\lambda}_\ell = [\mathbf{t}_\ell] \text{ mod } \Lambda_C. \quad (3.12)$$

Finally, the  $\ell^{\text{th}}$  encoder sends the index  $i_\ell \in \{1, \dots, 2^R\}$  of  $\boldsymbol{\lambda}_\ell$  to the decoder.

### Decompression

It will be useful to collect the dithers and sources' realizations in matrices  $\mathbf{U} \triangleq [\mathbf{u}_1 \cdots \mathbf{u}_L]^\dagger$  and  $\mathbf{S} \triangleq [\mathbf{s}_1 \cdots \mathbf{s}_L]^\dagger$ , respectively.

For a fixed full-rank integer matrix  $\mathbf{A}$ , the decoder first recovers the codeword matrix  $\boldsymbol{\Lambda} \triangleq [\boldsymbol{\lambda}_1 \cdots \boldsymbol{\lambda}_L]^\dagger$  from the indices  $i_1, \dots, i_L$ , then removes the dithers and computes

$$\begin{aligned} \widehat{\mathbf{V}} &= [\mathbf{A} (\boldsymbol{\Lambda} - \mathbf{U})] \text{ mod } \Lambda_C \\ &\stackrel{(a)}{=} [\mathbf{A} (\mathbf{T} - \mathbf{U})] \text{ mod } \Lambda_C \\ &\stackrel{(b)}{=} [\mathbf{A} (\mathbf{S} + \mathbf{Q})] \text{ mod } \Lambda_C \\ &\stackrel{\text{w.h.p.}}{=} \mathbf{A} (\mathbf{S} + \mathbf{Q}) \end{aligned} \quad (3.13)$$

where  $\text{mod } \Lambda_C$  operates on each row,  $\widehat{\mathbf{V}} \triangleq [\widehat{\mathbf{v}}_1 \cdots \widehat{\mathbf{v}}_L]^\dagger$ ,  $\widehat{\mathbf{v}}_\ell$  is an estimate of  $\mathbf{v}_\ell$ ,  $\mathbf{T} \triangleq [\mathbf{t}_1 \cdots \mathbf{t}_L]^\dagger$ , (a) follows from the distributive law, (b) follows from substituting by  $\mathbf{T} = \mathbf{S} + \mathbf{U} + \mathbf{Q}$ ,  $\mathbf{Q} \triangleq [\mathbf{q}_1 \cdots \mathbf{q}_L]^\dagger$ ,  $\mathbf{q}_k \triangleq -[\mathbf{s}_k + \mathbf{u}_k] \text{ mod } \Lambda_F$  is independent of  $\mathbf{s}_k$  and uniformly distributed over  $\mathcal{V}(\Lambda_F)$  by the Crypto Lemma and the last inequality holds from Lemma 2 with high probability if all rows of  $\mathbf{A} (\mathbf{S} + \mathbf{Q})$  lies with high probability in  $\mathcal{V}(\Lambda_C)$  which happens if

$$\frac{1}{T} \mathbb{E} \|\mathbf{a}_m^\dagger (\mathbf{S} + \mathbf{Q})\|^2 < \theta_C, \quad m = 1, \dots, L.$$

This can be guaranteed by setting  $\theta_F = d$  and  $\theta_C = \max_m \mathbf{a}_m^\dagger (\mathbf{K}_{SS} + d\mathbf{I}) \mathbf{a}_m + \epsilon$ ,

where  $\frac{1}{T}\mathbb{E}[\mathbf{S}\mathbf{S}^\dagger] = \mathbf{K}_{SS}$  is the covariance matrix of the  $L$  sources,  $\frac{1}{T}\mathbb{E}[\mathbf{Q}\mathbf{Q}^\dagger] = d\mathbf{I}$  is the effective covariance matrix of the quantization noise  $\mathbf{Q}$  and  $\epsilon$  goes to zero as the blocklength goes to infinity.

Assuming correct recovery  $\widehat{\mathbf{v}}_m = \mathbf{v}_m$ , the decoder applies the inverse of  $\mathbf{A}$  to obtain

$$\begin{aligned}\widehat{\mathbf{S}} &\triangleq \mathbf{A}^{-1}\widehat{\mathbf{V}} = \mathbf{A}^{-1}\mathbf{V} \\ &= \mathbf{S} + \mathbf{Q}.\end{aligned}$$

**Lemma 7** ([Ordentlich and Erez, 2017]). *For a given covariance matrix  $\mathbf{K}_{SS}$  and distortion level  $d$ , the symmetric IFSC achievable rate with parallel decomposition is*

$$R_{IFSC}(\mathbf{K}_{SS}, d) = \min_{\substack{\mathbf{A} \in \mathbb{Z}^{L \times L} \\ \text{Rank}(\mathbf{A})=L}} \frac{1}{2} \log^+ \left( \frac{\max_{m=1, \dots, L} \mathbf{a}_m^\dagger (\mathbf{K}_{SS} + d\mathbf{I}) \mathbf{a}_m}{d} \right). \quad (3.14)$$

### 3.3.3 Asymmetric Integer-Forcing Source Coding

Let us recall the asymmetric IFSC introduced in [He and Nazer, 2016].

For a full-rank integer matrix  $\mathbf{A}$ , assume that the combinations  $\mathbf{v}_1, \dots, \mathbf{v}_L$  have been re-indexed (i.e., the rows of  $\mathbf{A}$ ) such that their effective variances are monotonically increasing (i.e.,  $\mathbb{E}\|\mathbf{v}_1\|^2 \leq \dots \leq \mathbb{E}\|\mathbf{v}_L\|^2$ ). Furthermore, assume that the sources are re-indexed (i.e., the columns of  $\mathbf{A}$ , columns and rows of  $\mathbf{K}_{SS}$  as well as the diagonal elements of  $\mathbf{D}$ ) such that the full-rank integer matrix  $\mathbf{A}$  has full-rank sub-matrices  $\mathbf{A}_{s,[1:m]}$ , for  $m = 1, \dots, L$ .

Furthermore, define a permutation  $\pi_F$  such that  $d_{\pi_F(L)} \leq \dots \leq d_{\pi_F(1)}$ .

#### Codebook

Generate nested lattice codebooks  $\mathcal{C}_\ell \triangleq \Lambda_{F,\ell} \cap \mathcal{V}(\Lambda_{C,\ell})$  with rates  $R_\ell = \frac{1}{2} \log \left( \frac{\theta_{C,\ell}}{\theta_{F,\ell}} \right)$  using nested lattices  $\Lambda_{C,L} \subseteq \dots \subseteq \Lambda_{C,1} \subseteq \Lambda_{F,\pi_F(1)} \subseteq \dots \subseteq \Lambda_{F,\pi_F(L)}$  selected using Lemma 2 with parameters  $\theta_{F,\ell} = d_\ell$  and  $\theta_{C,\ell}$  (to be chosen later), where  $d_\ell$  is the  $\ell^{\text{th}}$

distortion level.

**Remark 4.** *Note that for the symmetric rate case  $R$ , the monotonically increasing effective variances  $\mathbb{E}\|\mathbf{v}_1\|^2 \leq \dots \leq \mathbb{E}\|\mathbf{v}_L\|^2$  induces a monotonically increasing distortion levels  $d_1 \leq \dots \leq d_L$  where  $\pi_F$  is the identity permutation in this case.*

### Compression

The compression part is similar to IFSC in Section 3.3.2, however with asymmetric fine lattice  $\Lambda_{F,\ell}$  and coarse lattice  $\Lambda_{C,\ell}$  such that the  $\ell^{\text{th}}$  encoder obtains

$$\begin{aligned} \mathbf{t}_\ell &= \mathcal{Q}_{\Lambda_{F,\ell}}(\mathbf{s}_\ell + \mathbf{u}_\ell) \\ \boldsymbol{\lambda}_\ell &= [\mathbf{t}_\ell] \bmod \Lambda_{C,\ell} \end{aligned} \quad (3.15)$$

where  $\mathbf{u}_\ell$  is a random dither that is independent of  $\mathbf{s}_\ell$  and uniformly distributed over  $\mathcal{V}(\Lambda_{F,\ell})$ .

It is useful to write the  $i^{\text{th}}$  combination as

$$\mathbf{v}_i^\dagger = \mathbf{a}_i^\dagger(\mathbf{T} - \mathbf{U}), \quad i = 1, \dots, L, \quad (3.16)$$

where  $\mathbf{T} = \mathbf{S} + \mathbf{U} + \mathbf{Q}$ ,  $\mathbf{Q} \triangleq [\mathbf{q}_1 \ \dots \ \mathbf{q}_L]^\dagger$ ,  $\mathbf{q}_\ell \triangleq -[\mathbf{s}_\ell + \mathbf{u}_\ell] \bmod \Lambda_{F,\ell}$  and is independent of  $\mathbf{s}_\ell$  and uniformly distributed over  $\mathcal{V}(\Lambda_{F,\ell})$  from the Crypto Lemma.

### Algebraic Successive Decompression

Recall that in parallel decompression in (3.13), we found that by computing  $[\mathbf{A}(\boldsymbol{\Lambda} - \mathbf{U})] \bmod \Lambda_C = [\mathbf{A}([\mathbf{T}] \bmod \Lambda_C - \mathbf{U})] \bmod \Lambda_C$  and using the distributive law, we were able to recover  $[\mathbf{A}(\mathbf{T} - \mathbf{U})] \bmod \Lambda_C$ , which can be written as  $[\mathbf{A}(\mathbf{S} + \mathbf{Q})] \bmod \Lambda_C$ .

This was only possible since we were using a single coarse lattice  $\Lambda_C$ . Unfortunately, here at the  $m^{\text{th}}$  decoding step, we take  $\bmod \Lambda_{C,m}$  and this result does not

hold. Alternatively, at the  $m^{\text{th}}$  decoding step, we can compute

$$[\mathbf{L}(\mathbf{\Lambda} - \mathbf{U})] \bmod \Lambda_{C,m} = [\mathbf{L}(\mathbf{T} - \mathbf{U})] \bmod \Lambda_{C,m} = [\mathbf{L}(\mathbf{S} + \mathbf{Q})] \bmod \Lambda_{C,m}$$

where the first equality holds using the distributive law if and only if  $\mathbf{L}$  is an upper triangular integer matrix. This is due to the fact that, the  $m^{\text{th}}$  row of  $\mathbf{L}\mathbf{\Lambda}$  only contains  $\bmod \Lambda_{C,\ell}$  operations for  $\ell \geq m$  and for those values of  $\ell$  we have  $\Lambda_{C,\ell} \subseteq \Lambda_{C,m}$  (i.e.,  $\Lambda_{C,m}$  is finer than all "inner"  $\bmod \Lambda_{C,\ell}$  operations).

Furthermore, the upper triangular property of  $\mathbf{L}$  means that the  $m^{\text{th}}$  combination will only contain the source vectors  $\mathbf{s}_m, \dots, \mathbf{s}_L$ . Using previously decoded combinations  $\mathbf{v}_1, \dots, \mathbf{v}_{m-1}$  (assuming correct decoding) as side information, we can obtain the missing part of the  $m^{\text{th}}$  combination (i.e., fill out the zero elements in the  $m^{\text{th}}$  row of the upper triangular matrix  $\mathbf{L}$ ).

Towards this end, let us define a strictly lower triangular integer matrix  $\mathbf{C}$  where its  $m^{\text{th}}$  row  $\mathbf{c}_m^\dagger$  contains the coefficients of previously successfully decoded combinations  $\mathbf{v}_1, \dots, \mathbf{v}_{m-1}$ , hence the strictly upper triangular condition on the matrix  $\mathbf{C}$ .

Next, we discuss the details of our algebraic successive decompression. The decoder first recovers the lattice codewords  $\boldsymbol{\lambda}_1, \dots, \boldsymbol{\lambda}_L$  from the indices  $i_1, \dots, i_L$ , then computes

$$\begin{aligned} \widehat{\mathbf{v}}_m^\dagger &= \left[ \boldsymbol{\ell}_m^\dagger (\mathbf{\Lambda} - \mathbf{U}) - \mathbf{c}_m^\dagger \widehat{\mathbf{V}} \right] \bmod \Lambda_{C,m} \\ &\stackrel{(a)}{=} \left[ \boldsymbol{\ell}_m^\dagger (\mathbf{T} - \mathbf{U}) - \mathbf{c}_m^\dagger \widehat{\mathbf{V}} \right] \bmod \Lambda_{C,m} \\ &\stackrel{(b)}{=} \left[ (\boldsymbol{\ell}_m^\dagger + \mathbf{c}_m^\dagger \mathbf{A}) (\mathbf{T} - \mathbf{U}) \right] \bmod \Lambda_{C,m} \\ &\stackrel{(c)}{=} \left[ (\boldsymbol{\ell}_m^\dagger + \mathbf{c}_m^\dagger \mathbf{A}) (\mathbf{S} + \mathbf{Q}) \right] \bmod \Lambda_{C,m} \\ &\stackrel{(d)}{=} \left[ [\boldsymbol{\ell}_m^\dagger + \mathbf{c}_m^\dagger \mathbf{A}] \bmod p \times (\mathbf{S} + \mathbf{Q}) \right] \bmod \Lambda_{C,m} \\ &\stackrel{(e)}{=} \left[ [\mathbf{a}_m^\dagger] \bmod p \times (\mathbf{S} + \mathbf{Q}) \right] \bmod \Lambda_{C,m} \\ &= \left[ \mathbf{a}_m^\dagger (\mathbf{S} + \mathbf{Q}) \right] \bmod \Lambda_{C,m}, \quad m = 1, \dots, L \end{aligned} \tag{3.17}$$

where  $\widehat{\mathbf{V}} \triangleq [\widehat{\mathbf{v}}_1 \cdots \widehat{\mathbf{v}}_L]^\dagger$ ,  $\mathbf{c}_m^\dagger \widehat{\mathbf{V}}$  is available at the  $m^{\text{th}}$  decoding step since  $C_{m,i} = 0$  for  $i \geq m$ , (a) follows from the distributive law, (b) holds from assuming correct decoding for previous combinations (i.e.,  $\widehat{\mathbf{v}}_i = \mathbf{v}_i$  for  $i = 1, \dots, m-1$ ) and using (3.16), (c) holds from  $\mathbf{T} = \mathbf{S} + \mathbf{U} + \mathbf{Q}$ ,  $\mathbf{Q} \triangleq [\mathbf{q}_1 \cdots \mathbf{q}_L]^\dagger$ ,  $\mathbf{q}_k \triangleq -[\mathbf{s}_k + \mathbf{u}_k] \bmod \Lambda_{F,k}$  is independent of  $\mathbf{s}_k$  and uniformly distributed over  $\mathcal{V}(\Lambda_{F,k})$  by the Crypto Lemma, (d) holds from [Ordentlich et al., 2014, Theorem 2 (c)] and (e) holds from Lemma 28 in Appendix B which states that for any full-rank integer matrix  $\mathbf{A}$  with full-rank sub-matrices  $\mathbf{A}_{[1:m]}$  for  $m = 1, \dots, L$ , we can select an upper triangular integer matrix  $\mathbf{L}$  and a strictly lower triangular integer matrix  $\mathbf{C}$  such that

$$[\mathbf{L} + \mathbf{CA}] \bmod p = [\mathbf{A}] \bmod p. \quad (3.18)$$

Furthermore, the  $m^{\text{th}}$  estimated combination  $\widehat{\mathbf{v}}_m^\dagger = \mathbf{v}_m^\dagger$ ,  $m = 1, \dots, L$ , if  $\mathbf{a}_m^\dagger (\mathbf{S} + \mathbf{Q}) \in \mathcal{V}(\Lambda_{C,m})$  which happens with high probability if

$$\frac{1}{T} \mathbb{E} \|\mathbf{a}_m^\dagger (\mathbf{S} + \mathbf{Q})\|^2 < \theta_{C,m}, \quad m = 1, \dots, L.$$

This can be guaranteed by setting  $\theta_{F,\ell} = d_\ell$  for  $\ell = 1, \dots, L$  and  $\theta_{C,m} = \mathbf{a}_m^\dagger (\mathbf{K}_{SS} + \mathbf{D}) \mathbf{a}_m + \epsilon$ , where  $\frac{1}{T} \mathbb{E} [\mathbf{SS}^\dagger] = \mathbf{K}_{SS}$  is the covariance matrix of the  $L$  sources,  $\frac{1}{T} \mathbb{E} [\mathbf{QQ}^\dagger] \triangleq \mathbf{D} = \text{diag}(d_1, \dots, d_L)$  and  $\epsilon$  goes to zero as the blocklength goes to infinity.

Finally, the decoder applies the inverse of  $\mathbf{A}$  to obtain

$$\begin{aligned} \widehat{\mathbf{S}} &\triangleq \mathbf{A}^{-1} \widehat{\mathbf{V}} = \mathbf{A}^{-1} \mathbf{V} \\ &= \mathbf{S} + \mathbf{Q}. \end{aligned}$$

**Remark 5.** *The advantage from using  $L$  nested coarse lattices instead of a single one as in the parallel decomposition, is that each coarse lattice  $\Lambda_{C,m}$  should tolerate only one combination  $\mathbf{v}_m$  (i.e.,  $\mathbf{v}_m \in \mathcal{V}(\Lambda_{C,m})$  w.h.p.) instead of tolerating all combinations*

$\mathbf{v}_1, \dots, \mathbf{v}_L$  (i.e.,  $\mathbf{v}_m \in \mathcal{V}(\Lambda_C)$  w.h.p. for  $m = 1, \dots, L$ ).

**Theorem 2** ([Bakoury and Nazer, 2017]). *For a given distortion matrix  $\mathbf{D}$  and covariance matrix  $\mathbf{K}_{SS}$ , the asymmetric achievable rates for IFSC with algebraic successive decomposition are*

$$R_{SIFSC,\ell}(\mathbf{K}_{SS}, \mathbf{D}) = \min_{\mathbf{A} \in \mathbb{Z}^{L \times L}} \frac{1}{2} \log^+ \left( \frac{\mathbf{a}_\ell^\dagger (\mathbf{K}_{SS} + \mathbf{D}) \mathbf{a}_\ell}{d_\ell} \right), \quad \ell = 1, \dots, L \quad (3.19)$$

where the minimization over all integer matrices  $\mathbf{A}$  such that  $\text{Rank}(\mathbf{A}_{[1:m]}) = m$  for  $m = 1, \dots, L$  and  $\mathbf{a}_1^\dagger (\mathbf{K}_{SS} + \mathbf{D}) \mathbf{a}_1 \leq \dots \leq \mathbf{a}_L^\dagger (\mathbf{K}_{SS} + \mathbf{D}) \mathbf{a}_L$ .

Early, we have assumed that the sources have been re-indexed such that the matrix  $\mathbf{A}$  has full-rank sub-matrices  $\mathbf{A}_{[1:m]}$  for  $m = 1, \dots, L$ . Later, in our work, we will need to write the achievable rates in terms of the original source order.

**Lemma 8.** *Define the permutation  $\pi_{SIFSC}$  as the combinations re-ordering that we did in the beginning to ensure that after re-ordering, we have  $\mathbf{a}_{\pi_{SIFSC}(1)}^\dagger (\mathbf{K}_{SS} + \mathbf{D}) \mathbf{a}_{\pi_{SIFSC}(1)} \leq \dots \leq \mathbf{a}_{\pi_{SIFSC}(L)}^\dagger (\mathbf{K}_{SS} + \mathbf{D}) \mathbf{a}_{\pi_{SIFSC}(L)}$  and the permutation  $\pi_{\text{rank}}$  as the source re-ordering such that  $\text{Rank}(\mathbf{A}_{\pi_{SIFSC}([1:m]), \pi_{\text{rank}}([1:m])}) = m$  for  $m = 1, \dots, L$ . The achievable rates in Theorem 2 in terms of the original source order can be written as*

$$R_{SIFSC, \pi_{\text{rank}}(\ell)}(\mathbf{K}_{SS}, \mathbf{D}) = \min_{\mathbf{A} \in \mathbb{Z}^{L \times L}} \frac{1}{2} \log^+ \left( \frac{\mathbf{a}_{\pi_{SIFSC}(\ell)}^\dagger (\mathbf{K}_{SS} + \mathbf{D}) \mathbf{a}_{\pi_{SIFSC}(\ell)}}{d_{\pi_{\text{rank}}(\ell)}} \right), \quad \ell = 1, \dots, L \quad (3.20)$$

where  $\mathbf{D} = \text{diag}(d_1, \dots, d_L)$  and  $d_\ell$  is the  $\ell^{\text{th}}$  distortion level at the  $\ell^{\text{th}}$  source.

**Remark 6.** *Note that, to achieve the compression rates in (3.14) or (3.19), all sources need to know the covariance matrix  $\mathbf{K}_{SS}$ . On the other hand, to achieve the compression rates in (3.9), the  $\ell^{\text{th}}$  source only needs to know its variance  $K_{SS,\ell,\ell}$ .*

### 3.3.4 Symmetric Integer-Forcing Source Coding with Outage

In the case where  $\mathbf{K}_{SS}$  is not fully known to all sources (i.e., the  $\ell^{\text{th}}$  source only knows  $K_{SS,\ell,\ell}$ ), we must tolerate some probability of outage in order to exploit the

correlations between  $\mathbf{s}_1, \dots, \mathbf{s}_L$ . Specifically, for a given symmetric target distortion  $d_t$ , we fix a rate  $R$  that ensures that the decoder can successfully decompress  $\widehat{\mathbf{s}}_1, \dots, \widehat{\mathbf{s}}_L$  with probability  $1 - \rho_s$ . We use the symmetric IFSC scheme from Section 3.3.2 with target distortion  $d_t$  and fixed symmetric rate  $R$  which can be determined using a bisection search such that

$$p_{\text{outage}}(R, d_t) \triangleq \mathbb{P}(R_{\text{IFSC}}(\mathbf{K}_{SS}, d_t) > R) = \rho_s, \quad (3.21)$$

Then, using Lemma 2, we choose a codebook  $\mathcal{C} \triangleq \Lambda_F \cap \mathcal{V}(\Lambda_C)$  with rate  $R$ . The lattice quantizer  $\mathcal{Q}_{\Lambda_F}(\cdot)$  for this codebook should induce the target distortion level  $d_t$ , which suggests choosing  $\theta_F = d_t$  and  $\theta_C = d_t \times 2^{2R}$ .

The compression and decompression processes are similar to the symmetric IFSC with full knowledge of  $\mathbf{K}_{SS}$ . However, the codebook should be generated and held fixed to attain the desired outage probability  $\rho_s$  and should not be generated/adapted according to the current realization of  $\mathbf{K}_S S$  (assuming that  $\mathbf{K}_S S$  has a distribution as we will see later in the C-RAN application).

### 3.3.5 Opportunistic Integer-Forcing Source Coding with Outage

Note that, under fixed symmetric compression rate  $R$  the achievable distortion levels under SU compression in (3.9) can be written as

$$d_{\text{SU},\ell} \triangleq \frac{K_{SS,\ell,\ell}}{2^R - 1} \quad (3.22)$$

For some covariance matrix realizations  $\mathbf{K}_{SS}$ ,  $d_{\text{SU},\ell}$  may in fact be smaller than the fixed symmetric distortion  $d_t$  in (3.21) that attains the desired outage probability  $\rho_s$ . This observation suggests the following opportunistic scheme that combines both IFSC and SUC schemes. First, we choose a lattice codebook with a fine lattice that induces a distortion level  $d_t$  as in Section 3.3.4. Then, for  $\ell$  such that  $d_{\text{SU},\ell} < d_t$ ,

the  $\ell^{\text{th}}$  encoder scales its observation using a parameter  $\beta_\ell$  such that the decoder reconstructs  $\mathbf{s}_\ell$  up to distortion  $d_{\text{SU},\ell}$  before forming the linear combinations as in the IFSC scheme. For the remaining  $\ell$  such that  $d_{\text{SU},\ell} > d_t$ , we proceed as in the basic IFSC scheme. Note that the effective variance of the combinations will be reduced. Next, we present the opportunistic scheme in details.

### Codebook

Select a nested lattice pair  $\Lambda_F \subseteq \Lambda_C$  using Lemma 2 with parameters  $\theta_F = d_t$  and  $\theta_C = d_t 2^{2R}$ , where  $d_t$  is the target symmetric distortion. The nested lattice pair forms the lattice codebook  $\mathcal{C} \triangleq \Lambda_F \cap \mathcal{V}(\Lambda_C)$  with rate  $R$ .

### Compression

Using the codebook  $\mathcal{C}$ , the  $\ell^{\text{th}}$  encoder maps its observation  $\mathbf{s}_\ell$  to the lattice codeword

$$\boldsymbol{\lambda}_\ell = [\mathcal{Q}_{\Lambda_F}(\beta_\ell \mathbf{s}_\ell + \mathbf{u}_\ell)] \bmod \Lambda_C \quad (3.23)$$

where  $\mathbf{u}_\ell$  is a random dither uniformly distributed over  $\mathcal{V}(\Lambda_F)$  and  $\beta_\ell = 1$  whenever  $d_{\text{SU},\ell} > d_t$ . However, when  $d_{\text{SU},\ell} < d_t$  we have

$$R_{\text{SU},\ell}(\mathbf{K}_{SS}, d_t) \triangleq \frac{1}{2} \log \left( \frac{K_{SS,\ell,\ell} + d_t}{d_t} \right) < R \quad (3.24)$$

and we can better utilize the corresponding fronthaul link by scaling up  $\mathbf{s}_\ell$  using  $\beta_\ell > 1$  such that

$$\beta_\ell = \sqrt{\frac{d_t(2^{2R} - 1) - \epsilon}{K_{SS,\ell,\ell}}}. \quad (3.25)$$

where  $\epsilon$  goes to zero as the blocklength goes to infinity.

## Decompression

First, the decoder recovers

$$\begin{aligned}
\tilde{\mathbf{s}}_\ell &\triangleq [\boldsymbol{\lambda}_\ell - \mathbf{u}_\ell] \bmod \Lambda_C \\
&\stackrel{(a)}{=} [\beta_\ell \mathbf{s}_\ell + \tilde{\mathbf{q}}_\ell] \bmod \Lambda_C \\
&\stackrel{(b)}{=} \begin{cases} [\mathbf{s}_\ell + \tilde{\mathbf{q}}_\ell] \bmod \Lambda_C & \text{if } d_{\text{SU},\ell} > d_t \\ \beta_\ell \mathbf{s}_\ell + \tilde{\mathbf{q}}_\ell & \text{if } d_{\text{SU},\ell} < d_t \end{cases} \quad (3.26)
\end{aligned}$$

where  $\tilde{\mathbf{q}}_\ell = -[\beta_\ell \mathbf{s}_\ell + \mathbf{u}_\ell] \bmod \Lambda_F$  is independent of  $\mathbf{s}_\ell$  and uniformly distributed over  $\mathcal{V}(\Lambda_F)$  (due to the Crypto Lemma), (a) holds from the distributive law and (b) holds with high probability if  $\beta_\ell^2 K_{SS,\ell,\ell} + d_t < \theta_C$  which holds by choosing  $\beta_\ell$  as in (3.25).

Defining

$$\mathbf{t}_\ell = \tilde{\mathbf{s}}_\ell / \beta_\ell = \begin{cases} [\mathbf{s}_\ell + \mathbf{q}_\ell] \bmod \Lambda_C & \text{if } d_{\text{SU},\ell} > d_t \\ \mathbf{s}_\ell + \mathbf{q}_\ell & \text{if } d_{\text{SU},\ell} < d_t \end{cases}$$

where  $\mathbf{q}_\ell \triangleq \tilde{\mathbf{q}}_\ell / \beta_\ell$  and  $\frac{1}{T} \mathbb{E} \|\mathbf{q}_\ell\|^2 = d_t / \beta_\ell^2$ , the decoder then forms linear combinations

$$\begin{aligned}
\hat{\mathbf{v}}_m &= \left[ \sum_{\ell=1}^L a_{m,\ell} \mathbf{t}_\ell \right] \bmod \Lambda_C \\
&\stackrel{(a)}{=} \left[ \sum_{\ell=1}^L a_{m,\ell} (\mathbf{s}_\ell + \mathbf{q}_\ell) \right] \bmod \Lambda_C \stackrel{(b)}{=} \sum_{\ell=1}^L a_{s,m,\ell} (\mathbf{s}_\ell + \mathbf{q}_\ell) \quad (3.27)
\end{aligned}$$

where (a) holds from the distributive law and (b) holds w.h.p. if

$$\frac{1}{T} \mathbb{E} \|\mathbf{v}_m\|^2 = \mathbf{a}_m^\dagger (\mathbf{K}_{SS} + \mathbf{D}) \mathbf{a}_m < \theta_C,$$

where  $\mathbf{D} = \text{diag}(d_1, \dots, d_L)$  is the covariance matrix of the quantization noise  $\mathbf{Q}$  and  $d_\ell = d_t / \beta_\ell^2$ .

To guarantee correct recovery with probability at least  $1 - \rho_s$  (i.e.,

$\mathbb{P}(R_{\text{IFSC,op}}(\mathbf{K}_{SS}, d_t) > R) < \rho_s$ ),  $d_t$  should be chosen such that

$$\max_m \mathbf{a}_m^\dagger (\mathbf{K}_{SS} + \mathbf{D}) \mathbf{a}_m \geq \theta_C \quad (3.28)$$

with probability  $\rho_s$ . Finally, assuming correct recovery, the decoder applies the inverse of  $\mathbf{A}$  to obtain

$$\widehat{\mathbf{S}} \triangleq \mathbf{A}^{-1} \mathbf{V} = \mathbf{S} + \mathbf{Q}. \quad (3.29)$$

**Theorem 3.** *Under fixed compression rate  $R$  and for a target outage probability  $\rho_s$ , the achievable distortion levels using opportunistic IFSC are given by*

$$\mathbf{D} = \text{diag}(d_t/\beta_1^2, \dots, d_t/\beta_L^2) \quad (3.30)$$

$$\beta_\ell = \begin{cases} 1 & \text{if } d_t \leq \frac{K_{SS,\ell,\ell}}{2^{2R} - 1} \\ \sqrt{\frac{2^{2R} - 1}{K_{SS,\ell,\ell}}} d_t & \text{if } d_t > \frac{K_{SS,\ell,\ell}}{2^{2R} - 1} \end{cases} \quad (3.31)$$

where  $d_t$  is chosen such that  $\mathbb{P}(R_{\text{IFSC,op}}(\mathbf{K}_{SS}, d_t) > R) = \rho_s$  and

$$R_{\text{IFSC,op}}(\mathbf{K}_{SS}, d_t) = \min_{\substack{\mathbf{A} \in \mathbb{Z}^{L \times L} \\ \text{Rank}(\mathbf{A})=L}} \max_{\ell} \frac{1}{2} \log^+ \left( \frac{\mathbf{a}_\ell^\dagger (\mathbf{K}_{SS} + \mathbf{D}) \mathbf{a}_\ell}{d_t} \right). \quad (3.32)$$

## Chapter 4

# Uplink Cloud-Radio Access Networks

In this chapter, we study the uplink C-RAN, under symmetric or total fronthaul capacity constraints, and propose an end-to-end low complexity IF scheme. In this scheme, we use IFSC to convey noisy versions of the BSs' observations to the CP, then use IF equalization to decode the users' messages. We also establish approximate optimality, in the sense that the end-to-end IF scheme achieves a constant gap from the optimal outage probability when the channel is known only to the receiver (CSIR). We also explore the important case when the channel is only locally known at the receiver side (i.e., each BS only knows the channels from all users to itself).

### 4.1 System Model

Consider the uplink C-RAN scenario shown in Fig. 4.1, where a set  $\mathcal{K} \triangleq \{1, \dots, K\}$  of single-antenna users communicate to a set  $\mathcal{L} \triangleq \{1, \dots, L\}$  of single-antenna base stations<sup>1</sup>. The BSs are connected to the CP via noiseless fronthaul links with finite capacities  $C_1, \dots, C_L$  as shown in Fig. 4.1. The fronthaul links either exhibit individual rate constraints<sup>2</sup>  $C_\ell = C_{\text{sym}}, \forall \ell \in \mathcal{L}$ , or a total rate constraint  $\sum_{\ell=1}^L C_\ell = C_{\text{tot}}$ , depending on the physical structure of the network.

---

<sup>1</sup>For simplicity, we assume single-antenna BSs, however, the proposed schemes can be extended directly to deal with multiple-antenna BSs as in [Bakoury and Nazer, 2017].

<sup>2</sup>We assume symmetric fronthaul links constraints, however an extension to asymmetric individual rate constraints is straightforward

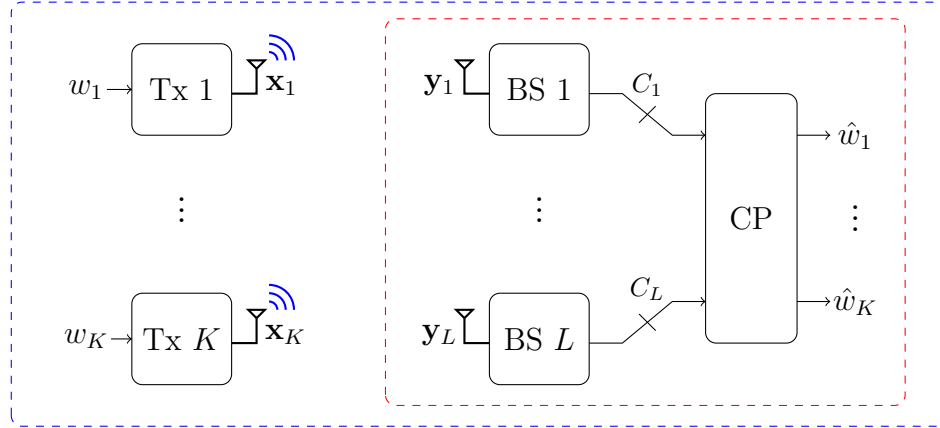


**Figure 4.1:** Uplink C-RAN architecture with  $K$  users and  $L$  BSs. The red dashed rectangle represents the distributed lossy compression sub-problem, while the blue dashed rectangle represents the end-to-end channel coding problem

#### 4.1.1 The End-to-End Channel Coding Problem

The  $k^{\text{th}}$  user encodes its message  $w_k \in \{1, 2, \dots, 2^{TR}\}$ , with symmetric rate  $R$ , into a length- $T$  codeword  $\mathbf{x}_k \triangleq [x_k(1) \cdots x_k(T)]^\dagger \in \mathbb{R}^T$  satisfying the standard power constraint  $\|\mathbf{x}_k\|^2 \leq TP$ . The  $\ell^{\text{th}}$  BS receives  $y_\ell(t) \in \mathbb{R}$  at time  $t$  and the vector of all received signals  $\mathbf{y}(t) \triangleq [y_1(t) \cdots y_L(t)]^\dagger$  at time  $t$  can be expressed as

$$\mathbf{y}(t) = \mathbf{H}\mathbf{x}(t) + \mathbf{z}(t) \quad (4.1)$$

where  $\mathbf{H} \in \mathbb{R}^{L \times K}$  is the channel matrix which is only known to the receivers (i.e., CSIR),  $\mathbf{x}(t) = [x_1(t) \cdots x_K(t)]^\dagger$  is the vector of transmitted symbols at time  $t$ , and  $\mathbf{z}(t)$  is i.i.d.  $\mathcal{N}(0, 1)$ . For simplicity, we focus on real-valued channels and note that complex-valued channels can be handled via their real-valued decompositions [Zhan et al., 2014]. We also consider both cases, namely global CSIR and Local CSIR. In global CSIR, all BSs know the channel matrix  $\mathbf{H}$ , while in local CSIR, the  $\ell^{\text{th}}$  BS knows only its local channel  $\mathbf{H}_{\ell, \mathcal{K}}$  (i.e., the channel from all users  $\mathcal{K}$  to itself).

The  $\ell^{\text{th}}$  BS maps its observation  $\mathbf{y}_\ell \triangleq [y_\ell(1) \cdots y_\ell(T)]^\dagger$  to an index  $i_\ell \in$

$\{1, \dots, 2^{TC_\ell}\}$  and forwards it to the CP through the fronthaul link. Upon receiving indices  $i_1, \dots, i_L$ , the CP uses these indices to make estimates  $\hat{w}_1, \dots, \hat{w}_K$  of the transmitted messages.

We say that a symmetric rate  $R$  is achievable if, for any  $\epsilon > 0$  and  $T$  large enough, there exists encoders and decoders that can attain  $\mathbb{P}(\cup_{k=1}^K \{\hat{w}_k \neq w_k\}) \leq \epsilon$  average probability of error at most  $\epsilon$ . Since we assume that  $\mathbf{H}$  is not known to the transmitters, each user has to tolerate some outage probability.

For a target symmetric rate  $R$ , we define the *outage probability* of a scheme as

$$p_{\text{outage}}(R) \triangleq \mathbb{P}(R_{\text{scheme}}(\mathbf{H}) < R)$$

where  $R_{\text{scheme}}(\mathbf{H})$  is the achievable symmetric rate under  $\mathbf{H}$  for this particular scheme. Similarly, for a target outage probability  $\rho$ , we define the *symmetric outage rate* as

$$R_{\text{outage}}(\rho) \triangleq \sup \{R : p_{\text{outage}}(R) \leq \rho\}.$$

#### 4.1.2 The Distributed Lossy Compression Sub-problem

In compression-based strategies, each BS uses the fronthaul link to send a compressed version of its observation to the CP rather than decoding locally, and can thus be oblivious to the codebooks employed by the users. The  $\ell^{\text{th}}$  BS maps its received signal  $\mathbf{y}_\ell \triangleq [y_\ell(1) \cdots y_\ell(T)]^\dagger$  to an index  $i_\ell \in \{1, \dots, 2^{TR_\ell^s}\}$ , where  $R_\ell^s$  is the compression rate, and forwards it to the CP through a fronthaul link with fixed capacity  $C_\ell$  (i.e.,  $R_\ell^s \leq C_\ell$ ). Upon receiving indices  $i_1, \dots, i_L$ , the CP first reconstructs the signals  $\hat{\mathbf{y}}_1, \dots, \hat{\mathbf{y}}_L$  where  $\hat{\mathbf{y}}_\ell \triangleq [\hat{y}_\ell(1) \cdots \hat{y}_\ell(T)]$ , then uses these reconstructions to make estimates  $\hat{w}_1, \dots, \hat{w}_K$  of the transmitted messages.

Note that the CP can use other techniques to recover the messages  $w_1, \dots, w_K$  from the indices  $i_1, \dots, i_L$ , however recovering  $\hat{\mathbf{y}}_1, \dots, \hat{\mathbf{y}}_L$  first simplifies the fronthaul network to the well studied distributed lossy compression problem which allows us to

use one of the efficient schemes proposed in Chapter 3 to convey the BSs' observations to the CP.

Due to the limited fronthaul capacity, each decompressed signal

$$\hat{y}_\ell(t) = y_\ell(t) + q_\ell(t), \quad \forall \ell \in \mathcal{L}$$

suffers from a quantization noise  $q_\ell(t)$ , which is characterized via its mean-squared error (MSE) (i.e., distortion level)  $\frac{1}{T}\mathbb{E}\left[\sum_{t=1}^T(q_\ell(t))^2\right]$ , which depends on the fronthaul link capacity  $C_\ell$  and the compression strategy. We assume that the  $\hat{y}_\ell(t)$  are unbiased estimates of  $y_\ell(t)$ , since this facilitates the interface between source and channel coding by allowing the latter to assume that the quantization noise is uncorrelated with the transmitted codewords.

The end-to-end effective channel can be written as

$$\hat{\mathbf{y}}(t) = \mathbf{H}\mathbf{x}(t) + \mathbf{z}(t) + \mathbf{q}(t), \quad (4.2)$$

where  $\hat{\mathbf{y}}(t) \triangleq [\hat{y}_1(t) \cdots \hat{y}_L(t)]^\dagger$  and  $\mathbf{q}(t) \triangleq [q_1(t) \cdots q_L(t)]^\dagger$ .

For the distributed lossy compression sub-problem, we denote the effective covariance matrix for BSs' observations  $\mathbf{Y} \triangleq [\mathbf{y}_1 \cdots \mathbf{y}_L]^\dagger$  as  $\mathbf{K}_{\mathbf{Y}\mathbf{Y}} \triangleq \frac{1}{T}\mathbb{E}[\mathbf{Y}\mathbf{Y}^\dagger] = P\mathbf{H}\mathbf{H}^\dagger + \mathbf{I}$ . Furthermore, the achievable compression rates via particular scheme are denoted by  $R_{\text{scheme},\ell}^s(\mathbf{H}, d_1, \dots, d_L) \leq C_\ell, \forall \ell \in \mathcal{L}$  for distortions  $d_1, \dots, d_L$ . It is worth noting that for the local CSIR scenario, the  $\ell^{\text{th}}$  BS knows only  $K_{\mathbf{Y}\mathbf{Y},\ell,\ell} \triangleq P\|\mathbf{H}_{\ell,\mathcal{K}}\|^2 + 1$ .

For the special case where the fronthaul network has symmetric rate constraints  $C_1 = \cdots = C_L = C_{\text{sym}}$ , the distortion achievable by a compression scheme is given by,

$$d_{\text{scheme}}(\rho_s) \triangleq \inf \{d : p_{\text{outage}}^s(C_{\text{sym}}, d) \leq \rho_s\}$$

where  $p_{\text{outage}}^s(C_{\text{sym}}, d)$  is given in (3.1),  $\rho_s < \rho$  is the target compression outage and  $\rho$  is the end-to-end outage probability.

## 4.2 Conventional Receivers for Uplink C-RAN

In this section, we go over the techniques proposed in literature to deal with both channel coding and distributed source coding problems. We assume fronthaul rate allocation  $C_1, \dots, C_L$ .

**Remark 7.** (*Local CSIR*) Under local CSIR, the channel outage probability constraint is reduced to  $1 - \rho_s$ , since the remaining probability  $\rho_s$  is reserved for the decompression outage event. In our work, we choose  $\rho_s = \rho/2$ .

### 4.2.1 “Single-User” Decoding

The simplest conventional scheme to convey  $w_1, \dots, w_K$  to the CP is to use parallel single user decoders for both; the decompression and the channel decoding stages.

In this scheme, each BS uses the single-user compression scheme, discussed in Section 3.2.1, to independently convey its observation to the CP through its dedicated fronthaul link. The CP independently recovers  $\hat{\mathbf{y}}_\ell$  for  $\ell = 1, \dots, L$ , applies a linear equalizer  $\mathbf{B}$  to its reconstructed observations to get

$$\tilde{\mathbf{Y}} = \mathbf{B}\hat{\mathbf{Y}}$$

where  $\hat{\mathbf{Y}} \triangleq [\hat{\mathbf{y}}_1 \cdots \hat{\mathbf{y}}_L]^\dagger$ , and then applies a single-user decoder to each row of  $\tilde{\mathbf{Y}}$  to recover the individual codewords. Thus, each row of  $\mathbf{B}$  should be selected to maximize the SINR for the desired codeword, which corresponds to the MMSE equalization vector.

**Lemma 9.** For a given channel matrix  $\mathbf{H}$ , the achievable symmetric rate using SU compression and MMSE linear receiver is

$$R_{SUC,MMSE}(\mathbf{H}, \mathbf{D}) = \frac{1}{2} \min_{k \in \mathcal{K}} \log \left( 1 + \frac{P(\mathbf{b}_k^\dagger \mathbf{H}_{\mathcal{L},k})^2}{\mathbf{b}_k^\dagger (\mathbf{I} + \mathbf{D}) \mathbf{b}_k + P \sum_{i \neq k} (\mathbf{b}_k^\dagger \mathbf{H}_{\mathcal{L},i})^2} \right) \quad (4.3)$$

where  $\mathbf{b}_k^\dagger = P\mathbf{H}_{\mathcal{L},k}^\dagger \left( P \sum_{j=1}^K \mathbf{H}_{\mathcal{L},j} \mathbf{H}_{\mathcal{L},j}^\dagger + \mathbf{I} + \mathbf{D} \right)^{-1}$  is the  $\ell^{\text{th}}$  row of the MMSE equalization matrix  $\mathbf{B}$ ,  $\mathbf{H}_{\mathcal{L},k}$  is the  $k^{\text{th}}$  column of the channel matrix  $\mathbf{H}$ ,  $\mathbf{D} = \text{diag}(d_{SU,1}, \dots, d_{SU,L})$  and

$$d_{SU,\ell} = \frac{\|\mathbf{H}_{\ell,\mathcal{K}}\|^2 P + 1}{2^{2C_\ell} - 1}, \quad \forall \ell \in \mathcal{L}.$$

See [Tse and Viswanath, 2005, Section 8.3.3] for more details on MMSE decoders.

**Remark 8.** *Since the SU compression does not exploit the correlation between the BSs observations (i.e., does not depend on cross channels), it is suitable for both cases; local CSIR and global CSIR.*

#### 4.2.2 Successive Decoding

Using successive decoding can enhance the performance of both decompression and channel decoding. In this scheme, first the CP successively reconstructs  $\widehat{\mathbf{y}}_{\pi_s(1)}, \dots, \widehat{\mathbf{y}}_{\pi_s(L)}$  for some decompression order  $\pi_s : \mathcal{L} \rightarrow \mathcal{L}$ . Next, the CP uses MMSE decoder with successive interference cancellation (MMSE-SIC) to cancel out the effect of previously decoded codewords  $\mathbf{x}_{\pi_c(1)}, \dots, \mathbf{x}_{\pi_c(k-1)}$  (assuming successful decoding), for some decoding order  $\pi_c : \mathcal{K} \rightarrow \mathcal{K}$ , before decoding the current codeword  $\mathbf{x}_{\pi_c(k)}$ , and then equalizes the result to get

$$\widetilde{\mathbf{y}}_k^\dagger = \mathbf{b}_k^\dagger \left( \widehat{\mathbf{Y}} - \sum_{i=1}^{k-1} \mathbf{H}_{\mathcal{L},\pi_c(i)} \mathbf{x}_{\pi_c(i)}^\dagger \right), \quad (4.4)$$

which is subsequently fed to a single-user decoder to recover  $\mathbf{x}_{\pi_c(k)}$  for  $k = 1, \dots, K$ .

**Lemma 10.** *For a given channel matrix  $\mathbf{H}$ , the achievable symmetric rate using WZ compression and MMSE-SIC is*

$$R_{WZ,MMSE-SIC}(\mathbf{H}, \mathbf{D}) = \frac{1}{2} \max_{\pi_c} \min_{k \in \mathcal{K}} \log \left( 1 + \frac{P(\mathbf{b}_k^\dagger \mathbf{H}_{\mathcal{L}, \pi_c(k)})^2}{\mathbf{b}_k^\dagger (\mathbf{I} + \mathbf{D}) \mathbf{b}_k + P \sum_{i>k} (\mathbf{b}_k^\dagger \mathbf{H}_{\mathcal{L}, \pi_c(i)})^2} \right) \quad (4.5)$$

where  $\mathbf{b}_k^\dagger = P \mathbf{H}_{\mathcal{L}, \pi_c(k)}^\dagger (P \sum_{j \geq k} \mathbf{H}_{\mathcal{L}, \pi_c(j)} \mathbf{H}_{\mathcal{L}, \pi_c(j)}^\dagger + \mathbf{I} + \mathbf{D})^{-1}$  is the MMSE-SIC equalization vector and  $\mathbf{D} \triangleq \text{diag}(d_{WZ,1}, \dots, d_{WZ,L})$  is chosen such that

$$\frac{1}{2} \log \left( \frac{|\mathbf{P} \mathbf{H}_{\mathcal{T}_\ell, \mathcal{K}} (\mathbf{H}_{\mathcal{T}_\ell, \mathcal{K}})^\dagger + \mathbf{I} + \mathbf{D}_{\mathcal{T}_\ell}|}{|\mathbf{P} \mathbf{H}_{\mathcal{T}_{\ell-1}, \mathcal{K}} (\mathbf{H}_{\mathcal{T}_{\ell-1}, \mathcal{K}})^\dagger + \mathbf{I} + \mathbf{D}_{\mathcal{T}_{\ell-1}}|} \right) - \frac{1}{2} \log(d_{WZ, \pi_s(\ell)}) = C_{\pi_s(\ell)}, \quad \forall \ell \in \mathcal{L} \quad (4.6)$$

where  $\mathcal{T}_\ell \triangleq \{\pi_s(1), \dots, \pi_s(\ell)\}$ ,  $\pi_s$  is the decompression order and  $\pi_c$  is the channel decoding order.

See [Tse and Viswanath, 2005, Section 8.3.3] for more details on MMSE decoders with SIC.

**Remark 9.** (Global CSIR) It can be shown that, for a fixed  $\mathbf{D}_{\mathcal{T}_{\ell-1}}$ ,  $R_{WZ, \pi_s(\ell)}^s(\mathbf{H}, \mathbf{D}_{\mathcal{T}_\ell})$ , given in Lemma 4, is monotonically decreasing in  $d_{WZ, \pi_s(\ell)}$ . This means that the optimal  $d_{WZ, \pi_s(\ell)}$  for the global CSIR case can be obtained successively for  $\ell = 1, \dots, L$  (e.g., using a bisection search method) such that  $R_{WZ, \pi_s(\ell)}^s(\mathbf{H}, \mathbf{D}_{\mathcal{T}_\ell}) = C_{\pi_s(\ell)}$ , for a given fronthaul rate allocation  $C_1, \dots, C_L$ .

**Remark 10.** (Local CSIR) Under local CSIR,  $\mathbf{H}$  is only known to the CP. Thus, the WZ compression rates in Lemma 4 are not known to the BSs and we can not set the distortion levels accordingly. Furthermore, it is not clear how to optimize for the asymmetric distortion levels  $d_1, \dots, d_L$  to satisfy a certain outage probability  $\rho_s$ . Hence, we set a symmetric distortion  $d_t$  such that

$$\mathbb{P} \left( \bigcup_{\ell=1}^L \{R_{WZ, \ell}^s(\mathbf{H}, d_t \mathbf{I}) > C_\ell\} \right) \leq \rho_s. \quad (4.7)$$

where  $R_{WZ, \ell}^s(\mathbf{H}, d_t \mathbf{I})$  is given in Lemma 4.

It is worth noting that, the Wyner-Ziv compression scheme requires searching over all  $L!$  decompression orders, which can be computationally expensive. To circumvent this issue, [Zhou and Yu, 2016] proposed a heuristic ordering by placing the effective variance of  $\mathbf{y}_1, \dots, \mathbf{y}_L$  in increasing order. Numerical simulations indicate that this heuristic ordering operates close to the performance of optimal ordering on average.

### 4.2.3 Joint Decoding

In this scheme, we employ a BT quantize-and-bin strategy [Berger, 1977] as a compression scheme to convey the BSs' observations to the CP. The BT rate region is evaluated for Gaussian test channels and with a symmetric distortion constraint. This converts the channel to a virtual MAC as mentioned earlier. The best performance for the channel decoding part given  $\hat{\mathbf{Y}}$ , is attained by simultaneously decoding all codewords  $\mathbf{x}_1, \dots, \mathbf{x}_K$  via a joint maximum likelihood (ML) decoder. Although, the implementation complexity for both BT compression and joint ML decoding scales exponentially with number of users/BSs, we include it as a benchmark for our schemes.

**Lemma 11.** *For a given channel matrix  $\mathbf{H}$ , the achievable symmetric rate using BT compression scheme and joint ML decoding is*

$$R_{BT,ML}(\mathbf{H}, d_{BT}\mathbf{I}) = \min_{\mathcal{S} \subseteq \mathcal{K}} \frac{1}{2|\mathcal{S}|} \log \left( \left| \frac{P}{d_{BT} + 1} \mathbf{H}_{\mathcal{L},\mathcal{S}} \mathbf{H}_{\mathcal{L},\mathcal{S}}^\dagger + \mathbf{I} \right| \right). \quad (4.8)$$

where  $d_{BT}$  is chosen (e.g., using a bisection search) such that

$$\frac{1}{2L} \log \left| \mathbf{I} + \frac{1}{d_{BT}} \mathbf{K}_{YY} \right| = \min_{\ell} C_{\ell} \quad (4.9)$$

Lemma 11 follows from using joint typicality analysis and can be considered a special case of [Zhou and Yu, 2014, Proposition 1].

**Remark 11.** (Local CSIR) *For local CSIR, one can still implement the BT quantize-and-bin strategy by fixing  $d_{BT}$ , independent of the channel matrix  $\mathbf{H}$ , to the smallest value that satisfies*

$$\mathbb{P} \left( R_{BT}^s(\mathbf{H}, d_{BT}) > \min_{\ell} C_{\ell} \right) \leq \rho_s$$

where  $R_{BT}^s(\mathbf{H}, d_{BT})$  is given by (3.4).

### 4.3 Integer-Forcing C-RAN Architecture

For this section, we assume that we have symmetric rate constraints on the fronthaul links  $C_1 = \dots = C_L = C_{\text{sym}}$ , however, the scheme can be directly extended to the asymmetric constraints setting as we will see in Chapter 7.

#### 4.3.1 Architecture

The end-to-end integer-forcing architecture for C-RAN is illustrated in Figure 4.2. It employs one of the integer-forcing source coding schemes in Section 3.3, to convey the channel observations to the CP, which then recovers the transmitted messages via integer-forcing channel decoding discussed in Chapter 9. Specifically, for full-rank integer matrices  $\mathbf{A}_s$  and  $\mathbf{A}_c$ , the CP first recovers integer-linear combinations  $\mathbf{v}_{s,m}^\dagger = \mathbf{a}_{s,m}^\dagger \widehat{\mathbf{Y}}$  for  $m = 1, \dots, L$ , solves for the BSs observations  $\widehat{\mathbf{Y}} \triangleq [\widehat{\mathbf{y}}_1 \ \dots \ \widehat{\mathbf{y}}_L]^\dagger$ , then recovers integer-linear combinations  $\mathbf{v}_{c,m}^\dagger = \mathbf{a}_{c,m}^\dagger \mathbf{X}$  for  $m = 1, \dots, L$ , then finally solves for  $\mathbf{X} \triangleq [\mathbf{x}_1 \ \dots \ \mathbf{x}_K]^\dagger$ .

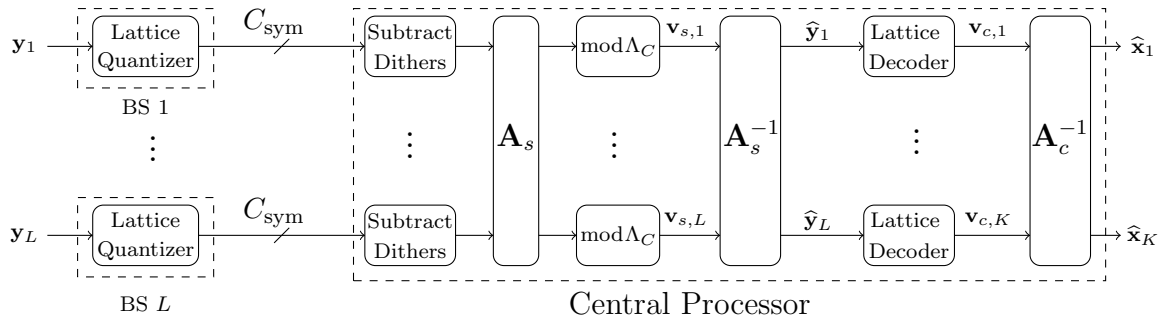


**Figure 4.2:** Integer-forcing architecture for C-RAN with symmetric distortion.

For completeness, let us assume that the CP already recovered  $\widehat{\mathbf{Y}}$  up to distortion levels  $d_1, \dots, d_L$  and recall briefly the IF channel decoding part.

In order to decode  $\mathbf{x}_1, \dots, \mathbf{x}_K$ , the CP first decodes integer-linear combinations of the transmitted codewords, and then solves for the desired codewords. Specifically, in order to decode the combinations

$$\mathbf{v}_{c,m}^\dagger \triangleq \mathbf{a}_{c,m}^\dagger \mathbf{X}, \quad m = 1, \dots, K$$

where  $\mathbf{a}_{c,m} \in \mathbb{Z}^K$ , the CP first applies linear equalizers  $\mathbf{b}_{c,m}^\dagger$  to get effective channels

$$\begin{aligned} \tilde{\mathbf{y}}_m^\dagger &= \mathbf{b}_{c,m}^\dagger \widehat{\mathbf{Y}} \\ &= \underbrace{\mathbf{a}_{c,m}^\dagger \mathbf{X}}_{\text{lattice codeword}} + \underbrace{(\mathbf{b}_{c,m}^\dagger \mathbf{H} - \mathbf{a}_{c,m}^\dagger) \mathbf{X} + \mathbf{b}_{c,m}^\dagger (\mathbf{Z} + \mathbf{Q})}_{\text{effective noise}} \\ &= \mathbf{v}_{c,m}^\dagger + \mathbf{z}_{\text{eff},m}^\dagger, \quad m = 1, \dots, K \end{aligned} \quad (4.10)$$

where  $\mathbf{z}_{\text{eff},m}^\dagger = (\mathbf{b}_{c,m}^\dagger \mathbf{H} - \mathbf{a}_{c,m}^\dagger) \mathbf{X} + \mathbf{b}_{c,m}^\dagger (\mathbf{Z} + \mathbf{Q})$  is the effective noise due to the scaled AWGN  $\mathbf{b}_{c,m}^\dagger \mathbf{Z}$ , the scaled quantization noise  $\mathbf{b}_{c,m}^\dagger \mathbf{Q}$  and the mismatch between the equalized channel  $\mathbf{b}_{c,m}^\dagger \mathbf{H}$  and the integer vector  $\mathbf{a}_{c,m}^\dagger$ . The CP then employs single-user decoders to decode  $\mathbf{v}_{c,1}, \dots, \mathbf{v}_{c,K}$ , and finally solves for  $\mathbf{x}_1, \dots, \mathbf{x}_K$ .

The effective variance of  $\mathbf{z}_{\text{eff},m}$  is

$$\sigma_{\text{eff},m}^2 \triangleq \frac{1}{T} \mathbb{E} \|\mathbf{z}_{\text{eff},m}\|^2 = \|\mathbf{b}_{c,m}^\dagger \mathbf{H} - \mathbf{a}_{c,m}^\dagger\|^2 P + \mathbf{b}_{c,m}^\dagger (\mathbf{I} + \mathbf{D}) \mathbf{b}_{c,m} \quad (4.11)$$

where  $\mathbf{D} \triangleq \text{diag}(d_1, \dots, d_L)$  is the covariance matrix of the quantization noise  $\mathbf{Q}$ .

Using the MMSE equalizer that minimizes the noise variance in (4.11)

$$\mathbf{b}_{c,m}^\dagger = P \mathbf{a}_{c,m}^\dagger \mathbf{H}^\dagger (P \mathbf{H} \mathbf{H}^\dagger + \mathbf{I} + \mathbf{D})^{-1},$$

and applying Woodbury's matrix identity, we can write (4.11) as

$$\sigma_{\text{eff},m}^2 = \mathbf{a}_{c,m}^\dagger (P^{-1} \mathbf{I} + \mathbf{H}^\dagger (\mathbf{I} + \mathbf{D})^{-1} \mathbf{H})^{-1} \mathbf{a}_{c,m} = \|\mathbf{F}_c \mathbf{a}_{c,m}\|^2 \quad (4.12)$$

where  $\mathbf{F}_c$  is any matrix satisfies the decomposition  $\mathbf{F}_c^\dagger \mathbf{F}_c = (P^{-1} \mathbf{I} + \mathbf{H}^\dagger (\mathbf{I} + \mathbf{D})^{-1} \mathbf{H})^{-1}$ .

**Lemma 12.** [Zhan et al., 2014, Theorem 4] For a given channel matrix  $\mathbf{H}$  and distortion matrix  $\mathbf{D}$ , the achievable symmetric rate for the integer-forcing strategy with parallel channel decoding is

$$R_{IFCC}(\mathbf{H}, \mathbf{D}) = \max_{\substack{\mathbf{A}_c \in \mathbb{Z}^{K \times K} \\ \text{rank}(\mathbf{A}_c) = K}} \min_{m \in \mathcal{K}} \frac{1}{2} \log^+ \left( \frac{P}{\|\mathbf{F}_c \mathbf{a}_{c,m}\|^2} \right). \quad (4.13)$$

**Remark 12.** Similar to MMSE-SIC, successive decoding for the combinations  $\mathbf{v}_{c,1}, \dots, \mathbf{v}_{c,K}$  is possible and improves the achievable symmetric rate for IF receivers on average. See [Ordentlich et al., 2013] for more details.

**Remark 13.** Note that both symmetric integer-forcing source coding and integer-forcing channel coding only need parallel encoding/decoding.

Finally, the end-to-end IF performance can be measured by the next 3 Theorems.

**Theorem 4.** The achievable symmetric rate for the integer-forcing C-RAN strategy with global CSIR, parallel decomposition and parallel channel decoding is

$$\begin{aligned} R_{IF-CRAN}(\mathbf{H}) &= \max_{d, \mathbf{A}_c \in \mathbb{Z}^{K \times K}} \min_{m \in \mathcal{K}} \frac{1}{2} \log^+ \left( \frac{P}{\|\mathbf{F}_c \mathbf{a}_{c,m}\|^2} \right) \\ &\text{subject to} \quad \text{Rank}(\mathbf{A}_c) = K \\ &\quad R_{IFSC}^s(\mathbf{H}, d) \leq C_{sym}, \end{aligned} \quad (4.14)$$

where  $R_{IFSC}^s(\mathbf{H}, d)$  is given by (3.14) and  $\mathbf{F}_c$  is any matrix satisfying the decomposition  $\mathbf{F}_c^\dagger \mathbf{F}_c = (P^{-1} \mathbf{I} + \frac{1}{d+1} \mathbf{H}^\dagger \mathbf{H})^{-1}$ .

Furthermore, the performance can be enhanced by using asymmetric distortions for IFSC.

**Theorem 5.** The achievable symmetric rate for the IF C-RAN strategy with global CSIR, algebraic SIC decomposition and parallel channel decoding is

$$R_{IF-CRAN}(\mathbf{H}) = \max_{\mathbf{D}, \mathbf{A}_c \in \mathbb{Z}^{K \times K}} \min_{m \in \mathcal{K}} \frac{1}{2} \log^+ \left( \frac{P}{\|\mathbf{F}_c \mathbf{a}_{c,m}\|^2} \right)$$

$$\begin{aligned} \text{subject to} \quad & \text{Rank}(\mathbf{A}_c) = K \\ & R_{IFSC,\ell}^s(\mathbf{H}, \mathbf{D}) \leq C_{sym}, \forall \ell \in \mathcal{L} \end{aligned} \quad (4.15)$$

where  $R_{IFSC,\ell}^s(\mathbf{H}, \mathbf{D})$  is given by (3.19) and  $\mathbf{F}_c$  is any matrix satisfying the decomposition  $\mathbf{F}_c^\dagger \mathbf{F}_c = (P^{-1} \mathbf{I} + \mathbf{H}^\dagger (\mathbf{I} + \mathbf{D})^{-1} \mathbf{H})^{-1}$ .

It can be shown that the two optimization problems in (4.14) and (4.15) are non-convex problems. In the following section, we propose sub-optimal algorithms for choosing the integer matrices  $\mathbf{A}_s$ ,  $\mathbf{A}_c$  and the distortion levels  $\mathbf{D}$ .

**Theorem 6.** *The achievable symmetric rate for the IF C-RAN strategy with local CSIR, opportunistic IFSC and parallel IF channel decoding is*

$$\begin{aligned} R_{IF-CRAN}(\mathbf{H}) = \max_{d_t, \mathbf{A}_c \in \mathbb{Z}^{K \times K}} \quad & \min_{m \in \mathcal{K}} \frac{1}{2} \log^+ \left( \frac{P}{\|\mathbf{F}_c \mathbf{a}_{c,m}\|^2} \right) \\ \text{subject to} \quad & \mathbb{P}(R_{IFSC,op}^s(\mathbf{H}, d_t) > C_{sym}) \leq \rho_s \end{aligned} \quad (4.16)$$

where  $R_{IFSC,op}^s(\mathbf{H}, d_t)$  is given by (3.32),  $\mathbf{F}_c$  is any matrix satisfying the decomposition  $\mathbf{F}_c^\dagger \mathbf{F}_c = (P^{-1} \mathbf{I} + \mathbf{H}^\dagger (\mathbf{I} + \mathbf{D})^{-1} \mathbf{H})^{-1}$ ,  $\rho_s$  is the compression outage probability,  $\mathbf{D} = \text{diag}(d_t/\beta_1^2, \dots, d_t/\beta_L^2)$  and  $\beta_\ell$  is given by (3.31).

### 4.3.2 Optimization Algorithms

In this section, we propose algorithms that can be used to select the parameters of the IF-CRAN scheme proposed in Section 4.3.

#### IF-CRAN with Symmetric Distortion

The optimization problems in (4.14), (4.15) and (4.16) are challenging problems due to the integer constraints on  $\mathbf{A}_c$  and  $\mathbf{A}_s$ . For a fixed distortion matrix  $\mathbf{D}$  ( $d$  for the symmetric case), the problem of finding the optimal  $\mathbf{A}_s$  to meet the fronthaul constraint or finding the optimal integer matrix  $\mathbf{A}_c$  given  $\mathbf{A}_s$  to maximize the IF C-RAN symmetric rate are linked to the shortest vectors problem [Bremner, 2012].

For a fixed matrix  $\mathbf{A}_c$ , the overall rate in (4.14) is monotonically increasing in  $d$ . Using a bisection search, we can quickly converge to the smallest  $d$  that meets the fronthaul constraint (i.e.,  $R_{\text{IFSC}}(\mathbf{H}, d) = C_{\text{sym}}$ ). During each iteration in the search,  $\mathbf{A}_s$  can be optimized using an LLL reduction [Lenstra et al., 1982] on  $\mathbf{F}_s$ , which provides approximate guarantees. A detailed algorithm is given in Algorithm 1. Finally, an approximate solution for the integer matrix  $\mathbf{A}_c$  can be obtained using an LLL reduction on the basis  $\mathbf{F}_c$ .

---

**Algorithm 1** Symmetric IFSC

---

```

1: procedure SIFSC( $P, \mathbf{H}, C_{\text{sym}}, \text{tol}$ )
2:   Initialization: Set  $d_{\min} = 0$  and  $d_{\max} = d$  large enough such that  $R_{\text{IFSC}}(\mathbf{H}, d) < C_{\text{sym}}$ .
3:   while  $C_{\text{sym}} - R_{\text{IFSC}}(\mathbf{H}, d) > \text{tol}$  or  $R_{\text{IFSC}}(\mathbf{H}, d) > C_{\text{sym}}$  do
4:     if  $R_{\text{IFSC}}(\mathbf{H}, d) < C_{\text{sym}}$  then
5:        $d_{\max} = d/2$ .
6:     else
7:        $d_{\min} = d/2$ .
8:     end if
9:      $d = (d_{\min} + d_{\max})/2$ .
10:     $\mathbf{F}_s = \text{chol}((1 + \frac{1}{d})\mathbf{I} + \frac{1}{d}P\mathbf{H}\mathbf{H}^\dagger)$ 
11:     $\mathbf{A}_s = \text{LLL-reduction}(\mathbf{F}_s)$ .
12:     $R_{\text{IFSC}}(\mathbf{H}, d) = \frac{1}{2} \log^+(\|\mathbf{F}_s \mathbf{a}_{s,L}\|^2)$ 
13:  end while
14:  return  $d$ .
15: end procedure

```

---

**IF-CRAN with Asymmetric Distortion**

In the symmetric case, we were able to decouple the problem of choosing the distortion level  $d$  from the problem of choosing the integer matrix  $\mathbf{A}_c$ . However, in the case of asymmetric distortion levels in (4.15), the problems of distortion selection and integer matrix selection are more tightly coupled. In order to tackle this problem, we initially set all distortion levels to the symmetric value  $d$  such that  $R_{\text{IFSC},\ell}(\mathbf{H}, d\mathbf{I}) = C_{\text{sym}}$ , fix the integer matrix  $\mathbf{A}_s$ , then find the distortion levels  $d_1, \dots, d_L$  such that

$R_{\text{IFSC},\ell}(\mathbf{H}, \mathbf{D}) = C_{\text{sym}}, \forall \ell \in \mathcal{L}$ . With  $\mathbf{A}_s$  fixed, the last step is equivalent to solving  $L$  linear equations in  $\mathbf{D}$ .

Note that, for algebraic successive cancellation to work, we need the sub-matrices  $\mathbf{A}_{s,[1:m]}$  to be full-rank which can be achieved by permuting the BSs (i.e., columns of a full-rank matrix  $\mathbf{A}_s$ ). A detailed algorithm is given in Algorithm 2.

---

**Algorithm 2** Asymmetric IFSC

---

- 1: **procedure** AIFSC( $\mathbf{K}_{YY}, C_{\text{sym}}$ )
- 2:   Initialization: Fix  $d_\ell = d, \forall \ell$  and solve  $d = \text{SIFSC}(\mathbf{H}, C_{\text{sym}}, \text{tol})$ .
- 3:   Fix  $\mathbf{A}_s$  and find  $\pi_{\text{IF}} : \{1, \dots, L\} \rightarrow \{1, \dots, L\}$  s.t.  $\text{rank}(\mathbf{A}_{s,[1:m],\pi_{\text{IF}}([1:m])}) = m, \forall m = 1, \dots, L$ .
- 4:   Find distortion levels  $d_1, \dots, d_L$  that satisfies

$$\mathbf{C}[d_1 \cdots d_L]^\dagger = \mathbf{e} \quad (4.17)$$

where  $\mathbf{C} = 2^{C_{\text{sym}}} \times \mathbf{I} - \mathbf{A}_{s,\mathcal{L},\pi_{\text{IF}}(\mathcal{L})} \odot \mathbf{A}_{s,\mathcal{L},\pi_{\text{IF}}(\mathcal{L})}$  and  $e_\ell = \mathbf{a}_{s,\pi_{\text{IF}}(\ell)}^\dagger \mathbf{K}_{YY} \mathbf{a}_{s,\pi_{\text{IF}}(\ell)}, \forall \ell \in \mathcal{L}$ .

- 5:   **return**  $\mathbf{D} = \text{diag}(d_1, \dots, d_L)$ .
  - 6: **end procedure**
- 

**Remark 14.** *The asymmetric distortion levels obtained from Algorithm 2 are upper-bounded by the distortion level obtained from Algorithm 1. This is because the symmetric distortion  $d$  that satisfies  $R_{\text{IFSC}}(\mathbf{H}, d) = C_{\text{sym}}$  (i.e., Algorithm 2 result) also guarantees that  $R_{\text{IFSC},\ell}(\mathbf{H}, d\mathbf{I}) \leq C_{\text{sym}}, \forall \ell \in \mathcal{L}$ , since for both cases, the integer matrix  $\mathbf{A}_s$  is the same and in IFSC with parallel decoding, all rates are constrained by the combination with the largest variance. Second, decreasing one distortion level only increases the compression rate of the corresponding BS and simultaneously decreases the rate of the other BSs.*

## 4.4 IF Outage Upper Bound

As noted in [Zhan et al., 2014], for some channel realizations  $\mathbf{H}$ , the achievable rate of IF channel coding can be far from the MIMO capacity. However, [Domanovitz and

[Erez, 2018] quantifies the measure of such channels  $\mathbf{H}$  for the important special case of Gaussian fading (i.e.,  $\mathbf{H} \sim \mathcal{N}(\mathbf{0}, \mathbf{I})$ ). A similar story holds for IF source coding as shown in [Domanovitz and Erez, 2017]: for certain covariance matrices of the form  $P\mathbf{H}\mathbf{H}^\dagger + \mathbf{I}$ , the performance falls short of BT compression, but, for i.i.d. Gaussian  $\mathbf{H}$ , the measure of such “difficult” channels can be bounded. Here, we combine ideas from the proofs in [Domanovitz and Erez, 2018, Domanovitz and Erez, 2017] to bound the measure of channels for which our IF-CRAN scheme falls significantly below the uplink C-RAN capacity.

To this end, we apply Theorem 1 to find that, using the eigenvalue decomposition  $\mathbf{U}\mathbf{S}_2\mathbf{U}^\dagger = \frac{P}{d+1}\mathbf{H}^\dagger\mathbf{H} + \mathbf{I}$ , the IF rate in (4.14) can be bounded by

$$\begin{aligned} R_{\text{IF-CRAN}}(\mathbf{H}) &= -\frac{1}{2} \log \left( \lambda_K^2 \left( \mathbf{S}_2^{-\frac{1}{2}} \mathbf{U}^\dagger \right) \right) \geq \frac{1}{2} \log \left( \frac{\lambda_1^2 \left( \mathbf{S}_2^{\frac{1}{2}} \mathbf{U}^\dagger \right)}{K^2} \right) \\ &= \frac{1}{2} \log \left( \min_{\mathbf{a} \in \mathbb{Z}^K: \mathbf{a} \neq \mathbf{0}} \frac{\|\mathbf{S}_2^{\frac{1}{2}} \mathbf{U}^\dagger \mathbf{a}\|^2}{K^2} \right). \end{aligned} \quad (4.18)$$

We now recall a result from [Domanovitz and Erez, 2018] that provides a bound on the outage probability for integer-forcing over i.i.d. Gaussian fading. We make a slight modification to the original proof by using the Banaszczyk transference theorem from Theorem 1 to exchange  $\alpha(K)$  in [Domanovitz and Erez, 2018, Equation 36] with  $K^2$ , which yields the following theorem, whose form is more convenient for our analysis.

**Theorem 7** ([Domanovitz and Erez, 2018, Theorem 1]). *For the Gaussian MAC (i.e.,  $C_{\text{sym}} = \infty$  and  $d = 0$ ), we have*

$$\mathbb{P} \left( \min_{\mathbf{a} \in \mathbb{Z}^K: \mathbf{a} \neq \mathbf{0}} \|\mathbf{S}_1^{\frac{1}{2}} \mathbf{U}^\dagger \mathbf{a}\|^2 < 2^{\frac{2(C - \Delta C_{\text{MAC}})}{K}} K^2 \right) \leq \gamma(K) 2^{-\Delta C_{\text{MAC}}} \quad (4.19)$$

where  $\Delta C_{\text{MAC}} > 0$  is some constant, the orthogonal matrix  $\mathbf{U}$  and the diagonal matrix  $\mathbf{S}_1$  comes from the eigenvalue decomposition  $\mathbf{U}\mathbf{S}_1\mathbf{U}^\dagger = P\mathbf{H}^\dagger\mathbf{H} + \mathbf{I}$ ,  $C = \frac{1}{2} \log |\mathbf{S}_1|$  is the MAC capacity and  $\gamma(K)$  is defined in [Domanovitz and Erez, 2018, Equation (59)]

as  $c(K)$  with replacing  $\alpha(K)$  by  $K^2$ .

Let us define the probability that the difference between the IF C-RAN achievable rate and a cut-set bound on the sum capacity is larger than some positive constant  $\Delta C$  as

$$P_{\text{diff}}(\Delta C) \triangleq \mathbb{P}(KR_{\text{IF-CRAN}}(\mathbf{H}) < C_{\text{upper}}(\mathbf{H}) - \Delta C)$$

where  $\Delta C > 0$  is some constant and  $C_{\text{upper}}(\mathbf{H}) \triangleq \min\{LC_{\text{sym}}, \frac{1}{2} \log(|P\mathbf{H}^{\dagger}\mathbf{H} + \mathbf{I}|)\}$  is a cut-set bound for the sum capacity and the probability is taken with respect to  $\mathbf{H} \sim \mathcal{N}(\mathbf{0}, \mathbf{I})$ .

**Theorem 8.** *For the uplink C-RAN channel with i.i.d. Gaussian fading,  $\mathbf{H} \sim \mathcal{N}(\mathbf{0}, \mathbf{I})$ , the probability that the integer-forcing C-RAN strategy with global CSIR, parallel decompression, and parallel channel decoding cannot operate within  $\Delta C$  of the sum-capacity is upper bounded as follows:*

$$P_{\text{diff}}(\Delta C) \leq \gamma(\max\{K, L\}) 2^{-\Delta C/3} \quad (4.20)$$

where  $\gamma(\max\{K, L\})$  is defined in [Domanovitz and Erez, 2017, Equation (45)] as  $c(\max\{K, L\})$  and only depends on  $\max\{K, L\}$ .

*Proof.* The proof closely follows that of [Domanovitz and Erez, 2018, Theorem 1]. We start by bounding  $P_{\text{diff}}(\Delta C)$  as

$$\begin{aligned} P_{\text{diff}}(\Delta C) &= \mathbb{P}(KR_{\text{IF-CRAN}}(\mathbf{H}) < C_{\text{upper}}(\mathbf{H}) - \Delta C | \mathcal{A}) P(\mathcal{A}) \\ &\quad + \mathbb{P}(KR_{\text{IF-CRAN}}(\mathbf{H}) < C_{\text{upper}}(\mathbf{H}) - \Delta C | \mathcal{A}^c) P(\mathcal{A}^c) \\ &\leq \underbrace{\mathbb{P}(KR_{\text{IF-CRAN}}(\mathbf{H}) < C_{\text{upper}}(\mathbf{H}) - \Delta C | \mathcal{A})}_{(i)} + \underbrace{\mathbb{P}(\mathcal{A}^c)}_{(ii)}. \end{aligned} \quad (4.21)$$

where  $\mathcal{A} \triangleq \{R_{\text{IFSC}}^s(\mathbf{H}, d^*) < R_{\text{BT}}^s(\mathbf{H}, d^*) + \Delta R\}$  is the event that the IFSC rate is within a constant  $\Delta R > 0$  (to be chosen later) from the BT compression rate and  $d^* > 0$  is the distortion that saturates the fronthaul rate constraint  $R_{\text{IFSC}}^s(\mathbf{H}, d^*) = C_{\text{sym}}$ . For the rest of the proof, we will omit  $d^*$  from  $R_{\text{IFSC}}^s(\mathbf{H}, d^*)$  and  $R_{\text{BT}}^s(\mathbf{H}, d^*)$  for the sake of conciseness.

In order for the end-to-end IF scheme to work correctly, we need both the IF

source coding part to work (i.e., to be able to recover the BSs observations correctly) and the IF channel coding part to work (i.e., to be able to recover the users' messages correctly). Consequently, one interpretation to this bound is that (ii) measures the probability that the IFSC rate  $R_{\text{IFSC}}^s(\mathbf{H})$  is not within a constant  $\Delta R$  from the BT rate  $R_{\text{BT}}^s(\mathbf{H})$  (i.e., the source coding part is the bottleneck), while (i) measures the probability that the IFCC rate  $KR_{\text{IF-CRAN}}(\mathbf{H})$  is not within a constant  $\Delta C$  from the cut-set bound  $C_{\text{upper}}(\mathbf{H})$ , given that the IFSC rate is within a constant  $\Delta R$  from the BT rate (i.e., the channel coding part is the bottleneck). For the rest of the proof, we will eliminate  $d^*$  from  $R_{\text{IFSC}}^s(\mathbf{H}, d^*)$  and  $R_{\text{BT}}^s(\mathbf{H}, d^*)$  for clarity and try to bound both (i) and (ii).

Using [Domanovitz and Erez, 2017, Theorem 1], we immediately have the upper bound (ii)  $\leq \gamma(L)2^{-\Delta R}$  where  $\gamma(L)$  is defined in [Domanovitz and Erez, 2017, Equation (45)]. Next, in order to bound (i), we use (4.18) to get

$$\begin{aligned} (i) &\leq \mathbb{P}_{\mathbf{U}, \mathbf{S}_1} \left( \min_{\mathbf{a}} \|\mathbf{S}_2^{1/2} \mathbf{U}^\dagger \mathbf{a}\|^2 < K^2 2^{2(C_{\text{upper}}(\mathbf{H}) - \Delta C)/K} \mid \mathcal{A} \right) \\ &= \mathbb{P}_{\mathbf{S}_1} \left[ \mathbb{P}_{\mathbf{U} \mid \mathbf{S}_1} \left( \min_{\mathbf{a}} \|\mathbf{S}_2^{1/2} \mathbf{U}^\dagger \mathbf{a}\|^2 < K^2 2^{-2\Delta C/K} \min\{|\mathbf{S}_1|^{1/K}, 2^{2LC_{\text{sym}}/K}\} \mid \mathcal{A} \right) \right] \end{aligned} \quad (4.22)$$

where the minimization is over all non-zero integer vectors  $\mathbf{a} \in \mathbb{Z}^K \setminus \{\mathbf{0}\}$  and  $\mathbf{U}$ ,  $\mathbf{S}_1$  and  $\mathbf{S}_2$  come from the eigenvalue decompositions  $\mathbf{U}\mathbf{S}_1\mathbf{U}^\dagger = P\mathbf{H}^\dagger\mathbf{H} + \mathbf{I}$  and  $\mathbf{U}\mathbf{S}_2\mathbf{U}^\dagger = \frac{P}{d^*+1}\mathbf{H}^\dagger\mathbf{H} + \mathbf{I}$ .

We now proceed to bound the inner probability in (4.22) for any value of  $\mathbf{S}_1$ .

$$\begin{aligned} &\mathbb{P}_{\mathbf{U} \mid \mathbf{S}_1} \left( \min_{\mathbf{a}} \|\mathbf{S}_2^{1/2} \mathbf{U}^\dagger \mathbf{a}\|^2 < K^2 2^{-2\Delta C/K} \min\{|\mathbf{S}_1|^{1/K}, 2^{2LC_{\text{sym}}/K}\} \mid \mathcal{A} \right) \\ &\stackrel{(a)}{=} \mathbb{P}_{\mathbf{U} \mid \mathbf{S}_1} \left( \min_{\mathbf{a}} \|\tilde{\mathbf{S}}_2^{1/2} \mathbf{U}^\dagger \mathbf{a}\|^2 < K^2 2^{-2\Delta C/K} \min \left\{ \left( \frac{|\mathbf{S}_1|}{|\mathbf{S}_2|} \right)^{1/K}, \frac{2^{2LC_{\text{sym}}/K}}{|\mathbf{S}_2|^{1/K}} \right\} \mid \mathcal{A} \right) \\ &\stackrel{(b)}{\leq} \mathbb{P}_{\mathbf{U} \mid \mathbf{S}_1} \left( \min_{\mathbf{a}} \|\tilde{\mathbf{S}}_2^{1/2} \mathbf{U}^\dagger \mathbf{a}\|^2 < K^2 2^{-\frac{2\Delta C}{K}} \min \left\{ (d^* + 1)^{\frac{L}{K}}, \frac{2^{\frac{2LC_{\text{sym}}}{K}}}{2^{\frac{2R_{\text{BT}}^s(\mathbf{H})}{K}}} \left( \frac{d^* + 1}{d^*} \right)^{\frac{L}{K}} \right\} \mid \mathcal{A} \right) \\ &\stackrel{(c)}{\leq} \mathbb{P}_{\mathbf{U} \mid \mathbf{S}_1} \left( \min_{\mathbf{a}} \|\tilde{\mathbf{S}}_2^{1/2} \mathbf{U}^\dagger \mathbf{a}\|^2 < K^2 2^{-\frac{2\Delta C}{K}} \min \left\{ (d^* + 1)^{\frac{L}{K}}, 2^{\frac{2\Delta R}{K}} \left( \frac{d^* + 1}{d^*} \right)^{\frac{L}{K}} \right\} \mid \mathcal{A} \right) \end{aligned} \quad (4.23)$$

where (a) holds from  $\tilde{\mathbf{S}}_2 \triangleq \frac{\mathbf{S}_2}{|\mathbf{S}_2|^{1/K}}$ , (b) holds from  $|\mathbf{S}_2| = |\frac{1}{d^*+1}(\mathbf{S}_1 + d^*\mathbf{I})| > |\frac{1}{d^*+1}\mathbf{S}_1|$

and  $R_{\text{BT}}^s(\mathbf{H}) = \frac{1}{2} \log \left| \frac{1}{d^*} \mathbf{K}_{YY} + \mathbf{I} \right| = \frac{1}{2} \log \left| \frac{d^*+1}{d^*} \mathbf{S}_2 \right|$  and (c) holds from  $R_{\text{BT}}^s(\mathbf{H}) \geq R_{\text{IFSC}}^s(\mathbf{H}) - \Delta R = LC_{\text{sym}} - \Delta R$  given  $\mathcal{A}$ .

Next, we partition the space of possible values of  $\mathbf{S}_1$  into  $\mathcal{B}$  and  $\mathcal{B}^c$ , where  $\mathcal{B} \triangleq \left\{ \frac{1}{2} \log |\mathbf{S}_1| > LC_{\text{sym}} - L/2 - \Delta R \right\}$  and bound  $d^*$  depending on the event  $\mathcal{B}$  as in Lemma 29 in Appendix C. Using (4.23), we can upper bound (i) by

$$\begin{aligned}
& \mathbb{P}_{\mathbf{S}_1} \left[ \mathbb{P}_{\mathbf{U}|\mathbf{S}_1} \left( \min_{\mathbf{a}} \|\tilde{\mathbf{S}}_2^{1/2} \mathbf{U}^\dagger \mathbf{a}\|^2 < K^2 2^{-2(\Delta C - \Delta R)/K} \left( \frac{d^*+1}{d^*} \right)^{L/K} \middle| \mathcal{A}, \mathcal{B} \right) \mathbf{1}_{\mathcal{B}} \right] \\
& + \mathbb{P}_{\mathbf{S}_1} \left[ \mathbb{P}_{\mathbf{U}|\mathbf{S}_1} \left( \min_{\mathbf{a}} \|\tilde{\mathbf{S}}_2^{1/2} \mathbf{U}^\dagger \mathbf{a}\|^2 < K^2 2^{-2\Delta C/K} (d^*+1)^{L/K} \middle| \mathcal{A}, \mathcal{B}^c \right) \mathbf{1}_{\mathcal{B}^c} \right] \\
& \stackrel{(a)}{\leq} \mathbb{P}_{\mathbf{S}_1} \left[ \mathbb{P}_{\mathbf{U}|\mathbf{S}_1} \left( \min_{\mathbf{a}} \|\tilde{\mathbf{S}}_2^{1/2} \mathbf{U}^\dagger \mathbf{a}\|^2 < K^2 2^{-2(\Delta C - \Delta R)/K} 2^{2(\Delta R + L)/K} \middle| \mathcal{A}, \mathcal{B} \right) \mathbf{1}_{\mathcal{B}} \right] \\
& + \mathbb{P}_{\mathbf{S}_1} \left[ \mathbb{P}_{\mathbf{U}|\mathbf{S}_1} \left( \min_{\mathbf{a}} \|\tilde{\mathbf{S}}_2^{1/2} \mathbf{U}^\dagger \mathbf{a}\|^2 < K^2 2^{-2\Delta C/K} 2^{L/K} \middle| \mathcal{A}, \mathcal{B}^c \right) \mathbf{1}_{\mathcal{B}^c} \right] \\
& \stackrel{(b)}{\leq} \gamma(K) 2^{-(\Delta C - 2\Delta R)} 2^L + \gamma(K) 2^{-(\Delta C)} 2^{L/2}
\end{aligned} \tag{4.24}$$

where  $\mathbf{1}$  is the indicator function, (a) holds from Lemma 29 in Appendix C and (b) holds from Theorem 7 by substituting  $\Delta C_{\text{MAC}} = \Delta C - 2\Delta R - L$  and  $\Delta C_{\text{MAC}} = \Delta C - L/2$ , respectively.

The rest of the proof follows by combining (i) and (ii) and taking  $\Delta R = \frac{\Delta C}{3}$  so that the exponential terms in (ii) and (4.24) are  $\frac{\Delta C}{3}$ .  $\square$

For a fixed sum rate  $R$ , define the optimal outage probability as  $p_{\text{optimal}}(R) \triangleq \mathbb{P}(C(\mathbf{H}) < R)$ , where  $C(\mathbf{H})$  is the sum capacity of the uplink C-RAN channel.

**Theorem 9.** *For a positive constant  $\Delta C$ , the outage probability for the integer-forcing C-RAN strategy with global CSIR, parallel decompression, and parallel channel decoding is bounded by*

$$p_{\text{IF-CRAN}}(R - \Delta C) \leq p_{\text{optimal}}(R) + \gamma(\max\{K, L\}) 2^{-\Delta C/3}. \tag{4.25}$$

*Proof.* Using the law of total probability, the IF-CRAN outage probability can be written as

$$p_{\text{IF-CRAN}}(R - \Delta C) = \mathbb{P}(\{KR_{\text{IF-CRAN}} \leq R - \Delta C\} \cap \{C(\mathbf{H}) \geq R\})$$

$$\begin{aligned}
& + \mathbb{P} (KR_{\text{IF-CRAN}} \leq R - \Delta C | C(\mathbf{H}) < R) \mathbb{P} (C(\mathbf{H}) < R) \\
& \leq \mathbb{P} (KR_{\text{IF-CRAN}} \leq C(\mathbf{H}) - \Delta C) + \mathbb{P} (C(\mathbf{H}) < R) \\
& \leq \mathbb{P} (KR_{\text{IF-CRAN}} \leq C_{\text{upper}}(\mathbf{H}) - \Delta C) + \mathbb{P} (C(\mathbf{H}) < R) \\
& \leq \gamma(\max\{K, L\}) 2^{-\Delta C/3} + p_{\text{optimal}}(R) \tag{4.26}
\end{aligned}$$

where  $C_{\text{upper}}(\mathbf{H}) \triangleq \min \{LC_{\text{sym}}, \frac{1}{2} \log |P\mathbf{H}^{\dagger}\mathbf{H} + \mathbf{I}|\}$  is a cut-set bound on the sum capacity of the uplink C-RAN channel and we used Theorem 8 in the last step.  $\square$

## 4.5 Numerical Results

For our simulations, we generated 1000 realizations for the channel matrix  $\mathbf{H}$ , each elementwise i.i.d.  $\mathcal{N}(0, 1)$ . Since joint decoding and joint decompression recently proved to achieve the capacity within a constant gap [Ganguly and Kim, 2017], we plot Berger-Tung (BT) compression with symmetric distortion and joint maximum likelihood (ML) decoding as a benchmark.

In general, we expect the advantage conferred by IF channel coding to be more pronounced when  $K > L$  (i.e., higher interference), while that of IF source coding ought to be more pronounced when  $K < L$  (i.e., higher correlation). This is because when the number of users is larger than the number of BSs (i.e.,  $K > L$ ), conventional linear receivers (e.g., ZF and MMSE) fail to achieve the optimal degrees of freedom, while the IF receiver does. On the other hand, when the number of BSs is larger than the number of users (i.e.,  $K < L$ ), exploiting the correlation between the BSs' observations using IF source coding becomes more important.

### 4.5.1 Global CSIR

We start by assuming global CSIR and fixing  $\text{SNR} = 25$  dB. Fig. 4.3 and 4.4 show the symmetric outage rates versus the fronthaul rate  $C_{\text{sym}}$  for outage probability  $\rho = 0.05$  and  $\rho = 0.02$  and for the case when  $K > L$  and  $K < L$ , respectively.

The performance of asymmetric integer-forcing source coding (AIFSC) compres-

sion with integer-forcing channel coding (IFCC) decoding, IFSC with IFCC decoding and optimized<sup>3</sup> Wyner-Ziv compression (WZC) with MMSE successive interference cancellation (MMSE-SIC) decoding are plotted. In Fig 4-4, we also plot the performance of the WZC with heuristic decompression order (heuristic WZC), single-user compression (SUC) and parallel MMSE decoding without SIC. We note that the difference between heuristic WZC and optimal WZC can be large at limited fronthaul rate constraint  $C_{\text{sym}}$ .

Since the asymmetric distortion levels in Algorithm 2 are bounded below by the symmetric distortion level in Algorithm 1, we see in both figures that the performance of AIFSC compression with IFCC decoding is bounded below by the performance of IFSC compression with IFCC decoding. Notice that the IF strategies outperforms conventional schemes in the high fronthaul capacity regime. This is expected, since as  $C_{\text{sym}}$  increases, the C-RAN converges to a MAC, where IFCC is already known to outperforms conventional linear decoders [Zhan et al., 2014]. More importantly, the IF strategy (e.g., IFSC with IFCC and AIFSC with IFCC) still performs close to WZ compression with MMSE decoding in low and moderate fronthaul capacity regimes while retaining the advantage of its lower implementation complexity. It is worth noting that IFSC, IFCC and MMSE only use parallel single-user decoding while AIFSC, WZC and MMSE-SIC uses sequential decoding.

For the global CSIR scenario, we find the IF strategies are competitive with optimized Wyner-Ziv successive strategies coupled with successive MMSE decoding, however IF strategies can be implemented using parallel single-user decoders.

#### 4.5.2 Local CSIR

Regarding local CSIR, where each BS only knows the channel gains to itself, Fig. 4-5 and Fig. 4-6 compare the performance of local IFSC compression with IFCC decoding

---

<sup>3</sup>with an optimized decompression order

and opportunistic IFSC with IFCC decoding to conventional (parallel and successive) compression and decoding schemes when  $K < L$ . At high SNR or  $C_{\text{sym}}$  regimes, the performance can be ordered from the highest symmetric rate to the lowest as follows: opportunistic IFSC with IFCC, then local IFSC with IFCC, SUC with MMSE-SIC then WZC with MMSE-SIC. The poor performance for WZC (even compared to SUC) is due to the challenge to choose asymmetric distortion levels to achieve a certain outage probability which left us with assuming symmetric distortion levels for WZC. Since local IFSC can be considered a special case of opportunistic IFSC where we do not recover any BS's observation before forming the integer-linear combinations, we can see that its performance is always bounded above by the performance of opportunistic IFSC.

Fig. 4.7 and Fig. 4.8 show the same strategies when  $K > L$  and  $\rho = 0.1$ . In this case, the advantage of IF schemes over the conventional schemes are more noticeable. The poor performance of local IFSC at small fronthaul capacity relative to the opportunistic IFSC and SUC that we see in Fig. 4.5 and Fig. 4.7 can be attributed to the fact that asymmetric distortion schemes better utilize the fronthaul links at small fronthaul capacity.

Finally, Fig. 4.9 and Fig. 4.10 show the same strategies for a square channel matrix  $\mathbf{H}$  (i.e.,  $K = L$ ). Opportunistic IFSC with IFCC has the best performance almost through all SNR and  $C_{\text{sym}}$  values. Furthermore, the more pronounced difference between the opportunistic IFSC and local IFSC emphasizes the advantage of eliminating some outage events at some BSs.

Overall, we find compression strategies with asymmetric distortion levels (e.g., opportunistic IFSC and SUC for local CSIR and asymmetric IFSC and WZC for global CSIR) have advantages in limited fronthaul rate constraint or high SNR regimes.

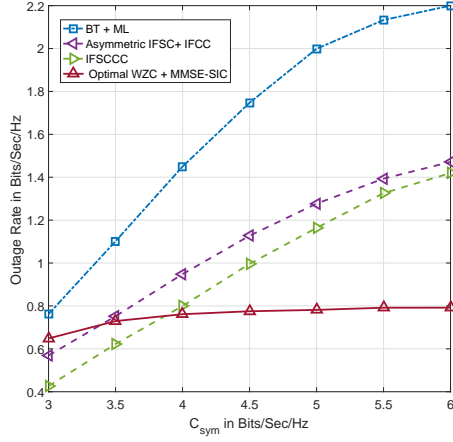


**Figure 4-3:** 5% outage rate for global CSIR with  $K = 6$ ,  $L = 3$  and  $SNR = 25$  dB.

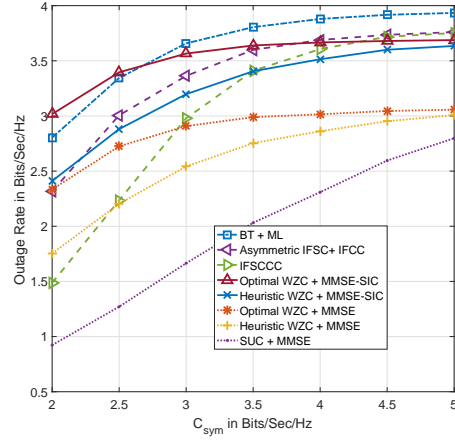


**Figure 4-4:** 2% outage rate for global CSIR with  $K = 3$ ,  $L = 6$  and  $SNR = 25$  dB.

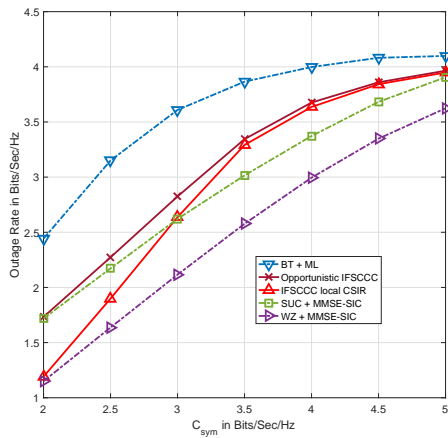


**Figure 4-5:** 10% outage rate for local CSIR Scenario with  $K = 3$ ,  $L = 6$  and  $SNR = 25$  dB.

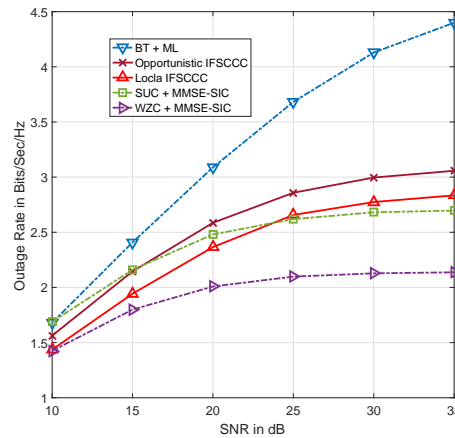


**Figure 4-6:** 10% outage rate for local CSIR Scenario with  $K = 3$ ,  $L = 6$  and  $C = 3$  bits/sec/Hz.

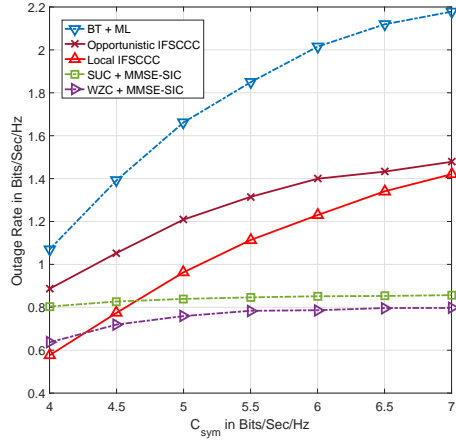


**Figure 4-7:** 10% outage rate for local CSIR Scenario with  $K = 6$ ,  $L = 3$  and  $SNR = 25$  dB.

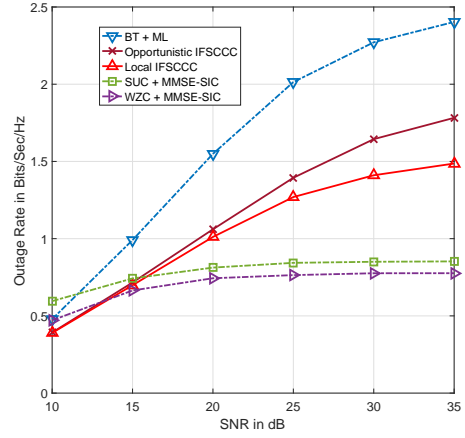


**Figure 4-8:** 10% outage rate for local CSIR Scenario with  $K = 6$ ,  $L = 3$  and  $C = 6$  bits/sec/Hz.

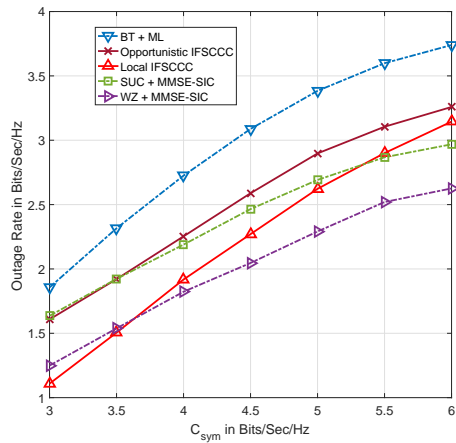


**Figure 4-9:** 10% outage rate for local CSIR Scenario with  $K = L = 6$  and  $SNR = 25$  dB.

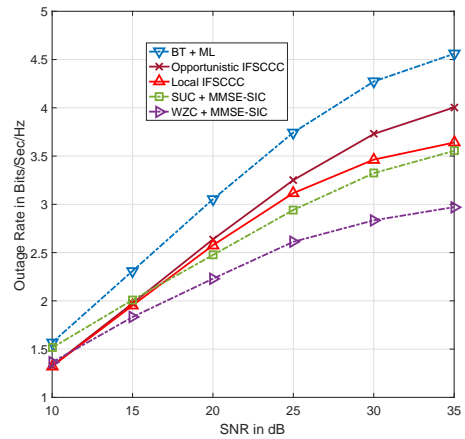


**Figure 4-10:** 10% outage rate for local CSIR Scenario with  $K = L = 6$  and  $C = 6$  bits/sec/Hz.

## Chapter 5

# Distributed Lossy Decompression

### 5.1 Problem Formulation

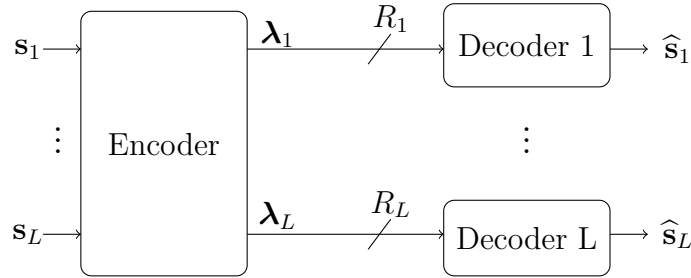


**Figure 5.1:** The distributed decompression problem.

Consider the distributed decompression problem in Fig. 5.1, where we have a single encoder with  $T$  i.i.d. realizations of  $L$  sources  $\mathbf{s}(1), \dots, \mathbf{s}(T)$  distributed according to a Gaussian distribution with zero-mean and a covariance matrix  $\mathbf{K}_{SS}$  and  $L$  decoders. The  $m^{\text{th}}$  decoder is interested in the  $m^{\text{th}}$  source vector  $\mathbf{s}_m \triangleq [s_m(1) \cdots s_m(T)]^\dagger$ . The encoder has a function  $\mathcal{E} : \mathbb{R}^T \times \cdots \times \mathbb{R}^T \rightarrow \{1, \dots, 2^{TR_1}\} \times \cdots \times \{1, \dots, 2^{TR_L}\}$  that maps  $(\mathbf{s}_1, \dots, \mathbf{s}_L)$  to indices  $(i_1, \dots, i_L) \triangleq \mathcal{E}(\mathbf{s}_1, \dots, \mathbf{s}_L)$  with rate tuple  $(R_1, \dots, R_L)$ . The  $m^{\text{th}}$  decoder has access only to the  $m^{\text{th}}$  index  $i_m$  upon which it uses a function  $\mathcal{D}_m : \{1, \dots, 2^{TR_m}\} \rightarrow \mathbb{R}^T$  to recover  $\hat{\mathbf{s}}_m = \mathcal{D}_m(i_m)$ . Since the rate  $R_m$  is finite, we can write the  $m^{\text{th}}$  reconstruction as  $\hat{\mathbf{s}}_m \triangleq \mathbf{s}_m + \tilde{\mathbf{q}}_m$  where  $\tilde{\mathbf{q}}_m$  is a quantization noise<sup>1</sup>. The quantization noise  $\tilde{\mathbf{Q}} \triangleq [\tilde{\mathbf{q}}_1 \cdots \tilde{\mathbf{q}}_L]^\dagger$  is characterized by its effective covariance

<sup>1</sup>We assume here unbiased estimates  $\hat{\mathbf{s}}_m$  for  $\mathbf{s}_m$ , hence zero-mean quantization noise  $\tilde{\mathbf{q}}_m$ .

matrix

$$\frac{1}{T}\mathbb{E}[\tilde{\mathbf{Q}}\tilde{\mathbf{Q}}^\dagger].$$

Suppose, for reasons to be clear later, that we are interested in recovering  $\hat{\mathbf{s}}_1, \dots, \hat{\mathbf{s}}_L$  with a desired effective covariance matrix  $\mathbf{\Omega}$  for the quantization noise. The rates  $R_\ell(\mathbf{K}_{SS}, \mathbf{\Omega})$  for  $\ell \in \mathcal{L}$  are said to be achievable if for any  $\epsilon > 0$  and  $T$  large enough, there exists mappings  $\mathcal{E}$  and  $\mathcal{D}_m$ ,  $m = 1, \dots, L$ , such that

$$\frac{1}{T}\mathbb{E}\left[\sum_{t=1}^T \tilde{q}_{i,t}\tilde{q}_{j,t}\right] \leq \Omega_{i,j} + \epsilon, \quad \forall i, j \in \mathcal{L}.$$

This desired correlation  $\mathbf{\Omega}$  can be useful in some applications like the downlink C-RAN, which we will see in Chapter 6, where introducing correlation between quantization noise across different BSs helps reducing the effective variance of the quantization noise when combined at the receivers [Park et al., 2013].

## 5.2 Conventional Compression Schemes

### 5.2.1 Single-User Compression

The simplest scheme is to use  $L$  parallel single-user encoders to quantize each source independently (i.e.,  $i_\ell$  only depends on  $\mathbf{s}_\ell$ ). This implies that the quantization noise at different decoders is uncorrelated and we end up with a diagonal covariance matrix  $\mathbf{\Omega}$ . Under i.i.d. Gaussian codebooks, the following rates are achievable.

**Lemma 13.** *For a given source covariance matrix  $\mathbf{K}_{SS}$  and a target diagonal quantization covariance matrix  $\mathbf{\Omega} = \text{diag}(\Omega_{1,1}, \dots, \Omega_{L,L})$ , the achievable rates for the SU compression are*

$$R_{SU,\ell} = \frac{1}{2} \log \left( \frac{K_{SS,\ell,\ell} + \Omega_{\ell,\ell}}{\Omega_{\ell,\ell}} \right), \quad \forall \ell \in \mathcal{L}, \quad (5.1)$$

where  $K_{SS,\ell,\ell}$  is the  $(\ell, \ell)^{\text{th}}$  element of  $\mathbf{K}_{SS}$  (i.e., the variance of the  $\ell^{\text{th}}$  source) and  $\Omega_{\ell,\ell}$  is the  $(\ell, \ell)^{\text{th}}$  element of  $\mathbf{\Omega}$  (i.e., the  $\ell^{\text{th}}$  distortion level).

**Remark 15.** *Under fixed rates, single-user encoding minimizes the sum of the achievable distortions  $\sum_{\ell=1}^L \Omega_{\ell,\ell}$ . However, the quantization noise is uncorrelated (i.e., diagonal  $\mathbf{\Omega}$ ).*

### 5.2.2 Multivariate Compression

The idea behind multivariate compression is to apply a joint typicality encoder that searches for the indices  $i_1, \dots, i_L \in \{1, \dots, 2^{TR_1}\} \times \dots \times \{1, \dots, 2^{TR_L}\}$  such that the corresponding reconstructions  $\hat{\mathbf{s}}_1, \dots, \hat{\mathbf{s}}_L$  at the decoders are jointly typical with the source vectors  $\mathbf{s}_1, \dots, \mathbf{s}_L$  according to a distribution (i.e., Gaussian test channel) with the desired covariance matrix  $\mathbf{\Omega}$ .

**Lemma 14.** *[Park et al., 2013, Lemma 2] For a target covariance matrix  $\mathbf{\Omega}$ , the achievable rate region for the multivariate compression is given by any rate tuple  $(R_{MV,1}, \dots, R_{MV,L})$  that satisfies*

$$\sum_{i \in \mathcal{T}} \frac{1}{2} \log(K_{SS,i,i} + \Omega_{i,i}) - \frac{1}{2} \log |\mathbf{\Omega}_{\mathcal{T},\mathcal{T}}| \leq \sum_{i \in \mathcal{T}} R_{MV,i}, \quad \forall \mathcal{T} \subseteq \{1, \dots, L\}, \quad (5.2)$$

where  $K_{SS,i,i}$  is the  $(i, i)^{th}$  element of  $\mathbf{K}_{SS}$  and  $\Omega_{i,i}$  is the  $(i, i)^{th}$  element of  $\mathbf{\Omega}$ .

**Remark 16.** *The achievable rates in Lemma 14, can also be obtained using analog successive compression (i.e., successive single-user encoders) which has smaller implementation complexity.*

## 5.3 The Reverse Integer-Forcing Source Coding

Now, we introduce a simple, yet effective, scheme to create correlations between the quantization noise  $\mathbf{q}_1, \dots, \mathbf{q}_L$  without using neither joint typicality encoding nor a successive compression. We call this scheme reverse integer-forcing source coding (RIFSC), since it mimics IFSC as proposed for distributed lossy compression in Chapter 3. However, instead of recovering integer-linear combinations of the sources, we

create correlation between the quantization noise by forming integer-linear combinations of the quantizers' outputs. We also extend our results to include an algebraic successive cancellation strategy, which can attain a larger class of covariance matrices.

### 5.3.1 Parallel Reverse Integer-Forcing Source Coding

The basic idea behind the RIFSC is to use nested lattice codebooks to quantize the source vectors, then form integer-linear combinations of the quantizers' outputs. These integer-linear combinations are still valid codewords, due to the closure property of lattice codebooks. Furthermore, since the  $m^{\text{th}}$  decoder is interested in recovering the  $m^{\text{th}}$  source  $\mathbf{s}_m$  and not in an integer-linear combinations of  $\mathbf{s}_1, \dots, \mathbf{s}_L$ , we need to pre-invert the sources in the analog domain before quantization.

Let  $\mathbf{A} \in \mathbb{Z}^{L \times L}$  be a full-rank integer matrix containing the coefficients of the integer-linear combinations. Furthermore, define a permutation  $\pi_C$  such that

$$K_{SS, \pi_C(1), \pi_C(1)} + d \|\mathbf{a}_{\pi_C(1)}\|^2 \leq \dots \leq K_{SS, \pi_C(L), \pi_C(L)} + d \|\mathbf{a}_{\pi_C(L)}\|^2$$

where  $d > 0$  is the target distortion level and  $\mathbf{a}_\ell$  is the  $\ell^{\text{th}}$  row of the matrix  $\mathbf{A}$ .

#### Codebook

Select nested lattices  $\Lambda_{C, \pi_C(L)} \subseteq \dots \subseteq \Lambda_{C, \pi_C(1)} \subseteq \Lambda_F$  using Lemma 2 with parameters  $\theta_F = d$ , where  $d$  is the symmetric distortion and  $\theta_{C,L} \leq \dots \leq \theta_{C,1}$ , to be chosen later. Each nested lattice pair  $\Lambda_{C, \ell} \subseteq \Lambda_F$  forms a lattice codebook  $\mathcal{C}_\ell \triangleq \Lambda_F \cap \mathcal{V}(\Lambda_{C, \ell})$  with rate  $R_\ell = \frac{1}{2} \log \left( \frac{\theta_{C, \ell}}{\theta_F} \right)$ .

## Compression

First, the encoder pre-inverts the full-rank integer matrix  $\mathbf{A}$  and uses it to obtain the combinations

$$\mathbf{V} = \mathbf{A}^{-1}\mathbf{S} \quad (5.3)$$

where  $\mathbf{V} \triangleq [\mathbf{v}_1 \cdots \mathbf{v}_L]^\dagger$  and  $\mathbf{S} \triangleq [\mathbf{s}_1 \cdots \mathbf{s}_L]^\dagger$ .

Second, the encoder adds random dither matrix  $\mathbf{U} \triangleq [\mathbf{u}_1 \cdots \mathbf{u}_L]^\dagger$  to  $\mathbf{V}$ , where  $\mathbf{u}_1, \dots, \mathbf{u}_L$  are independent dithers uniformly distributed over  $\mathcal{V}(\Lambda_F)$ , then quantizes the result to obtain

$$\Phi = \mathcal{Q}_{\Lambda_F}(\mathbf{V} + \mathbf{U}) \quad (5.4)$$

where the quantizer  $\mathcal{Q}_{\Lambda_F}$  operates on each row separately.

Next, the encoder forms the integer-linear combinations  $\mathbf{T} = \mathbf{A}\Phi$  and applies  $\text{mod } \Lambda_{C,m}$  to the  $m^{\text{th}}$  row of  $\mathbf{T}$  (i.e.,  $\mathbf{t}_m$ ) to obtain the lattice codewords

$$\boldsymbol{\lambda}_m = [\mathbf{t}_m] \text{ mod } \Lambda_{C,m}, \quad m = 1, \dots, L. \quad (5.5)$$

Finally, the index  $i_m \in \{1, \dots, 2^{TR_m}\}$  of  $\boldsymbol{\lambda}_m \in \mathcal{C}_m$  is forwarded to the  $m^{\text{th}}$  decoder.

## Decompression

Upon receiving  $i_m$ , the  $m^{\text{th}}$  decoder recovers  $\boldsymbol{\lambda}_m$  then removes the dithers and take  $\text{mod } \Lambda_{C,m}$  to get

$$\begin{aligned} \widehat{\mathbf{s}}_m^\dagger &= [\boldsymbol{\lambda}_m^\dagger - \mathbf{a}_m^\dagger \mathbf{U}] \text{ mod } \Lambda_{C,m} \\ &\stackrel{(a)}{=} [\mathbf{t}_m^\dagger - \mathbf{a}_m^\dagger \mathbf{U}] \text{ mod } \Lambda_{C,m} \\ &= [\mathbf{a}_m^\dagger \Phi - \mathbf{a}_m^\dagger \mathbf{U}] \text{ mod } \Lambda_{C,m} \\ &\stackrel{(b)}{=} [\mathbf{a}_m^\dagger (\mathbf{V} + \mathbf{U} + \mathbf{Q}) - \mathbf{a}_m^\dagger \mathbf{U}] \text{ mod } \Lambda_{C,m} \end{aligned}$$

$$\begin{aligned}
&= [\mathbf{s}_m^\dagger + \mathbf{a}_m^\dagger \mathbf{Q}] \bmod \Lambda_{C,m} \\
&\stackrel{\text{w.h.p.}}{=} \mathbf{s}_m^\dagger + \mathbf{a}_m^\dagger \mathbf{Q}
\end{aligned} \tag{5.6}$$

where  $\mathbf{a}_m^\dagger$  is the  $m^{\text{th}}$  row of the matrix  $\mathbf{A}$ , (a) follows from the distributive law, (b) follows from defining  $\mathbf{Q} \triangleq [\mathbf{q}_1 \ \cdots \ \mathbf{q}_L]^\dagger$  and for  $\ell = 1, \dots, L$ , we have  $\mathbf{q}_\ell = -[\mathbf{v}_\ell + \mathbf{u}_\ell] \bmod \Lambda_F$  is independent of  $\mathbf{v}_\ell$  and uniformly distributed over  $\mathcal{V}(\Lambda_F)$  by the Crypto Lemma and finally the last equality follows from the second property of Lemma 2 with high probability if

$$\frac{1}{T} \mathbb{E} \|\mathbf{s}_m^\dagger + \mathbf{a}_m^\dagger \mathbf{Q}\|^2 < \theta_{C,m}. \tag{5.7}$$

By setting  $\theta_F = d$  and  $\theta_{C,m} = K_{SS,m,m} + d \|\mathbf{a}_m\|^2 + \epsilon$  where  $\epsilon$  goes to zero as  $T$  goes to infinity, we satisfy (5.7) and the  $m^{\text{th}}$  decoder is able to recover (5.6) with high probability. Finally, Fig. 5-2 shows a detailed diagram for the encoder and decoders of the RIFSC.

**Remark 17.** Note that  $\tilde{\mathbf{Q}} \triangleq \mathbf{A}\mathbf{Q}$  is the final correlated noise and the correlation is determined by the integer matrix  $\mathbf{A}$  along with  $\theta_F = d$  since the effective covariance matrix of  $\tilde{\mathbf{Q}}$  is

$$\frac{1}{T} \mathbb{E}[\tilde{\mathbf{Q}}\tilde{\mathbf{Q}}^\dagger] = d\mathbf{A}\mathbf{A}^\dagger.$$

**Theorem 10.** For a given covariance matrix  $\mathbf{K}_{SS}$ , target covariance matrix  $\mathbf{\Omega} = d\mathbf{A}\mathbf{A}^\dagger$  for a full-rank integer matrix  $\mathbf{A} \in \mathbb{Z}^{L \times L}$  and distortion level  $d > 0$ , the following rates are achievable using reverse integer-forcing source coding

$$R_{RIFSC,\ell} \triangleq \frac{1}{2} \log \left( \frac{K_{SS,\ell,\ell} + d \|\mathbf{a}_\ell\|^2}{d} \right), \quad \ell = 1, \dots, L, \tag{5.8}$$

where  $K_{SS,\ell,\ell}$  is the  $(\ell, \ell)^{\text{th}}$  element of  $\mathbf{K}_{SS}$ .

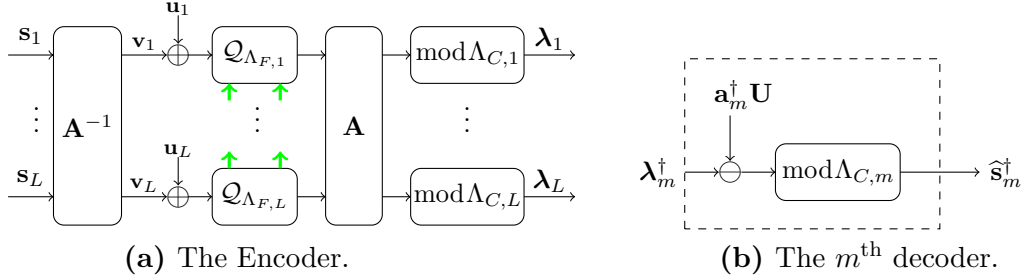


**Figure 5.2:** Reverse Integer-Forcing Source Coding. Green arrows indicate successive encoding.

### 5.3.2 Successive Reverse Integer-Forcing Compression

Instead of using a single fine lattice, one can better approximate a desired covariance matrix by using  $L$  nested fine lattices  $\Lambda_{F,1} \subseteq \dots \subseteq \Lambda_{F,L}$  (i.e.,  $L$  different lattice quantizers) with  $L$  different second moments  $\theta_{F,L} \leq \dots \leq \theta_{F,1}$ . Since the encoder forms integer-linear combinations of the quantizers outputs, this limits us to the finest resolution  $\theta_{F,L}$  leading us back to the previous result with a single resolution (i.e., single fine lattice  $\Lambda_{F,L}$ ). In order to solve this problem, we propose a "digital" successive quantization approach to eliminate the fine lattices  $\{\Lambda_{F,k}, k > m\}$  from the  $m^{\text{th}}$  compression step.

For a full-rank integer matrix  $\mathbf{A}$ , assume that the sources are re-indexed (i.e., the columns of  $\mathbf{A}$ , columns and rows of  $\mathbf{K}_{SS}$  as well as the diagonal elements of  $\mathbf{D}$ ) such that their distortion levels are monotonically increasing (i.e.,  $d_L \leq \dots \leq d_1$ ). Furthermore, assume that the combinations  $\mathbf{a}_1^\dagger(\mathbf{V} + \mathbf{Q}), \dots, \mathbf{a}_L^\dagger(\mathbf{V} + \mathbf{Q})$  has been re-indexed (i.e., rows of  $\mathbf{A}$ ) such that the full-rank integer matrix  $\mathbf{A}$  has full-rank sub-matrices  $\mathbf{A}_{s,[1:m]}$ , for  $m = 1, \dots, L$ . Finally, similar to the parallel compression in Section 5.3.1, we define a permutation  $\pi_C$  such that  $\mathbb{E}\|\mathbf{s}_{\pi_C(1)}^\dagger + \mathbf{a}_{\pi_C(1)}^\dagger \mathbf{Q}\|^2 \leq \dots \leq \mathbb{E}\|\mathbf{s}_{\pi_C(L)}^\dagger + \mathbf{a}_{\pi_C(L)}^\dagger \mathbf{Q}\|^2$  which determines the nested coarse lattices order.

### Codebook

Generate nested lattice codebooks  $\mathcal{C}_\ell \triangleq \Lambda_{F,\ell} \cap \mathcal{V}(\Lambda_{C,\ell})$  with rates  $R_\ell = \frac{1}{2} \log \left( \frac{\theta_{C,\ell}}{\theta_{F,\ell}} \right)$  using nested lattices  $\Lambda_{C,\pi_C(L)} \subseteq \cdots \subseteq \Lambda_{C,\pi_C(1)} \subseteq \Lambda_{F,1} \subseteq \cdots \subseteq \Lambda_{F,L}$  selected using Lemma 2 with parameters  $\theta_{F,\ell} = d_\ell$  and  $\theta_{C,\ell}$  (to be chosen later), where  $d_\ell$  is the  $\ell^{\text{th}}$  distortion level.

### Compression

Similar to the parallel compression, the encoder starts by pre-inverting an integer matrix  $\mathbf{A}$ , with full-rank sub-matrices  $\mathbf{A}_{[1:m]}$  for  $m = 1, \dots, L$ , and using it to obtain the combinations

$$\mathbf{V} = \mathbf{A}^{-1}\mathbf{S} \quad (5.9)$$

where  $\mathbf{V} \triangleq [\mathbf{v}_1, \dots, \mathbf{v}_L]^\dagger$  and  $\mathbf{S} \triangleq [\mathbf{s}_1, \dots, \mathbf{s}_L]^\dagger$ .

Second, the encoder adds the dither and quantizes to get

$$\mathbf{\Phi} = \begin{bmatrix} \mathcal{Q}_{\Lambda_{F,1}}(\mathbf{v}_1 + \mathbf{u}_1 + \mathbf{g}_1)^\dagger \\ \vdots \\ \mathcal{Q}_{\Lambda_{F,L}}(\mathbf{v}_L + \mathbf{u}_L + \mathbf{g}_L)^\dagger \end{bmatrix} \quad (5.10)$$

where  $\mathbf{u}_1, \dots, \mathbf{u}_L$  independent dithers with  $\mathbf{u}_\ell$  uniformly distributed over  $\mathcal{V}(\Lambda_{F,\ell})$  and  $\mathbf{g}_1, \dots, \mathbf{g}_L$  are some auxiliary variables to be chosen later.

Next, unlike in the parallel compression, the encoder uses a lower triangular integer matrix  $\mathbf{L}$  to form the combinations

$$\mathbf{T} = \mathbf{L}\mathbf{\Phi}. \quad (5.11)$$

Since each row of  $\mathbf{\Phi}$  is quantized with a different resolution (i.e., different fine lattice), using a lower triangular integer matrix  $\mathbf{L}$  allows  $\mathbf{t}_m$  (i.e., the  $m^{\text{th}}$  row of  $\mathbf{T}$ ) to only contain the quantizers' outputs with resolutions lower (coarser) than  $\theta_{F,m}$

(i.e.,  $\Lambda_{F,\ell}$  for  $\ell \leq m$ ).

Finally, the encoder forms the lattice codewords

$$\boldsymbol{\lambda}_m = [\mathbf{t}_m] \bmod \Lambda_{C,m}, \quad m = 1, \dots, L, \quad (5.12)$$

where  $\mathbf{t}_m$  is the  $m^{\text{th}}$  row of  $\mathbf{T}$  and  $\boldsymbol{\lambda}_m \in \mathcal{C}_m$ , then the index  $i_m \in \{1, \dots, 2^{TR_m}\}$  of  $\boldsymbol{\lambda}_m$  is sent to the  $m^{\text{th}}$  decoder.

### Decompression

Defining  $\mathbf{U} \triangleq [\mathbf{u}_1 \ \dots \ \mathbf{u}_L]^\dagger$ ,  $\mathbf{Q} \triangleq [\mathbf{q}_1 \ \dots \ \mathbf{q}_L]^\dagger$ ,  $\mathbf{q}_k \triangleq -[\mathbf{v}_k + \mathbf{u}_k + \mathbf{g}_k] \bmod \Lambda_{F,k}$ , which by the Crypto Lemma is uniformly distributed over  $\mathcal{V}(\Lambda_{F,k})$  for  $k = 1, \dots, L$  and  $\mathbf{G} \triangleq [\mathbf{g}_1 \ \dots \ \mathbf{g}_L]^\dagger$ , we can write  $\mathbf{T}$  as

$$\begin{aligned} \mathbf{T} &= \mathbf{L}\boldsymbol{\Phi} \\ &\stackrel{(a)}{=} \mathbf{L}(\mathbf{V} + \mathbf{U} + \mathbf{Q} + \mathbf{G}) \\ &\stackrel{(b)}{=} \mathbf{L}(\mathbf{V} + \mathbf{U} + \mathbf{Q} + \mathbf{C}\boldsymbol{\Phi}) \\ &\stackrel{(c)}{=} \mathbf{L}(\mathbf{V} + \mathbf{U} + \mathbf{Q} + \mathbf{C}(\mathbf{V} + \mathbf{U} + \mathbf{Q} + \mathbf{G})) \\ &\stackrel{(d)}{=} \mathbf{L}(\mathbf{I} + (\mathbf{I} - \mathbf{C})^{-1}\mathbf{C})(\mathbf{V} + \mathbf{U} + \mathbf{Q}) \\ &\stackrel{(e)}{=} \mathbf{L}\mathbf{F}(\mathbf{V} + \mathbf{U} + \mathbf{Q}) \end{aligned} \quad (5.13)$$

where (a) holds from  $\mathbf{Q} \triangleq [\mathbf{q}_1 \ \dots \ \mathbf{q}_L]^\dagger$ , (b) follows from choosing a recursive solution  $\mathbf{G} \triangleq \mathbf{C}\boldsymbol{\Phi}$  for some strictly upper triangular integer matrix  $\mathbf{C}$ , (c) holds as (a) by the substitution  $\boldsymbol{\Phi} = \mathbf{V} + \mathbf{U} + \mathbf{Q} + \mathbf{G}$ , (d) holds from solving the recursive equation

$$\mathbf{G} = \mathbf{C}(\mathbf{V} + \mathbf{U} + \mathbf{Q} + \mathbf{G})$$

for  $\mathbf{G}$  and (e) from defining  $\mathbf{F} \triangleq (\mathbf{I} + (\mathbf{I} - \mathbf{C})^{-1}\mathbf{C})$  which is proved in Appendix E to be an upper triangular integer matrix with unit diagonal entries.

Finally, the  $m^{\text{th}}$  decoder removes the dithers  $\boldsymbol{\ell}_m^\dagger \mathbf{F} \mathbf{U}$  from (5.13) and applies mod  $\Lambda_{C,m}$  to recover

$$\begin{aligned}
& [\boldsymbol{\lambda}_m^\dagger - \boldsymbol{\ell}_m^\dagger \mathbf{F} \mathbf{U}] \bmod \Lambda_{C,m} \\
& \stackrel{(a)}{=} [\mathbf{t}_m^\dagger - \boldsymbol{\ell}_m^\dagger \mathbf{F} \mathbf{U}] \bmod \Lambda_{C,m} \\
& = [\boldsymbol{\ell}_m^\dagger \mathbf{F} (\mathbf{V} + \mathbf{Q})] \bmod \Lambda_{C,m} \\
& \stackrel{(b)}{=} [[\boldsymbol{\ell}_m^\dagger \mathbf{F}] \bmod p (\mathbf{V} + \mathbf{Q})] \bmod \Lambda_{C,m} \\
& \stackrel{(c)}{=} [[\mathbf{a}_m^\dagger] \bmod p (\mathbf{V} + \mathbf{Q})] \bmod \Lambda_{C,m} \\
& \stackrel{(d)}{=} [\mathbf{a}_m^\dagger (\mathbf{V} + \mathbf{Q})] \bmod \Lambda_{C,m} \\
& = [\mathbf{s}_m^\dagger + \mathbf{a}_m^\dagger \mathbf{Q}] \bmod \Lambda_{C,m} \\
& \stackrel{\text{w.h.p.}}{=} \mathbf{s}_m^\dagger + \mathbf{a}_m^\dagger \mathbf{Q} \tag{5.14}
\end{aligned}$$

where (a) follows from the distributive law, (b) and (d) follows from [Ordentlich et al., 2014, Theorem 2 (c)], (c) follows from Lemma 30 in Appendix D which states that, for any full-rank integer matrix  $\mathbf{A}$  with full-rank sub-matrices  $\mathbf{A}_{[1:m]}$  for  $m = 1, \dots, L$ , there exists lower triangular integer matrix  $\mathbf{L}$  and strictly upper triangular integer matrix  $\mathbf{C}$  such that  $[\mathbf{L}\mathbf{F}] \bmod p = [\mathbf{A}] \bmod p$  and the last inequality holds with high probability if

$$\frac{1}{T} \mathbb{E} \|\mathbf{s}_m^\dagger + \mathbf{a}_m^\dagger \mathbf{Q}\|^2 < \theta_{C,m}.$$

Finally, setting  $\theta_m = K_{SS,m,m} + \mathbf{a}_m^\dagger \mathbf{D} \mathbf{a}_m + \epsilon$ , where  $\epsilon$  goes to zero as the blocklength goes to infinity insures that with high probability the  $m^{\text{th}}$  decoder recovers  $\widehat{\mathbf{s}}_m^\dagger = \mathbf{s}_m^\dagger + \mathbf{a}_m^\dagger \mathbf{Q}$ .

**Remark 18.** In Lemma 30, after obtaining  $\mathbf{F}$ , we can find the corresponding  $\mathbf{C}$  using

$$\mathbf{C} = \mathbf{I} - \mathbf{F}^{-1}. \tag{5.15}$$

**Theorem 11.** For a given covariance matrix  $\mathbf{K}_{SS}$ , target covariance matrix  $\mathbf{\Omega} = \mathbf{A}\mathbf{D}\mathbf{A}^\dagger$  for a full-rank  $\mathbf{A} \in \mathbb{Z}^{L \times L}$  with full-rank sub-matrices  $\mathbf{A}_{[1:m]}$  for  $m = 1, \dots, L$ , distortion matrix  $\mathbf{D} = \text{diag}(d_1, \dots, d_L)$  and  $d_L \leq \dots \leq d_1$ , the following rates are achievable using successive reverse integer-forcing source coding

$$R_{SRIFSC,\ell}(\mathbf{K}_{SS}, \mathbf{\Omega}) \triangleq \frac{1}{2} \log \left( \frac{K_{SS,\ell,\ell} + \mathbf{a}_\ell^\dagger \mathbf{D} \mathbf{a}_\ell}{d_\ell} \right), \ell = 1, \dots, L. \quad (5.16)$$

**Lemma 15.** Define the permutation  $\pi_{SRIFSC}$  as the source re-ordering that we used to ensure that  $d_{\pi_{SRIFSC}(L)} \leq \dots \leq d_{\pi_{SRIFSC}(1)}$  and the permutation  $\pi_{rank}$  as the combination re-ordering such that  $\text{Rank}(\mathbf{A}_{\pi_{rank}([1:m]), \pi_{SRIFSC}([1:m])}) = m$  for  $m = 1, \dots, L$ . The achievable rates in Theorem 11 in terms of the original source order can be written as

$$R_{SRIFSC, \pi_{SRIFSC}(\ell)}(\mathbf{K}_{SS}, \mathbf{\Omega}) \triangleq \frac{1}{2} \log \left( \frac{K_{SS, \pi_{rank}(\ell), \pi_{rank}(\ell)} + \mathbf{a}_{\pi_{rank}(\ell)}^\dagger \mathbf{D} \mathbf{a}_{\pi_{rank}(\ell)}}{d_{\pi_{SRIFSC}(\ell)}} \right), \ell = 1, \dots, L \quad (5.17)$$

where  $\mathbf{D} = \text{diag}(d_1, \dots, d_L)$ .

**Remark 19.** The permutations  $\pi_{SRIFSC}$  and  $\pi_{rank}$  are essential for the algebraic successive compression to work and determines which source should be mapped to which combination, however the permutation  $\pi_C$  is only used to define the nesting order of the coarse lattices.

Finally, we present the next theorem that compares the performance of the proposed successive reverse integer-forcing source coding to that of the multivariate compression [Park et al., 2013].

**Theorem 12.** For a given covariance matrix  $\mathbf{K}_{SS}$  and a desired covariance matrix  $\mathbf{\Omega}$  that can be decomposed into  $\mathbf{\Omega} = \mathbf{A}\mathbf{D}\mathbf{A}^\dagger$ , where  $\mathbf{A}$  is any unimodular integer matrix and  $\mathbf{D}$  is a real positive diagonal matrix, we have

$$\sum_{\ell=1}^L R_{SRIFSC,\ell}(\mathbf{K}_{SS}, \mathbf{\Omega}) = \sum_{\ell=1}^L R_{MV,\ell}(\mathbf{K}_{SS}, \mathbf{\Omega}) \quad (5.18)$$

where  $R_{RIFSC,\ell}(\mathbf{K}_{SS}, \boldsymbol{\Omega})$  are the achievable rates using the RIFSC, while  $R_{MV,\ell}(\mathbf{K}_{SS}, \boldsymbol{\Omega})$  are the achievable rates using the multivariate compression in Lemma 14.

*Proof.* We proceed as in Lemma 15. First, find a permutation  $\pi_1$  such that  $d_{\pi_1(L)} \leq \dots \leq d_{\pi_1(1)}$ . Next, since  $\mathbf{A}$  is a full-rank matrix, there exists a permutation  $\pi_2$  such that  $\text{Rank}(\mathbf{A}_{\pi_2([1:m]),\pi_1([1:m])}) = m$  for  $m = 1, \dots, L$ . By permuting the sources and combinations by  $\pi_1$  and  $\pi_2$ , respectively we get the following achievable sum-rate

$$\begin{aligned}
& \sum_{\ell=1}^L R_{\text{SRIFSC},\ell}(\mathbf{K}_{SS}, \boldsymbol{\Omega}) \\
& \stackrel{(a)}{=} \sum_{\ell=1}^L \frac{1}{2} \log \left( \frac{K_{SS,\pi_2(\ell),\pi_2(\ell)} + \mathbf{a}_{\pi_2(\ell),\pi_1(\mathcal{L})}^\dagger \mathbf{D}_{\pi_1(\mathcal{L}),\pi_1(\mathcal{L})} \mathbf{a}_{\pi_2(\ell),\pi_1(\mathcal{L})}}{d_{\pi_1(\ell)}} \right) \\
& = \frac{1}{2} \log \left( \frac{\prod_{\ell=1}^L \left( K_{SS,\pi_2(\ell),\pi_2(\ell)} + \mathbf{a}_{\pi_2(\ell),\pi_1(\mathcal{L})}^\dagger \mathbf{D}_{\pi_1(\mathcal{L}),\pi_1(\mathcal{L})} \mathbf{a}_{\pi_2(\ell),\pi_1(\mathcal{L})} \right)}{\prod_{\ell=1}^L d_{\pi_1(\ell)}} \right) \\
& = \frac{1}{2} \log \left( \frac{\prod_{\ell=1}^L \left( K_{SS,\ell,\ell} + \mathbf{a}_\ell^\dagger \mathbf{D} \mathbf{a}_\ell \right)}{\prod_{\ell=1}^L d_\ell} \right) \\
& = \frac{1}{2} \log \left( \frac{\prod_{\ell=1}^L \left( K_{SS,\ell,\ell} + \mathbf{a}_\ell^\dagger \mathbf{D} \mathbf{a}_\ell \right)}{|\mathbf{A} \mathbf{D} \mathbf{A}^\dagger|} \right) + \frac{1}{2} \log(|\mathbf{A}|^2) \\
& \stackrel{(b)}{=} \sum_{\ell=1}^L \frac{1}{2} \log \left( K_{SS,\ell,\ell} + \mathbf{a}_\ell^\dagger \mathbf{D} \mathbf{a}_\ell \right) - \frac{1}{2} \log(|\boldsymbol{\Omega}|) + \frac{1}{2} \log(|\mathbf{A}|^2) \\
& = \sum_{\ell=1}^L \frac{1}{2} \log \left( K_{SS,\ell,\ell} + \Omega_{\ell,\ell} \right) - \frac{1}{2} \log(|\boldsymbol{\Omega}|) + \frac{1}{2} \log(|\mathbf{A}|^2) \\
& \stackrel{(c)}{=} \sum_{\ell=1}^L R_{\text{MV},\ell}(\mathbf{K}_{SS}, \boldsymbol{\Omega}) + \frac{1}{2} \log(|\mathbf{A}|^2) \\
& \stackrel{(d)}{=} \sum_{\ell=1}^L R_{\text{MV},\ell}(\mathbf{K}_{SS}, \boldsymbol{\Omega}) \tag{5.19}
\end{aligned}$$

where (a) holds by applying Theorem 11 to the sources re-indexed by  $\pi_1$  and using the integer matrix  $\mathbf{A}_{\pi_2(\mathcal{L}),\pi_1(\mathcal{L})}$  with full-rank sub-matrices  $\mathbf{A}_{\pi_2([1:m]),\pi_1([1:m])}$  for  $m = 1, \dots, L$  instead of  $\mathbf{A}$  when forming  $\mathbf{V}$  in (5.9), (b) holds from  $\mathbf{\Omega} = \mathbf{A}\mathbf{D}\mathbf{A}^\dagger$ , (c) holds from Lemma 14 and (d) holds from noting that  $|\mathbf{A}| = \pm 1$  for unimodular matrices.

□

## Chapter 6

# Downlink Cloud-Radio Access Networks

In this chapter, we study the downlink C-RAN, under total fronthaul capacity constraints. We propose an end-to-end low complexity IF scheme, in which we use the RIFSC proposed in Chapter 5 to convey the users' codewords, with correlated quantization noises, to the BSs. This transforms the downlink C-RAN to a virtual broadcast channel, for which we can use the reverse compute-and-forward [Hong and Caire, 2012] to decode integer-linear combinations of the BSs codewords at the user side, then map these combinations to the users' messages. The parameters of the scheme can be optimized using our duality result that will be established in the next chapter.

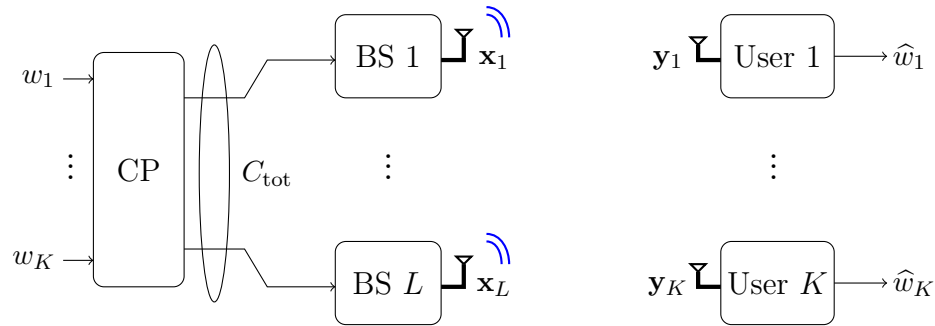


**Figure 6.1:** The downlink C-RAN channel model.

## 6.1 System Model

Consider the downlink C-RAN scenario shown in Fig. 6.1, where a CP is connected to a set  $\mathcal{L}$  of single-antenna BSs through noiseless fronthaul links with finite rates  $C_1, \dots, C_L$  as shown in Fig. 6.1. The CP wants to communicate  $K$  messages  $w_k \in \{1, \dots, 2^{TR_k}\}$ , with rate  $R_k$ , for  $k \in \mathcal{K}$ , to a set of single-antenna users  $\mathcal{K}$ , where the  $k^{\text{th}}$  user is interested in  $w_k$ . The fronthaul links either exhibit symmetric rate constraints<sup>1</sup>  $C_\ell = C_{\text{sym}}, \forall \ell \in \mathcal{L}$ , or a total rate constraint  $\sum_{\ell=1}^L C_\ell = C_{\text{tot}}$ , depending on the physical structure of the network.

### 6.1.1 The End-to-End Broadcast Channel

The CP maps the messages  $w_1, \dots, w_K$  into indices  $i_1, \dots, i_L$ , where  $i_\ell \in \{1, \dots, 2^{TC_\ell}\}$  for  $\ell = 1, \dots, L$ , then forwards  $i_\ell$  to the  $\ell^{\text{th}}$  BS through the fronthaul link. Next, the  $\ell^{\text{th}}$  BS transmits signal  $\mathbf{x}_\ell \in \mathbb{R}^T$  for  $\ell = 1, \dots, L$  and the received signal across all users is

$$\mathbf{Y} = \mathbf{H}\mathbf{X} + \mathbf{Z} \quad (6.1)$$

where  $\mathbf{Y} \triangleq [\mathbf{y}_1 \ \dots \ \mathbf{y}_K]^\dagger$ ,  $\mathbf{y}_k \in \mathbb{R}^T$  is the received signal at the  $k^{\text{th}}$  user,  $\mathbf{H} \in \mathbb{R}^{K \times L}$  is the channel matrix from the  $L$  BSs to the  $K$  users which is known to the CP, all BSs and all users,  $\mathbf{X} \triangleq [\mathbf{x}_1 \ \dots \ \mathbf{x}_L]^\dagger$  and  $\mathbf{Z} \in \mathbb{R}^{K \times T}$  is i.i.d.  $\mathcal{N}(0, 1)$ . The BSs have total power constraint  $\text{Tr}(\mathbf{X}\mathbf{X}^\dagger) \leq TP_{\text{total}}$ . The  $k^{\text{th}}$  user makes an estimate  $\hat{w}_k$  of the transmitted message based on its received signal  $\mathbf{y}_k$ . We say that the rates  $R_1, \dots, R_K$  are achievable if, for any  $\epsilon > 0$  and  $T$  large enough there exists encoders and decoders that attain average probability of error at most  $\epsilon$  (i.e.,  $\mathbb{P}(\cup_{k=1}^K \{\hat{w}_k \neq w_k\}) \leq \epsilon$ ).

---

<sup>1</sup>We assume symmetric fronthaul links constraints, however an extension to asymmetric individual rate constraints is straightforward.

### 6.1.2 Compression-Based Strategies for Downlink C-RAN

In compression-based strategies for the downlink C-RAN, the CP jointly encodes the messages  $w_1, \dots, w_K$  into channel codewords  $\mathbf{s}_1, \dots, \mathbf{s}_L$  (since we have  $L$  BSs) rather than locally encoding each one at a separate BS. These strategies allows the BSs to be oblivious to the codebooks employed by the users. The CP then compresses the  $\ell^{\text{th}}$  codeword  $\mathbf{s}_\ell$  into an index  $i_\ell \in \{1, \dots, 2^{T C_\ell}\}$  and forwards it to the  $\ell^{\text{th}}$  BS through the fronthaul link. Upon receiving the index  $i_\ell$ , the  $\ell^{\text{th}}$  BS reconstructs the signal  $\widehat{\mathbf{s}}_\ell$ , then uses it to transmit  $\mathbf{x}_\ell = \widehat{\mathbf{s}}_\ell$ .

Due to the limited fronthaul capacity, the decompressed signal at the  $\ell^{\text{th}}$  BS

$$\widehat{\mathbf{s}}_\ell = \mathbf{s}_\ell + \mathbf{q}_\ell, \forall \ell \in \mathcal{L} \quad (6.2)$$

suffers from a zero-mean quantization noise  $\mathbf{q}_\ell$ . The quantization noise  $\mathbf{Q} \triangleq [\mathbf{q}_1 \ \dots \ \mathbf{q}_L]^\dagger$  is characterized by its covariance matrix  $\frac{1}{T} \mathbb{E}[\mathbf{Q}\mathbf{Q}^\dagger]$ , which depends on the fronthaul rates  $C_1, \dots, C_L$  and the compression strategy used at the CP/BSs. Similar to the uplink, we assume zero-mean quantization noise, since this implies that the quantization noises  $\mathbf{q}_1, \dots, \mathbf{q}_L$  are independent of the channel codewords  $\mathbf{s}_1, \dots, \mathbf{s}_L$  which facilitates the interface between source and channel coding.

## 6.2 Conventional Receivers for Downlink C-RAN

In this section, we briefly summarize the successive encoding scheme proposed in [Park et al., 2013]. First, for a specific encoding order  $\pi_c$ , the CP successively encodes the messages  $w_{\pi_c(1)}, \dots, w_{\pi_c(K)}$ , into channel codewords  $\widetilde{\mathbf{s}}_{\pi_c(1)}, \dots, \widetilde{\mathbf{s}}_{\pi_c(K)}$  of length  $T$  as done in the dirty paper coding (DPC) [Costa, 1983]. Denote the diagonal matrix  $\mathbf{P} \triangleq \text{diag}(P_1, \dots, P_K) = \frac{1}{T} \mathbb{E}[\widetilde{\mathbf{S}}\widetilde{\mathbf{S}}^\dagger]$  as the effective covariance matrix of  $\widetilde{\mathbf{S}} \triangleq [\widetilde{\mathbf{s}}_1 \ \dots \ \widetilde{\mathbf{s}}_K]^\dagger$ .

Second, the CP applies a linear beamforming matrix  $\mathbf{B} \in \mathbb{R}^{L \times K}$  to obtain  $\mathbf{S} \triangleq \mathbf{B}\widetilde{\mathbf{S}}$ , where  $\mathbf{S} \triangleq [\mathbf{s}_1 \ \dots \ \mathbf{s}_L]^\dagger$ . Next, the CP jointly compresses the equalized codewords

$\mathbf{s}_1 \cdots \mathbf{s}_L$  and forwards it to the BSs through the fronthaul links. This is done using the novel multivariate compression scheme discussed in 5.2.2. The multivariate compression scheme helps creating correlation between quantization noise across BSs. Since the quantization noise is going to be combined (naturally by the wireless channel) at the user side, the correlation can be chosen to reduce their effective variance at the receiver, hence improve the end-to-end performance. Finally, the BSs recover and re-transmit  $\mathbf{X} = \mathbf{S} + \mathbf{Q}$ , where the quantization noise  $\mathbf{Q}$  has an effective covariance matrix  $\frac{1}{T}\mathbb{E}[\mathbf{Q}\mathbf{Q}^\dagger] = \mathbf{\Omega}$ .

**Lemma 16.** *For a beamforming matrix  $\mathbf{B}$ , diagonal coding power matrix  $\mathbf{P}$ , effective covariance matrix  $\mathbf{\Omega}$  and encoding order  $\pi_c$ , the rates achievable by DPC and multivariate compression are*

$$R_{DPC,\pi_c(k)}(\mathbf{H}) = \frac{1}{2} \log \left( 1 + \frac{\left( \mathbf{h}_{\pi_c(k)}^\dagger \mathbf{b}_{\pi_c(k)} \right)^2 P_{\pi_c(k)}}{1 + \mathbf{h}_{\pi_c(k)}^\dagger \left( \sum_{\ell=k+1}^K \mathbf{b}_{\pi_c(\ell)} \mathbf{b}_{\pi_c(\ell)}^\dagger + \mathbf{\Omega} \right) \mathbf{h}_{\pi_c(k)}} \right) \quad (6.3)$$

where  $\mathbf{B}$ ,  $\mathbf{\Omega}$  and  $\mathbf{P}$  should be chosen such that

$$\sum_{i \in \mathcal{T}} \frac{1}{2} \log \left( \mathbf{b}_i^\dagger \mathbf{P} \mathbf{b}_i + \Omega_{i,i} \right) - \frac{1}{2} \log |\mathbf{\Omega}_{\mathcal{T},\mathcal{T}}| \leq \sum_{i \in \mathcal{T}} C_i, \quad \forall \mathcal{T} \subseteq \{1, \dots, L\},$$

$$\text{Tr}(\mathbf{B}\mathbf{P}\mathbf{B}^\dagger + \mathbf{\Omega}) \leq P_{total}. \quad (6.4)$$

**Remark 20.** *The authors in [Park et al., 2013] have also proposed a successive convex approximation algorithm in order to optimize the parameters of the aforementioned scheme, for a given encoding permutation  $\pi_c$ .*

### 6.3 Integer-Forcing C-RAN Architecture

The end-to-end integer-forcing architecture for downlink C-RAN is illustrated in Figure 6.2. In this scheme, the CP first pre-codes/pre-inverts the messages allowing

each user at the end to map the decoded integer-linear combination of the transmitted codewords to its desired message. The CP encodes the messages using nested lattice channel codes, then uses the reverse-IFSC (RIFSC) proposed in Section 5.3 to convey these channel codewords to the BSs while introducing correlations between the quantization noises.

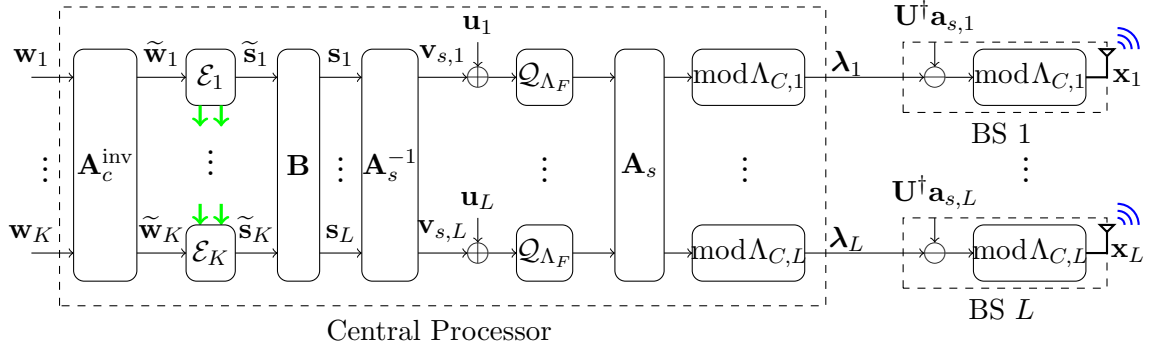


**Figure 6.2:** Integer-forcing architecture for Downlink C-RAN with symmetric distortion. The green arrows denote the successive encoding in [He et al., 2018, Section VI].

### 6.3.1 Channel Encoding

For simplicity, we only present integer-forcing beamforming for the special case of symmetric rates, and point to [He et al., 2018, Section VI] for the asymmetric case. The CP starts with "digitally" precoding the  $K$  messages  $w_1, \dots, w_K$  by forming

$$\widetilde{\mathbf{W}} = [\mathbf{A}_c^{\text{inv}} \mathbf{W}] \bmod p \quad (6.5)$$

where  $\widetilde{\mathbf{W}} \triangleq [\widetilde{\mathbf{w}}_1 \cdots \widetilde{\mathbf{w}}_K]^\dagger$ ,  $\mathbf{A}_c \in \mathbb{Z}^{K \times K}$  is a full-rank integer matrix,  $\mathbf{A}_c^{\text{inv}}$  is the algebraic inverse of the matrix  $\mathbf{A}_c$  over  $\mathbb{Z}_p$ ,  $\mathbf{W} \triangleq [\mathbf{w}_1 \cdots \mathbf{w}_K]^\dagger$ ,  $\mathbf{w}_k$  is the  $p$ -ary expansion of  $w_k$  and  $p$  is a prime. The precoded messages  $\widetilde{\mathbf{w}}_1, \dots, \widetilde{\mathbf{w}}_K$  are then mapped successively, as in Theorem [He et al., 2018, Theorem 6] to lattice codewords  $\widetilde{\mathbf{s}}_1, \dots, \widetilde{\mathbf{s}}_K$  of length  $T$  and power  $\frac{1}{T} \mathbb{E} \|\widetilde{\mathbf{s}}_k\|^2 = P_k$  for  $k = 1, \dots, K$  to form the channel

codeword matrix  $\tilde{\mathbf{S}} \triangleq [\tilde{\mathbf{s}}_1 \cdots \tilde{\mathbf{s}}_K]^\dagger$  with effective covariance matrix  $\frac{1}{T}\mathbb{E}[\tilde{\mathbf{S}}\tilde{\mathbf{S}}^\dagger] = \mathbf{P}$ , where  $\mathbf{P} = \text{diag}(P_1, \dots, P_K)$ . The precoding step in (6.5) allows the  $m^{\text{th}}$  user, after successfully decoding the real integer-linear combination

$$\mathbf{v}_{c,m}^\dagger \triangleq \mathbf{a}_{c,m}^\dagger \tilde{\mathbf{S}},$$

to map it back to

$$\begin{aligned} [\mathbf{a}_{c,m}^\dagger \tilde{\mathbf{W}}] \bmod p &= [\mathbf{a}_{c,m}^\dagger [\mathbf{A}_c^{\text{inv}} \mathbf{W}] \bmod p] \bmod p \\ &\stackrel{(a)}{=} [\mathbf{a}_{c,m}^\dagger \mathbf{A}_c^{\text{inv}} \mathbf{W}] \bmod p \\ &\stackrel{(b)}{=} [[\mathbf{a}_{c,m}^\dagger \mathbf{A}_c^{\text{inv}}] \bmod p \mathbf{W}] \bmod p \\ &= \mathbf{w}_m^\dagger \end{aligned} \tag{6.6}$$

which is the desired message at that user, where  $\mathbf{a}_{c,m}$  is the  $m^{\text{th}}$  row of  $\mathbf{A}_c$  and both (a) and (b) hold from the distributive law.

After forming the channel codeword matrix  $\tilde{\mathbf{S}}$ , the CP uses a beamforming matrix  $\mathbf{B} \in \mathbb{R}^{L \times K}$  to form

$$\mathbf{S} \triangleq [\mathbf{s}_1 \cdots \mathbf{s}_L]^\dagger = \mathbf{B}\tilde{\mathbf{S}}.$$

### 6.3.2 Backhaul Compression

In order to convey  $\mathbf{S}$  to the BSs (i.e., convey the  $\ell^{\text{th}}$  row of  $\mathbf{S}$  to the  $\ell^{\text{th}}$  BS) with correlated quantization noises, we use the RIFSC scheme proposed in Section 5.3. For simplicity of presentation, we summarize parallel RIFSC, however one can choose to use algebraic successive cancellation to enhance the end-to-end performance.

The CP uses a full-rank integer matrix  $\mathbf{A}_s$  to form linear combinations  $\mathbf{V}_s = \mathbf{A}_s^{-1}\mathbf{S}$ , then uses it to compute

$$\boldsymbol{\lambda}_m^\dagger = [\mathbf{a}_{s,m}^\dagger \mathcal{Q}_{\Lambda_F}(\mathbf{V}_s + \mathbf{U})] \bmod \Lambda_{C,m}, \quad m = 1, \dots, L, \tag{6.7}$$

where  $\mathbf{a}_{s,m}$  is the  $m^{\text{th}}$  row of  $\mathbf{A}_s$ ,  $\mathbf{U}$  is a random dither matrix discussed in Section 5.3. The CP then forwards the index  $i_m$  of  $\boldsymbol{\lambda}_m$  through the fronthaul link.

Finally, the  $\ell^{\text{th}}$  BS uses the index  $i_\ell$  to recover  $\boldsymbol{\lambda}_\ell$ , then removes the dithers, applies mod  $\Lambda_{C,\ell}$  to obtain

$$\begin{aligned}\widehat{\mathbf{s}}_\ell^\dagger &= \left[ \boldsymbol{\lambda}_\ell - \mathbf{a}_{s,\ell}^\dagger \mathbf{U} \right] \bmod \Lambda_{C,\ell} \\ &\stackrel{\text{w.h.p.}}{=} \mathbf{s}_\ell^\dagger + \mathbf{a}_{s,\ell}^\dagger \mathbf{Q}\end{aligned}\quad (6.8)$$

where the last equality holds with high probability as in (5.6), the quantization noise  $\mathbf{Q}$  has an effective covariance matrix  $\boldsymbol{\Omega} \triangleq \frac{1}{T} \mathbb{E}[\mathbf{Q}\mathbf{Q}^\dagger] = d\mathbf{A}_s\mathbf{A}_s^\dagger$  and  $d$  is the distortion level. Finally, the  $\ell^{\text{th}}$  BS transmits  $\mathbf{x}_\ell = \widehat{\mathbf{s}}_\ell$ .

**Remark 21** (RIFSC). *In case of parallel RIFSC, the linear equalizer  $\mathbf{B}$ , coding power matrix  $\mathbf{P}$ , integer matrix  $\mathbf{A}_s$  and distortion level  $d$  should be chosen to satisfy the constraints*

$$\begin{aligned}\frac{1}{2} \log \left( \frac{\mathbf{b}_\ell^\dagger \mathbf{P} \mathbf{b}_\ell + \|\mathbf{a}_{s,\ell}\|^2 d}{d} \right) &\leq C_\ell, \quad \forall \ell \in \mathcal{L} \\ \text{Tr}(\mathbf{B}\mathbf{P}\mathbf{B}^\dagger + \mathbf{A}_s \mathbf{D} \mathbf{A}_s^\dagger) &\leq P_{total}.\end{aligned}\quad (6.9)$$

**Remark 22** (SRIFSC). *In case of successive RIFSC, the linear equalizer  $\mathbf{B}$ , coding power matrix  $\mathbf{P}$ , integer matrix  $\mathbf{A}_s$  and distortion matrix  $\mathbf{D}$  should be chosen to satisfy the constraints*

$$\begin{aligned}\frac{1}{2} \log \left( \frac{\mathbf{b}_\ell^\dagger \mathbf{P} \mathbf{b}_\ell + \mathbf{a}_{s,\ell}^\dagger \mathbf{D} \mathbf{a}_{s,\ell}}{d_\ell} \right) &\leq C_\ell, \quad \forall \ell \in \mathcal{L} \\ \text{rank}(\mathbf{A}_{s,[1:m]}) &= m, \quad \forall m \in \mathcal{L} \\ d_L &\leq \dots \leq d_1 \\ \text{Tr}(\mathbf{B}\mathbf{P}\mathbf{B}^\dagger + \mathbf{A}_s \mathbf{D} \mathbf{A}_s^\dagger) &\leq P_{total}.\end{aligned}\quad (6.10)$$

### 6.3.3 Channel Decoding

The end-to-end channel can be written as

$$\mathbf{Y} = \mathbf{H} \left( \mathbf{B}\tilde{\mathbf{S}} + \mathbf{A}_s\mathbf{Q} \right) + \mathbf{Z} \quad (6.11)$$

where  $\mathbf{Y} = [\mathbf{y}_1 \cdots \mathbf{y}_K]^\dagger$ ,  $\mathbf{y}_k$  is the received signal at the  $k^{\text{th}}$  user.

As mentioned earlier in this section, the  $k^{\text{th}}$  user is interested in decoding  $\mathbf{v}_{c,k}^\dagger \triangleq \mathbf{a}_{c,k}^\dagger \tilde{\mathbf{S}}$ , which can be mapped later to the desired message  $\mathbf{w}_k^\dagger = \left[ \mathbf{a}_{c,k}^\dagger \tilde{\mathbf{W}} \right] \bmod p$ . In order to accomplish this, the  $k^{\text{th}}$  user equalizes (i.e., MMSE scaling) its received signal  $\mathbf{y}_k$  by  $v_k \in \mathbb{R}$  to get

$$\begin{aligned} \tilde{\mathbf{y}}_k^\dagger &\triangleq v_k \mathbf{y}_k^\dagger \\ &= \mathbf{v}_{c,k}^\dagger + \mathbf{z}_{\text{eff}}^\dagger \end{aligned} \quad (6.12)$$

where  $\mathbf{z}_{\text{eff}}^\dagger \triangleq (v_k \mathbf{h}_k^\dagger \mathbf{B} - \mathbf{a}_{c,k}^\dagger) \tilde{\mathbf{S}} + v_k \mathbf{z}_k^\dagger + v_k \mathbf{h}_k^\dagger \mathbf{A}_s \mathbf{Q}$  is an effective noise with effective variance

$$\sigma_{\text{eff},k}^2 \triangleq \frac{1}{T} \mathbb{E}(\|\mathbf{z}_{\text{eff}}\|^2) = \left\| \left( v_k \mathbf{h}_k^\dagger \mathbf{B} - \mathbf{a}_{c,k}^\dagger \right) \mathbf{P}^{\frac{1}{2}} \right\|^2 + (v_k)^2 + (v_k)^2 \mathbf{h}_k^\dagger \mathbf{A}_s \mathbf{D} \mathbf{A}_s^\dagger \mathbf{h}_k. \quad (6.13)$$

**Theorem 13.** *Similar to [Hong and Caire, 2011], it can be shown that the achievable sum-rate for the IF strategy is*

$$R_{\text{IF-CRAN}}(\mathbf{H}) = \max_{\substack{\mathbf{B} \in \mathbb{R}^{L \times K}, \mathbf{A}_c \in \mathbb{Z}^{K \times K} \\ \mathbf{D} = \text{diag}(d_1, \dots, d_L) \\ \mathbf{P} = \text{diag}(P_1, \dots, P_L)}} \sum_{k=1}^K \frac{1}{2} \log^+(\beta_k) \quad (6.14)$$

subject to

$$\text{Rank}(\mathbf{A}_c) = K$$

$$R_{\text{RIFSC},\ell}^s(\mathbf{B}\mathbf{P}\mathbf{B}^\dagger, \mathbf{D}) \leq C_\ell, \forall \ell \in \mathcal{L}$$

$$\text{Tr}(\mathbf{B}\mathbf{P}\mathbf{B}^\dagger + \mathbf{A}_s \mathbf{D} \mathbf{A}_s^\dagger) \leq P_{\text{total}}, \forall \ell \in \mathcal{L}$$

where  $\beta_k \triangleq P_k / \sigma_{\text{eff},k}^2$  is the  $k^{\text{th}}$  effective SINR for the  $k^{\text{th}}$  user and  $R_{\text{SRIFSC},\ell}^s(\mathbf{B}\mathbf{P}\mathbf{B}^\dagger, \mathbf{D})$

is given in (5.16). The proof of Theorem 13 follows the same steps in [He et al., 2018, Theorem 6], however, here we have the added quantization noise  $\mathbf{Q}$  with effective covariance matrix  $\mathbf{D}$ .

Finally, the MMSE equalizer that minimizes the variance in (7.17) and the corresponding variance are given by

$$v_k = \frac{\mathbf{a}_{c,k}^\dagger \mathbf{P} \mathbf{B}^\dagger \mathbf{h}_k}{1 + \mathbf{h}_k^\dagger (\mathbf{A}_s \mathbf{D} \mathbf{A}_s^\dagger + \mathbf{B} \mathbf{P} \mathbf{B}^\dagger) \mathbf{h}_k} \quad (6.15)$$

$$\sigma_{\text{eff},k}^2 = \|\mathbf{F}_{c,k} \mathbf{a}_{c,k}\|^2 \quad (6.16)$$

where  $\mathbf{F}_{c,k}$  is any matrix that satisfies the decomposition

$$\mathbf{F}_{c,k}^\dagger \mathbf{F}_{c,k} = \left( \mathbf{P}^{-1} + \mathbf{B}^\dagger \mathbf{h}_k \left( 1 + \mathbf{h}_k^\dagger \mathbf{A}_s \mathbf{D} \mathbf{A}_s^\dagger \mathbf{h}_k \right)^{-1} \mathbf{h}_k^\dagger \mathbf{B} \right)^{-1}.$$

Similar to the uplink, under fixed rate allocation  $C_1, \dots, C_L$  for the fronthaul network and assuming that the compression rates meet these constraints with equality, we write the achievable downlink distortion matrix  $\mathbf{D}$  in terms  $C_1, \dots, C_L$  as

$$\mathbf{D} = \text{diag}(\mathbf{R} \mathbf{e}) \quad (6.17)$$

where  $e_\ell \triangleq \mathbf{b}_\ell^\dagger \mathbf{P} \mathbf{b}_\ell$  is the  $\ell^{\text{th}}$  element of  $\mathbf{e}$ , while

$$\mathbf{R} \triangleq \begin{bmatrix} 2^{2C_1} - (a_{s,1,1})^2 & \dots & -(a_{s,1,L})^2 \\ \vdots & \ddots & \vdots \\ -(a_{s,L,1})^2 & \dots & 2^{2C_L} - (a_{s,L,L})^2 \end{bmatrix}^{-1}. \quad (6.18)$$

## Chapter 7

# Uplink-Downlink Integer-Forcing Duality through Algebraic Successive Decoding

In this chapter, we prove a sum-rate duality between the end-to-end IF schemes proposed in Chapters 4 and 6 for both the uplink and downlink C-RAN, respectively. Recent work in [He et al., 2018] proved the sum-rate IF duality between the uplink (i.e., MAC) and downlink (i.e., BC) channels where the authors only used channel codes. In compression-based strategies, the uplink (downlink) C-RAN channel however has additional source codes that are used to convey the BSs observations (channel codewords) from the BSs (CP) to the CP (BSs), respectively. These source codes adds to the complexity of establishing the duality, since the end-to-end transmission rates (i.e., channel code rate) depends on the distortion levels achieved in both directions (i.e., uplink and downlink directions) as we saw in Theorems 5 and 13. The distortion levels achieved depend consecutively on the compression rates allocation across the fronthaul links in both directions which may be different. In this work, we link both achievable distortion levels to the same compression rate allocation (e.g., the uplink compression rate allocation), even if this allocation was not achievable<sup>1</sup> for one direction (e.g., the downlink channel).

For clarity, in this chapter we denote all uplink parameters by superscript ul and all downlink parameters by superscript dl. We also assumes total fronthaul rates

---

<sup>1</sup>Even if the downlink rate allocation was not achievable, these downlink distortion levels can be achieved using different rate allocation, however, we write it in terms of the unachievable uplink rate allocation of the.

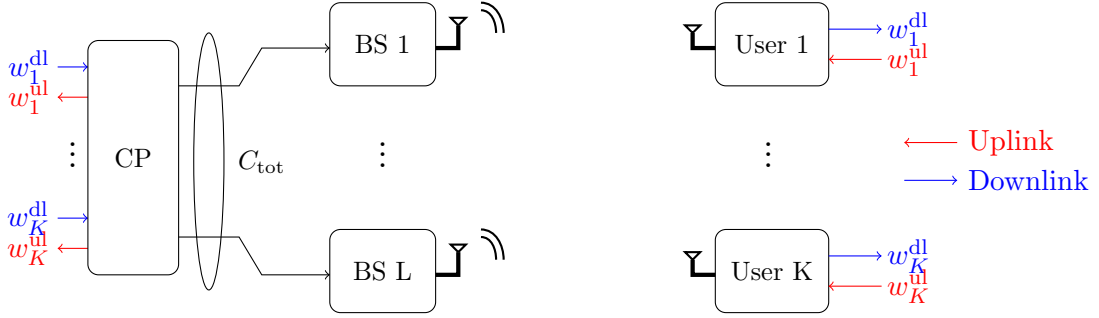


**Figure 7.1:** The Uplink and downlink C-RAN channel models.

constraint  $C_{\text{total}}$  and total power constraint  $P_{\text{total}}$ .

## 7.1 Uplink C-RAN

### 7.1.1 Uplink C-RAN Channel

In the uplink C-RAN, the  $k^{\text{th}}$  user has a message  $w_k^{\text{ul}} \in \{1, \dots, 2^{TR_k^{\text{ul}}}\}$  to the CP with rate  $R_k^{\text{ul}}$ . The  $k^{\text{th}}$  user maps  $w_k^{\text{ul}}$  to a lattice codeword  $\mathbf{s}_k^{\text{ul}} \in \mathbb{R}^T$  of length  $T$ , scales it using  $v_k^{\text{ul}} \in \mathbb{R}$ , then transmits  $\mathbf{x}_k^{\text{ul}} = v_k^{\text{ul}} \mathbf{s}_k^{\text{ul}}$ . The received signal at the BSs is given by

$$\mathbf{Y}^{\text{ul}} = \mathbf{H}^{\text{ul}} \mathbf{X}^{\text{ul}} + \mathbf{Z}^{\text{ul}}, \quad (7.1)$$

where  $\mathbf{Y}^{\text{ul}} \triangleq [\mathbf{y}_1^{\text{ul}} \dots \mathbf{y}_L^{\text{ul}}]^\dagger$ ,  $\mathbf{y}_\ell^{\text{ul}} \in \mathbb{R}^T$  is the received signal at the  $\ell^{\text{th}}$  BS,  $\mathbf{H}^{\text{ul}} \in \mathbb{R}^{L \times K}$  is the channel from all users to all BSs (assumed to be known to all terminals),  $\mathbf{X}^{\text{ul}} \triangleq [\mathbf{x}_1^{\text{ul}} \dots \mathbf{x}_K^{\text{ul}}]^\dagger = \mathbf{V}^{\text{ul}} \mathbf{S}^{\text{ul}}$ ,  $\mathbf{V}^{\text{ul}} \triangleq \text{diag}(v_1^{\text{ul}}, \dots, v_K^{\text{ul}})$  is the beamforming matrix,  $\mathbf{S}^{\text{ul}} \triangleq [\mathbf{s}_1^{\text{ul}} \dots \mathbf{s}_K^{\text{ul}}]^\dagger$  is the codeword matrix and  $\mathbf{Z}^{\text{ul}} \in \mathbb{R}^{L \times T}$  is i.i.d.  $\mathcal{N}(0, 1)$  noise. The BSs have a total power constraint<sup>2</sup>  $\text{Tr}(\mathbf{V}^{\text{ul}} \mathbf{P}^{\text{ul}} \mathbf{V}^{\text{ul}\dagger}) \leq P_{\text{total}}$ , where  $\mathbf{P}^{\text{ul}} \triangleq \frac{1}{T} \mathbb{E}[\mathbf{S}^{\text{ul}} \mathbf{S}^{\text{ul}\dagger}]$  is a diagonal coding power matrix. The  $\ell^{\text{th}}$  BS maps its received signal  $\mathbf{y}_\ell^{\text{ul}}$  into an index  $i_\ell^{\text{ul}} \in \{1, \dots, 2^{TC_\ell^{\text{ul}}}\}$ , where  $C_1^{\text{ul}}, \dots, C_L^{\text{ul}}$  are the  $L$  rates allocation to the  $L$  fronthaul links and satisfy  $\sum_{\ell=1}^L C_\ell^{\text{ul}} \leq C_{\text{total}}$ . Upon receiving the indices  $i_1^{\text{ul}}, \dots, i_L^{\text{ul}}$ ,

<sup>2</sup>Although standard uplink channel models employ individual power constraints on the users, a total power constraint is necessary here to enable us to establish uplink-downlink duality.

the CP makes estimates  $\hat{w}_1^{\text{ul}}, \dots, \hat{w}_K^{\text{ul}}$  of the transmitted messages. We say that the rates  $R_1^{\text{ul}}, \dots, R_K^{\text{ul}}$  are achievable if, for any  $\epsilon > 0$  and  $T$  large enough there exists encoders and decoders that attains average probability of error at most  $\epsilon$ .

### 7.1.2 Integer-Forcing for Uplink C-RAN

We begin with an overview of the integer-forcing scheme proposed in Chapter 4 for the uplink C-RAN, however, we assume here a total power constraints on the transmitters and that the channel  $\mathbf{H}$  is known at the transmitters (CSIT), hence we can allocate different rates to different transmitters. Without loss of generality, we assume for both the source and channel coding stages that the identity permutation is admissible [He et al., 2018, Definition 2], which will impose constraints on the effective noises and integer matrices.

Specifically, for the channel coding part, this means that we first permute the channel coding combinations  $\mathbf{v}_{c,1}^{\text{ul}}, \dots, \mathbf{v}_{c,K}^{\text{ul}}$  such that  $(\sigma_1^{\text{ul}})^2 \leq \dots \leq (\sigma_K^{\text{ul}})^2$ , then permute the  $K$  users such that the integer matrix  $\mathbf{A}_c^{\text{ul}}$  has full-rank sub-matrices  $\mathbf{A}_{c,[1:m]}^{\text{ul}}$  for  $m = 1, \dots, K$ .

On the other hand, for the source coding part, this means that we first permute the BSs such that  $d_L^{\text{ul}} \leq \dots \leq d_1^{\text{ul}}$ , then permutes the source coding combinations  $\mathbf{v}_{s,1}^{\text{ul}}, \dots, \mathbf{v}_{s,L}^{\text{ul}}$  such that the integer matrix  $\mathbf{A}_s^{\text{ul}}$  has full-rank sub-matrices  $\mathbf{A}_{s,[1:m]}^{\text{ul}}$  for  $m = 1, \dots, L$ .

**Uplink Source Coding.** The  $\ell^{\text{th}}$  BS uses a lattice codebook  $\mathcal{C}_\ell \triangleq \Lambda_{F,\ell} \cap \mathcal{V}(\Lambda_{C,\ell})$  with rate  $C_\ell^{\text{ul}}$  to quantize its observation  $\mathbf{y}_\ell^{\text{ul}}$ ,

$$\boldsymbol{\lambda}_\ell^{\text{ul}} = [\mathcal{Q}_{\Lambda_{F,\ell}}(\mathbf{y}_\ell^{\text{ul}} + \mathbf{u}_\ell^{\text{ul}})] \bmod \Lambda_{C,\ell} \quad (7.2)$$

where  $\mathbf{u}_\ell^{\text{ul}}$  is a random dither independent of  $\mathbf{y}_\ell^{\text{ul}}$  and uniformly distributed over  $\mathcal{V}(\Lambda_{F,\ell})$ . The  $\ell^{\text{th}}$  BS then forwards the index  $i_\ell^{\text{ul}} \in \{1, \dots, 2^{TC_\ell^{\text{ul}}}\}$  of  $\boldsymbol{\lambda}_\ell^{\text{ul}}$  to the CP

through the fronthaul link.

For a fixed integer matrix  $\mathbf{A}_s^{\text{ul}} \triangleq [\mathbf{a}_{s,1}^{\text{ul}} \cdots \mathbf{a}_{s,L}^{\text{ul}}]^\dagger$  with full-rank sub-matrices  $\mathbf{A}_{s,[1:m]}^{\text{ul}}$  for  $m = 1, \dots, L$ , the CP uses the integer-forcing source coding with algebraic successive cancellation in Section 3.3.3 to recover

$$\widehat{\mathbf{Y}}^{\text{ul}} = \mathbf{H}^{\text{ul}} \mathbf{V}^{\text{ul}} \mathbf{S}^{\text{ul}} + \mathbf{Z}^{\text{ul}} + \mathbf{Q}^{\text{ul}} \quad (7.3)$$

where  $\mathbf{Q}^{\text{ul}} \triangleq [\mathbf{q}_1^{\text{ul}} \cdots \mathbf{q}_L^{\text{ul}}]^\dagger$  has effective covariance matrix  $\mathbf{D}^{\text{ul}} \triangleq \frac{1}{T} \mathbb{E}[\mathbf{Q}^{\text{ul}} \mathbf{Q}^{\text{ul}\dagger}] = \text{diag}(d_1^{\text{ul}}, \dots, d_L^{\text{ul}})$ . Since  $\mathbf{A}_s^{\text{ul}}$  and  $\mathbf{D}^{\text{ul}}$  should be chosen such that, the successive IFSC rate  $R_{\text{SIFSC},\ell}^s = C_\ell$  for  $\ell = 1, \dots, L$ , we can write the distortion levels  $d_1^{\text{ul}}, \dots, d_L^{\text{ul}}$  in terms of the fronthaul rate allocation  $C_1^{\text{ul}}, \dots, C_L^{\text{ul}}$  as in the next Lemma.

**Lemma 17.** *For the uplink C-RAN with sum-rate backhaul constraint  $C_{\text{total}}$  and an integer matrix  $\mathbf{A}_s^{\text{ul}}$  that satisfies  $\text{rank}(\mathbf{A}_{s,[1:m]}^{\text{ul}}) = m, \forall m \in \mathcal{L}$ , the achievable distortion levels  $d_1^{\text{ul}}, \dots, d_L^{\text{ul}}$  can be written in terms of the rate allocation  $C_1^{\text{ul}}, \dots, C_L^{\text{ul}}$  as*

$$\mathbf{d}^{\text{ul}} = \mathbf{R}^{\text{ul}} \mathbf{e}^{\text{ul}} \quad (7.4)$$

where  $d_\ell^{\text{ul}}$  and  $e_\ell^{\text{ul}} \triangleq \mathbf{a}_{s,\ell}^{\text{ul}\dagger} (\mathbf{H}^{\text{ul}} \mathbf{V}^{\text{ul}} \mathbf{P}^{\text{ul}} \mathbf{V}^{\text{ul}\dagger} \mathbf{H}^{\text{ul}\dagger} + \mathbf{I}) \mathbf{a}_{s,\ell}^{\text{ul}}$  are the  $\ell^{\text{th}}$  elements of  $\mathbf{d}^{\text{ul}}$  and  $\mathbf{e}^{\text{ul}}$ , respectively, while

$$\mathbf{R}^{\text{ul}} \triangleq \begin{bmatrix} 2^{2C_1^{\text{ul}}} - (a_{s,1,1}^{\text{ul}})^2 & \cdots & -(a_{s,1,L}^{\text{ul}})^2 \\ \vdots & \ddots & \vdots \\ -(a_{s,L,1}^{\text{ul}})^2 & \cdots & 2^{2C_L^{\text{ul}}} - (a_{s,L,L}^{\text{ul}})^2 \end{bmatrix}^{-1}. \quad (7.5)$$

The proof of Lemma 17 follows from Theorem 2.

**Uplink Channel Coding.** The users draw their codewords  $\mathbf{s}_1^{\text{ul}}, \dots, \mathbf{s}_K^{\text{ul}}$  from nested lattice codebooks, which are selected via Lemma 2. After reconstructing the quantized BS observations  $\widehat{\mathbf{Y}}^{\text{ul}}$ , the CP proceeds to successively decode integer-linear combinations  $\mathbf{v}_{c,1}^{\text{ul}}, \dots, \mathbf{v}_{c,K}^{\text{ul}}$  of channel codewords  $\mathbf{s}_1^{\text{ul}}, \dots, \mathbf{s}_K^{\text{ul}}$ , as in [Nazer et al., 2016, Lemma 16], where

$$\mathbf{v}_{c,m}^{\text{ul}} \triangleq \sum_{k=1}^K a_{c,m,k}^{\text{ul}} \mathbf{s}_k^{\text{ul}}, \quad \forall m \in \mathcal{K}, \quad a_{c,m,k} \in \mathbb{Z}.$$

At the  $m^{\text{th}}$  channel decoding step (i.e., when decoding  $\mathbf{v}_{c,m}^{\text{ul}}$ ) and assuming correct decoding of  $\mathbf{v}_{c,1}^{\text{ul}}, \dots, \mathbf{v}_{c,m-1}^{\text{ul}}$ , the CP first employs a linear equalizer  $\mathbf{b}_m^{\text{ul}}$  to obtain

$$\mathbf{b}_m^{\text{ul}\dagger} \widehat{\mathbf{Y}}^{\text{ul}} = \mathbf{v}_{c,m}^{\text{ul}\dagger} + \underbrace{(\mathbf{b}_m^{\text{ul}\dagger} \mathbf{H}^{\text{ul}} \mathbf{V}^{\text{ul}} - \mathbf{a}_{c,m}^{\text{ul}\dagger}) \mathbf{S}^{\text{ul}} + \mathbf{b}_m^{\text{ul}\dagger} \mathbf{Z}^{\text{ul}} + \mathbf{b}_m^{\text{ul}\dagger} \mathbf{Q}^{\text{ul}}}_{\mathbf{z}_{\text{eff},m}^{\text{ul}\dagger}}$$

where the effective noise  $\mathbf{z}_{\text{eff},m}^{\text{ul}}$  has an effective variance

$$(\sigma_m^{\text{ul}})^2 \triangleq \frac{1}{T} \mathbb{E} \|\mathbf{z}_{\text{eff},m}^{\text{ul}}\|^2 = \|(\mathbf{b}_m^{\text{ul}\dagger} \mathbf{H}^{\text{ul}} \mathbf{V}^{\text{ul}} - \mathbf{a}_{c,m}^{\text{ul}\dagger}) \mathbf{P}^{\text{ul}\frac{1}{2}}\|^2 + \|\mathbf{b}_m^{\text{ul}}\|^2 + \mathbf{b}_m^{\text{ul}\dagger} \mathbf{D}^{\text{ul}} \mathbf{b}_m^{\text{ul}}. \quad (7.6)$$

Finally, it is worth noting that the MMSE equalizer that minimizes (7.6) and the corresponding variance are given by

$$\mathbf{b}_m^{\text{ul}\dagger} = \mathbf{a}_{c,m}^{\text{ul}\dagger} \mathbf{P}^{\text{ul}\dagger} \mathbf{V}^{\text{ul}\dagger} \mathbf{H}^{\text{ul}\dagger} (\mathbf{H}^{\text{ul}} \mathbf{V}^{\text{ul}} \mathbf{P}^{\text{ul}} \mathbf{V}^{\text{ul}\dagger} \mathbf{H}^{\text{ul}\dagger} + \mathbf{I} + \mathbf{D}^{\text{ul}})^{-1} \quad (7.7)$$

$$(\sigma_m^{\text{ul}})^2 = \|\mathbf{F}_c^{\text{ul}} \mathbf{a}_{c,m}^{\text{ul}}\|^2 \quad (7.8)$$

where  $\mathbf{F}_c^{\text{ul}}$  is any matrix that satisfies

$$\mathbf{F}_c^{\text{ul}\dagger} \mathbf{F}_c^{\text{ul}} = \left( (\mathbf{P}^{\text{ul}})^{-1} + \mathbf{V}^{\text{ul}\dagger} \mathbf{H}^{\text{ul}\dagger} (\mathbf{I} + \mathbf{D}^{\text{ul}})^{-1} \mathbf{H}^{\text{ul}} \mathbf{V}^{\text{ul}} \right)^{-1}. \quad (7.9)$$

**Lemma 18.** For an uplink channel  $\mathbf{H}^{\text{ul}}$ , beamforming matrix  $\mathbf{V}^{\text{ul}}$ , coding power matrix  $\mathbf{P}^{\text{ul}}$ , coding power vector  $\boldsymbol{\rho}^{\text{ul}} = \text{diag}(\mathbf{P}^{\text{ul}})$  and equalization matrix  $\mathbf{B}^{\text{ul}}$ , we can write (7.6) as

$$(\mathbf{I} - \text{diag}(\boldsymbol{\beta}^{\text{ul}}) \mathbf{M}^{\text{ul}}) \boldsymbol{\rho}^{\text{ul}} = \mathbf{J}^{\text{ul}} \boldsymbol{\beta}^{\text{ul}} \quad (7.10)$$

where  $\boldsymbol{\beta}^{\text{ul}} = [\beta_1^{\text{ul}} \dots \beta_K^{\text{ul}}]^\dagger$ ,  $\beta_k^{\text{ul}} = P_k^{\text{ul}} / (\sigma_k^{\text{ul}})^2$  is the  $k^{\text{th}}$  effective SINR,  $\mathbf{J}^{\text{ul}} = \text{diag}(J_1^{\text{ul}}, \dots, J_K^{\text{ul}})$ ,  $J_k^{\text{ul}} = \|\mathbf{b}_k^{\text{ul}}\|^2 + \sum_i \sum_j (b_{k,i}^{\text{ul}})^2 R_{i,j}^{\text{ul}} \|\mathbf{a}_{s,j}^{\text{ul}}\|^2$ ,  $M_{k,\ell}^{\text{ul}} = (\mathbf{b}_k^{\text{ul}\dagger} \mathbf{h}_\ell^{\text{ul}} v_\ell^{\text{ul}} - a_{c,k,\ell}^{\text{ul}})^2 + \sum_i \sum_j (b_{k,i}^{\text{ul}})^2 R_{i,j}^{\text{ul}} (\mathbf{a}_{s,j}^{\text{ul}\dagger} \mathbf{h}_\ell^{\text{ul}})^2 (v_\ell^{\text{ul}})^2$  is the  $(k, \ell)^{\text{th}}$  element of  $\mathbf{M}^{\text{ul}}$  and  $\mathbf{h}_\ell^{\text{ul}}$  is the  $\ell^{\text{th}}$  column of  $\mathbf{H}^{\text{ul}}$ .

The proof of Lemma 18 is given in Appendix F.

Finally, using the successive decoding in [Nazer et al., 2016, Lemma 16], the achievable rates for the uplink IF-CRAN can be written in terms of effective SINR as

$$R_{\text{UL-IF-CRAN},k}(\mathbf{H}^{\text{ul}}) = \frac{1}{2} \log^+ (\beta_k^{\text{ul}}), \forall k \in \mathcal{K} \quad (7.11)$$

where  $\beta_k^{\text{ul}} = P_k^{\text{ul}}/(\sigma_k^{\text{ul}})^2$  is the  $k^{\text{th}}$  effective SINR.

## 7.2 Downlink C-RAN

### 7.2.1 Downlink C-RAN Channel

In the downlink C-RAN, the CP has  $K$  messages  $w_k^{\text{dl}} \in \{1, \dots, 2^{TR_k^{\text{dl}}}\}$  with rate  $R_k^{\text{dl}}$ , for  $k = 1, \dots, K$ , to the  $K$  users where the  $k^{\text{th}}$  user is interested in the  $k^{\text{th}}$  message  $w_k^{\text{dl}}$ . The CP maps the  $K$  messages  $w_1^{\text{dl}}, \dots, w_K^{\text{dl}}$  into  $L$  indices  $i_1^{\text{dl}}, \dots, i_L^{\text{dl}}$ , where  $i_\ell^{\text{dl}} \in \{1, \dots, 2^{TC_\ell^{\text{dl}}}\}$  has a rate  $C_\ell^{\text{dl}}$  for  $\ell = 1, \dots, L$  and the rates satisfy  $\sum_{\ell=1}^L C_\ell^{\text{dl}} \leq C_{\text{total}}$ . The  $i_\ell^{\text{dl}}$  is then forwarded to the  $\ell^{\text{th}}$  BS through the fronthaul network. The  $\ell^{\text{th}}$  BS transmits the codeword  $\mathbf{x}_\ell \in \mathbb{R}^T$ .

The received signal across all users is

$$\mathbf{Y}^{\text{dl}} = \mathbf{H}^{\text{dl}}\mathbf{X}^{\text{dl}} + \mathbf{Z}^{\text{dl}} \quad (7.12)$$

where  $\mathbf{Y}^{\text{dl}} \triangleq [\mathbf{y}_1^{\text{dl}} \dots \mathbf{y}_K^{\text{dl}}]^\dagger$ ,  $\mathbf{y}_k^{\text{dl}} \in \mathbb{R}^T$  is the received signal at the  $k^{\text{th}}$  user,  $\mathbf{H}^{\text{dl}} \in \mathbb{R}^{K \times L}$  is the channel matrix from the  $L$  BSs to the  $K$  users,  $\mathbf{X}^{\text{dl}} \triangleq [\mathbf{x}_1^{\text{dl}} \dots \mathbf{x}_L^{\text{dl}}]^\dagger$  and  $\mathbf{Z}^{\text{dl}} \in \mathbb{R}^{K \times T}$  is i.i.d.  $\mathcal{N}(0, 1)$ . Similar to the uplink, we have a total power constraint  $\frac{1}{T}\mathbb{E}\text{Tr}(\mathbf{X}^{\text{dl}}\mathbf{X}^{\text{dl}\dagger}) \leq P_{\text{total}}$ <sup>3</sup>. The  $k^{\text{th}}$  user makes an estimate  $\hat{w}_k^{\text{dl}}$  of the transmitted message based on  $\mathbf{y}_k^{\text{dl}}$ . We say that the rates  $R_1^{\text{dl}}, \dots, R_K^{\text{dl}}$  are achievable if, for any  $\epsilon > 0$  and  $T$  large enough there exists encoders and decoders that attains average probability of error at most  $\epsilon$ .

<sup>3</sup>We assume equal power constraints  $P_{\text{total}}$  between the uplink and downlink channels since we are seeking to prove duality between both proposed IF schemes, however, in a practical system, both constraints should not be equal and the BSs usually have more power.

### 7.2.2 Integer-Forcing for Downlink C-RAN

For the channel coding part, we use the integer-forcing beamforming strategy introduced for the downlink channel in [Hong and Caire, 2012] for symmetric powers, then extended in [He et al., 2018] to the asymmetric powers setting. For the source coding part, we use the successive reverse integer-forcing source coding (SRIFSC) in Section 5.3.2.

#### Downlink Channel Encoding.

The CP successively, as in [He et al., 2018, Section VI], maps the messages  $\mathbf{w}_1^{\text{dl}}, \dots, \mathbf{w}_K^{\text{dl}}$  to lattice codewords  $\mathbf{s}_1^{\text{dl}}, \dots, \mathbf{s}_K^{\text{dl}}$  with coding power matrix  $\mathbf{P}^{\text{dl}} \triangleq \frac{1}{T} \mathbb{E}[\mathbf{S}^{\text{dl}} \mathbf{S}^{\text{dl}\dagger}]$ , where  $\mathbf{S}^{\text{dl}} \triangleq [\mathbf{s}_1^{\text{dl}} \dots \mathbf{s}_K^{\text{dl}}]^\dagger$  is the channel codeword matrix,  $\mathbf{w}_k^{\text{dl}}$  is the  $p$ -ary expansion of  $w_k^{\text{dl}}$  and  $p$  is a prime.

Briefly, for a fixed integer matrix  $\mathbf{A}_c^{\text{dl}}$  with full-rank sub-matrices  $\mathbf{A}_{c,[1:m]}^{\text{dl}}$  for  $m = 1, \dots, K$ , the CP first forms the precoded messages  $\tilde{\mathbf{w}}_1^{\text{dl}}, \dots, \tilde{\mathbf{w}}_K^{\text{dl}}$  by successively applying the inverse of  $[\mathbf{A}_{c,[1:m]}^{\text{dl}}] \bmod p$  over  $\mathbb{Z}_p$  to the messages  $\mathbf{w}_1^{\text{dl}}, \dots, \mathbf{w}_K^{\text{dl}}$ , then map  $\tilde{\mathbf{w}}_m^{\text{dl}}$  to the lattice codeword  $\mathbf{s}_m^{\text{dl}}$  for each encoding step  $m = 1, \dots, K$ .

Next, the CP uses a beamforming matrix  $\mathbf{B}^{\text{dl}} \in \mathbb{R}^{L \times K}$  to form  $\tilde{\mathbf{S}}^{\text{dl}} = \mathbf{B}^{\text{dl}} \mathbf{S}^{\text{dl}}$ , where  $\tilde{\mathbf{S}}^{\text{dl}} \triangleq [\tilde{\mathbf{s}}_1^{\text{dl}} \dots \tilde{\mathbf{s}}_L^{\text{dl}}]^\dagger$ .

**Downlink Source Coding.** The CP then compresses  $\tilde{\mathbf{s}}_1^{\text{dl}}, \dots, \tilde{\mathbf{s}}_L^{\text{dl}}$  using the SRIFSC discussed in Section 5.3.2. This can be done by first pre-inverting  $\tilde{\mathbf{S}}^{\text{dl}}$  with integer matrix  $\mathbf{A}_s^{\text{dl}}$  which has full-rank submatrices  $\mathbf{A}_{s,[1:m]}^{\text{dl}}$  for  $m = 1, \dots, L$  to get

$$\mathbf{V}_s^{\text{dl}} = (\mathbf{A}_s^{\text{dl}})^{-1} \tilde{\mathbf{S}}^{\text{dl}} \quad (7.13)$$

where  $\mathbf{V}_s^{\text{dl}} \triangleq [\mathbf{v}_{s,1}^{\text{dl}} \dots \mathbf{v}_{s,L}^{\text{dl}}]^\dagger$ . Next, using lattice codebooks  $\mathcal{C}_\ell \triangleq \Lambda_{F,\ell} \cap \mathcal{V}(\Lambda_{C,\ell})$ , the CP quantizes and forms integer-linear combinations

$$\boldsymbol{\lambda}_m^{\text{dl}} = \left[ \sum_{k=1}^m L_{m,k}^{\text{dl}} \mathcal{Q}_{\Lambda_{F,k}}(\mathbf{v}_{s,k}^{\text{dl}} + \mathbf{u}_k^{\text{dl}} + \mathbf{g}_k^{\text{dl}}) \right] \bmod \Lambda_{C,m} \quad (7.14)$$

where  $\mathbf{u}_1^{\text{dl}}, \dots, \mathbf{u}_L^{\text{dl}}$  are independent dithers,  $L_{m,k}^{\text{dl}}$  is the  $(m, k)^{\text{th}}$  element of the lower triangular matrix  $\mathbf{L}^{\text{dl}}$  and  $\mathbf{g}_k^{\text{dl}}$  is the  $k^{\text{th}}$  row of the matrix  $\mathbf{G}^{\text{dl}}$  discussed in Section 5.3.2.

The BSs then recover and re-transmit

$$\mathbf{X}^{\text{dl}} = \tilde{\mathbf{S}}^{\text{dl}} + \tilde{\mathbf{Q}}^{\text{dl}}$$

where  $\tilde{\mathbf{Q}}^{\text{dl}} \triangleq \mathbf{A}_s^{\text{dl}} \mathbf{Q}^{\text{dl}}$  and  $\mathbf{Q}^{\text{dl}}$  has effective covariance matrix  $\mathbf{D}^{\text{dl}} \triangleq \frac{1}{T} \mathbb{E}[\mathbf{Q}^{\text{dl}} \mathbf{Q}^{\text{dl}\dagger}]$ . Since the achievable rates for both integer-forcing schemes (i.e., uplink and downlink) depend on the achievable distortion levels, the next lemma helps us to express the distortion levels achieved in the downlink channel in terms of the uplink parameters.

**Lemma 19.** *For the downlink C-RAN with sum-rate capacity constraint  $C_{\text{total}}$ , the following distortion levels  $d_1^{\text{dl}}, \dots, d_L^{\text{dl}}$  are achievable using the SRIFSC compression scheme*

$$\mathbf{d}^{\text{dl}} = \mathbf{R}^{\text{dl}} \mathbf{e}^{\text{dl}} \quad (7.15)$$

where  $d_\ell^{\text{dl}}$  and  $e_\ell^{\text{dl}} \triangleq \mathbf{b}_\ell^{\text{dl}\dagger} \mathbf{P}^{\text{dl}} \mathbf{b}_\ell^{\text{dl}}$  are the  $\ell^{\text{th}}$  elements of  $\mathbf{d}^{\text{dl}}$  and  $\mathbf{e}^{\text{dl}}$ , respectively, while

$$\mathbf{R}^{\text{dl}} \triangleq \begin{bmatrix} 2^{2C_1^{\text{ul}}} - (a_{s,1,1}^{\text{dl}})^2 & \dots & -(a_{s,1,L}^{\text{dl}})^2 \\ \vdots & \ddots & \vdots \\ -(a_{s,L,1}^{\text{dl}})^2 & \dots & 2^{2C_L^{\text{ul}}} - (a_{s,L,L}^{\text{dl}})^2 \end{bmatrix}^{-1}$$

where  $C_1^{\text{ul}}, \dots, C_L^{\text{ul}}$  are the uplink rate allocation. Furthermore, if we choose integer matrix  $\mathbf{A}_s^{\text{dl}} = \mathbf{A}_s^{\text{ul}\dagger}$ , we have  $\mathbf{R}^{\text{dl}} = \mathbf{R}^{\text{ul}}$ .

The proof of Lemma 19 is given in Appendix F.

**Downlink Channel Decoding.** The  $k^{\text{th}}$  user attempt decoding  $\mathbf{v}_{c,k}^{\text{dl}\dagger} = \mathbf{a}_{c,k}^{\text{dl}\dagger} \mathbf{S}^{\text{dl}}$ , which (if successfully decoded) can be mapped back to its desired message  $\mathbf{w}_k^{\text{dl}}$ . To do so, it equalizes its received signal, using  $v_k^{\text{dl}}$ , to get

$$\begin{aligned} \tilde{\mathbf{y}}_k^{\text{dl}\dagger} &\triangleq v_k^{\text{dl}} \mathbf{y}_k^{\text{dl}\dagger} \\ &= \mathbf{v}_{c,k}^{\text{dl}\dagger} + \mathbf{z}_{\text{eff}}^{\text{dl}\dagger} \end{aligned} \quad (7.16)$$

where  $\mathbf{z}_{\text{eff}}^{\text{dl}\dagger} \triangleq (v_k^{\text{dl}} \mathbf{h}_k^{\text{dl}\dagger} \mathbf{B}^{\text{dl}} - \mathbf{a}_{c,k}^{\text{dl}\dagger}) \mathbf{S}^{\text{dl}} + v_k^{\text{dl}} \mathbf{z}_k^{\text{dl}\dagger} + v_k^{\text{dl}} \mathbf{h}_k^{\text{dl}\dagger} \mathbf{A}_s^{\text{dl}} \mathbf{Q}^{\text{dl}}$  is an effective noise with effective variance

$$(\sigma_k^{\text{dl}})^2 \triangleq \frac{1}{T} \mathbb{E}(\|\mathbf{z}_{\text{eff}}^{\text{dl}}\|^2) = \left\| \left( v_k^{\text{dl}} \mathbf{h}_k^{\text{dl}\dagger} \mathbf{B}^{\text{dl}} - \mathbf{a}_{c,k}^{\text{dl}\dagger} \right) \mathbf{P}^{\text{dl}\frac{1}{2}} \right\|^2 + (v_k^{\text{dl}})^2 + (v_k^{\text{dl}})^2 \mathbf{h}_k^{\text{dl}\dagger} \mathbf{A}_s^{\text{dl}} \mathbf{D}^{\text{dl}} \mathbf{A}_s^{\text{dl}\dagger} \mathbf{h}_k^{\text{dl}}. \quad (7.17)$$

**Lemma 20.** *Let*

$$\boldsymbol{\beta}^{\text{dl}} \triangleq \begin{bmatrix} P_1^{\text{dl}} / (\sigma_1^{\text{dl}})^2 \\ \vdots \\ P_K^{\text{dl}} / (\sigma_K^{\text{dl}})^2 \end{bmatrix} \quad \text{and} \quad \boldsymbol{\rho}^{\text{dl}} \triangleq \begin{bmatrix} P_1^{\text{dl}} \\ \vdots \\ P_K^{\text{dl}} \end{bmatrix} \quad (7.18)$$

denote the effective SINR and coding power vectors, respectively, then (7.17) can be written as

$$(\mathbf{I} - \text{diag}(\boldsymbol{\beta}^{\text{dl}}) \mathbf{M}^{\text{dl}}) \boldsymbol{\rho}^{\text{dl}} = \mathbf{J}^{\text{dl}} \boldsymbol{\beta}^{\text{dl}} \quad (7.19)$$

where  $M_{\ell,k}^{\text{dl}} = (\mathbf{h}_\ell^{\text{dl}\dagger} \mathbf{b}_k^{\text{dl}} v_\ell^{\text{dl}} - a_{c,\ell,k}^{\text{dl}})^2 + \sum_i \sum_j b_{i,k}^{\text{dl}2} R_{j,i}^{\text{dl}} (\tilde{\mathbf{a}}_{s,j}^{\text{dl}\dagger} \mathbf{h}_\ell^{\text{dl}})^2 (v_\ell^{\text{dl}})^2$  is the  $(\ell, k)^{\text{th}}$  element of  $\mathbf{M}^{\text{dl}}$ ,  $\mathbf{h}_\ell^{\text{dl}}$  is the  $\ell^{\text{th}}$  column of  $\mathbf{H}^{\text{dl}}$ ,  $\tilde{\mathbf{a}}_{s,j}^{\text{dl}}$  is the  $j^{\text{th}}$  column of  $\mathbf{A}_s^{\text{dl}}$  and  $\mathbf{J}^{\text{dl}} = \text{diag}((v_1^{\text{dl}})^2, \dots, (v_K^{\text{dl}})^2)$ .

The proof of Lemma 20 is given in Appendix F.

Finally, the asymmetric achievable rates for downlink IF-CRAN can be written in terms of effective SINR as

$$R_{\text{DL-IF-CRAN},k}(\mathbf{H}^{\text{dl}}) = \frac{1}{2} \log^+ (\beta_k^{\text{dl}}), \forall k \in \mathcal{K} \quad (7.20)$$

where  $\beta_k^{\text{dl}} = P_k^{\text{dl}} / (\sigma_k^{\text{dl}})^2$  is the  $k^{\text{th}}$  effective SINR. This follows directly from [He et al., 2018, Theorem 6].

### 7.3 Duality

**Lemma 21.** *For the dual channel  $\mathbf{H}^{dl} = \mathbf{H}^{ul\dagger}$  and by choosing  $C_\ell^{dl} = C_\ell^{ul}$  for  $\ell = 1, \dots, L$ ,  $\mathbf{B}^{dl} = \mathbf{B}^{ul\dagger}$ ,  $\mathbf{V}^{dl} = \mathbf{V}^{ul}$ ,  $\mathbf{A}_c^{dl} = \mathbf{A}_c^{ul\dagger}$  and  $\mathbf{A}_s^{dl} = \mathbf{A}_s^{ul\dagger}$ , we have*

$$\mathbf{R}^{dl} = \mathbf{R}^{ul\dagger} \quad (7.21)$$

$$\mathbf{M}^{dl} = \mathbf{M}^{ul\dagger} \quad (7.22)$$

and the distortion matrix  $\mathbf{D}^{dl} = \text{diag}(\mathbf{R}^{dl}\mathbf{e}^{dl})$  is achievable even though the downlink compression rate allocation  $C_1^{dl}, \dots, C_L^{dl}$  may not be achievable.

The proof of Lemma 21 is straightforward and follows from both Lemma 18 and Lemma 20.

**Theorem 14.** *Let  $R_{IF-CRAN}^{ul}$  be the achievable sum-rate using integer-forcing equalization and compression for a given uplink channel  $\mathbf{H}^{ul}$ , integer matrices  $\mathbf{A}_c^{ul}$  and  $\mathbf{A}_s^{ul}$ , coding power matrix  $\mathbf{P}^{ul}$ , equalization matrix  $\mathbf{B}^{ul}$  and beamforming matrix  $\mathbf{V}^{ul}$  that satisfies the total power constraint  $P_{total}$ . Then, for the dual downlink channel  $\mathbf{H}^{dl} = \mathbf{H}^{ul\dagger}$ , we can achieve a sum-rate  $\sum_{k=1}^K R_{DL-IF-CRAN,k} \geq \sum_{k=1}^K R_{UL-IF-CRAN,k}$ .*

*Proof.* We start by defining a *Z-matrix* as any square matrix that has non-positive off-diagonal elements. The *Z-matrix* is called an *M-matrix* if it has eigenvalues with positive real parts. Next, we borrow the next theorem from the theory of non-negative matrices.

**Lemma 22.** *[Plemmons, 1977, Theorem 1] Let  $\mathbf{L}$  be a *Z-matrix*, then the following statements are equivalent.*

1.  $\mathbf{L}$  is an *M-matrix*.
2.  $\mathbf{L}^{-1}$  exists and non-negative.
3. There exists  $\mathbf{x} \geq 0$  such that  $\mathbf{L}\mathbf{x} > 0$ .
4. Every real eigenvalue of  $\mathbf{L}$  is positive.

Now back to our proof. It follows from Lemma 21 that by setting  $\mathbf{B}^{\text{dl}}, \mathbf{V}^{\text{dl}}, \mathbf{A}_c^{\text{dl}}$  and  $\mathbf{A}_s^{\text{dl}}$ , we have  $\mathbf{M}^{\text{dl}} = \mathbf{M}^{\text{ul}\dagger}$ . Furthermore, from (7.5), it follows that  $(\mathbf{R}^{\text{ul}})^{-1}$  is a Z-matrix. Furthermore, we can write the uplink achievable distortion levels  $(\mathbf{D}^{\text{ul}}) \geq 0$  as a solution for  $(\mathbf{R}^{\text{ul}})^{-1}\mathbf{x} = \mathbf{e}^{\text{ul}}$ , where  $\mathbf{e}^{\text{ul}} > 0$ . From Lemma 22, it follows that  $(\mathbf{R}^{\text{ul}})^{-1}$  is an M-matrix and that  $\mathbf{R}^{\text{ul}}$  is a non-negative matrix. Following the same argument we can prove that  $(\mathbf{R}^{\text{dl}})^{-1}$  is an M-matrix and that  $\mathbf{R}^{\text{dl}}$  is a non-negative matrix. Now looking at the  $(k, \ell)^{\text{th}}$  element of  $\mathbf{M}^{\text{ul}}$ , we can show that  $\mathbf{M}^{\text{ul}}$  is a non-negative matrix as well (same result holds for  $\mathbf{M}^{\text{dl}}$  since  $\mathbf{M}^{\text{dl}} = \mathbf{M}^{\text{ul}\dagger}$ ).

Next, we repeat the same argument for the matrix  $(\mathbf{I} - \text{diag}(\boldsymbol{\beta}^{\text{ul}})\mathbf{M}^{\text{ul}})$  instead of  $(\mathbf{R}^{\text{ul}})^{-1}$ . Looking at the off-diagonal elements of  $(\mathbf{I} - \text{diag}(\boldsymbol{\beta}^{\text{ul}})\mathbf{M}^{\text{ul}})$  (i.e., the off diagonal elements of  $-\text{diag}(\boldsymbol{\beta}^{\text{ul}})\mathbf{M}^{\text{ul}}$ ), it follows that  $(\mathbf{I} - \text{diag}(\boldsymbol{\beta}^{\text{ul}})\mathbf{M}^{\text{ul}})$  is a Z-matrix. Furthermore, since we have a positive uplink power allocation  $\boldsymbol{\rho}^{\text{ul}} \geq 0$  that is a solution for (7.10) for positive  $\mathbf{J}^{\text{ul}}\boldsymbol{\beta}^{\text{ul}}$ , we have that  $(\mathbf{I} - \text{diag}(\boldsymbol{\beta}^{\text{ul}})\mathbf{M}^{\text{ul}})$  is an M-matrix.

By setting  $\boldsymbol{\beta}^{\text{dl}} = \boldsymbol{\beta}^{\text{ul}}$  and noting that both  $\text{diag}(\boldsymbol{\beta}^{\text{ul}})\mathbf{M}^{\text{dl}}$  and  $\text{diag}(\boldsymbol{\beta}^{\text{ul}})\mathbf{M}^{\text{ul}}$  have the same eigenvalues, we deduce that there exists a unique non-negative downlink coding power vector

$$\boldsymbol{\rho}^{\text{dl}} = (\mathbf{I} - \text{diag}(\boldsymbol{\beta}^{\text{dl}})\mathbf{M}^{\text{dl}})^{-1}\mathbf{J}^{\text{dl}}\boldsymbol{\beta}^{\text{dl}} \quad (7.23)$$

that satisfies (7.19).

Finally, it remains to check that this coding power vector satisfies the total power constraints. To this end, define

$$\begin{aligned} \boldsymbol{\rho}_{tot}^{\text{ul}} &\triangleq \mathbf{N}^{\text{ul}}\boldsymbol{\rho}^{\text{ul}} \in \mathbb{R}^K \\ \boldsymbol{\rho}_{tot}^{\text{dl}} &\triangleq \mathbf{N}^{\text{dl}}\boldsymbol{\rho}^{\text{dl}} \in \mathbb{R}^L \end{aligned}$$

as the power allocated across transmitters for the uplink and downlink, where  $\mathbf{N}^{\text{ul}} = \text{diag}((v_1^{\text{ul}})^2, \dots, (v_K^{\text{ul}})^2)$  and  $N_{\ell, k}^{\text{dl}} = (b_{\ell, k}^{\text{dl}})^2 + \sum_{j=1}^L \sum_{i=1}^L (a_{s, \ell, j}^{\text{dl}})^2 R_{j, i}^{\text{dl}} (b_{i, k}^{\text{dl}})^2$ ,  $\forall \ell \in \mathcal{L}$  and  $\forall k \in \mathcal{K}$ .

Since  $\boldsymbol{\rho}^{\text{ul}}$  satisfies the total power constraint, we have

$$\begin{aligned} P_{\text{total}} &= \mathbf{1}^\dagger \boldsymbol{\rho}_{tot}^{\text{ul}} \\ &= \mathbf{1}^\dagger \mathbf{N}^{\text{ul}} (\mathbf{I} - \text{diag}(\boldsymbol{\beta}^{\text{ul}})\mathbf{M}^{\text{ul}})^{-1} \mathbf{J}^{\text{ul}} \boldsymbol{\beta}^{\text{ul}} \\ &= \mathbf{1}^\dagger \mathbf{N}^{\text{ul}} (\mathbf{I} - \text{diag}(\boldsymbol{\beta}^{\text{ul}})\mathbf{M}^{\text{ul}})^{-1} \text{diag}(\boldsymbol{\beta}^{\text{ul}}) \mathbf{J}^{\text{ul}} \mathbf{1} \end{aligned}$$

$$\begin{aligned}
&= \mathbf{1}^\dagger \mathbf{N}^{\text{ul}} (\text{diag}(\boldsymbol{\beta}^{\text{ul}})^{-1} - \mathbf{M}^{\text{ul}})^{-1} \mathbf{J}^{\text{ul}} \mathbf{1} \\
&= \mathbf{1}^\dagger \mathbf{J}^{\text{dl}\dagger} (\text{diag}(\boldsymbol{\beta}^{\text{dl}})^{-1} - \mathbf{M}^{\text{dl}\dagger})^{-1} \mathbf{J}^{\text{ul}} \mathbf{1} \\
&= \mathbf{1}^\dagger \text{diag}(\boldsymbol{\beta}^{\text{dl}}) \mathbf{J}^{\text{dl}\dagger} (\mathbf{I} - \mathbf{M}^{\text{dl}\dagger} \text{diag}(\boldsymbol{\beta}^{\text{dl}}))^{-1} \mathbf{J}^{\text{ul}} \mathbf{1} \\
&= \boldsymbol{\beta}^{\text{dl}\dagger} \mathbf{J}^{\text{dl}\dagger} (\mathbf{I} - \mathbf{M}^{\text{dl}\dagger} \text{diag}(\boldsymbol{\beta}^{\text{dl}}))^{-1} \mathbf{J}^{\text{ul}} \mathbf{1} \\
&= \boldsymbol{\beta}^{\text{dl}\dagger} \mathbf{J}^{\text{dl}\dagger} (\mathbf{I} - \mathbf{M}^{\text{dl}\dagger} \text{diag}(\boldsymbol{\beta}^{\text{dl}}))^{-1} \mathbf{N}^{\text{dl}\dagger} \mathbf{1} \\
&= \boldsymbol{\rho}_{\text{tot}}^{\text{dl}\dagger} \mathbf{1}.
\end{aligned}$$

Finally using (7.11) and (7.20), similar to [He et al., 2018], and since the achievable SINRs for the uplink and downlink are equal, we have our result.  $\square$

**Theorem 15.** *Let  $R_{DL-IF-CRAN}$  be the achievable rates using integer-forcing equalization and compression for a given downlink channel  $\mathbf{H}_d$ , integer matrices  $\mathbf{A}_{d,c}$  and  $\mathbf{A}_{d,s}$ , coding power matrix  $\mathbf{P}_d$ , equalization matrix  $\mathbf{V}_d$  and beamforming matrix  $\mathbf{B}_d$  that satisfies the total power constraint  $P_{\text{total}}$ . Then, for the dual uplink channel  $\mathbf{H}_u = \mathbf{H}_d^\dagger$ , we can achieve a sum-rate  $\sum_{k=1}^K R_{UL-IF-CRAN,k} \geq \sum_{k=1}^K R_{DL-IF-CRAN,k}$ .*

The proof is similar to the proof of Theorem 14.

## 7.4 Downlink C-RAN Optimization Algorithm Based on Duality

Our approach is to first choose  $\mathbf{A}_c^{\text{ul}}$ ,  $\mathbf{B}^{\text{ul}}$ ,  $\mathbf{A}_s^{\text{ul}}$  and  $\mathbf{D}^{\text{ul}}$  while maximizing the sum-rate of the corresponding dual uplink channel  $\mathbf{H}^{\text{ul}} = \mathbf{H}^{\text{dl}\dagger}$ , then set  $\mathbf{A}_c^{\text{dl}}$ ,  $\mathbf{B}^{\text{dl}}$ ,  $\mathbf{A}_s^{\text{dl}}$  and  $\mathbf{D}^{\text{dl}}$  as in Theorem 14 to achieve at least the same sum-rate as the dual uplink channel.

Unfortunately, optimizing  $\mathbf{A}_c^{\text{ul}}$ ,  $\mathbf{B}^{\text{ul}}$ ,  $\mathbf{A}_s^{\text{ul}}$  and  $\mathbf{D}^{\text{ul}}$  for the corresponding uplink channel is also challenging. However, in Chapter 4, we proposed a suboptimal solution for individual symmetric fronthaul rate constraints, which demonstrated good performance via simulations. Hence, we use Algorithm 3 which is adapted for sum-rate fronthaul links constraint to optimize the dual uplink channel. The details for the optimization algorithm is given below in Algorithm 4. It is worth noting that, at the end of Algorithm 3 and before using Algorithm 4, we need to permute the BSs

such that we have full-rank sub-matrices  $\mathbf{A}_{s,[1:m]}^{\text{ul}}$  for  $m = 1, \dots, L$ .

---

**Algorithm 3** Uplink IF-CRAN
 

---

```

1: procedure UIFCRAN( $\mathbf{H}^{\text{ul}}, \mathbf{V}^{\text{ul}}, \mathbf{P}^{\text{ul}}, C_{\text{total}}, \text{tol}$ )
2:   Initialization: Set  $d_{\text{min}} = 0$  and  $d_{\text{max}} = d$  large enough such that
    $\sum_{\ell=1}^L R_{\text{SIFSC},\ell}^s(\mathbf{H}^{\text{ul}}) < C_{\text{total}}$ .
3:   while  $C_{\text{total}} - \sum_{\ell=1}^L R_{\text{SIFSC},\ell}^s(\mathbf{H}^{\text{ul}}) > \text{tol}$  or  $\sum_{\ell=1}^L R_{\text{SIFSC},\ell}^s(\mathbf{H}^{\text{ul}}) > C_{\text{total}}$  do
4:     if  $\sum_{\ell=1}^L R_{\text{SIFSC},\ell}^s(\mathbf{H}^{\text{ul}}) < C_{\text{total}}$  then
5:        $d_{\text{max}} = d/2$ .
6:     else
7:        $d_{\text{min}} = d/2$ .
8:     end if
9:      $d = (d_{\text{min}} + d_{\text{max}})/2$ .
10:     $\mathbf{F}_s^{\text{ul}} = \text{chol}((1 + \frac{1}{d})\mathbf{I} + \frac{1}{d}P\mathbf{H}^{\text{ul}}\mathbf{V}^{\text{ul}}\mathbf{P}^{\text{ul}}\mathbf{V}^{\text{ul}\dagger}\mathbf{H}^{\text{ul}\dagger})$ 
11:     $\mathbf{A}_s^{\text{ul}} = \text{LLL-reduction}(\mathbf{F}_s^{\text{ul}})$ .
12:     $R_{\text{SIFSC},\ell}^s(\mathbf{H}^{\text{ul}}) = \frac{1}{2} \log^+(\|\mathbf{F}_s^{\text{ul}}\mathbf{a}_{s,\ell}^{\text{ul}}\|^2)$ 
13:  end while
14:  return  $d$ .
15: end procedure

```

---



---

**Algorithm 4** Downlink IF-CRAN
 

---

```

1: procedure DIFCRAN( $\mathbf{H}^{\text{dl}}, C_{\text{total}}, \text{tol}$ )
2:   Initialization: Set  $\mathbf{H}^{\text{ul}} = \mathbf{H}^{\text{dl}\dagger}$ ,  $\mathbf{V}^{\text{ul}} = \mathbf{I}$  and  $\mathbf{P}^{\text{ul}} = \frac{\text{SNR}}{K}\mathbf{I}$ .
3:    $d^{\text{ul}} = \text{UIFCRAN}(\mathbf{H}^{\text{ul}}, \mathbf{V}^{\text{ul}}, \mathbf{P}^{\text{ul}}, C_{\text{total}}, \text{tol})$ .
4:   Calculate  $\mathbf{R}^{\text{ul}}$  using (7.5).
5:   Calculate  $\mathbf{F}_c^{\text{ul}}$  using (7.9).
6:    $\mathbf{A}_c^{\text{ul}} = \text{LLL-reduction}(\mathbf{F}_c^{\text{ul}})$ .
7:   Calculate  $\mathbf{B}^{\text{ul}}$  using (7.7).
8:   Set  $\mathbf{A}_c^{\text{dl}} = \mathbf{A}_c^{\text{ul}\dagger}$ ,  $\mathbf{B}^{\text{dl}} = \mathbf{B}^{\text{ul}\dagger}$ ,  $\mathbf{A}_s^{\text{dl}} = \mathbf{A}_s^{\text{ul}\dagger}$  and  $\mathbf{D}^{\text{dl}} = \text{diag}(\mathbf{R}^{\text{ul}\dagger}\mathbf{e}^{\text{dl}})$  according to
   Theorem 14
9:   return  $(\mathbf{A}_c^{\text{dl}}, \mathbf{B}^{\text{dl}}, \mathbf{A}_s^{\text{dl}}, \mathbf{D}^{\text{dl}})$ .
10: end procedure

```

---

Finally, it is worth noting that similar to [He et al., 2018], one can develop an iterative algorithm based on our IF duality result, in which each time we optimize the parameters at the receiver side for one direction (e.g., uplink), then use the duality to move these parameters to the transmitter side of the other direction (e.g., downlink), then repeat. However, preliminary simulations showed no extra gain from

iteratively going back and forth between the uplink and downlink channels, hence we only propose one-shot algorithm for downlink parameter optimization.

## 7.5 Numerical Results

In this section, we show the performance (in terms of average sum-rate in bits/sec/Hz) of the proposed IF architecture and compare it to independent compression with successive channel encoding as well as multivariate compression with successive channel encoding. The optimization of the rate achieved by multivariate compression with dirty paper encoding is carried out jointly using the successive convex approximation algorithm proposed in [Park et al., 2013]. (Note that this optimization must be performed over all  $K!$  possible decoding orders.) For more details about multivariate compression, we refer the readers to [Park et al., 2013].

For our simulations, we generated 500 realizations for the channel matrix  $\mathbf{H}^{\text{dl}}$ , each elementwise i.i.d.  $\mathcal{N}(0, 1)$ . We also fix the number of BSs to  $L = 4$ . Figure 7.2 shows the case of  $L = 4$  users where we fix the total SNR = 30dB and plot the average sum-rate with the sum-rate of the backhaul network  $C_{\text{sym}}$ . The performance of the proposed IF scheme is quite close to that of multivariate compression combined with dirty paper coding, and has an advantage over multivariate compression with single-user decoding as well as single-user compression and channel coding. Figure 7.3 shows the average sum-rate against the SNR for fixed total backhaul rate  $C_{\text{total}} = 20$  for the same  $4 \times 4$  channel. Again, we observe that our integer-forcing scheme is competitive with multivariate compression combined with dirty paper coding, and outperforms schemes that rely on single-user source coding and/or channel coding.

We also note that, rather than a “one-shot” algorithm, we can iterate between the uplink and downlink to optimize the parameters. However, our simulations did not show any significant performance improvement for this iterative algorithm.

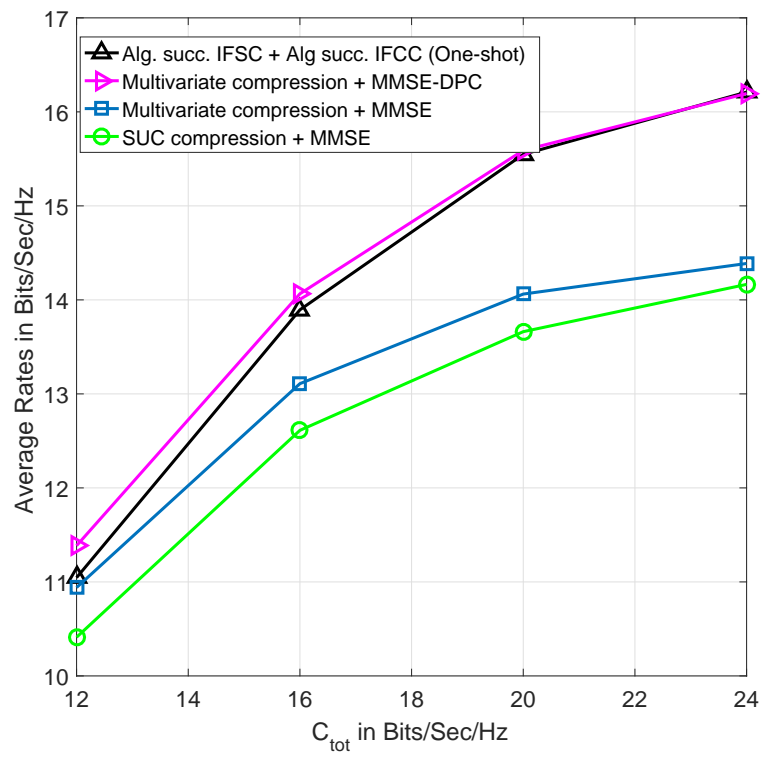


**Figure 7.2:** The average sum-rate for  $K = 4$  and  $\text{SNR} = 30\text{dB}$

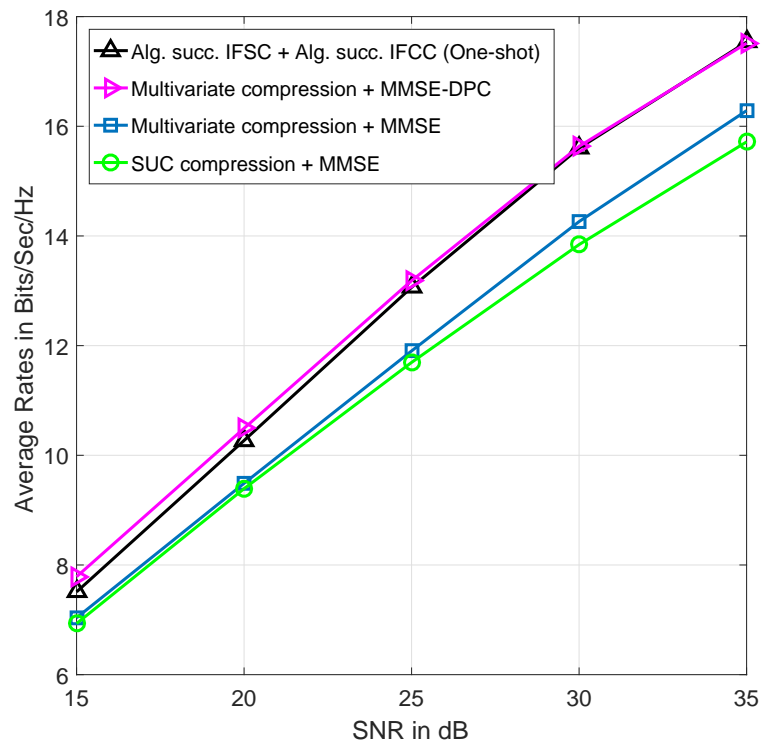


**Figure 7.3:** The average sum-rate for  $K = 4$  and  $C_{\text{sym}} = 20$  Bits/Sec/Hz.

## Chapter 8

# Integer-Forcing Interference Alignment

For the  $K$ -user MIMO interference channel, some form of interference alignment is often needed to attain the highest possible rates. For the important special case of linear alignment strategies, many iterative optimization algorithms have been proposed that aim to maximize the signal-to-interference-and-noise ratio (SINR) at each receiver. Recent work [Ntranos et al., 2013] has demonstrated the advantages of integer-forcing interference alignment (IFIA), which combines both signal space and signal scale interference alignment. This chapter proposes a class of iterative optimization algorithms for IFIA and demonstrates its advantages via simulations.

### 8.0.1 Notation

We denote the matrix resulting from dropping the  $k^{\text{th}}$  column of matrix  $\mathbf{A}$  by  $\mathbf{A}_{\sim k}$  and the vector resulting from dropping the  $k^{\text{th}}$  entry of vector  $\mathbf{a}$  by  $\mathbf{a}_{\sim k}$ . In this chapter, we refer to the transmitter or the receiver index by superscripts. Particularly, we index the transmitters by  $\ell$  and the receivers by  $k$ . Subscripts is used to index the elements in a vector (or vectors in a matrix).

### 8.0.2 System Model

For our system model, we assume the  $\ell^{\text{th}}$  transmitter is equipped with  $N_{\text{Tx}}^{[\ell]}$  antennas and the  $k^{\text{th}}$  receiver has  $N_{\text{Rx}}^{[k]}$  antennas. We let  $T$  denotes the coding blocklength.

The  $\ell^{\text{th}}$  transmitter has a *message*  $w^{[\ell]}$  that is drawn independently and uniformly from  $\{1, 2, \dots, 2^{nR^{[\ell]}}\}$ , where  $R^{[\ell]}$  denotes the rate of  $w^{[\ell]}$  measured in bits per channel

use. The  $\ell^{\text{th}}$  transmitter is equipped with an encoder  $\mathcal{E}^{[\ell]} : \{1, 2, \dots, 2^{nR^{[\ell]}}\} \rightarrow \mathbb{R}^T$  which maps the message  $w^{[\ell]}$  into a codeword  $\mathbf{s}^{[\ell]} = \mathcal{E}^{[\ell]}(w^{[\ell]})$ . The  $\ell^{\text{th}}$  transmitter creates a channel input matrix

$$\mathbf{X}^{[\ell]} = \mathbf{v}^{[\ell]} \mathbf{s}^{[\ell]\dagger} \quad (8.1)$$

where  $\mathbf{v}^{[\ell]} \in \mathbb{R}^{N_{\text{Tx}}^{[\ell]}}$  is a beamforming vector. The resulting channel input satisfies an average power constraint

$$\frac{1}{T} E[\text{Tr}(\mathbf{X}^{[\ell]} \mathbf{X}^{[\ell]\dagger})] \leq \rho \quad (8.2)$$

where  $\rho$  is the average power available at each transmitter (assuming symmetric power constraint across all transmitters).

The  $k^{\text{th}}$  receiver observes the channel output

$$\mathbf{Y}^{[k]} = \sum_{\ell=1}^K \mathbf{H}^{[k,\ell]} \mathbf{X}^{[\ell]} + \mathbf{Z}^{[k]} \quad (8.3)$$

where  $\mathbf{H}^{[k,\ell]} \in \mathbb{R}^{N_{\text{Rx}}^{[k]} \times N_{\text{Tx}}^{[\ell]}}$  is the channel matrix from the  $\ell^{\text{th}}$  transmitter to the  $k^{\text{th}}$  receiver and  $\mathbf{Z}^{[k]} \in \mathbb{R}^{N_{\text{Rx}}^{[k]} \times T}$  is elementwise i.i.d.  $\mathcal{N}(0, 1)$  representing the AWGN at receiver  $k$ . The  $k^{\text{th}}$  receiver applies an equalization matrix  $\mathbf{U}^{[k]} \in \mathbb{R}^{N_{\text{Rx}}^{[k]} \times M^{[k]}}$  to the channel output and obtains an effective channel output

$$\tilde{\mathbf{Y}}^{[k]} = \mathbf{U}^{[k]\dagger} \mathbf{Y}^{[k]}. \quad (8.4)$$

Each receiver  $k$  is equipped with a decoder  $\mathcal{D}^{[k]} : \mathbb{R}^{M^{[k]} \times T} \rightarrow \{1, 2, \dots, 2^{nR^{[k]}}\}$  that decodes  $\hat{w}^{[k]} = \mathcal{D}^{[k]}(\tilde{\mathbf{Y}}^{[k]})$ .

**Remark 23.** *The  $M^{[k]}$  equalization vectors (columns of  $\mathbf{U}^{[k]}$ ) needed to decode  $w^{[k]}$  depend on the decoding technique used at the  $k^{\text{th}}$  decoder.*

We call the rate tuple  $(R^{[1]}, \dots, R^{[K]})$  is achievable if for any  $\epsilon > 0$  and for large

enough  $T$ , there exist encoders, beamforming matrices, equalization matrices and decoders such that

$$\Pr \left( \bigcup_{k=1}^K \{\hat{w}^{[k]} \neq w^{[k]}\} \right) < \epsilon. \quad (8.5)$$

## 8.1 Signal Space Alignment and Max-SINR Algorithm

As mentioned earlier, interference alignment can be performed at both the signal level, using structure codes, and the signal space, using beamforming vectors. The later type of interference alignment aims to creating an interference-free space that can be used by the desired signal. This is done by aligning the interference signals, using beamforming vectors, in one space and projecting the received signal, using equalization vectors, onto the space orthogonal to the interference. The work in [Cadambe and Jafar, 2008] focused on the high SNR regime by studying the degrees of freedom (DOF) achievable by interference alignment. While DOF is a good metric for the performance of the interference alignment schemes at high SNR regimes, it is not sufficient for the low or moderate SNR regimes. In [Gomadam et al., 2011], the authors studied this problem and proposed an algorithm called Max-SINR algorithm which aims to maximize the signal to interference and noise ratio (SINR) at the receiver successively. The SINR metric is a good choice for the low to moderate SNR regimes, since the achievable rate of the linear receiver is a monotonic function in the SINR.

### 8.1.1 Objective and Optimization Problem

For a fixed channel realization, the rate of the linear receivers can be written as

$$R^{[k]} = \frac{1}{2} \log \left( 1 + \text{SINR}^{[k]}(\mathbf{u}^{[k]}, \mathbf{v}^{[\ell]}, \forall \ell) \right) \quad (8.6)$$

where  $\text{SINR}^{[k]}(\mathbf{u}^{[k]}, \mathbf{v}^{[\ell]}, \forall \ell)$ , the SINR at the  $k^{\text{th}}$  receiver, is a function in the equalization vector  $\mathbf{u}^{[k]}$  and all the beamforming vectors  $\mathbf{v}^{[\ell]}$ .

In linear receivers, e.g., zero-forcing or MMSE receivers, the  $k^{\text{th}}$  receiver decodes directly its intended data stream  $\mathbf{s}^{[k]}$  treating the rest of interference data streams as noise (i.e.,  $\mathbf{s}^{[\ell]}, \forall \ell \neq k$ ). Thus,  $M^{[k]} = 1$  equalization vector  $\mathbf{u}^{[k]}$  is needed. The effective output can be expressed as

$$\tilde{\mathbf{y}}^{[k]\dagger} = \mathbf{u}^{[k]\dagger} \mathbf{Y}^{[k]} \quad (8.7)$$

$$= \underbrace{\mathbf{u}^{[k]\dagger} \mathbf{H}^{[k,k]} \mathbf{v}^{[k]} \mathbf{s}^{[k]\dagger}}_{\text{desired signal}} + \sum_{\ell \neq k} \underbrace{\mathbf{u}^{[k]\dagger} \mathbf{H}^{[k,\ell]} \mathbf{v}^{[\ell]} \mathbf{s}^{[\ell]\dagger}}_{\text{interference from the } \ell^{\text{th}} \text{ transmitter}} + \mathbf{u}^{[k]\dagger} \mathbf{Z}^{[k]} \quad (8.8)$$

where  $\mathbf{s}^{[\ell]}$  here is drawn from an i.i.d. Gaussian codebook of power  $\rho$  and each beamforming vector must satisfy  $\|\mathbf{v}^{[\ell]}\|^2 \leq 1$  to satisfy the power constraint<sup>1</sup>.

The resulting signal-to-interference-and-noise ratio (SINR) at the  $k^{\text{th}}$  receiver is

$$\text{SINR}^{[k]} = \frac{\rho \mathbf{u}^{[k]\dagger} \mathbf{H}^{[k,k]} \mathbf{v}^{[k]} \mathbf{v}^{[k]\dagger} \mathbf{H}^{[k,k]\dagger} \mathbf{u}^{[k]}}{\mathbf{u}^{[k]\dagger} \left( \rho \sum_{\ell \neq k} \mathbf{H}^{[k,\ell]} \mathbf{v}^{[\ell]} \mathbf{v}^{[\ell]\dagger} \mathbf{H}^{[k,\ell]\dagger} + \mathbf{I} \right)^{-1} \mathbf{u}^{[k]}} \quad (8.9)$$

Our goal is to choose  $\mathbf{u}^{[k]}$  and  $\mathbf{v}^{[\ell]}$  in order to maximize the sum rate. Formally, we want to solve the following optimization problem.

$$\max_{\mathbf{u}^{[k]}, \mathbf{v}^{[\ell]}} \sum_{k=1}^K \frac{1}{2} \log \left( 1 + \text{SINR}^{[k]} \right) \quad (8.10)$$

$$\text{subject to } \|\mathbf{v}^{[k]}\|^2 \leq 1, \forall k = 1, \dots, K$$

where  $\text{SINR}^{[k]}$  is given in (8.9).

---

<sup>1</sup>We employ unit-norm equalization and beamforming vectors ( $\mathbf{u}^{[k]}$  and  $\mathbf{v}^{[\ell]}$ , respectively) to make it easier to switch the roles of transmitters and receivers later in the dual channel.

It can be shown that simultaneously choosing  $\mathbf{u}^{[k]}$  and  $\mathbf{v}^{[\ell]}$  to solve 8.10 is a non-convex optimization problem.

### 8.1.2 Max-SINR Algorithm

The idea behind the Max-SINR algorithm is to use reciprocity of wireless networks to relax the non-convex problem into an iterative optimization problem. Precisely, the relaxation is done by, firstly, dividing the optimization over the unit-norm vectors  $\mathbf{u}^{[k]}$  and  $\mathbf{v}^{[\ell]}$  into two separate problems. Secondly, further relaxing the problem of finding the optimal beamforming vectors  $\mathbf{v}^{[\ell]}$  for a fixed  $\mathbf{u}^{[k]}$  using channel reciprocity.

To this end, let us consider the dual channel in which the roles of the transmitters and receivers are reversed. Define the dual channel matrix  $\overleftarrow{\mathbf{H}}^{[k,\ell]} = \mathbf{H}^{[\ell,k]\dagger}$  which represents the channel from the  $\ell^{\text{th}}$  transmitter ( $\ell^{\text{th}}$  receiver in the original problem) to the  $k^{\text{th}}$  receiver ( $k^{\text{th}}$  transmitter in the original problem). In the dual channel, the  $\mathbf{v}^{[\ell]}$  play the role of the equalization vectors and the  $\mathbf{u}^{[k]}$  play the role of the beamforming vectors.

For the prime channel, the relaxed optimization problem becomes

$$\max_{\mathbf{u}^{[k]}} \sum_{k=1}^K \frac{1}{2} \log \left( 1 + \text{SINR}^{[k]} \right) \quad (8.11)$$

For a fixed choice of beamforming vectors  $\mathbf{v}^{[\ell]}$ , the optimal solution of (8.11) can be expressed in closed form as

$$\mathbf{u}^{[k]} = \frac{\left( \rho \sum_{\ell \neq k} \mathbf{H}^{[k,\ell]} \mathbf{v}^{[\ell]} \mathbf{v}^{[\ell]\dagger} \mathbf{H}^{[k,\ell]\dagger} + \mathbf{I} \right)^{-1} \mathbf{H}^{[k,k]} \mathbf{v}^{[k]}}{\left\| \left( \rho \sum_{\ell \neq k} \mathbf{H}^{[k,\ell]} \mathbf{v}^{[\ell]} \mathbf{v}^{[\ell]\dagger} \mathbf{H}^{[k,\ell]\dagger} + \mathbf{I} \right)^{-1} \mathbf{H}^{[k,k]} \mathbf{v}^{[k]} \right\|}. \quad (8.12)$$

For the dual channel, the relaxed optimization problem becomes

$$\max_{\mathbf{v}^{[k]}} \sum_{k=1}^K \frac{1}{2} \log \left( 1 + \overleftarrow{\text{SINR}}^{[k]} \right). \quad (8.13)$$

Now, using the dual channel, while holding  $\mathbf{u}^{[k]}$  fixed, the optimal  $\mathbf{v}^{[k]}$  that maximizes (8.13) is

$$\mathbf{v}^{[k]} = \frac{\left( \rho \sum_{\ell \neq k} \overleftarrow{\mathbf{H}}^{[k,\ell]} \mathbf{u}^{[\ell]} \mathbf{u}^{[\ell]\dagger} \overleftarrow{\mathbf{H}}^{[k,\ell]\dagger} + \mathbf{I} \right)^{-1} \overleftarrow{\mathbf{H}}^{[k,k]} \mathbf{u}_i^{[k]}}{\left\| \left( \rho \sum_{\ell \neq k} \overleftarrow{\mathbf{H}}^{[k,\ell]} \mathbf{u}_j^{[\ell]} \mathbf{u}_j^{[\ell]\dagger} \overleftarrow{\mathbf{H}}^{[k,\ell]\dagger} + \mathbf{I} \right)^{-1} \overleftarrow{\mathbf{H}}^{[k,k]} \mathbf{u}^{[k]} \right\|}. \quad (8.14)$$

Finally, the Max-SINR algorithm uses (8.12) and (8.14) iteratively to optimize the beamforming and equalization vectors. For more details, we refer readers to [Gomadam et al., 2011].

## 8.2 Integer-Forcing Interference Alignment

In this section, we give a high-level overview of the IFIA strategy, which builds on previous results for compute-and-forward and integer-forcing from [Nazer and Gastpar, 2011, Zhan et al., 2014, Ordentlich et al., 2014, Ntranos et al., 2013, Nazer et al., 2016]. Our framework inherits the alignment idea from [Ntranos et al., 2013] as well as the expanded framework for the compute-and-forward technique from [Nazer et al., 2016]. For details, we refer readers to [Nazer et al., 2016]. Fig. 8-1 shows the structure of the IFIA transmitters and receivers.

### 8.2.1 Achievable Rates

Let us assume that the  $\ell^{\text{th}}$  transmitter selects a codeword  $\mathbf{s}_\ell \in \mathbb{R}^n$  with power  $\rho_\ell = \frac{1}{n} \mathbb{E} \|\mathbf{s}^{[\ell]}\|^2$  and a beamforming vector  $\mathbf{v}^{[\ell]}$  that meets the overall power constraint

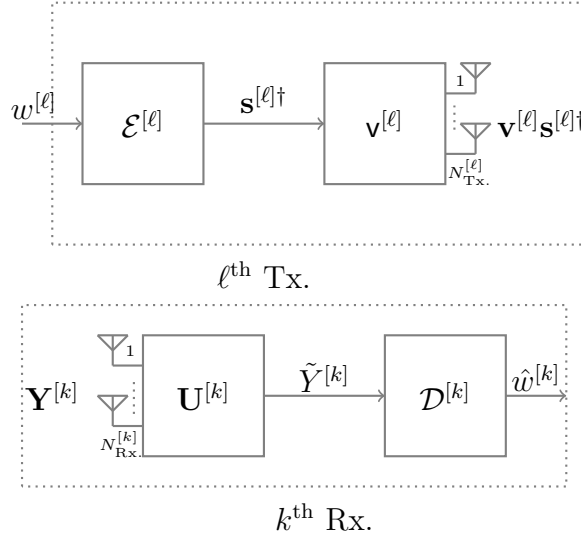


**Figure 8.1:** The structure of the  $\ell^{\text{th}}$  Tx. and the  $k^{\text{th}}$  Rx. for IFIA scheme

$\rho_\ell \|\mathbf{v}^{[\ell]}\|^2 = \rho$ . Let  $\mathbf{P} = \text{diag}(\rho_1, \dots, \rho_K)$  be the diagonal matrix of coding powers and  $\mathbf{S} \triangleq [\mathbf{s}^{[1]} \dots \mathbf{s}^{[K]}\dagger]$  denote the matrix of transmitted codewords. We define the beamforming matrix  $\mathbf{V}$  as

$$\mathbf{V} \triangleq \begin{bmatrix} \mathbf{v}^{[1]} & \cdots & \mathbf{0}_{N_{\text{Tx}}^{[1]}} \\ \vdots & \ddots & \vdots \\ \mathbf{0}_{N_{\text{Tx}}^{[K]}} & \cdots & \mathbf{v}^{[K]} \end{bmatrix} \quad (8.15)$$

where  $\mathbf{0}_N$  refers to the zero column vector of length  $N$ . Recall that  $\mathbf{H}^{[k,\ell]}$  is the channel matrix from the  $\ell^{\text{th}}$  transmitter to the  $k^{\text{th}}$  receiver. By defining the channel matrix from all the  $K$  transmitters to the  $k^{\text{th}}$  receiver as

$$\mathbf{H}^{[k]} \triangleq [\mathbf{H}^{[k,1]} \dots \mathbf{H}^{[k,K]}], \quad (8.16)$$

we can compactly write the  $k^{\text{th}}$  receiver's observation as

$$\mathbf{Y}^{[k]} = \mathbf{H}^{[k]} \mathbf{V} \mathbf{S} + \mathbf{Z}^{[k]}. \quad (8.17)$$

The  $k^{\text{th}}$  receiver's goal is to recover  $M^{[k]}$  integer-linear combinations of codewords which can be solved later for the desired codeword  $\mathbf{s}^{[k]}$ . The  $m^{\text{th}}$  combination is given by

$$\mathbf{r}_m^{[k]\dagger} = \mathbf{a}_m^{[k]\dagger} \mathbf{S}, \quad m = 1, \dots, M^{[k]} \quad (8.18)$$

where  $\mathbf{a}_m^{[k]} \in \mathbb{Z}^K$  is the integer vector containing the coefficients of the  $m^{\text{th}}$  linear combination.

To recover the integer combination  $\mathbf{r}_m^{[k]}$ , the  $k^{\text{th}}$  receiver applies the equalization vector  $\mathbf{u}_m^{[k]}$ , the  $m^{\text{th}}$  column of the matrix  $\mathbf{U}^{[k]}$ , and obtains effective channel output

$$\tilde{\mathbf{y}}_m^{[k]\dagger} = \mathbf{u}_m^{[k]\dagger} \mathbf{Y}^{[k]} \quad (8.19)$$

$$= \underbrace{\mathbf{r}_m^{[k]\dagger}}_{\text{Desired combination}} + \underbrace{\mathbf{z}_{\text{eff},m}^{[k]\dagger}}_{\text{Effective noise}} \quad (8.20)$$

where  $\mathbf{z}_{\text{eff},m}^{[k]\dagger} = (\mathbf{u}_m^{[k]\dagger} \mathbf{H}^{[k]} \mathbf{V} - \mathbf{a}_m^{[k]\dagger}) \mathbf{S} + \mathbf{u}_m^{[k]\dagger} \mathbf{Z}^{[k]}$  is the effective noise due to the mismatch between the actual effective channel  $\mathbf{u}_m^{[k]\dagger} \mathbf{H}^{[k]} \mathbf{V}$  and the desired integer vector  $\mathbf{a}_m^{[k]\dagger}$  plus the amplified AWGN after equalization. The power of the effective noise  $\mathbf{z}_{\text{eff},m}^{[k]}$  is given by

$$\left( \sigma_{\text{eff},m}^{[k]} \right)^2 = \frac{1}{n} \mathbb{E} \left[ \|\mathbf{z}_{\text{eff},m}^{[k]}\|^2 \right] = \|(\mathbf{u}_m^{[k]\dagger} \mathbf{H}^{[k]} \mathbf{V} - \mathbf{a}_m^{[k]\dagger}) \mathbf{P}^{\frac{1}{2}}\|^2 + \|\mathbf{u}_m^{[k]}\|^2. \quad (8.21)$$

In order to decode the  $m^{\text{th}}$  integer-combination  $\mathbf{r}_m^{[k]}$  at the  $k^{\text{th}}$  receiver, all participating users with non-zero coefficient in  $\mathbf{a}_m^{[k]\dagger}$  should design their codebook to tolerate noise power  $(\sigma_{\text{eff},m}^{[k]})^2$  given in (8.21). Successfully decoding the  $m^{\text{th}}$  integer-combination  $\mathbf{r}_m^{[k]}$  at the  $k^{\text{th}}$  receiver results in a set of constraints called the *computation*

rates for the participating users, given as

$$R_{\text{comp},m,\ell}^{[k]} = \frac{1}{2} \log^+ \left( \frac{\rho_\ell}{\left(\sigma_{\text{eff},m}^{[k]}\right)^2} \right) \quad \text{for } a_{m,\ell}^{[k]} \neq 0 \quad (8.22)$$

where  $a_{m,\ell}^{[k]}$  is the  $\ell^{\text{th}}$  entry of  $\mathbf{a}_m^{[k]\dagger}$ . Here  $R_{\text{comp},m,\ell}^{[k]}$  is a rate constraint on user  $\ell$  only if this user participates in the  $m^{\text{th}}$  integer-combination at the  $k^{\text{th}}$  receiver (i.e.,  $a_{m,\ell}^{[k]} \neq 0$ ). The message from the  $\ell^{\text{th}}$  transmitter (user) might participate in multiple combinations at multiple receivers. Thus, the achievable rate for the  $\ell^{\text{th}}$  transmitter is the minimum computation rate among these combinations

$$R^{[\ell]} = \min_{k=1,\dots,K} \min_{m:a_{m,\ell}^{[k]} \neq 0} R_{\text{comp},m,\ell}^{[k]}. \quad (8.23)$$

It is worth noting, as we will see later, that usually the computation rate constraints are ordered in a descending order (i.e.,  $R_{\text{comp},1,\ell}^{[k]} \geq R_{\text{comp},2,\ell}^{[k]} \geq \dots \geq R_{\text{comp},K,\ell}^{[k]}, \forall \ell, k$ ).

The rate expression in (8.23) can be further improved by implementing *algebraic successive cancellation* introduced in [Ordentlich et al., 2014] which relaxes some of the computation rate constraints in (8.23). We first review the basic idea of algebraic successive cancellation and then show the improved achievable rates region.

Algebraic successive cancellation can be achieved by using previously decoded integer-combinations to eliminate some of the users codewords participating in the subsequent integer-combinations. This relaxes the corresponding computation rate constraints on these, no longer participating, users.

In order to capture the order in which the codewords can be eliminated from the integer-combinations, we define a *mapping*  $\mathcal{I}^{[k]}$  as a set of pair of the form  $(m, \ell)$ , where  $\ell \in \{1, \dots, K\}$  denotes the user index,  $m \in \{1, \dots, M^{[k]}\}$  denotes the integer-combination index and  $(m, \ell) \in \mathcal{I}^{[k]}$  means that the  $\ell^{\text{th}}$  user can not

be canceled out while decoding the  $m^{\text{th}}$  integer-combination (i.e.,  $R_{\text{comp},m,\ell}^{[k]}$  is a constraint on  $R^{[\ell]}$ ). Only some mappings are *admissible* (depending on the integer matrix  $\mathbf{A}^{[k]} \triangleq [\mathbf{a}_1^{[k]}, \dots, \mathbf{a}_{M^{[k]}}^{[k]}]^\dagger$ ). A mapping  $\mathcal{I}^{[k]}$  is said to be admissible if there exists a lower unitriangular<sup>2</sup> matrix  $\mathbf{L}^{[k]} \in \mathbb{R}^{M^{[k]} \times M^{[k]}}$  such that the  $(m, \ell)^{\text{th}}$  entry of  $\mathbf{L}^{[k]} \mathbf{A}^{[k]}$  is equal to zero for all  $(m, \ell) \notin \mathcal{I}^{[k]}$ . The admissible mapping  $\mathcal{I}^{[k]}$  captures the possible assignments of the computation rates to the users.

For any choice of integer matrices  $\mathbf{A}^{[k]}$ , beamforming matrix  $\mathbf{V}$ , equalization matrices  $\mathbf{U}^{[k]}$ , coding power matrix  $\mathbf{P}$  and admissible mappings  $\mathcal{I}^{[k]}$ , the following rates are achievable

$$R^{[\ell]} = \min_{k=1, \dots, K} \min_{m: (m, \ell) \in \mathcal{I}^{[k]}} R_{\text{comp},m,\ell}^{[k]} \quad (8.24)$$

For an in-depth discussion of the achievability proof, we refer interested readers to [Ordentlich et al., 2014, Ntranos et al., 2013] and [Nazer et al., 2016].

### 8.2.2 Integer Matrix $\mathbf{A}^{[k]}$ structure

In the simple case where the  $k^{\text{th}}$  receiver wants to decode all of the codewords ( $K$  codewords), we need  $K$  independent integer-combinations such that

$$\text{rank}(\mathbf{A}^{[k]}) = K. \quad (8.25)$$

Decoding all the codewords is essential in a multiple-access channel, where the receiver is interested in all transmitted codewords. However, in the interference channel, this overconstrains the user rates as we will have  $K$  computation rate constraints while the receiver only desires one message.

The  $k^{\text{th}}$  receiver can choose to decode fewer integer-combinations (i.e.,  $M^{[k]}$  instead of  $K$ ), then solve for the desired codeword. In order to solve for the desired codeword,

---

<sup>2</sup>lower triangular matrix whose diagonal elements are equal to 1

the following conditions are needed:

$$\text{rank}(\mathbf{A}^{[k]}) = M^{[k]}, \quad (8.26)$$

$$\text{rank}(\mathbf{A}_{\sim k}^{[k]}) = M^{[k]} - 1. \quad (8.27)$$

The first condition, in (8.26), means that the  $M^{[k]}$  integer-combinations should be independent (since there is no need to decode additional dependent combination with possibly lower computation rates). The second condition in (8.27) means that the coefficients of the interference codewords, in the  $M^{[k]}$  integer-combinations, should be aligned in no more than  $M^{[k]} - 1$  dimensional space.

**Example 1.** *In order to visualize (8.26) and (8.27), lets consider the case when  $K = 3$  and  $M^{[1]} = 2$ . An example of the integer-combinations that could be decoded at receiver 1 are*

$$\mathbf{r}_1^{[1]} = 2\mathbf{s}^{[1]} + \mathbf{s}^{[2]} + 2\mathbf{s}^{[3]} \quad (8.28)$$

$$\mathbf{r}_2^{[1]} = 6\mathbf{s}^{[1]} + 2(\mathbf{s}^{[2]} + 2\mathbf{s}^{[3]}). \quad (8.29)$$

It can be shown that  $\mathbf{s}^{[1]} = \frac{\mathbf{r}_2^{[1]} - 2\mathbf{r}_1^{[1]}}{2}$ . The integer matrices  $\mathbf{A}^{[1]}$  and  $\mathbf{A}_{\sim 1}^{[1]}$  are

$$\mathbf{A}^{[1]} = \begin{bmatrix} 2 & 1 & 2 \\ 6 & 2 & 4 \end{bmatrix} \quad (8.30)$$

$$\mathbf{A}_{\sim 1}^{[1]} = \begin{bmatrix} 1 & 2 \\ 2 & 4 \end{bmatrix} \quad (8.31)$$

which satisfy the conditions in (8.26) and (8.27). Fig. 8.2 illustrates (8.26) and (8.27) for this example.

### 8.2.3 Objective and Optimization Problem

Using equation (8.24), the problem of maximizing the sum of the user rates achieved by IFIA strategy can be written as

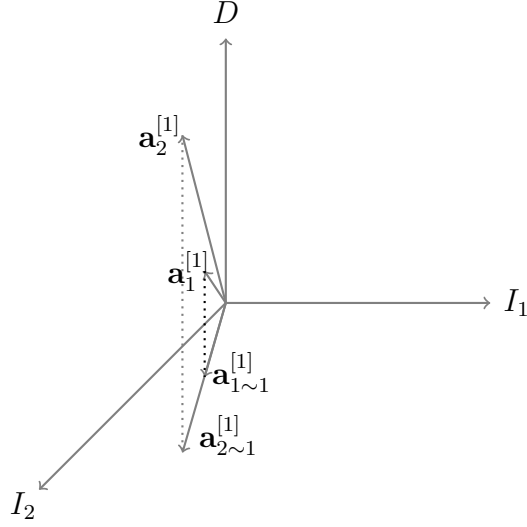


Figure 8.2: Example 1

$$\max_{\mathcal{I}^{[k]}, \mathbf{U}^{[k]}, \mathbf{v}^{[\ell]}, \mathbf{A}^{[k]} \in \mathbb{Z}^{M^{[k]} \times K}, \mathbf{P}} \sum_{\ell=1}^K \min_{k=1, \dots, K} \min_{m: (m, \ell) \in \mathcal{I}^{[k]}} \frac{1}{2} \log^+ \left( \frac{\rho_\ell}{\left( \sigma_{\text{eff}, m}^{[k]} \right)^2} \right) \quad (8.32)$$

$$\begin{aligned} \text{subject to} \quad & \|\mathbf{v}^{[\ell]}\|^2 \leq 1 \quad \forall \ell = 1, \dots, K \\ & \text{rank}(\mathbf{A}^{[k]}) = M^{[k]} \\ & \text{rank}(\mathbf{A}_{\sim k}^{[k]}) = M^{[k]} - 1 \end{aligned}$$

(8.32) is a challenging non convex optimization problem. It does not only has the non convexity of choosing  $\mathbf{U}^{[k]}$  and  $\mathbf{v}^{[\ell]}$  jointly as we saw before, but it also has an integer programming part for choosing  $\mathbf{A}^{[k]} \in \mathbb{Z}^{M^{[k]} \times K}$ . Furthermore, the mapping  $\mathcal{I}^{[k]}$  between the computation rates and the user rates does not have an explicit form that we can use. Hence, in this work, we try to relax this challenging problem to a more tractable problem that we can solve.

### 8.2.4 Problem Relaxation

Since (8.2) can be written as  $\rho_\ell \|\mathbf{v}^{[\ell]}\|^2 \leq \rho$ , one can use this to relax the problem of optimizing over the coding power matrix  $\mathbf{P}$  by absorbing it into the choice of the beamforming vectors  $\mathbf{v}^{[\ell]}$ . This can be done by selecting

$$\rho_\ell \|\mathbf{v}^{[\ell]}\|^2 = \rho, \quad \forall \ell = 1, \dots, K. \quad (8.33)$$

Also, assuming that all the users participate in all the combinations, this relaxes the need to optimize over  $\mathcal{I}^{[k]}$ . Taking this into consideration, the relaxed problem is now

$$\begin{aligned} & \max_{\mathbf{U}^{[k]}, \mathbf{v}^{[\ell]}, \mathbf{A}^{[k]} \in \mathbb{Z}^{M^{[k]} \times K}} \sum_{\ell=1}^K \min_{k=1, \dots, K} \min_{m=1, \dots, M^{[k]}} \frac{1}{2} \log^+ \left( \frac{\rho_\ell}{\left(\sigma_{\text{eff}, m}^{[k]}\right)^2} \right) & (8.34) \\ \text{subject to} & \quad \|\mathbf{v}^{[\ell]}\|^2 \leq 1 \quad \forall \ell = 1, \dots, K \\ & \quad \text{rank}(\mathbf{A}^{[k]}) = M^{[k]} \\ & \quad \text{rank}(\mathbf{A}_{\sim k}^{[k]}) = M^{[k]} - 1 \end{aligned}$$

Note that  $\rho_\ell$  is a function in  $\mathbf{v}^{[\ell]}$ , which makes the numerator inside the log also depends on  $\mathbf{v}^{[\ell]}$ . By replacing  $\rho_\ell$  by its lower bound  $\rho$  the relaxed problem becomes

$$\begin{aligned} & \min_{\mathbf{U}^{[k]}, \mathbf{v}^{[\ell]}, \mathbf{A}^{[k]} \in \mathbb{Z}^{M^{[k]} \times K}} \max_{k=1, \dots, K} \max_{m=1, \dots, M^{[k]}} \left(\sigma_{\text{eff}, m}^{[k]}\right)^2 & (8.35) \\ \text{subject to} & \quad \|\mathbf{v}^{[\ell]}\|^2 \leq 1 \quad \forall \ell = 1, \dots, K \\ & \quad \text{rank}(\mathbf{A}^{[k]}) = M^{[k]} \\ & \quad \text{rank}(\mathbf{A}_{\sim k}^{[k]}) = M^{[k]} - 1 \end{aligned}$$

Unfortunately, even (8.35) can be shown to be a non-convex problem. To this

end, we propose a suboptimal iterative algorithm.

First, we choose  $\mathbf{V}$  and  $\mathbf{U}^{[k]}$  for a fixed integer matrix  $\mathbf{A}^{[k]}$ . This can be done as in [Gomadani et al., 2011], using the duality results in [He et al., 2018]. We also propose a novel solution method using convex optimization.

Second, we select  $\mathbf{A}^{[k]}$  while keeping  $\mathbf{V}$  and  $\mathbf{U}^{[k]}$  fixed. A suboptimal algorithm for this subproblem is given in the next subsection.

### 8.3 Aligned LLL

In this section, we discuss how to choose the integer-combinations coefficients  $\mathbf{A}^{[k]}$  to maximize the sum of computation rates at the  $k^{\text{th}}$  receiver. For simplicity, we propose an algorithm to optimize the integer matrix  $\mathbf{A}^{[k]}$  for a fixed  $M^{[k]} = 2$  (decode two integer-combinations) and given matrices  $\mathbf{V}$  and  $\mathbf{U}^{[k]}$ .

It has been shown in [Zhan et al., 2014] that for a given equivalent channel  $\mathbf{H}^{[k]}\mathbf{V}$ , coding power matrix  $\mathbf{P}$  and integer vector  $\mathbf{a}_m^{[k]}$ , the optimal equalization vector  $\mathbf{u}_{\text{opt},m}^{[k]}$  that minimizes (8.21) is given by the MMSE equalizer

$$\mathbf{u}_{\text{opt},m}^{[k]\dagger} = \mathbf{a}_m^{[k]\dagger} \mathbf{P}^\dagger \mathbf{V}^\dagger \mathbf{H}^{[k]\dagger} (\mathbf{I} + \mathbf{H}^{[k]} \mathbf{V} \mathbf{P} \mathbf{V}^\dagger \mathbf{H}^{[k]\dagger})^{-1}. \quad (8.36)$$

Substituting with (8.36) we can rewrite (8.21) as

$$(\sigma_{\text{eff},m}^{[k]})^2 = \mathbf{a}_m^{[k]\dagger} (\mathbf{P} - \mathbf{P} \mathbf{V}^\dagger \mathbf{H}^{[k]\dagger} (\mathbf{I} + \mathbf{H}^{[k]} \mathbf{V} \mathbf{P} \mathbf{V}^\dagger \mathbf{H}^{[k]\dagger})^{-1} \mathbf{H}^{[k]} \mathbf{V} \mathbf{P}) \mathbf{a}_m^{[k]} \quad (8.37)$$

$$\triangleq \|\mathbf{F}^{[k]} \mathbf{a}_m^{[k]}\|^2 \quad (8.38)$$

where  $\mathbf{F}^{[k]} = (\mathbf{P}^{-1} + \mathbf{V}^\dagger \mathbf{H}^{[k]\dagger} \mathbf{H}^{[k]} \mathbf{V})^{-\frac{1}{2}}$  and the last inequality follows from Woodbury's matrix identity.

Recall that, for a fixed  $\mathbf{U}^{[k]}$  and  $\mathbf{v}^{[\ell]}$ , (8.35) is relaxed to

$$\min_{\mathbf{A}^{[k]} \in \mathbb{Z}^{M^{[k]} \times K}} \max_{m=1, \dots, M^{[k]}} (\sigma_{\text{eff},m}^{[k]})^2 \quad (8.39)$$

$$\begin{aligned} \text{subject to} \quad & \text{rank}(\mathbf{A}^{[k]}) = M^{[k]} \\ & \text{rank}(\mathbf{A}_{\sim k}^{[k]}) = M^{[k]} - 1 \end{aligned}$$

which can be shown to be equivalent to

$$\begin{aligned} \min_{\mathbf{A}^{[k]} \in \mathbb{Z}^{M^{[k]} \times K}} \quad & \prod_{m=1}^{M^{[k]}} \left( \sigma_{\text{eff},m}^{[k]} \right)^2 \quad (8.40) \\ \text{subject to} \quad & \text{rank}(\mathbf{A}^{[k]}) = M^{[k]} \\ & \text{rank}(\mathbf{A}_{\sim k}^{[k]}) = M^{[k]} - 1 \end{aligned}$$

Combining (8.37) with (8.40), such a problem is equivalent to finding the shortest  $M^{[k]}$  vectors in the lattice spanned by  $\mathbf{F}^{[k]}$  satisfying the constraints in (8.40).

Finding the shortest and independent  $M^{[k]}$  vectors in a lattice spanned by  $\mathbf{F}^{[k]}$  is, in general, a hard problem. Some polynomial time algorithms (e.g., LLL algorithm [Lenstra et al., 1982]) can provide a good approximation, but there is no guarantee for satisfying the conditions in (8.26) and (8.27). In order to solve this, we introduce a lattice reduction method that we call the aligned LLL algorithm to obtain the desired  $\mathbf{A}^{[k]}$ . For general case ( $M^{[k]} \geq 2$ ), a generalization of this aligned LLL algorithm is given in Appendix G as well as simulation results.

For a fixed  $M^{[k]} = 2$  (i.e.,  $\mathbf{A}^{[k]} \in \mathbb{Z}^{2 \times K}$ ), we need to align the coefficients of the  $K - 1$  interference codewords into a single combination. Recall that  $\mathbf{a}_m^{[k]\dagger}$  is the  $m^{\text{th}}$  row of  $\mathbf{A}^{[k]}$  for  $m = 1, 2$  and  $\mathbf{a}_{m \sim k}^{[k]\dagger}$  is the vector resulting from dropping the  $k^{\text{th}}$  entry of vector  $\mathbf{a}_m^{[k]\dagger}$  (i.e., dropping the coefficient of the desired codeword). At the  $k^{\text{th}}$  receiver, the constraints in (8.26) and (8.27) can be rewritten as constraints for  $\mathbf{a}_1^{[k]\dagger}$  and  $\mathbf{a}_2^{[k]\dagger}$  such that

$$\mathbf{a}_{1 \sim k}^{[k]} = b_{1,2}^{[k]} \mathbf{a}_{\text{int}}^{[k]} \quad (8.41)$$

$$\mathbf{a}_{2 \sim k}^{[k]} = b_{2,2}^{[k]} \mathbf{a}_{\text{int}}^{[k]} \quad (8.42)$$

$$a_{1,k}^{[k]} = b_{1,1}^{[k]} \quad (8.43)$$

$$a_{2,k}^{[k]} = b_{2,1}^{[k]} \quad (8.44)$$

$$\text{rank} \left( \begin{bmatrix} b_{1,1}^{[k]} & b_{1,2}^{[k]} \\ b_{2,1}^{[k]} & b_{2,2}^{[k]} \end{bmatrix} \right) = 2 \quad (8.45)$$

where  $\mathbf{a}_{\text{int}}^{[k]} \in \mathbb{Z}^{K-1}$  and  $b_{m,i}^{[k]} \in \mathbb{Z}, \forall i, m = 1, 2$ .

Here the vector  $\mathbf{a}_{\text{int}}^{[k]}$  represents the coefficients of an aligned function. Recall that  $\mathbf{S} \triangleq [\mathbf{s}^{[1]} \ \dots \ \mathbf{s}^{[K]}]^\dagger$  denote the matrix of codewords and let  $(\mathbf{S}^\dagger)_{\sim k}$  be the matrix resulting from dropping the  $k^{\text{th}}$  column of  $\mathbf{S}^\dagger$  (i.e., dropping the desired codeword). Another way to view this, is to define an aligned function of interfering codewords as

$$\mathbf{g}^{[k]} = (\mathbf{S}^\dagger)_{\sim k} \mathbf{a}_{\text{int}}^{[k]}. \quad (8.46)$$

Now, we decode two independent integer-combinations  $\mathbf{r}_1^{[k]}$  and  $\mathbf{r}_2^{[k]}$  given by

$$\mathbf{r}_1^{[k]} = b_{1,1}^{[k]} \mathbf{s}^{[k]} + b_{1,2}^{[k]} \mathbf{g}^{[k]}, \quad (8.47)$$

$$\mathbf{r}_2^{[k]} = b_{2,1}^{[k]} \mathbf{s}^{[k]} + b_{2,2}^{[k]} \mathbf{g}^{[k]}. \quad (8.48)$$

If  $\mathbf{r}_1^{[k]}$  and  $\mathbf{r}_2^{[k]}$  are decoded successfully, we can solve for  $\mathbf{s}^{[k]}$  (and  $\mathbf{g}^{[k]}$ ). Our goal is to find the optimal (or a good approximation)  $\mathbf{a}_1^{[k]\dagger}$  and  $\mathbf{a}_2^{[k]\dagger}$  given by the structure in (8.41)-(8.44) to minimize the product of effective noise powers  $\prod_{m=1,2} \|\mathbf{F}^{[k]} \mathbf{a}_m^{[k]}\|^2$ .

We propose a method based on Minkowski's second theorem [Cassels, 1957]. The method allows us to get a theoretical lower-bound on the computation sum rate. For any chosen interference function  $\mathbf{g}^{[k]}$  in (8.46), we choose two independent integer

vectors  $\mathbf{b}_1^{[k]} = [b_{1,1}^{[k]} \ b_{1,2}^{[k]}]^\dagger$  and  $\mathbf{b}_2^{[k]} = [b_{2,1}^{[k]} \ b_{2,2}^{[k]}]^\dagger$  to minimize  $\prod_{m=1}^2 (\sigma_{\text{eff},m}^{[k]})^2$  which can be written as

$$\prod_{m=1}^2 (\sigma_{\text{eff},m}^{[k]})^2 = \prod_{m=1}^2 \|\mathbf{F}^{[k]} \mathbf{a}_m^{[k]}\|^2 \quad (8.49)$$

$$= \prod_{m=1}^2 \|b_{m,1}^{[k]} \mathbf{f}_k^{[k]} + b_{m,2}^{[k]} \mathbf{F}_{\sim k}^{[k]} \mathbf{a}_{\text{int}}^{[k]}\|^2 \quad (8.50)$$

$$= \prod_{m=1}^2 \|\mathbf{F}_{\text{red}}^{[k]} \mathbf{b}_m^{[k]}\|^2 \quad (8.51)$$

where  $\mathbf{F}_{\text{red}}^{[k]} = \begin{bmatrix} \mathbf{f}_k^{[k]} & \mathbf{F}_{\sim k}^{[k]} \mathbf{a}_{\text{int}}^{[k]} \end{bmatrix}$  represents the basis of a new reduced lattice. The first column of this basis corresponds to the desired signal  $\mathbf{s}^{[k]}$ , while the second column corresponds to the interference function  $\mathbf{g}^{[k]}$ .

Since there is no constraints on  $\mathbf{b}_1^{[k]}$  and  $\mathbf{b}_2^{[k]}$  other than independence, (8.51) means that minimizing  $\prod_{m=1}^2 (\sigma_{\text{eff},m}^{[k]})^2$  (for a given fixed  $\mathbf{a}_{\text{int}}^{[k]}$ ) is now mapped to finding the two shortest non-zero vectors in this new lattice with basis  $\mathbf{F}_{\text{red}}^{[k]}$ . The optimal  $\mathbf{b}_1^{[k]}$  and  $\mathbf{b}_2^{[k]}$  are given as a function of  $\mathbf{a}_{\text{int}}^{[k]}$  by

$$\mathbf{b}_1^{[k]} = \arg \min_{\mathbf{b} \in \mathbb{Z}^2, \mathbf{b} \neq \mathbf{0}} \|\mathbf{F}_{\text{red}}^{[k]} \mathbf{b}\|^2 \quad (8.52)$$

$$\mathbf{b}_2^{[k]} = \arg \min_{\mathbf{b} \in \mathbb{Z}^2: \text{rank}([\mathbf{b}_1^{[k]} \ \mathbf{b}])=2} \|\mathbf{F}_{\text{red}}^{[k]} \mathbf{b}\|^2. \quad (8.53)$$

Note that a lattice reduction algorithm (e.g., the LLL algorithm) can be used to give the optimal solution since  $\dim(\mathbf{F}_{\text{red}}^{[k]}) = 2$ . The remaining question is how to select  $\mathbf{a}_{\text{int}}^{[k]}$ ?

From [Feng et al., 2013] and (8.51), the powers of the effective noise in the two integer-combinations are given by the first and second successive minima of the reduced lattice  $\mathbf{F}_{\text{red}}^{[k]}$  such that  $(\sigma_{\text{eff},1}^{[k]})^2 = \lambda_1^2(\mathbf{F}_{\text{red}}^{[k]})$  and  $(\sigma_{\text{eff},2}^{[k]})^2 = \lambda_2^2(\mathbf{F}_{\text{red}}^{[k]})$ . We can write

the sum of the computation rates as

$$\sum_{m=1}^2 R_{\text{comp},m}^{[k]} = \frac{1}{2} \sum_{m=1}^2 \log \left( \frac{\rho}{(\sigma_{\text{eff},m}^{[k]})^2} \right) \quad (8.54)$$

$$= \frac{1}{2} \log \left( \frac{\rho^2}{\prod_{m=1}^2 \lambda_m^2(\mathbf{F}_{\text{red}}^{[k]})} \right) \quad (8.55)$$

$$\stackrel{(a)}{\geq} \frac{1}{2} \log \left( \frac{\rho^2}{4 |\det(\mathbf{F}_{\text{red}}^{[k]\dagger} \mathbf{F}_{\text{red}}^{[k]})|} \right) \quad (8.56)$$

where (a) is due to Minkowski's second theorem [Cassels, 1957]. Furthermore, we can write  $\det(\mathbf{F}_{\text{red}}^{[k]\dagger} \mathbf{F}_{\text{red}}^{[k]})$  as

$$\det(\mathbf{F}_{\text{red}}^{[k]\dagger} \mathbf{F}_{\text{red}}^{[k]}) = \|\mathbf{f}_k^{[k]}\|^2 \|\mathbf{F}_{\sim k}^{[k]} \mathbf{a}_{\text{int}}^{[k]}\|^2 - (\mathbf{f}_k^{[k]\dagger} \mathbf{F}_{\sim k}^{[k]} \mathbf{a}_{\text{int}}^{[k]})^2 \quad (8.57)$$

$$= \mathbf{a}_{\text{int}}^{[k]\dagger} \mathbf{F}_{\sim k}^{[k]\dagger} \|\mathbf{f}_k^{[k]}\| \left( \mathbf{I} - \frac{\mathbf{f}_k^{[k]} \mathbf{f}_k^{[k]\dagger}}{\|\mathbf{f}_k^{[k]}\|^2} \right) \|\mathbf{f}_k^{[k]}\| \mathbf{F}_{\sim k}^{[k]} \mathbf{a}_{\text{int}}^{[k]} \quad (8.58)$$

$$= \|\mathbf{G}^{[k]} \mathbf{a}_{\text{int}}^{[k]}\|^2 \quad (8.59)$$

where  $\mathbf{G}^{[k]}$  can be obtained by Cholesky factorization of  $(\mathbf{F}_{\sim k}^{[k]\dagger} \|\mathbf{f}_k^{[k]}\| \left( \mathbf{I} - \frac{\mathbf{f}_k^{[k]} \mathbf{f}_k^{[k]\dagger}}{\|\mathbf{f}_k^{[k]}\|^2} \right) \|\mathbf{f}_k^{[k]}\| \mathbf{F}_{\sim k}^{[k]})$ . Since minimizing the determinant in (8.57) results in the sharpest bound in (8.56), the interference function  $\mathbf{g}^{[k]}$  (i.e.,  $\mathbf{a}_{\text{int}}^{[k]}$ ) can be obtained by lattice reduction on  $\mathbf{G}^{[k]}$ :

$$\mathbf{a}_{\text{int}}^{[k]} = \arg \min_{\mathbf{a} \in \mathbb{Z}^{K-1}} \|\mathbf{G}^{[k]} \mathbf{a}\|^2. \quad (8.60)$$

Choosing  $\mathbf{a}_{\text{int}}^{[k]}$  as in (8.60) guarantees that  $\|\mathbf{G}^{[k]} \mathbf{a}_{\text{int}}^{[k]}\|^2$  is the shortest vector in a lattice with basis  $\mathbf{G}^{[k]}$  (i.e.,  $\lambda_1^2(\mathbf{G}^{[k]})$ ) and as a result we can bound the sum of the computation rates as

$$\sum_{m=1}^2 R_{\text{comp},m}^{[k]} \geq \frac{1}{2} \log \left( \frac{\text{SNR}^2}{4 \lambda_1^2(\mathbf{G}^{[k]})} \right) \quad (8.61)$$

$$\stackrel{(a)}{\geq} \frac{1}{2} \log \left( \frac{\text{SNR}^2}{4(K-1) \det(\mathbf{G}^{[k]})^{\frac{2}{K-1}}} \right) \quad (8.62)$$

where (a) is due to Minkowski's first theorem [Cassels, 1957]. Algorithm 5 shows the details of the aligned LLL algorithm for  $M^{[k]} = 2$ .

---

**Algorithm 5** Proposed Method A for decoding two integer-combinations

---

1. Step 1: Using the LLL algorithm, find the shortest vector in the lattice  $\mathbf{G}^{[k]}$

$$\mathbf{a}_{\text{int}}^{[k]} = \arg \min_{\mathbf{a} \in \mathbb{Z}^{K-1}} \|\mathbf{G}^{[k]} \mathbf{a}\|^2$$

where  $\mathbf{G}^{[k]}$  can be obtained by factoring  $\mathbf{G}^{[k]\dagger} \mathbf{G}^{[k]} = \mathbf{F}_{\sim k}^{[k]\dagger} \|\mathbf{f}_k^{[k]}\| \left( \mathbf{I} - \frac{\mathbf{f}_k^{[k]} \mathbf{f}_k^{[k]\dagger}}{\|\mathbf{f}_k^{[k]}\|^2} \right) \|\mathbf{f}_k^{[k]}\| \mathbf{F}_{\sim k}^{[k]}$  using Cholesky decomposition.

2. Step 2: Using the LLL algorithm, find the shortest two vectors in the lattice  $\mathbf{F}_{\text{red}}^{[k]} = [\mathbf{f}_k^{[k]} \quad \mathbf{F}_{\sim k}^{[k]} \mathbf{a}_{\text{int}}^{[k]}]$

$$\mathbf{b}_i^{[k]} = \arg \min_{\mathbf{b} \in \mathbb{Z}^2: \text{rank}([\mathbf{b}_1^{[k]}, \dots, \mathbf{b}_{i-1}^{[k]}, \mathbf{b}])=i} \|\mathbf{F}_{\text{red}}^{[k]} \mathbf{b}\|^2, \quad i = 1, 2$$

3. Step 3: Calculate the integer matrix  $\mathbf{A}^{[k]}$  using

$$\tilde{\mathbf{A}}^{[k]} = \begin{bmatrix} b_{1,1}^{[k]} & b_{1,2}^{[k]} \mathbf{a}_{\text{int}}^{[k]} \\ b_{2,1}^{[k]} & b_{2,2}^{[k]} \mathbf{a}_{\text{int}}^{[k]} \end{bmatrix}$$

$$\mathbf{A}^{[k]} = \mathbf{L}^{[k]} (\tilde{\mathbf{A}}^{[k]})$$

where  $\mathbf{L}^{[k]}$  is a permutation matrix which puts column 1 in between columns  $k$  and  $k+1$  of  $\tilde{\mathbf{A}}^{[k]}$ .

---

## 8.4 Beamforming and Equalization

In this section, we propose two methods to optimize beamforming matrix  $\mathbf{V}$  and equalization matrix  $\mathbf{U}^{[k]}$  while fixing  $\mathbf{A}^{[k]}$ . Even after fixing  $\mathbf{A}^{[k]}$ , jointly optimizing

$\mathbf{V}$  and  $\mathbf{U}^{[k]}$  is a non-convex problem, and we will relax this joint optimization problem into two separate optimization problems.

For any given beamforming matrix,  $\mathbf{V}$ , the columns of the optimal equalization matrix  $\mathbf{U}^{[k]}$  is always in the form of MMSE equalizer as in (8.36). On the other hand, for a given equalization matrix  $\mathbf{U}^{[k]}$ , we develop two algorithms to update the beamforming matrix  $\mathbf{V}$ . The first algorithm relaxes the problem of choosing  $\mathbf{V}$ , given  $\mathbf{A}^{[k]}$  and  $\mathbf{U}^{[k]}$ , to a convex optimization problem. Then uses a convex optimization toolbox, like the CVX package [Grant and Boyd, 2014], to solve the relaxed convex problem. The second algorithm optimizes  $\mathbf{V}$  given  $\mathbf{U}^{[k]}$  using the idea of channel reciprocity and uplink-downlink duality for integer-forcing [He et al., 2018]. Both algorithms are iterative optimization algorithms in the sense that, we keep updating  $\mathbf{U}^{[k]}$  and  $\mathbf{V}$  given  $\mathbf{A}^{[k]}$  using these two methods. By the end of each iteration, the integer matrix  $\mathbf{A}^{[k]}$  can be updated using the aligned LLL algorithm introduced in Section 8.3 for fixed  $\mathbf{V}$  and  $\mathbf{U}^{[k]}$ .

We use the CVX package to solve the convex optimization problem for our first algorithm, thus we name the first algorithm CVX-IFIA. The second algorithm is called Dual-IFIA since it borrows the idea of duality for integer-forcing from [He et al., 2018].

#### 8.4.1 CVX-IFIA

Recall that our focus has been shifted towards maximizing the sum of the computation rates rather than the sum of the user rates. This method further relaxes this goal by maximizing the worst computation rate (i.e., largest effective noise power) across all the receivers. Since this computation rate will be mapped to one of the user rates, this corresponds to maximizing the symmetric rate.

The relaxed problem can be written as

$$\begin{aligned} \mathbb{P}1 : \quad & \min_{\mathbf{V}, \mathbf{U}^{[k]}} \left( \max_{k,m} (\sigma_{\text{eff},m}^{[k]})^2 \right) \\ & s.t. \quad \|\mathbf{v}^{[\ell]}\|^2 \leq 1, \quad \forall \ell. \end{aligned} \tag{8.63}$$

As mentioned earlier, the joint optimization problem  $\mathbb{P}1$  is a non-convex optimization problem. However, for a fixed  $\mathbf{U}^{[k]}$ ,  $\mathbb{P}1$  can be rewritten as

$$\begin{aligned} \mathbb{P}2 : \quad & \min_{\mathbf{V}} \left( \max_{k,m} (\sigma_{\text{eff},m}^{[k]})^2 \right) \\ & s.t. \quad \|\mathbf{v}^{[\ell]}\|^2 \leq 1, \quad \forall \ell. \end{aligned} \tag{8.64}$$

which is a convex optimization problem. Since for any fixed beamforming matrix  $\mathbf{V}$ , (8.36) gives the columns of the optimal  $\mathbf{U}^{[k]}$ , one can iteratively optimize  $\mathbf{U}^{[k]}$  and  $\mathbf{V}$  using (8.36) and the solution of (8.64). The details of the algorithm is presented in Algorithm 2. To guarantee better performance, the CVX-IFIA algorithm is initialized by the beamforming vectors given by the Max-SINR algorithm described in Section 8.1.

#### 8.4.2 Dual-IFIA

Before giving the details of the algorithm, we introduce the dual channel and dual network for the IFIA. The dual channel for IFIA is a bit trickier than the dual channel for linear receivers (introduced in Section 8.1). This is because the number of transmitted codewords (beamforming vectors) from each transmitter and the number of decoded combinations (equalization vectors) at each receiver are not always equal anymore. In the primal network, each receiver  $k$  wants to decode  $M^{[k]}$  combinations and solve for the desired single codeword  $\mathbf{s}^{[k]}$  sent by the  $k^{\text{th}}$  transmitter. Overall, we have  $M = \sum_{k=1}^K M^{[k]} \geq K$  combinations decoded at all the receivers.

In the dual network, the receivers and transmitters roles are reversed. The  $\ell^{\text{th}}$  pri-

mal receiver becomes the  $\ell^{\text{th}}$  dual transmitter and the  $k^{\text{th}}$  primal transmitter becomes the  $k^{\text{th}}$  dual receiver (i.e., the dual channel matrix  $\overleftarrow{\mathbf{H}}^{[k,\ell]} = \mathbf{H}^{[\ell,k]\dagger}$ ). In addition, the beamforming (equalization) vectors of the primal network become the equalization (beamforming) vectors of the dual network, respectively. As a result, in the dual network, each dual transmitter  $\ell$  wants to send  $M^{[\ell]}$  messages, while each dual receiver  $k$  wants to decode only one combination of these messages. We have dual beamforming matrices  $\overleftarrow{\mathbf{V}}^{[\ell]} \in \mathbb{R}^{N_{\text{Rx}}^{[\ell]} \times M^{[\ell]}}$  and the dual equalization vectors  $\overleftarrow{\mathbf{u}}^{[k]} \in \mathbb{R}^{N_{\text{Tx}}^{[k]}}$ . Let  $\mathbf{A} = [\mathbf{A}^{[1]\dagger} \ \dots \ \mathbf{A}^{[K]\dagger}]^\dagger \in \mathbb{Z}^{M \times K}$  be the integer matrix of the primal channel, the dual integer matrix can be represented as

$$\overleftarrow{\mathbf{A}} = \mathbf{A}^\dagger \in \mathbb{Z}^{K \times M} \quad (8.65)$$

where  $K$  here represents the total number of combinations and  $M$  represents the total number of the transmitted messages. Define the channel to the  $k^{\text{th}}$  dual receiver as

$$\overleftarrow{\mathbf{H}}^{[k]} = \left[ \overleftarrow{\mathbf{H}}^{[k,1]} \ \dots \ \overleftarrow{\mathbf{H}}^{[k,K]} \right]. \quad (8.66)$$

Following the same steps as in the primal IFIA, the  $k^{\text{th}}$  dual receiver decodes a single combination and we can write the power of the effective noise on this combination as

$$(\overleftarrow{\sigma}_{\text{eff}}^{[k]})^2 \triangleq \|\overleftarrow{\mathbf{u}}^{[k]\dagger}\|^2 + (\overleftarrow{\mathbf{u}}^{[k]\dagger} \overleftarrow{\mathbf{H}}^{[k]} \overleftarrow{\mathbf{V}} - \overleftarrow{\mathbf{a}}^{[k]\dagger}) \overleftarrow{\mathbf{P}} (\overleftarrow{\mathbf{u}}^{[k]\dagger} \overleftarrow{\mathbf{H}}^{[k]} \overleftarrow{\mathbf{V}} - \overleftarrow{\mathbf{a}}^{[k]\dagger})^\dagger$$

where  $\overleftarrow{\mathbf{V}}$  is the block diagonal matrix of  $[\overleftarrow{\mathbf{V}}^{[1]} \ \dots \ \overleftarrow{\mathbf{V}}^{[K]}]$  and  $\overleftarrow{\mathbf{P}}$  is the diagonal coding power matrix with diagonal elements

$$\overleftarrow{P}_{i,i} = \frac{\rho}{\|\overleftarrow{\mathbf{v}}_i\|^2}, \quad i = 1, \dots, M \quad (8.67)$$

where  $\overleftarrow{\mathbf{v}}_i$  is the  $i^{\text{th}}$  column of the matrix  $\overleftarrow{\mathbf{V}}$ .

The optimal equalization vector  $\overleftarrow{\mathbf{u}}^{[k]\dagger}$  which minimizes the effective noise power

$\overleftarrow{\sigma}_{\text{eff}}^{[k]}$  at the  $k^{\text{th}}$  dual receiver is

$$\overleftarrow{\mathbf{u}}_{\text{opt}}^{[k]\dagger} = \overleftarrow{\mathbf{A}}^{[k]} \overleftarrow{\mathbf{P}}^\dagger \overleftarrow{\mathbf{V}}^\dagger \overleftarrow{\mathbf{H}}^{[k]\dagger} (\mathbf{I} + \overleftarrow{\mathbf{H}}^{[k]} \overleftarrow{\mathbf{V}} \overleftarrow{\mathbf{P}} \overleftarrow{\mathbf{V}}^\dagger \overleftarrow{\mathbf{H}}^{[k]\dagger})^{-1}. \quad (8.68)$$

In order to update  $\mathbf{V}$ , we use the equalization vectors  $\overleftarrow{\mathbf{u}}^{[k]}$  at the  $k^{\text{th}}$  dual receiver (after normalizing) and map it to the beamforming vectors  $\mathbf{v}^{[k]}$  for the  $k^{\text{th}}$  primal transmitter. Finally, We can iteratively use the closed form expressions in (8.36) and (8.68) to optimize the beamforming and equalization vectors. The details of the the proposed algorithm is given in Algorithm 6.

## 8.5 Simulation Results

We now briefly investigate the performance of our iterative algorithms. In our simulations, we consider the case of 500 channel realizations. Figure 8.3 shows the sum rate of three users obtained after 20 iterations of each algorithm. For the first plot, we have set  $K = 3$  and  $M^{[k]} = 2, \forall k$  (i.e., all terminals have two antennas). Recall that this scenario satisfies the feasibility conditions in [Yetis et al., 2010] for the existence of a linear strategy. The elements of the channel matrices  $\mathbf{H}^{[k,\ell]}$  are drawn i.i.d.  $\mathcal{N}(0, 1)$ . Notice that the Max-SINR algorithm is a special case of the IFIA algorithm where the integer matrix  $\mathbf{A}$  is set to the identity matrix. Thus, we can pick the maximum sum rate between any IFIA algorithm as well as Max-SINR without changing our decoding framework. In Fig 8.3, “max all” represents the maximum rate achieved among “Dual-IFIA”, “ CVX-IFIA” and “Max-SINR”. “Decode All” is the scenario where  $M^{[k]} = 3, \forall k$  and thus there is no interference alignment. For clarity, we have omitted the plot of  $\max(\text{Max-SINR}, \text{Dual-IFIA})$  as well as  $\max(\text{Max-SINR}, \text{CVX-IFIA})$  since they are close to “max all”. From Fig 8.3, it can be observed that our IFIA algorithms attain the same slope as the Max-SINR algorithm. The performance can be ordered from the highest sum rate to the lowest as follows: “max all”,

---

**Algorithm 6** Dual/CVX-IFIA Iterative Optimization
 

---

Given Iteration Number, power constraint  $\rho$  and  $\mathbf{H}^{[k,\ell]}, \forall k, \ell$ .

1. Initialization: counter=0,  $\mathbf{v}^{[k]}, \mathbf{U}^{[k]}, \rho_k = \rho, \forall k$ .
  2. Run Max SINR algorithm and update  $\mathbf{v}^{[k]}$  and  $\mathbf{U}^{[k]}, \forall k$ .
  3. Choose  $\mathbf{A}$  using Algorithm 1.
  4. Optimize  $\mathbf{U}^{[k]}$  using (8.36),  $\forall k$ .
  5. **while** counter < Iteration Number **do**
  6.
    - (a) **if** Dual-IFIA
      - i. Set  $\overleftarrow{\mathbf{A}} = \mathbf{A}^\dagger, \overleftarrow{\mathbf{H}}^{[k,\ell]} = \mathbf{H}^{[\ell,k]\dagger}$  and  $\overleftarrow{\mathbf{V}}^{[k]} = \mathbf{U}^{[k]}$ .
      - ii. Optimize  $\overleftarrow{\mathbf{u}}^{[k]\dagger}$  using (8.68),  $\forall k$ .
      - iii. **if**  $\|\overleftarrow{\mathbf{u}}^{[k]}\|^2 > 1$  **then**
      - iv.     Normalize  $\overleftarrow{\mathbf{u}}^{[k]}$ .
      - v.     **end if**
      - vi.    Set  $\mathbf{v}^{[k]} = \overleftarrow{\mathbf{u}}^{[k]}, \forall k$ .
    - else if** CVX-IFIA
      - i.    Using CVX package, solve P2
      - ii.   Optimize  $\mathbf{U}^{[k]}$  using (8.36),  $\forall k$ .
    - end if**
  - (b)    Update  $\rho_k = \rho / \|\mathbf{v}^{[k]}\|^2, \forall k$ .
  - (c)    Update  $\mathbf{A}$  using Algorithm 1.
  - (d)    counter=counter+1.
7. **end while**
8. Optimize  $\mathbf{U}^{[k]}$  using (8.36),  $\forall k$ .
9. Output  $\rho_k, \mathbf{A}^{[k]}, \mathbf{v}^{[k]}$  and  $\mathbf{U}^{[k]}, \forall k$ .
-

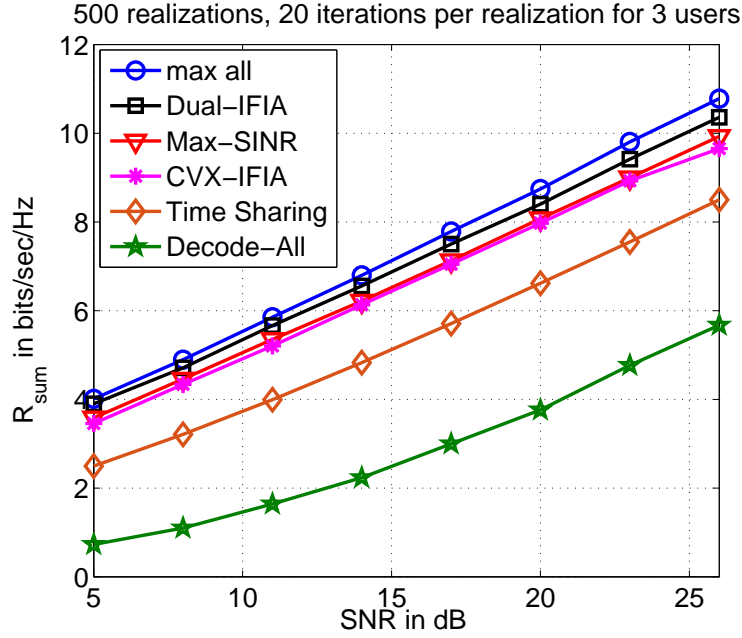


**Figure 8-3:**  $K = 3$ ,  $N_{\text{Tx}}^{[k]} = N_{\text{Rx}}^{[k]} = 2$ ,  $M^{[k]} = 2, \forall k$ .

“Dual-IFIA”, “Max-SINR”, “CVX-IFIA”, “time sharing”, and “Decode All”.

For comparison, Fig 8-4 shows the sum rates for 4 users ( $K = 4$ ), which is no longer a feasible scenario [Yetis et al., 2010] for linear strategies in terms of degrees-of-freedom. For clarity, we omit the plot of  $\max(\text{Max-SINR}, \text{CVX-IFIA})$  and  $\max(\text{Max-SINR}, \text{Dual-IFIA})$ , since they are only slightly higher than Dual-IFIA. In Fig 8-4, “Decode All” is the scenario where  $M^{[k]} = 4, \forall k$  and “max all” represents the maximum rate achieved among “Dual-IFIA”, “Max-SINR”, “CVX-IFIA”, and “Decode All”. It can be seen that IFIA outperforms Max-SINR significantly. It also outperforms “time sharing” at low SNR.

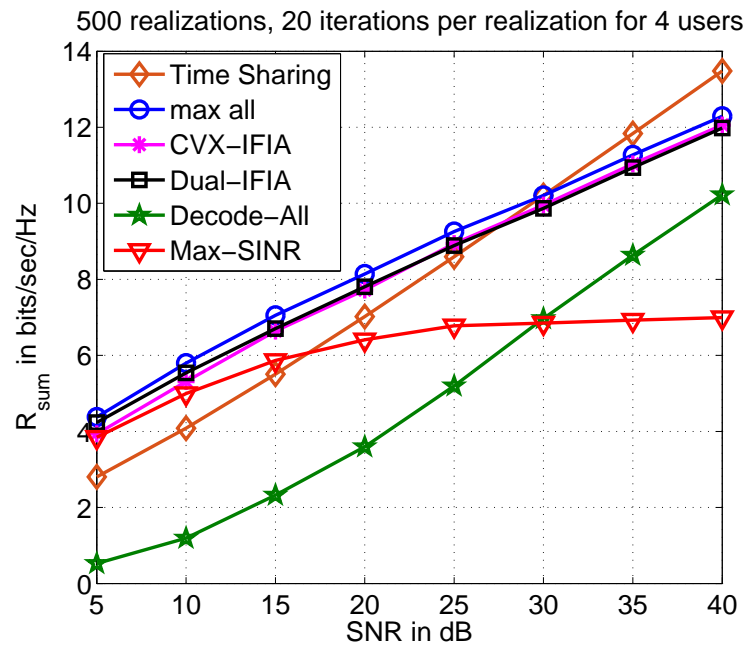


Figure 8.4:  $K = 4$ ,  $N_{\text{Tx}}^{[k]} = N_{\text{Rx}}^{[k]} = 2$ ,  $M^{[k]} = 2, \forall k$ .

## Chapter 9

# Time-Varying Integer-Forcing Receivers

In many important scenarios, the channel may vary significantly within the span of a single codeword. For instance, under orthogonal frequency-division multiplexing (OFDM), channel variation will occur across OFDM symbols if the channel is frequency-selective [Knopp and Humblet, 2000]. In this chapter, we extend the integer-forcing (IF) receiver to the time-varying channel setting and compare its performance with conventional linear receivers.

### 9.1 Channel Models

For simplicity, we assume a discrete-time communication system

$$\mathbf{y}(t) = \mathbf{H}(t)\mathbf{x}(t) + \mathbf{z}(t), \quad t = 1, \dots, T \quad (9.1)$$

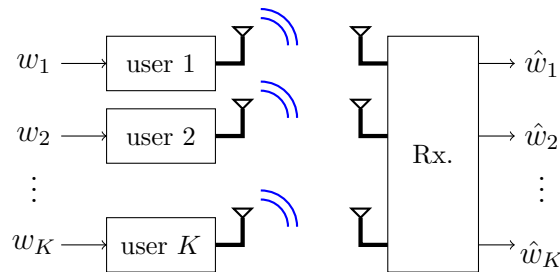


**Figure 9.1:** MIMO MAC channel with  $K$  users

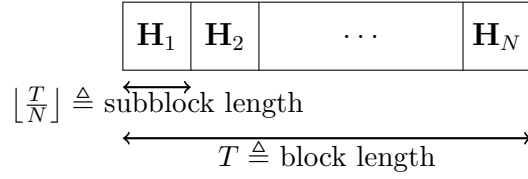


**Figure 9.2:** The block fading model.

where  $\mathbf{y}(t) \in \mathbb{R}^K$  is the received signal,  $\mathbf{H}(t) \in \mathbb{R}^{K \times K}$  is the real-valued<sup>1</sup> channel matrix,  $\mathbf{x}(t) \triangleq [x_1(t) \cdots x_K(t)]^\dagger$  is the vector of channel inputs,  $T$  is the block length, and  $\mathbf{z}(t) \sim \mathcal{N}(\mathbf{0}, \mathbf{I})$  is additive Gaussian noise. This system represents a MIMO channel or MIMO MAC as in Fig 9.1.

### 9.1.1 Static Channels

Previously proposed IF schemes assume that the channel is fixed through the codeword (i.e.,  $\mathbf{H}(t) = \mathbf{H}$ ,  $t = 1, \dots, T$ ), hence the communication system in (9.1) can be written as

$$\mathbf{Y} = \mathbf{H}\mathbf{X} + \mathbf{Z} \quad (9.2)$$

where  $\mathbf{Y} \triangleq [\mathbf{y}(1) \cdots \mathbf{y}(T)]$ ,  $\mathbf{X} \triangleq [\mathbf{x}(1) \cdots \mathbf{x}(T)]$  and  $\mathbf{Z} \triangleq [\mathbf{z}(1) \cdots \mathbf{z}(T)]$ .

### 9.1.2 Block Fading Channels

In this more general model, the channel is assumed to be fixed within a subblock, but changes from subblock to another. Formally, we model the block fading channel as

$$\mathbf{H}(t) = \mathbf{H}_n, \quad (n-1) \left\lfloor \frac{T}{N} \right\rfloor + 1 \leq t \leq n \left\lfloor \frac{T}{N} \right\rfloor, \quad n = 1, \dots, N \quad (9.3)$$

where  $N$  is the number of the subblocks in each block as shown in Figure 9.2.

The received signal during subblock  $n$  can be written as

<sup>1</sup>For simplicity, we consider real-valued channels since complex-valued channels can be handled using a real-valued decomposition [Nazer and Gastpar, 2011].

$$\mathbf{Y}_n = \mathbf{H}_n \mathbf{X}_n + \mathbf{Z}_n, \forall n = 1, \dots, N \quad (9.4)$$

where  $\mathbf{X}_n \triangleq [\mathbf{x}((n-1)\lfloor T/N \rfloor + 1) \cdots \mathbf{x}(n\lfloor T/N \rfloor)]$ ,  $\mathbf{Y}_n \triangleq [\mathbf{y}((n-1)\lfloor T/N \rfloor + 1) \cdots \mathbf{y}(n\lfloor T/N \rfloor)]$  and  $\mathbf{Z}_n \triangleq [\mathbf{z}((n-1)\lfloor T/N \rfloor + 1) \cdots \mathbf{z}(n\lfloor T/N \rfloor)]$  are the transmitted signal, received signal, and AWGN during the  $n^{\text{th}}$  subblock, respectively. It will be useful to define  $\mathbf{Y}_1^N \triangleq \{\mathbf{Y}_1, \dots, \mathbf{Y}_N\}$  and  $\mathbf{H}_1^N \triangleq \{\mathbf{H}_1, \dots, \mathbf{H}_N\}$  as the set of observations and channel matrices across all  $N$  subblocks, respectively.

## 9.2 Problem Formulation

Consider the MIMO MAC shown in Figure 9.1, where a set  $\mathcal{K} \triangleq \{1, \dots, K\}$  of single-antenna transmitters want to communicate to a common receiver with  $K$  antennas. The  $k^{\text{th}}$  transmitter has a message  $w_k \in \{1, \dots, 2^{TR}\}$ , where  $R$  (in bits/channel use) denotes the symmetric rate. Using an encoder, the  $k^{\text{th}}$  transmitter maps  $w_k$  into a channel input (codeword)  $\mathbf{x}_k \triangleq [x_k(1) \cdots x_k(T)]^\dagger$  where it satisfies an average power constraint  $\frac{1}{T} \sum_{t=1}^T (x_k(t))^2 \leq \text{SNR}$ . The receiver uses a decoder to obtain estimates  $\hat{w}_1, \dots, \hat{w}_K$  of the messages from its observations  $\mathbf{Y}_1^N$ . We say  $R(\mathbf{H}_1^N)$  is an achievable symmetric rate if there exists encoders and decoders such that the average error probability vanishes as long as  $R < R(\mathbf{H}_1^N)$ . Since the channel is only known to the receiver (CSIR), the transmitters should be willing to tolerate some outage probability  $\rho$ . The outage happens when the transmitting rate  $R > R(\mathbf{H}_1^N)$ . The outage probability is  $P_{\text{outage}}(R) = \Pr\{R > R(\mathbf{H}_1^N)\}$ . On the other hand, the *outage rate* is  $R_{\text{outage}}(\rho) = \max\{R : P_{\text{outage}}(R) \leq \rho\}$ .

## 9.3 Conventional Block Fading Receivers

Since the channel is not static, the effective noise statistics are not fixed and can not be considered identically distributed anymore.

### 9.3.1 Joint ML Receiver

The joint ML receiver for the static case can be directly extended to the block fading case.

**Theorem 16.** (*Joint ML Receiver*): For a fixed set of channel matrices  $\mathbf{H}_1^N$ , joint ML decoding is optimal and achieves the following rate

$$R_{\text{ML}}(\mathbf{H}_1^N) = \min_{\mathcal{S} \subseteq \{1, \dots, K\}} \frac{1}{2N|\mathcal{S}|} \sum_{n=1}^N \log \det(\mathbf{I} + \text{SNR} \mathbf{H}_{n, \mathcal{K}, \mathcal{S}} \mathbf{H}_{n, \mathcal{K}, \mathcal{S}}^\dagger) \quad (9.5)$$

where  $\mathbf{H}_{n, \mathcal{K}, \mathcal{S}}$  is the submatrix consisting of the columns of  $\mathbf{H}_n$  with indices in the set  $\mathcal{S}$ . The proof follows from using i.i.d. Gaussian encoding and simultaneous joint typicality decoding.

### 9.3.2 MMSE Linear Receiver

Linear receivers are often employed as a means of reducing the implementation complexity of multiple-input multiple-output (MIMO) decoding. The basic idea is to first separate the data streams via linear equalization and then recover them via single-user decoding. However, in many scenarios, conventional linear receivers fall short of the performance of optimal joint ML decoding of the data streams.

In order to decode  $\mathbf{x}_m$ , the receiver equalizes  $\mathbf{Y}_n$  using an adaptive equalizer  $\mathbf{b}_{n,m}^\dagger$  for  $n = 1, \dots, N$ , to get

$$\begin{aligned} \tilde{\mathbf{y}}_{n,m}^\dagger &= \mathbf{b}_{n,m}^\dagger \mathbf{Y}_n \\ &= (\mathbf{b}_{n,m}^\dagger \mathbf{h}_{n,m}) \mathbf{x}_{n,m}^\dagger + \mathbf{z}_{\text{eff},n,m}^\dagger \end{aligned} \quad (9.6)$$

where  $\mathbf{h}_{n,m}$  is the  $m^{\text{th}}$  column of  $\mathbf{H}_n$ ,  $\mathbf{b}_{n,m}^\dagger$  is the  $m^{\text{th}}$  row of the equalizer  $\mathbf{B}_n$  and  $\mathbf{z}_{\text{eff},n,m}^\dagger = \sum_{k \neq m} (\mathbf{b}_{n,m}^\dagger \mathbf{h}_{n,m}) \mathbf{x}_{n,k}^\dagger + \mathbf{b}_{n,m}^\dagger \mathbf{Z}_n$  is the effective noise during the  $n^{\text{th}}$  subblock and  $\mathbf{x}_{n,m}$  is the  $n^{\text{th}}$  subvector of the  $m^{\text{th}}$  codeword  $\mathbf{x}_m$ . Note that the total effective

noise  $\mathbf{z}_{\text{eff},m}^\dagger \triangleq [\mathbf{z}_{\text{eff},1,m}^\dagger \cdots \mathbf{z}_{\text{eff},N,m}^\dagger]$  is not identically distributed anymore across the  $N$  subblocks since both the channel  $\mathbf{h}_{n,k}$  and the beamforming vectors  $\mathbf{b}_{n,m}$  are no longer static.

For this *elliptical* noise (i.e., not identically distributed across subblocks), we propose two different MMSE linear receivers.

The first MMSE receiver approximates this elliptical noise to a spherical noise (i.e., identically distributed across subblocks), then uses a conventional SUD.

**Theorem 17.** (*Linear AM-MMSE receiver*): For a fixed set of channel matrices  $\mathbf{H}_1^N$  and a fixed set of equalization matrices  $\mathbf{B}_1^N \triangleq \{\mathbf{B}_1, \dots, \mathbf{B}_N\}$ , the achievable rate for the AM-MMSE receiver is

$$R_{AM,Linear}(\mathbf{H}_1^N, \mathbf{B}_1^N) = \min_{m=1, \dots, N_{Tx}} \frac{1}{2} \log \left( \frac{1}{\frac{1}{N} \sum_{n=1}^N \frac{1}{1 + \text{SINR}_{n,m}}} \right)$$

$$\text{SINR}_{n,m} = \frac{\text{SNR}(\mathbf{b}_{n,m}^\dagger \mathbf{h}_{n,m})^2}{\|\mathbf{b}_{n,m}\|^2 + \text{SNR} \sum_{i \neq m} (\mathbf{b}_{n,m}^\dagger \mathbf{h}_{n,i})^2}. \quad (9.7)$$

where  $\mathbf{b}_{n,m}^\dagger$  is the  $m^{\text{th}}$  row of the equalization matrix  $\mathbf{B}_n$ ,  $\mathbf{h}_{n,m}$  is the  $m^{\text{th}}$  column of the channel matrix  $\mathbf{H}_n$  and  $\text{SINR}_{n,m}$  is the signal to interference and noise ratio. The proof of Theorem 17 follows from Theorem 19 by plugging in  $\mathbf{A} = \mathbf{I}$ .

The second MMSE receivers uses the ambiguity decoder in [Loeliger, 1997] which successfully decodes the desired codeword if the entropy of the noise falls below a certain threshold.

**Theorem 18.** (*Linear GM-MMSE receiver*): For a fixed set of channel matrices  $\mathbf{H}_1^N$  and a fixed set of equalization matrices  $\mathbf{B}_1^N$ , the achievable rate for the GM-MMSE receiver is

$$R_{GM,Linear}(\mathbf{H}_1^N, \mathbf{B}_1^N) = \min_{m=1, \dots, N_{Tx}} \frac{1}{N} \sum_{n=1}^N \frac{1}{2} \log(1 + \text{SINR}_{n,m}) \quad (9.8)$$

where  $\text{SINR}_{n,m}$  is given in (9.7). The proof follows from plugging in  $\mathbf{A} = \mathbf{I}$  in Theorem

20. For both AM-MMSE and GM-MMSE receivers, the optimal equalization matrix  $\mathbf{B}_n$  is

$$\mathbf{B}_{\text{MMSE},n} = \text{SNR} \mathbf{H}_n^\dagger (\mathbf{I} + \text{SNR} \mathbf{H}_n \mathbf{H}_n^\dagger)^{-1}.$$

## 9.4 Block Fading IF Receiver

We now propose a class of IF receivers for the block fading case. The IF receiver decodes integer-linear combinations

$$\begin{aligned} \mathbf{v}_m^\dagger &\triangleq \mathbf{a}_m^\dagger \mathbf{X} \\ &= \sum_{\ell=1}^K a_{m,\ell} \mathbf{x}_\ell^\dagger, \quad m = 1, \dots, K \end{aligned}$$

where  $\mathbf{a}_m \in \mathbb{Z}^K$  is the  $m^{\text{th}}$  row of a full-rank matrix  $\mathbf{A} \triangleq [\mathbf{a}_1 \cdots \mathbf{a}_K]^\dagger$ , then applies the inverse of  $\mathbf{A}$  to  $\mathbf{V} \triangleq [\mathbf{v}_1 \cdots \mathbf{v}_K]^\dagger = \mathbf{A} \mathbf{X}$  in order to recover the codewords  $\mathbf{X}$ .

In order to decode  $\mathbf{v}_m^\dagger$ , the receiver applies an adaptive equalizer  $\mathbf{b}_{n,m}^\dagger$  to obtain the effective channel

$$\begin{aligned} \tilde{\mathbf{y}}_{n,m}^\dagger &= \mathbf{b}_{n,m}^\dagger \mathbf{Y}_n \\ &= \mathbf{a}_m^\dagger \mathbf{X}_n + \mathbf{z}_{\text{eff},n,m}^\dagger, \quad n = 1, \dots, N, \end{aligned} \quad (9.9)$$

where  $\mathbf{z}_{\text{eff},n,m}^\dagger = (\mathbf{b}_{n,m}^\dagger \mathbf{H}_n - \mathbf{a}_m^\dagger) \mathbf{X}_n + \mathbf{b}_{n,m}^\dagger \mathbf{Z}_n$  is the effective noise encountered during the  $n^{\text{th}}$  subblock.

It is important to note that the integer coefficient vector  $\mathbf{a}_m$  is fixed and does not depend on the subblock index  $n$ , since changing it will destroy the closure property of the underlying lattice codebook. It can be argued, similarly to [Zhan et al., 2014], that the effective variance of  $\mathbf{z}_{\text{eff},n,m}$  is

$$\sigma_{\text{eff},n,m}^2(\mathbf{H}_n, \mathbf{b}_{n,m}, \mathbf{a}_m) \triangleq \frac{N}{T} \mathbb{E} \|\mathbf{z}_{\text{eff},n,m}\|^2 = \|\mathbf{b}_{n,m}^\dagger\|^2 + \text{SNR} \|\mathbf{b}_{n,m}^\dagger \mathbf{H}_n - \mathbf{a}_m^\dagger\|^2. \quad (9.10)$$

Finally, the effective channel seen by the  $m^{\text{th}}$  decoder across subblocks is

$$\tilde{\mathbf{y}}_m^\dagger = \mathbf{a}_m^\dagger \mathbf{X} + \mathbf{z}_{\text{eff},m}^\dagger \quad (9.11)$$

where  $\tilde{\mathbf{y}}_m^\dagger = [\tilde{\mathbf{y}}_{1,m}^\dagger \cdots \tilde{\mathbf{y}}_{N,m}^\dagger]$  and  $\mathbf{z}_{\text{eff},m}^\dagger = [\mathbf{z}_{\text{eff},1,m}^\dagger \cdots \mathbf{z}_{\text{eff},N,m}^\dagger]$ . Like the MMSE receiver,  $\mathbf{z}_{\text{eff},m}$  is not identically distributed and we will evaluate the rates for both AM and GM decoders.

**Theorem 19.** (*AM-IF receiver*): For a given set  $\mathbf{H}_1^N$ , the achievable symmetric rate for AM-IF receiver is

$$R_{AM,IF}(\mathbf{H}_1^N) = \max_{\substack{\mathbf{A} \in \mathbb{Z}^{K \times K} \\ \text{rank}(\mathbf{A})=K}} \min_{m=1,\dots,K} \frac{1}{2} \log^+ \left( \frac{\text{SNR}}{\|\mathbf{F}_{eq} \mathbf{a}_m\|^2} \right). \quad (9.12)$$

where  $\mathbf{F}_{eq}$  is any matrix that satisfies  $\mathbf{F}_{eq}^\dagger \mathbf{F}_{eq} = \frac{1}{N} \sum_{n=1}^N \mathbf{F}_n^\dagger \mathbf{F}_n$  where  $\mathbf{F}_n = (\text{SNR}^{-1} \mathbf{I} + \mathbf{H}_n^\dagger \mathbf{H}_n)^{-1/2}$ . The proof of Theorem 19 is given in Appendix A.1

**Theorem 20.** (*GM-IF receiver*): For a given set  $\mathbf{H}_1^N$ , the achievable symmetric rate for GM-IF receiver is

$$R_{GM,IF}(\mathbf{H}_1^N) = \max_{\substack{\mathbf{A} \in \mathbb{Z}^{K \times K} \\ \text{rank}(\mathbf{A})=K}} \min_{m=1,\dots,K} \frac{1}{2} \log^+ \left( \frac{\text{SNR}}{\prod_{n=1}^N \|\mathbf{F}_n \mathbf{a}_m\|^{\frac{2}{N}}} \right) \quad (9.13)$$

where  $\mathbf{F}_n = (\text{SNR}^{-1} \mathbf{I} + \mathbf{H}_n^\dagger \mathbf{H}_n)^{-1/2}$ . The proof of Theorem 20 is given in Appendix A.2

Note that the AM of the noise variance is greater than its GM due to AM-GM inequality, therefore, the rate of the GM-IF receiver is at least as high as the rate of the AM-IF receiver. Also note that, we can find approximate solutions for the integer matrix  $\mathbf{A}$  of the AM-IF receiver by applying the LLL algorithm [Bremner, 2012] to the basis  $\mathbf{F}_{eq}$ . However, the problem of choosing  $\mathbf{A}$  to optimize the GM-IF rate expression does not directly correspond to a lattice reduction problem. It remains

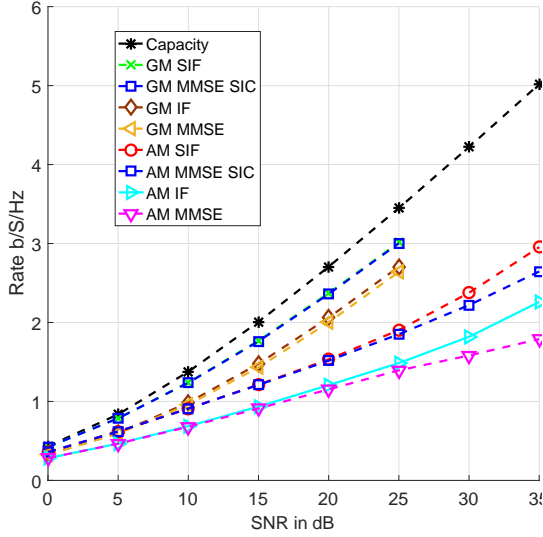


**Figure 9-3:** Outage rates  
at  $\rho = 0.1$ ,  $N = 8$ ,  $K = 2$   
and  $N_{\text{Rx}} = 2$ .

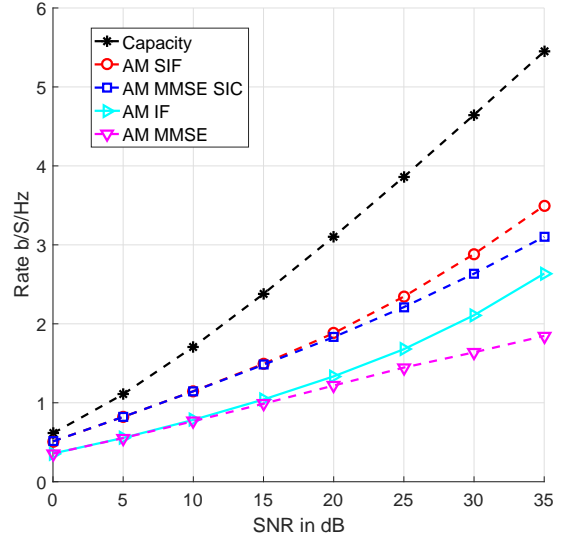


**Figure 9-4:** Outage rates  
at  $\rho = 0.1$ ,  $N = 8$ ,  $K = 3$   
and  $N_{\text{Rx}} = 3$ .

an open problem to find a polynomial-time algorithm that outputs a near-optimal integer matrix  $\mathbf{A}$  for the GM-IF receiver.

## 9.5 Simulation Results

Fig. 9-3 and Fig. 9-4 show the outage rate of IF receivers compared to the MMSE linear receivers and the joint ML receiver. We also include both MMSE and IF receivers with successive interference cancellation [Ordentlich et al., 2013]. The plots are generated from 10000 channel realizations, where each is drawn according to an i.i.d. Gaussian distribution. The outage probability  $\rho$  is 0.1. It is worth mentioning that for both MMSE and IF strategies, we expect the GM receiver to outperform the AM receiver since the GM SINR is at least as high as the AM SINR due to the AM-GM inequality. We also expect the IF receiver's rate (AM or GM) to be as high as the MMSE receiver's rate since the IF receiver with  $\mathbf{A} = \mathbf{I}$  is the MMSE receiver.

The performance can be ordered from the highest symmetric rate to the lowest as follows: "GM-SIF", "GM-MMSE-SIC", "GM-IF", "GM-MMSE", "AM-SIF", "AM-

MMSE-SIC”, ”AM-IF” and ”AM-MMSE”. It is worth noting that the IF-GM receiver requires exhaustive searching all possible<sup>2</sup> integer matrices  $\mathbf{A}$  since the problem of maximizing its symmetric rate does not correspond to a lattice reduction algorithm. It is also noted that the gain of IF receivers over MMSE receivers for both AM and GM schemes becomes more pronounced as the number of users increases and at high SNR.

---

<sup>2</sup>To limit the search space, in our simulations we only searched over all integer vectors with norm less than  $\sqrt{\text{SNR}}$ .

## Chapter 10

# Conclusion and Future Work

### 10.1 Summary

In this dissertation, we proposed several low-complexity architectures for next-generation wireless network topologies, such as C-RANs. Specifically, since the performance of integer-forcing encoding/decoding approaches the joint encoding/decoding performance for both source and channel coding separately, we build upon this and propose an end-to-end integer-forcing architectures for the C-RANs that combine both integer-forcing channel and source coding.

We started our work by studying the uplink C-RAN, where we proposed an end-to-end integer-forcing architecture in which the BSs use integer-forcing source coding to convey their observations to the CP. Our work in this problem also resulted in a simpler proof for integer-forcing source coding with algebraic successive decoding and iterative algorithms to optimize the associated parameters of the end-to-end integer-forcing architecture. We also showed that the proposed IF C-RAN architecture achieves the optimal outage probability within a constant gap.

Later, we proposed a novel standalone low-complexity compression strategy for the distributed decompression problem, namely the reverse integer-forcing source coding. The reverse IFSC strategy creates a correlation between the quantization noise across distributed decoders. Furthermore, we extended the reverse IFSC to include algebraic successive encoding, which achieves a wider class of target covariance matrices. The reverse IFSC with algebraic successive encoding achieves the same performance as

multivariate compression for a certain class of target covariance matrices. Specifically, if the target covariance matrix can be decomposed using a unimodular integer matrix and real diagonal matrix, then reverse IFSC sum rate is the same as the multivariate compression sum rate.

For the downlink C-RAN, we used the reverse IFSC to develop an end-to-end IF architecture that showed, via simulations, almost the same performance as sequential encoding strategies (i.e., multivariate compression and dirty paper coding) with lower implementation complexity. We also established a duality between the sum-rate achievable using IF in the uplink C-RAN and the sum-rate achievable using IF in the downlink, under total power and total fronthaul link capacity constraints.

We also developed algorithms to optimize the performance of IFIA proposed for the Gaussian interference channel, namely the aligned LLL reduction algorithm. Using the aligned LLL reduction algorithm, the performance of IFIA was also shown to outperform the Max-SINR algorithm in low and moderate SNR regimes.

Finally, we studied the impact of channel variation on integer-forcing receivers for the simple case of MAC where we showed that integer-forcing linear receivers still retain an advantage over conventional linear receivers for MAC.

## 10.2 Future Work

Coding over frequency (e.g., OFDM systems) sometimes suffers from block fading channels. Hence, extending the proposed time-varying integer-forcing MAC receivers to other wireless applications (e.g., C-RAN and Ad-Hoc) is an interesting direction.

Also, finding other applications for IFSC beyond communications such as image processing, where Wyner-Ziv based schemes [Puri et al., 2007] proved enhanced performance in video encoding/decoding.

Another direction is to study coded distributed compression. Consider a dense

wireless sensor network, where each sensor compresses its observation and sends it to a master processor. The master processor has access to a number of cores, which can be used to decompress the sensors (correlated) observations. One natural candidate is to use IFSC, since it exploits the correlation between the observations and yet uses parallel single-user decoders which naturally distribute the computation load over the distributed cores. Specifically, each core can compute one modulo operation and then a centralized "fusion" node can combine these results to get the required observations. In the case, we have a number of cores equal to the number of observations, we can use IFSC directly as in the uplink C-RAN. However, if we have more cores than observations, we can use extra cores (with coding) to better minimize the computation delay, since some of the cores can experience delay due to several reasons. We can also use extra cores to minimize the work done per processor, or the communication between processors. One potential candidate to minimize the delay is to use a maximum distance separable (MDS) code to determine the combinations that each core should recover. However, since pre-existing MDS codes are not optimized to minimize the effective variance of the integer-linear combinations as we saw in IFSC, we may end up with very high compression rates (or high distortion in case of fixed compression rates).

Another interesting direction is whether we can prove a channel-source coding duality between reverse compute-and-forward and reverse integer-forcing source coding.

## Appendix A

# Arithmetic Mean and Geometric Mean Decoders

### A.1 AM Decoder

Consider the point to point channel

$$\mathbf{y}^\dagger = \mathbf{a}^\dagger \mathbf{X} + \mathbf{z}_{\text{eff}}^\dagger,$$

where  $\mathbf{a} \in \mathbb{Z}^K$ ,  $\mathbf{X} \triangleq [\mathbf{x}_1 \ \cdots \ \mathbf{x}_K]^\dagger$ ,  $\mathbf{x}_k = [\boldsymbol{\lambda}_k + \mathbf{u}_k] \bmod \Lambda_C$  is a lattice codeword,  $\mathbf{u}_k \sim \text{Unif}(\mathcal{V}(\Lambda_F))$  is a random dither independent of  $\boldsymbol{\lambda}_k$ ,  $\boldsymbol{\lambda}_k \in \mathcal{C} \triangleq \mathcal{V}(\Lambda_C) \cap \Lambda_F$  for  $k = 1, \dots, L$ ,  $\Lambda_F$  and  $\Lambda_C$  are nested lattices generated using Lemma 2 with parameters  $\theta_F$  and  $\theta_C$ , respectively,  $\mathbf{z}_{\text{eff}}^\dagger = [\mathbf{z}_{\text{eff},1}^\dagger, \dots, \mathbf{z}_{\text{eff},N}^\dagger]$  is the effective noise through the block and  $\mathbf{z}_{\text{eff},n}^\dagger = (\mathbf{b}_n^\dagger \mathbf{H}_n - \mathbf{a}^\dagger) \mathbf{X}_n + \mathbf{b}_n^\dagger \mathbf{Z}_n$  is the noise through the subblock  $n$ .

Furthermore, assume that  $\Lambda_C$  can be decomposed, by construction, into

$$\Lambda_c = \underbrace{\tilde{\Lambda}_c \times \dots \times \tilde{\Lambda}_c}_{N \text{ times}} \tag{A.1}$$

where  $\tilde{\Lambda}_c$  is a lattice of dimension  $\frac{T}{N}$ . This is equivalent to coding over an effective<sup>1</sup> blocklength  $\frac{T}{N}$ .

---

<sup>1</sup>We assume that  $\frac{T}{N}$  goes to infinity, as  $T$  goes to infinity. However, in practice, using an effective blocklength  $\frac{T}{N}$  instead of  $T$  should result in a penalty.

The AM decoder estimates  $\boldsymbol{\lambda}_{\text{eff}} = \left[ \sum_{k=1}^K a_k \boldsymbol{\lambda}_k \right] \bmod \Lambda_C$  by computing

$$\widehat{\boldsymbol{\lambda}}_{\text{eff}} = \left[ \mathcal{Q}_{\Lambda_F} \left( \mathbf{y} - \sum_{k=1}^K a_k \mathbf{u}_k \right) \right] \bmod \Lambda_C. \quad (\text{A.2})$$

**Lemma 23.** (*AM decoder achievable rate*): For a given set of channels  $\mathbf{H}_1^N$ , the achievable symmetric rate for AM decoders is

$$R(\mathbf{H}_1^N) = \frac{1}{2} \log^+ \left( \frac{\text{SNR}}{\sigma_{AM}^2} \right) \quad (\text{A.3})$$

where  $\sigma_{AM}^2 = \frac{1}{N} \sum_{n=1}^N \sigma_n^2$  and  $\sigma_n^2 = \text{SNR} \|\mathbf{b}_n^\dagger \mathbf{H}_n - \mathbf{a}^\dagger\|^2 + \|\mathbf{b}_n^\dagger\|^2$ .

*Proof.* The AM decoder estimates

$$\begin{aligned} \widehat{\boldsymbol{\lambda}}_{\text{eff}} &= \left[ \mathcal{Q}_{\Lambda_F} \left( \mathbf{y} - \sum_{k=1}^K a_k \mathbf{u}_k \right) \right] \bmod \Lambda_C \\ &\stackrel{(a)}{=} \left[ \mathcal{Q}_{\Lambda_F} \left( [\mathbf{y}^\dagger - \mathbf{a}^\dagger \mathbf{U}] \bmod \Lambda_C \right) \right] \bmod \Lambda_C \\ &\stackrel{(b)}{=} \left[ \mathcal{Q}_{\Lambda_F} \left( \left[ \sum_{k=1}^K a_k \boldsymbol{\lambda}_k + \mathbf{z}_{\text{eff}} \right] \bmod \Lambda_C \right) \right] \bmod \Lambda_C \\ &\stackrel{(c)}{=} \left[ \mathcal{Q}_{\Lambda_F} \left( \sum_{k=1}^K a_k \boldsymbol{\lambda}_k + \mathbf{z}_{\text{eff}} \right) \right] \bmod \Lambda_C \\ &\stackrel{(d)}{=} \left[ \sum_{k=1}^K a_k \boldsymbol{\lambda}_k + \mathcal{Q}_{\Lambda_F}(\mathbf{z}_{\text{eff}}) \right] \bmod \Lambda_C \\ &\stackrel{(e)}{=} \left[ \sum_{k=1}^K a_k \boldsymbol{\lambda}_k \right] \bmod \Lambda_C \\ &= \boldsymbol{\lambda}_{\text{eff}} \end{aligned}$$

where (a), (b) and (c) holds from the distributive law, (d) holds since  $\sum_{k=1}^K a_k \boldsymbol{\lambda}_k \in \Lambda_F$  and finally (e) holds only if  $\mathbf{z}_{\text{eff}} \in \mathcal{V}(\Lambda_F)$ .

Note that, it follows from the Crypto Lemma that each dithered subvector  $\mathbf{x}_{n,m}^\dagger$  is uniform over  $\mathcal{V}(\tilde{\Lambda}_C)$ , hence  $\mathbf{x}_m^\dagger \triangleq [\mathbf{x}_{m,1}^\dagger \dots \mathbf{x}_{m,N}^\dagger]$  is uniform over  $\mathcal{V}(\Lambda_C)$ . From [Ordentlich and Erez, 2016, Theorem 3], we have that the mixture noise  $\mathbf{z}_{\text{eff}}$  is semi norm-ergodic and from Property 2 in Lemma 2, it follows that by choosing  $\theta_C = \text{SNR}$

and  $\theta_F = \sigma_{\text{AM}}^2 + \epsilon$  we have  $\Pr(\mathbf{z}_{\text{eff}} \notin \mathcal{V}(\Lambda_F)) \leq \epsilon'$  where  $\epsilon$  and  $\epsilon'$  goes to zero as  $T$  goes to infinity.  $\square$

This is equivalent to approximating the mixed noise  $\mathbf{z}_{\text{eff}}$  to a spherical noise with effective variance  $\sigma_{\text{AM}}^2$  for which we can use a classical lattice quantizer (i.e., nearest neighbor decoder) to decode the transmitted codeword affected by the spherical noise.

It is worth noting that, since we can bound the distribution of  $\mathbf{z}_{\text{eff}}$  with a Gaussian distribution having the same variance as in [Nazer and Gastpar, 2011], we can prove the previous lemma by using an ambiguity decoder [Loeliger, 1997] with a spherical decision region. This will become more clear in the next appendix when we define the ambiguity decoder.

Finally, from plugging in the optimal MMSE equalization matrix  $\mathbf{B}_{\text{MMSE},n} = \text{SNR} \mathbf{A} \mathbf{H}_n^\dagger (\mathbf{I} + \text{SNR} \mathbf{H}_n \mathbf{H}_n^\dagger)^{-1}$  and applying Woodbury's matrix identity we have

$$\sigma_{\text{AM}}^2 = \frac{1}{N} \sum_{n=1}^N \sigma_n^2 \quad (\text{A.4})$$

$$= \frac{1}{N} \sum_{n=1}^N \|\mathbf{F}_n \mathbf{a}\|^2 = \|\mathbf{F}_{\text{eq}} \mathbf{a}\|^2 \quad (\text{A.5})$$

where  $\mathbf{F}_{\text{eq}}$  is obtained by factoring  $\mathbf{F}_{\text{eq}}^\top \mathbf{F}_{\text{eq}} = \frac{1}{N} \sum_{n=1}^N \mathbf{F}_n^\top \mathbf{F}_n$  where  $\mathbf{F}_n = (\text{SNR}^{-1} \mathbf{I} + \mathbf{H}_n^\top \mathbf{H}_n)^{-1/2}$  which proves Theorem 19.

## A.2 GM Decoder

**Lemma 24.** [Nazer and Gastpar, 2011, Appendix A] Let  $\mathbf{z}_{\text{mix}}$  be the mixture noise

$$\mathbf{z}_{\text{mix}}^\dagger = \mathbf{c}_1^\dagger \mathbf{X} + \mathbf{c}_2^\dagger \mathbf{Z}$$

where  $\mathbf{Z} \in \mathbb{R}^{N_{Tx} \times T}$  is i.i.d.  $\mathcal{N}(0, 1)$ ,  $\mathbf{X} = [\mathbf{x}_1 \cdots \mathbf{x}_{N_{Tx}}]^\dagger$ ,  $\mathbf{x}_m$  is uniformly distributed over  $\mathcal{V}(\Lambda_C)$  and independent of  $\mathbf{Z}$ ,  $\mathbf{c}_1, \mathbf{c}_2 \in \mathbb{R}^{N_{Tx}}$  and  $\Lambda_C$  is a lattice with dimension  $T$  generated using Lemma 2, then there exists an i.i.d. Gaussian vector  $\mathbf{z}^*$  with variance

$\sigma^2$  equal to the effective variance of  $\mathbf{z}_{mix}$

$$\frac{1}{T} \mathbb{E}(\|\mathbf{z}_{mix}\|^2) \rightarrow \sigma^2 \text{ as } T \rightarrow \infty$$

and the pdf of  $\mathbf{z}_{mix}$  can be bounded by

$$f_{\mathbf{z}_{mix}}(\mathbf{z}) \leq e^{N_{Tx}c(T)T} f_{\mathbf{z}^*}(\mathbf{z})$$

where  $c(T)$  depends on the lattice  $\Lambda_C$  and  $c(T)T$  converges to a constant as  $T$  goes to  $\infty$ .

Using the previous lemma, we can upper-bound the pdf of the effective noise of the IF receiver for each subblock by a pdf of a Gaussian noise with the same effective variance as in the following lemma.

**Lemma 25** (Gaussian distribution upper bound). *Consider the effective noise  $\mathbf{z}_{eff}^\dagger = [\mathbf{z}_{eff,1}^\dagger \cdots \mathbf{z}_{eff,N}^\dagger]$ , where  $\mathbf{z}_{eff,n}$  and its effective variance  $\sigma_n^2$  are defined in Lemma 23, the distribution of  $\mathbf{z}_{eff}$  can be upper bounded by*

$$f_{\mathbf{z}_{eff}}(\mathbf{z}) \leq e^{N_{Tx}c(\frac{T}{N})T} f_{\mathbf{z}^*}(\mathbf{z}) \quad (\text{A.6})$$

where  $c(\frac{T}{N})T$  converges to a constant as  $T$  goes to  $\infty$ ,  $\mathbf{z}^{*\dagger} = [\mathbf{z}_1^{*\dagger} \cdots \mathbf{z}_N^{*\dagger}] \sim \mathcal{N}(\mathbf{0}, \Sigma)$  and

$$\Sigma = \begin{bmatrix} \sigma_1^2 \mathbf{I} & \cdots & \mathbf{0} \\ \vdots & \ddots & \vdots \\ \mathbf{0} & \cdots & \sigma_N^2 \mathbf{I} \end{bmatrix}.$$

*Proof.* Recall that by the Crypto Lemma, the subvector  $\mathbf{x}_{n,m}$  is uniformly distributed over  $\widetilde{\Lambda}_C$ , hence the vector  $\mathbf{x}_m = [\mathbf{x}_{1,m}^\dagger \cdots \mathbf{x}_{N,m}^\dagger]^\dagger$  is uniformly distributed over  $\Lambda_C \triangleq \widetilde{\Lambda}_C \times \cdots \times \widetilde{\Lambda}_C$ .

Now, the pdf of  $\mathbf{z}_{eff}$  can be written as

$$f_{\mathbf{z}_{eff}}(\mathbf{z}) \stackrel{(a)}{=} \prod_{n=1}^N f_{\mathbf{z}_{eff,n}}(\mathbf{z}_n) \stackrel{(b)}{\leq} \prod_{n=1}^N e^{N_{Tx}c(\frac{T}{N})\frac{T}{N}} f_{\mathbf{z}_n^*}(\mathbf{z}_n) \quad (\text{A.7})$$

$$\leq e^{N_{\text{T}}c(\frac{T}{N})T} f_{\mathbf{z}^*}(\mathbf{z})$$

where (a) holds from the fact that  $\mathbf{z}_{\text{eff},1}, \dots, \mathbf{z}_{\text{eff},N}$  are independent, (b) holds from using Lemma 24 and  $c(\frac{T}{N})T$  converges to a constant as  $T$  goes to  $\infty$ .  $\square$

Since the distribution of the mixed noise can be upper bounded by the distribution of a Gaussian noise with the same variance, a vanishing error probability under a Gaussian noise  $\mathbf{z}^*$  means a vanishing error probability under the mixed noise  $\mathbf{z}_{\text{eff}}$ . From this point on, we assume a non-identically distributed Gaussian noise. Instead of approximating this non-identically distributed noise to an identical one, which wastes some of the packing space, we develop a decoder that deals directly with the elliptically-shaped noise. This is possible using the ambiguity decoder in [Loeliger, 1997] and [El Gamal et al., 2004] with elliptical decision region.

For simplicity, we assume a non-dithered point-to-point channel, since we can remove the dithers at the receiver as in the AM decoder.

**Lemma 26.** *GM decoder achievable rate : Consider a point to point channel*

$$\mathbf{y} = \boldsymbol{\lambda}_{\text{eff}} + \mathbf{z}_{\text{eff}} \quad (\text{A.8})$$

where  $\boldsymbol{\lambda}_{\text{eff}} \in \mathcal{V}(\Lambda_C) \cap \Lambda_F$  is a lattice codeword of length  $T$ , the nested lattices  $\Lambda_C \subseteq \Lambda_F$  is generated using Lemma 2 with parameters  $\theta_F = \prod_{n=1}^N (\sigma_n^2)^{\frac{1}{N}}$  and  $\theta_C = \text{SNR}$ ,  $\mathbf{z}_{\text{eff}}^\dagger = [\mathbf{z}_{\text{eff},1}^\dagger \cdots \mathbf{z}_{\text{eff},N}^\dagger]$ , and  $\mathbf{z}_{\text{eff},n} \sim \mathcal{N}(\mathbf{0}, \sigma_n^2 \mathbf{I})$  for  $n = 1, \dots, N$ , then the following rate is achievable using the GM decoder

$$R_{GM} = \frac{1}{2} \log^+ \left( \frac{\text{SNR}}{\prod_{n=1}^N (\sigma_n^2)^{\frac{1}{N}}} \right). \quad (\text{A.9})$$

*Proof.* Define an ambiguity decoder  $\mathcal{D} : \mathbb{R}^T \rightarrow \Lambda_F$  as

$$\mathcal{D}(\mathbf{y}) = \hat{\boldsymbol{\lambda}} \text{ if } \begin{cases} 1. \mathbf{y} \in \Omega_{T,\epsilon} + \hat{\boldsymbol{\lambda}} \\ 2. \nexists \boldsymbol{\lambda}' \in \Lambda_F \text{ s.t. } \mathbf{y} \in \Omega_{T,\epsilon} + \boldsymbol{\lambda}' \text{ and } \boldsymbol{\lambda}' \neq \hat{\boldsymbol{\lambda}} \end{cases} \quad (\text{A.10})$$

with a decision region  $\Omega_{T,\epsilon} = \{\mathbf{z} \in \mathbb{R}^T : \mathbf{z}^\dagger \boldsymbol{\Sigma}^{-1} \mathbf{z} \leq T(1 + \epsilon)\}$ , where

$$\boldsymbol{\Sigma} = \begin{bmatrix} \sigma_1^2 \mathbf{I} & \dots & \mathbf{0} \\ \vdots & \ddots & \vdots \\ \mathbf{0} & \dots & \sigma_N^2 \mathbf{I} \end{bmatrix}.$$

In other words, the ambiguity decoder sends the region  $\boldsymbol{\lambda} + \Omega_{T,\epsilon}$  to  $\boldsymbol{\lambda}$ . Taking this into consideration, for a fixed decision region  $\Omega_{T,\epsilon}$  and fine lattice  $\Lambda_F$ , an error happens only if the elliptical noise  $\mathbf{z}_{\text{eff}}$  exceeds the decision region  $\Omega_{T,\epsilon}$  or there is an ambiguity about decoding the received signal  $\mathbf{y}$  (i.e., the intersection of two shifted decision regions is non-empty).

Formally, define the ambiguity  $\mathcal{A}$  and error  $\mathcal{E}$  events as

$$\begin{aligned} \mathcal{A} &= \{\mathbf{y} \in \{\Omega_{T,\epsilon} + \boldsymbol{\lambda}\} \cap \{\Omega_{T,\epsilon} + \boldsymbol{\lambda}'\}\} \\ \mathcal{E} &= \mathcal{A} \cup \{\mathbf{z}_{\text{eff}} \notin \Omega_{T,\epsilon}\}, \end{aligned} \quad (\text{A.11})$$

where  $\boldsymbol{\lambda} \neq \boldsymbol{\lambda}'$ . Using the union bound, the probability of error  $\mathcal{E}$ , given  $\Omega_{T,\epsilon}$  and  $\Lambda_F$ , is

$$P_e(\Omega_{T,\epsilon}, \Lambda_F) \leq \Pr(\mathbf{z}_{\text{eff}} \notin \Omega_{T,\epsilon}) + \Pr(\mathcal{A}). \quad (\text{A.12})$$

**Lemma 27.** *Now, define  $V_T \triangleq \text{Vol}(T\text{-dimensional unit ball})$  and  $G(\Lambda_C) = \frac{\sigma^2(\Lambda_C)}{\text{Vol}(\Lambda_C)^{2/T}}$  as the normalized second moment of lattice  $\Lambda_C$ . Then, from [Ordentlich and Erez, 2016, Definition 5] and for any  $\epsilon > 0$ , we have*

$$2\pi e G(\Lambda_C) \leq (1 + \epsilon)$$

for large enough  $T$  and  $\Lambda_C$  that is good for MSE quantization.

It would be also to write the rate of the lattice codebook as  $R = \frac{1}{T} \ln \left( \frac{\text{Vol}(\Lambda_C)}{\text{Vol}(\Lambda_F)} \right)$ .

By averaging over Loeliger ensemble of lattices as in [Loeliger, 1997], we get

$$\begin{aligned} \bar{P}_e(\Omega_{T,\epsilon}) &\leq \mathbb{E}_{\Lambda_F} (P_e(\Omega_{T,\epsilon}, \Lambda_F)) \\ &\leq \Pr(\mathbf{z}_{\text{eff}} \notin \Omega_{T,\epsilon}) + (1 + \delta(\epsilon)) \frac{\text{Vol}(\Omega_{T,\epsilon})}{\text{Vol}(\Lambda_F)} \\ &\stackrel{(a)}{\leq} \Pr(\mathbf{z}_{\text{eff}} \notin \Omega_{T,\epsilon}) + (1 + \delta(\epsilon)) \frac{\text{Vol}(\Omega_{T,\epsilon})}{\text{Vol}(\Lambda_C)} e^{TR} \\ &\stackrel{(b)}{\leq} \Pr(\mathbf{z}_{\text{eff}} \notin \Omega_{T,\epsilon}) + (1 + \delta(\epsilon)) e^{T(R - R_{GM} + \delta')} (2\pi e G(\Lambda_C))^{T/2} \end{aligned} \quad (\text{A.13})$$

$$\begin{aligned}
&\stackrel{(c)}{\leq} \epsilon + (1 + \delta(\epsilon))e^{T(R-R_{GM}+\delta')} (2\pi e G(\Lambda_C))^{T/2} \\
&\stackrel{(d)}{\leq} \epsilon'
\end{aligned}$$

where (a) holds from using codebook  $\Lambda_F \cap \mathcal{V}(\Lambda_C)$  with rate  $R = \frac{1}{T} \ln \left( \frac{\text{Vol}(\Lambda_C)}{\text{Vol}(\Lambda_F)} \right)$ , (b) holds from  $\text{Vol}(\Omega_{T,\epsilon}) = V_T(T(1+\epsilon))^{\frac{T}{2}} \det(\Sigma)^{\frac{1}{2}}$  and  $\left( \frac{\text{Vol}(\Lambda_C)}{V_T} \right)^{T/2} \geq \frac{T}{2\pi e} \text{Vol}(\Lambda_C)^{T/2} = \frac{T}{2\pi e} \left( \frac{\theta_C}{G(\Lambda_C)} \right) = \frac{T}{2\pi e} \left( \frac{\text{SNR}}{G(\Lambda_C)} \right)$ ,  $\delta' = \frac{1}{2} \log(1+\epsilon)$ , (c) holds from the asymptotic equipartition property for large enough  $T$  and finally (d) holds as long as  $R < R_{GM}$  where  $\epsilon'$  goes to zero as  $T$  goes to infinity.

Finally, as any random coding argument, as long as there is an ensemble of nested lattices such that the average probability of error converges to zero, there must be at least one nested lattice sequence such that the probability of error converges to zero.  $\square$

Finally, from plugging in the optimal MMSE equalization matrix  $\mathbf{B}_{\text{MMSE},n} = \text{SNR} \mathbf{A} \mathbf{H}_n^\dagger (\mathbf{I} + \text{SNR} \mathbf{H}_n \mathbf{H}_n^\dagger)^{-1}$  and applying Woodbury's matrix identity we can prove Theorem 20.

## Appendix B

### Existence of $\mathbf{L}$ and $\mathbf{C}$ in UL C-RAN

**Lemma 28.** *For any full-rank integer matrix  $\mathbf{A}$  with full-rank sub-matrices  $\mathbf{A}_{[1:m]}$  for  $m = 1, \dots, L$ , we can select an upper triangular integer matrix  $\mathbf{L}$  and a strictly lower triangular integer matrix  $\mathbf{C}$  such that*

$$[\mathbf{L} + \mathbf{C}\mathbf{A}] \bmod p = [\mathbf{A}] \bmod p. \quad (\text{B.1})$$

*Proof.* Since  $\mathbf{C}$  is a strictly lower triangular matrix, we can write (B.2) as

$$\begin{bmatrix} \ell_1^\dagger \\ \ell_2^\dagger \\ \vdots \\ \ell_L^\dagger \end{bmatrix} + \begin{bmatrix} \mathbf{0}^\dagger \\ C_{21}\mathbf{a}_1^\dagger \\ \vdots \\ \sum_{i=1}^{L-1} C_{L,i}\mathbf{a}_i^\dagger \end{bmatrix} \bmod p = \begin{bmatrix} \mathbf{a}_1^\dagger \\ \mathbf{a}_2^\dagger \\ \vdots \\ \mathbf{a}_L^\dagger \end{bmatrix} \bmod p. \quad (\text{B.2})$$

For the first row of (B.2) to hold, it suffices to choose  $\ell_1^\dagger = \mathbf{a}_1^\dagger$ . Next, since the first element in  $\ell_2$  is zero (i.e.,  $\ell_{21} = 0$ ) and in order to satisfy the first element in the second row in (B.2), we choose  $C_{21} = a_{11}^{\text{inv}} a_{21}$ . This sets the first element in the second row in the LHS to  $[C_{21}a_{11}] \bmod p = [a_{21}] \bmod p = \text{RHS}$ . To satisfy the rest of the equality for the rest of the elements in the second row, it follows that we have to choose the rest of  $\ell_2$  as  $\ell_{2,[2:L]} = \mathbf{a}_{2,[2:L]} - C_{21}\mathbf{a}_{1,[2:L]}$ .

Following the same steps for each row, generally, for  $m = 1, \dots, L - 1$ , it can be shown that (B.2) follows by choosing the  $(m + 1)^{\text{th}}$  row of  $\mathbf{L}$  and  $\mathbf{C}$  as

$$\begin{aligned} \mathbf{c}_{m+1,[1:m]}^\dagger &= \mathbf{a}_{m+1,[1:m]}^\dagger \mathbf{A}_{[1:m]}^{\text{inv}} \\ \ell_{m+1,[1:m]}^\dagger &= \mathbf{a}_{m+1,[m+1:L]}^\dagger - \mathbf{c}_{m+1,[1:m]}^\dagger \mathbf{A}_{[1:m],[m+1:L]}. \end{aligned} \quad (\text{B.3})$$

□

## Appendix C

### Bounding $d^*$

Recall that  $\mathbf{S}_1$  is the eigenvalue decomposition of

$$\mathbf{U}\mathbf{S}_1\mathbf{U}^\dagger = P\mathbf{H}^\dagger\mathbf{H} + \mathbf{I}.$$

**Lemma 29.** *Conditioning on  $\mathcal{A}$ , the distortion  $d^*$  that satisfies  $R_{\text{IFSC}}^S(\mathbf{H}, d^*) = C_{\text{sym}}$  satisfies the following inequalities*

$$d^* > 2^{-(2\Delta R/L+1)} \quad \text{if } \mathbf{S}_1 \in \mathcal{B} \quad (\text{C.1})$$

$$d^* < 1 \quad \text{if } \mathbf{S}_1 \in \mathcal{B}^c \quad (\text{C.2})$$

where  $\mathcal{B} = \{\frac{1}{2} \log |\mathbf{S}_1| > LC_{\text{sym}} - \Delta R - L/2\}$  and  $\mathcal{A} = \{R_{\text{IFSC}}^s(\mathbf{H}) < R_{\text{BT}}^s(\mathbf{H}) + \Delta R\}$ .

*Proof.* In order to prove (C.1), assume for the sake of contradiction that  $d^* \leq 2^{-(2\Delta R/L+1)}$  and  $\frac{1}{2} \log |\mathbf{S}_1| > LC_{\text{sym}} - \Delta R - L/2$ . Then, we have

$$\begin{aligned} LC_{\text{sym}} - \Delta R - L/2 &= LR_{\text{IFSC}}^s(\mathbf{H}) - \Delta R - L/2 \stackrel{(a)}{\geq} LR_{\text{BT}}^s(\mathbf{H}) - \Delta R - L/2 \\ &= \frac{1}{2} \log \left| \frac{1}{d^*} \mathbf{K}_{YY} + \mathbf{I} \right| - \Delta R - L/2 \\ &= \frac{1}{2} \log \left| \frac{P\mathbf{H}\mathbf{H}^\dagger + (d^* + 1)\mathbf{I}}{d^*} \right| - \Delta R - L/2 \\ &> \frac{1}{2} \log |\mathbf{S}_1| - \frac{L}{2} \log d^* 2^{2\Delta R/L+1} \stackrel{(b)}{>} \frac{1}{2} \log |\mathbf{S}_1| \end{aligned} \quad (\text{C.3})$$

where (a) holds from  $R_{\text{IFSC}}^s(\mathbf{H}) \geq R_{\text{BT}}^s(\mathbf{H})$  as shown in [Ordentlich and Erez, 2017] and (b) is a contradiction that holds if  $d^* < 2^{-(2\Delta R/L+1)}$ .

Now, in order to prove (C.2), assume that  $d^* \geq 1$  and  $\frac{1}{2} \log |\mathbf{S}_1| < LC_{\text{sym}} - L/2 -$

$\Delta R$  and note that

$$\begin{aligned}
LC_{\text{sym}} - L/2 - \Delta R &= LR_{\text{IFSC}}^s(\mathbf{H}) - L/2 - \Delta R \\
&\stackrel{(a)}{\leq} LR_{\text{BT}}^s(\mathbf{H}) - L/2 \\
&= \frac{1}{2} \log \left| \frac{P\mathbf{H}\mathbf{H}^\dagger + (d^* + 1)\mathbf{I}}{2d^*} \right| \\
&\stackrel{(b)}{\leq} \frac{1}{2} \log \left| \frac{P}{2d^*} \mathbf{H}\mathbf{H}^\dagger + \mathbf{I} \right| < \frac{1}{2} \log |\mathbf{S}_1| \tag{C.4}
\end{aligned}$$

where (a) holds from the fact that  $R_{\text{IFSC}}^s(\mathbf{H}) \leq R_{\text{BT}}^s(\mathbf{H}) + \Delta R$  and (b) follows from assuming  $d^* \geq 1$ . Finally, we reach a contradiction with our assumption. Hence, we have  $d^* < 1$ .  $\square$

## Appendix D

### Existence of $\mathbf{L}$ and $\mathbf{C}$ in DL C-RAN

**Lemma 30.** *For any full-rank integer matrix  $\mathbf{A}$  with full-rank submatrices  $\mathbf{A}_{[1:m]}$  for  $m = 1, \dots, L$ , there exists a lower triangular integer matrix  $\mathbf{L}$  and a strictly upper triangular integer matrix  $\mathbf{C}$  such that*

$$[\mathbf{L}\mathbf{F}] \bmod p = [\mathbf{A}] \bmod p \quad (\text{D.1})$$

*Proof.* Let us start by expanding  $\mathbf{L}\mathbf{F}$  as

$$\begin{aligned} \mathbf{L}\mathbf{F} &= [\ell_1 \quad \ell_2 \quad \dots \quad \ell_L] \begin{bmatrix} 1 & f_{1,2} & \dots & f_{1,L-1} & f_{1,L} \\ 0 & 1 & \dots & \vdots & \vdots \\ \vdots & \ddots & \ddots & f_{L-2,L-1} & f_{L-2,L} \\ 0 & 0 & \dots & 1 & f_{L-1,L} \\ 0 & 0 & \dots & 0 & 1 \end{bmatrix} \\ &= \left[ \ell_1 \quad \ell_2 + f_{1,2}\ell_1 \quad \ell_3 + f_{1,3}\ell_1 + f_{2,3}\ell_2 \quad \dots \quad \ell_L + \sum_{i=1}^{L-1} f_{i,L}\ell_i \right]. \end{aligned} \quad (\text{D.2})$$

where  $\ell_m$  is the  $m^{\text{th}}$  column of the matrix  $\mathbf{L}$ .

First, by setting  $\ell_1 = \mathbf{a}_1$ , the first column in (D.2) is satisfied. For the first element in the second column in (D.2) to be satisfied and since  $\ell_2$  has a leading zero (i.e.,  $\ell_{1,2} = 0$ ), we have to choose  $f_{1,2}$  such that  $[f_{1,2}\ell_{1,1}] \bmod p = [a_{1,2}] \bmod p$  which can be done by setting  $f_{1,2} = \ell_{1,1}^{\text{inv}} a_{1,2}$  where  $\ell_{1,1}^{\text{inv}}$  is the algebraic inverse of  $\ell_{1,1}$  as defined in (2.5). Hence, in order to satisfy the rest of the elements of the second column and with holding  $f_{1,2}\ell_1$  fixed, we have to choose  $\ell_{k,2} = a_{k,2} - f_{1,2}\ell_{k,1}$  for  $k > 1$ . Similarly, for the third column, we first choose

$$[f_{1,3}f_{2,3}]^\dagger = \mathbf{L}_{[1:2]}^{\text{inv}} \mathbf{A}_{[1:2],3}$$

then proceed to choose  $\ell_{k,3} = \mathbf{a}_{k,3} - f_{1,3}\ell_{k,1} - f_{2,3}\ell_{k,2}$  for  $k > 2$ .

Generally, we set  $\ell_1 = \mathbf{a}_1$  and for  $m = 1, \dots, L-1$ , the  $(m+1)^{\text{th}}$  columns of matrix  $\mathbf{F}$  and  $\mathbf{L}$  should be chosen as

$$\begin{aligned} \mathbf{F}_{[1:m],m+1} &= \mathbf{L}_{[1:m]}^{\text{inv}} \mathbf{A}_{[1:m],m+1} \\ \ell_{[m+1:L],m+1} &= \mathbf{a}_{[m+1:L],m+1} - \mathbf{L}_{[m+1:L],[1:m]} \mathbf{F}_{[1:m],m+1}, \quad k = m+1, \dots, L. \end{aligned} \quad (\text{D.3})$$

It is worth noting that the existence of the algebraic inverse  $\mathbf{L}_{[1:m]}^{\text{inv}}$  of the matrix  $\mathbf{L}_{[1:m]}$ , which is defined in (2.5), is guaranteed for  $m = 1, \dots, L$  since  $\mathbf{A}_{[1:m]}$  is full rank and we have

$$\begin{aligned} \det(\mathbf{A}_{[1:m]}) &= \det(\mathbf{L}_{[1:m]}) \det(\mathbf{F}_{[1:m]}) \\ &= \det(\mathbf{L}_{[1:m]}) \end{aligned} \quad (\text{D.4})$$

where the last equality holds from recalling that  $\mathbf{F}$  is an upper triangular matrices with unit diagonal, hence unit determinant.

□

## Appendix E

### Matrix $\mathbf{F}$ Properties

**Lemma 31.** *For a strictly upper triangular integer matrix  $\mathbf{C}$ , the matrix  $\mathbf{F} \triangleq \mathbf{I} + (\mathbf{I} - \mathbf{C})^{-1}\mathbf{C}$  is an upper triangular integer matrix with unit diagonal.*

*Proof.* First, the matrix  $\mathbf{F}$  is an integer-matrix since

$$\begin{aligned} \mathbf{F} &= \mathbf{I} + (\mathbf{I} - \mathbf{C})^{-1} \mathbf{C} \\ &\stackrel{(a)}{=} \mathbf{I} + \left( \sum_{k=0}^{\infty} \mathbf{C}^k \right) \mathbf{C} \\ &\stackrel{(b)}{=} \mathbf{I} + \left( \sum_{k=0}^{L-1} \mathbf{C}^k \right) \mathbf{C} \\ &= \sum_{k=0}^{L-1} \mathbf{C}^k \end{aligned} \tag{E.1}$$

where (a) holds from Taylor expansion, (b) holds from the fact that for a strictly upper triangular matrices  $\mathbf{C}^L = 0$ . Finally, since all powers of the matrix  $\mathbf{C}$ , higher than one, are strictly upper triangular matrices with integer entries, it follows that  $\mathbf{F}$  is an integer upper triangular matrix.  $\square$

## Appendix F

# Uplink Downlink Duality Appendix

### F.1 Proof of Lemma 18

We start by multiplying (7.6) by  $P_k^{\text{ul}}/(\sigma_k^{\text{ul}})^2$  to get

$$\begin{aligned}
& P_k^{\text{ul}} \\
&= \beta_k^{\text{ul}} \left( \sum_{\ell} (\mathbf{b}_k^{\text{ul}\dagger} \mathbf{h}_{\ell}^{\text{ul}} v_{\ell}^{\text{ul}} - a_{c,k,\ell}^{\text{ul}})^2 P_{\ell}^{\text{ul}} + \|\mathbf{b}_k^{\text{ul}}\|^2 + \sum_i (b_{k,i}^{\text{ul}})^2 d_i^{\text{ul}} \right) \\
&= \beta_k^{\text{ul}} \left( \sum_{\ell} (\mathbf{b}_k^{\text{ul}\dagger} \mathbf{h}_{\ell}^{\text{ul}} v_{\ell}^{\text{ul}} - a_{c,k,\ell}^{\text{ul}})^2 P_{\ell}^{\text{ul}} + \sum_i \sum_j (b_{k,i}^{\text{ul}})^2 C_{i,j}^{\text{ul}} \|\mathbf{a}_{s,j}^{\text{ul}}\|^2 \right. \\
&\quad \left. + \|\mathbf{b}_k^{\text{ul}}\|^2 + \sum_i \sum_j (b_{k,i}^{\text{ul}})^2 C_{i,j}^{\text{ul}} \mathbf{a}_{s,j}^{\text{ul}\dagger} (\mathbf{H}^{\text{ul}} \mathbf{V}^{\text{ul}} \mathbf{P}^{\text{ul}} \mathbf{V}^{\text{ul}\dagger} \mathbf{H}^{\text{ul}\dagger}) \mathbf{a}_{s,j}^{\text{ul}} \right) \\
&= \beta_k^{\text{ul}} \left( \sum_{\ell} (\mathbf{b}_k^{\text{ul}\dagger} \mathbf{h}_{\ell}^{\text{ul}} v_{\ell}^{\text{ul}} - a_{c,k,\ell}^{\text{ul}})^2 P_{\ell}^{\text{ul}} + J_{k,k}^{\text{ul}} \right. \\
&\quad \left. + \sum_i \sum_j (b_{k,i}^{\text{ul}})^2 C_{i,j}^{\text{ul}} \mathbf{a}_{s,j}^{\text{ul}\dagger} \left( \sum_{\ell} \mathbf{h}_{\ell}^{\text{ul}} \mathbf{h}_{\ell}^{\text{ul}\dagger} (v_{\ell}^{\text{ul}})^2 P_{\ell}^{\text{ul}} \right) \mathbf{a}_{s,j}^{\text{ul}} \right) \\
&= \beta_k^{\text{ul}} \sum_{\ell} M_{k,\ell}^{\text{ul}} P_{\ell}^{\text{ul}} + \beta_k^{\text{ul}} J_{k,k}^{\text{ul}} \tag{F.1}
\end{aligned}$$

Finally, (7.10) follows from the previous equation by taking  $k = 1, \dots, K$ .

## F.2 Proof of Lemma 20

Similar to Appendix F.1, multiplying (7.17) by  $P_k^{\text{dl}}/(\sigma_k^{\text{dl}})^2$ , we get

$$\begin{aligned}
P_k^{\text{dl}} &= \beta_k^{\text{dl}} \sum_{\ell} (\mathbf{b}_{\ell}^{\text{dl}\dagger} \mathbf{h}_k^{\text{dl}} v_k^{\text{dl}} - a_{c,k,\ell}^{\text{dl}})^2 P_{\ell}^{\text{dl}} + \beta_k^{\text{dl}} (v_k^{\text{dl}})^2 \\
&\quad + \beta_k^{\text{dl}} (v_k^{\text{dl}})^2 \sum_j (\mathbf{h}_k^{\text{dl}\dagger} \tilde{\mathbf{a}}_{s,j}^{\text{dl}})^2 d_j^{\text{dl}} \\
&= \beta_k^{\text{dl}} \sum_{\ell} (\mathbf{b}_{\ell}^{\text{dl}\dagger} \mathbf{h}_k^{\text{dl}} v_k^{\text{dl}} - a_{c,k,\ell}^{\text{dl}})^2 P_{\ell}^{\text{dl}} + \beta_k^{\text{dl}} (v_k^{\text{dl}})^2 \\
&\quad + \beta_k^{\text{dl}} \sum_j (\mathbf{h}_k^{\text{dl}\dagger} \tilde{\mathbf{a}}_{s,j}^{\text{dl}})^2 \mathbf{c}_{j,i}^{\text{dl}\dagger} \mathbf{e}^{\text{dl}} \\
&= \beta_k^{\text{dl}} \sum_{\ell} (\mathbf{b}_{\ell}^{\text{dl}\dagger} \mathbf{h}_k^{\text{dl}} v_k^{\text{dl}} - a_{c,k,\ell}^{\text{dl}})^2 P_{\ell}^{\text{dl}} + \beta_k^{\text{dl}} (v_k^{\text{dl}})^2 \\
&\quad + \beta_k^{\text{dl}} \sum_j \sum_i (\mathbf{h}_k^{\text{dl}\dagger} \tilde{\mathbf{a}}_{s,j}^{\text{dl}})^2 C_{j,i}^{\text{dl}} \mathbf{b}_i^{\text{dl}\dagger} \mathbf{P}^{\text{dl}} \mathbf{b}_i^{\text{dl}} \\
&= \beta_k^{\text{dl}} \sum_{\ell} (\mathbf{b}_{\ell}^{\text{dl}\dagger} \mathbf{h}_k^{\text{dl}} v_k^{\text{dl}} - a_{c,k,\ell}^{\text{dl}})^2 P_{\ell}^{\text{dl}} + \beta_k^{\text{dl}} (v_k^{\text{dl}})^2 \\
&\quad + \beta_k^{\text{dl}} \sum_{\ell} \sum_j \sum_i (\mathbf{h}_k^{\text{dl}\dagger} \tilde{\mathbf{a}}_{s,j}^{\text{dl}})^2 C_{j,i}^{\text{dl}} (b_{i,\ell}^{\text{dl}})^2 P_{\ell}^{\text{dl}} \\
&= \beta_k^{\text{dl}} \sum_{\ell} M_{k,\ell}^{\text{dl}} P_{\ell}^{\text{dl}} + \beta_k^{\text{dl}} J_{k,k}^{\text{dl}}. \tag{F.2}
\end{aligned}$$

Finally, (7.19) follows from the previous equation by taking  $k = 1, \dots, K$ .

## F.3 Proof of Lemma 19

We start by computing  $d_1^{\text{dl}}, \dots, d_L^{\text{dl}}$  such that

$$\frac{1}{2} \log \left( \frac{\mathbf{b}_{\ell}^{\text{dl}\dagger} \mathbf{P}^{\text{dl}} \mathbf{b}_{\ell}^{\text{dl}} + \mathbf{a}_{s,\ell}^{\text{dl}\dagger} \mathbf{D}^{\text{dl}} \mathbf{a}_{s,\ell}^{\text{dl}}}{d_{\ell}^{\text{dl}}} \right) = C_{\ell}^{\text{ul}}, \quad \ell = 1, \dots, L \tag{F.3}$$

where  $C_1^{\text{ul}}, \dots, C_L^{\text{ul}}$  is the uplink fronthaul rate allocation. Since  $d_1^{\text{dl}}, \dots, d_L^{\text{dl}}$  are not necessarily monotonically decreasing, the rates in (F.3) may not be achievable and so

are  $d_1^{\text{dl}}, \dots, d_L^{\text{dl}}$ .

In order to argue that  $d_1^{\text{dl}}, \dots, d_L^{\text{dl}}$  are indeed achievable, we find two permutations  $\pi_1$  and  $\pi_2$  such that  $d_{\pi_1(1)}^{\text{dl}}, \dots, d_{\pi_1(L)}^{\text{dl}}$  and  $\text{rank}(\mathbf{A}_{s, \pi_2([1:m]), \pi_1([1:m])}^{\text{dl}}) = m$  for  $m = 1, \dots, L$ .

This implies that the following rates are achievable

$$R_{\text{SRIFSC}, \ell}^s = \frac{1}{2} \log \left( \frac{\mathbf{b}_{\pi_2(\ell)}^{\text{dl}\dagger} \mathbf{P}^{\text{dl}} \mathbf{b}_{\pi_2(\ell)}^{\text{dl}} + \mathbf{a}_{s, \pi_2(\ell)}^{\text{dl}\dagger} \mathbf{D}^{\text{dl}} \mathbf{a}_{s, \pi_2(\ell)}^{\text{dl}}}{d_{\pi_1(\ell)}^{\text{dl}}} \right) \quad (\text{F.4})$$

if  $\sum_{\ell=1}^L R_{\text{SRIFSC}, \ell}^s \leq C_{\text{total}}$ .

The sum rate in the last equation can be written as

$$\begin{aligned} \sum_{\ell=1}^L R_{\text{SRIFSC}, \ell}^s &= \sum_{\ell=1}^L \frac{1}{2} \log \left( \frac{\mathbf{b}_{\pi_2(\ell)}^{\text{dl}\dagger} \mathbf{P}^{\text{dl}} \mathbf{b}_{\pi_2(\ell)}^{\text{dl}} + \mathbf{a}_{s, \pi_2(\ell)}^{\text{dl}\dagger} \mathbf{D}^{\text{dl}} \mathbf{a}_{s, \pi_2(\ell)}^{\text{dl}}}{d_{\pi_1(\ell)}^{\text{dl}}} \right) \\ &= \frac{1}{2} \log \left( \frac{\prod_{\ell=1}^L \mathbf{b}_{\pi_2(\ell)}^{\text{dl}\dagger} \mathbf{P}^{\text{dl}} \mathbf{b}_{\pi_2(\ell)}^{\text{dl}} + \mathbf{a}_{s, \pi_2(\ell)}^{\text{dl}\dagger} \mathbf{D}^{\text{dl}} \mathbf{a}_{s, \pi_2(\ell)}^{\text{dl}}}{\prod_{\ell=1}^L d_{\pi_1(\ell)}^{\text{dl}}} \right) \\ &= \frac{1}{2} \log \left( \frac{\prod_{\ell=1}^L \mathbf{b}_{\ell}^{\text{dl}\dagger} \mathbf{P}^{\text{dl}} \mathbf{b}_{\ell}^{\text{dl}} + \mathbf{a}_{s, \ell}^{\text{dl}\dagger} \mathbf{D}^{\text{dl}} \mathbf{a}_{s, \ell}^{\text{dl}}}{\prod_{\ell=1}^L d_{\ell}^{\text{dl}}} \right) \\ &= \sum_{\ell=1}^L \frac{1}{2} \log \left( \frac{\mathbf{b}_{\ell}^{\text{dl}\dagger} \mathbf{P}^{\text{dl}} \mathbf{b}_{\ell}^{\text{dl}} + \mathbf{a}_{s, \ell}^{\text{dl}\dagger} \mathbf{D}^{\text{dl}} \mathbf{a}_{s, \ell}^{\text{dl}}}{d_{\ell}^{\text{dl}}} \right) \end{aligned} \quad (\text{F.5})$$

$$= \sum_{\ell=1}^L C_{\ell}^{\text{ul}} \leq C_{\text{tot}}, \ell = 1, \dots, L. \quad (\text{F.6})$$

which indicates that the rates  $R_{\text{SRIFSC}, \ell}^s$  for  $\ell = 1, \dots, L$  are achievable and hence the distortion levels computed from (F.3).

## Appendix G

### Aligned LLL for general $M^{[k]}$

In this appendix, we propose two other methods for choosing the integer matrix  $\mathbf{A}^{[k]}$ , given  $\mathbf{U}^{[k]}$  and  $\mathbf{V}$ . These methods can be used for any  $M^{[k]}$  (if  $M^{[k]} = 1$  it is equivalent to Max-SINR algorithm). When we combine these methods with the proposed method in Section 8.3 and choose the best between them, we can slightly improve the performance.

Both methods start by first searching for the integer vector  $\mathbf{a}_{\text{int}}^{[k]}$  which constructs the interference function  $\mathbf{g}^{[k]}$  according to a certain criteria. Next, they search for the independent integer vectors  $\mathbf{b}_1^{[k]}$  and  $\mathbf{b}_2^{[k]}$  that minimize  $\prod_{i=1}^2 \|\mathbf{F}^{[k]} \mathbf{a}_i^{[k]}\|^2$  given this integer vector  $\mathbf{a}_{\text{int}}^{[k]}$ .

#### Method B

The intuition behind this method is to choose the interference function  $\mathbf{g}^{[k]}$  that has the smallest contribution on the effective noise power, regardless of the two integer-combinations in  $\mathbf{s}^{[k]}$  and  $\mathbf{g}^{[k]}$  (i.e., the integers  $b_{m,i}^{[k]}$ ).

##### G.0.1 Choosing the interference function $\mathbf{g}^{[k]}$

By eliminating the  $k^{\text{th}}$  column of  $\mathbf{F}^{[k]}$  that corresponds to the desired codeword, we can get  $\mathbf{a}_{\text{int}}^{[k]}$  by solving

$$\mathbf{a}_{\text{int}}^{[k]} = \arg \min_{\mathbf{a} \in \mathbb{Z}^{K-1}} \|\mathbf{F}_{\sim k}^{[k]} \mathbf{a}\|^2. \quad (\text{G.1})$$

Note that any lattice reduction algorithm (i.e., LLL) can be used to give an approximate solution for (G.1).

### G.0.2 Finding the best two integer-combinations in $\mathbf{g}^{[k]}$ and $\mathbf{s}^{[k]}$

For each interference function  $\mathbf{g}^{[k]}$  (i.e.,  $\mathbf{a}_{\text{int}}^{[k]}$ ), we can get the best combination of  $\mathbf{g}^{[k]}$  and the desired codeword  $\mathbf{s}^{[k]}$  as in (8.52) and (8.53).

### Method C

The difference between Methods *B* and *C* is that we choose the interference function  $\mathbf{g}^{[k]}$  (i.e.,  $\mathbf{a}_{\text{int}}^{[k]}$ ) to minimize  $\|\mathbf{F}^{[k]}\mathbf{a}_1^{[k]}\|^2$  instead of minimizing  $\|\mathbf{F}_{\sim k}^{[k]}\mathbf{a}_{1,\sim k}^{[k]}\|^2$ . This guarantees that the first integer-combination in (8.47) will have the lowest effective noise power. This can be done by finding the integer vector  $\mathbf{a}_1^{[k]}$  corresponding to the shortest vector in the lattice with basis  $\mathbf{F}^{[k]}$ , then dropping the  $k^{\text{th}}$  element to get  $\mathbf{a}_{\text{int}}^{[k]}$  as follows

$$\mathbf{a}_1^{[k]} = \arg \min_{\mathbf{a} \in \mathbb{Z}^K} \|\mathbf{F}^{[k]}\mathbf{a}\|^2 \quad (\text{G.2})$$

$$\mathbf{a}_{\text{int}}^{[k]} = \mathbf{a}_{1 \sim k}^{[k]}. \quad (\text{G.3})$$

Finding the best two integer-combinations in  $\mathbf{g}^{[k]}$  and  $\mathbf{s}^{[k]}$  follows as in Method *B*.

A comparison between the performance of the three methods are shown in Table G.1 for SNR = 25 dB. We also add the best (i.e., maximum) of all three methods to the comparison, where the maximum is taken for each channel realization  $\mathbf{H}$  separately. We denote the method previously discussed in Section 8.3 by method *A*. As we can see from Table G.1, none of the methods are consistently better (as the maximum is strictly higher than any one of them). It is worth noting that the rate per user for the 4-user case is higher than the rate per user for the 3-user case for SNR higher than

15 dB. This implies that time sharing between orthogonal groups of 3 users should be done in moderate and high SNR regimes.

	Method <i>A</i>	Method <i>B</i>	Method <i>C</i>	Best
3 users	9.8316	9.757 (-0.758%)	9.6541(-1.805%)	10.0808(+2.53%)
4 users	8.9254	8.5276(-4.45%)	8.1259(-8.95%)	9.3343(+4.58%)

**Table G.1:** The sum rate (in bits/Sec/Hz) for different methods at 25 dB

## G.1 Generalized Aligned LLL Algorithm

In Algorithm 7 we propose a generalized aligned LLL algorithm for  $M^{[k]}$  combinations.

---

**Algorithm 7** Generalized Aligned LLL for  $M^{[k]}$  integer-combinations.

---

1. Step 1: Using the LLL algorithm, find the shortest  $M^{[k]} - 1$  vectors in the lattice generated by  $\mathbf{F}^{[k]}$

Method *B*:  $\mathbf{a}_{\text{int},i}^{[k]} = \arg \min_{\mathbf{a} \in \mathbb{Z}^{K-1}} \|\mathbf{F}_{\sim k}^{[k]} \mathbf{a}\|^2$

Method *C*:

$$i) \mathbf{a}_i^{[k]} = \arg \min_{\mathbf{a} \in \mathbb{Z}^K} \|\mathbf{F}^{[k]} \mathbf{a}\|^2, \quad i = 1, \dots, M^{[k]} - 1$$

$$ii) \mathbf{a}_{\text{int},i}^{[k]} = \mathbf{a}_{i,\sim k}^{[k]}, \quad i = 1, \dots, M^{[k]} - 1$$

2. Step 2: Using the LLL algorithm, find the  $M^{[k]}$  shortest vectors in the lattice generated by  $\mathbf{F}_{\text{red}}^{[k]} = [\mathbf{f}_k^{[k]} \quad \mathbf{F}_{\sim k}^{[k]} \quad \bar{\mathbf{A}}^{[k]}]$

$$\mathbf{b}_i^{[k]} = \arg \min_{\mathbf{b} \in \mathbb{Z}^{M^{[k]}}, \text{rank}([\mathbf{b}_1^{[k]}, \dots, \mathbf{b}_{i-1}^{[k]}, \mathbf{b}])=i} \|\mathbf{F}_{\text{red}}^{[k]} \mathbf{b}\|^2, \quad i = 1, \dots, M^{[k]}$$

where  $\bar{\mathbf{A}}^{[k]} = [\mathbf{a}_{\text{int},1}^{[k]}, \dots, \mathbf{a}_{\text{int},M^{[k]}-1}^{[k]}]$

3. Step 3: Calculate the integer matrix  $\mathbf{A}^{[k]}$  using

$$\tilde{\mathbf{A}}^{[k]} = \begin{bmatrix} b_{1,1}^{[k]} & \sum_{j=1}^{M^{[k]}-1} b_{1,j+1}^{[k]} a_{\text{int},j,1} & \cdots & \sum_{j=1}^{M^{[k]}-1} b_{1,j+1}^{[k]} a_{\text{int},j,K-1} \\ \vdots & \vdots & \cdots & \vdots \\ b_{M^{[k]},1}^{[k]} & \sum_{j=1}^{M^{[k]}-1} b_{M^{[k]},j+1}^{[k]} a_{\text{int},j,1} & \cdots & \sum_{j=1}^{M^{[k]}-1} b_{M^{[k]},j+1}^{[k]} a_{\text{int},j,K-1} \end{bmatrix}$$

$$\mathbf{A}^{[k]} = \mathbf{L}^{[k]}(\tilde{\mathbf{A}}^{[k]})$$

where  $\mathbf{L}^{[k]}$  is a permutation matrix which put column 1 in between columns  $k$  and  $k + 1$  of  $\tilde{\mathbf{A}}^{[k]}$

---

## References

- Bakoury, I. E. and Nazer, B. (2017). Integer-forcing architectures for uplink cloud radio access networks. In *2017 55th Annual Allerton Conference on Communication, Control, and Computing (Allerton)*, pages 67–75.
- Banaszczyk, W. (1993). New bounds in some transference theorems in the geometry of numbers. *Mathematische Annalen*, 296(1):625–635.
- Berger, T. (1977). Multiterminal source coding. In *Lectures presented CISM Summer School on the Information Theory Approach to Communications*.
- Bremner, M. R. (2012). *Lattice Basis Reduction*. CRC Press.
- Cadambe, V. R. and Jafar, S. A. (2008). Interference alignment and the degrees of freedom for the K-user interference channel. *IEEE Transactions on Information Theory*, 54(8):3425–3441.
- Cassels, J. W. S. (1957). *An Introduction to Diophantine Approximations*. Cambridge University Press.
- Costa, M. (1983). Writing on dirty paper. *IEEE Transactions on Information Theory*, 29(3):439–441.
- Cover, T. M. and El Gamal, A. (1979). Capacity theorems for the relay channel. *IEEE Transactions on Information Theory*, 25(5):572–584.
- Domanovitz, E. and Erez, U. (2017). Achievability performance bounds for integer-forcing source coding. Available online: <https://arxiv.org/abs/1712.05431v1>.
- Domanovitz, E. and Erez, U. (2018). Outage behavior of integer forcing with random unitary pre-processing. *IEEE Transactions on Information Theory*, 64(4):2774–2790.
- El Gamal, H., Caire, G., and Damen, M. O. (2004). Lattice coding and decoding achieve the optimal diversity-multiplexing tradeoff of MIMO channels. *IEEE Transactions on Information Theory*, 50(6):968–985.
- Feng, C., Silva, D., and Kschischang, F. (2013). An algebraic approach to physical-layer network coding. *IEEE Transactions on Information Theory*, 59(11):7576–7596.

- Ganguly, S. and Kim, Y. (2017). On the capacity of cloud radio access networks. In *2017 IEEE International Symposium on Information Theory (ISIT)*, pages 2063–2067.
- Gesbert, D., Hanly, S., Huang, H., Shamai Shitz, S., Simeone, O., and Yu, W. (2010). Multi-cell MIMO cooperative networks: A new look at interference. *IEEE Journal on Selected Areas in Communications*, 28(9):1380–1408.
- Gomadam, K., Cadambe, V., and Jafar, S. (2011). A distributed numerical approach to interference alignment and applications to wireless interference networks. *IEEE Transactions on Information Theory*, 57(6):3309–3322.
- Grant, M. and Boyd, S. (2014). CVX: Matlab software for disciplined convex programming, version 2.1.
- He, W. and Nazer, B. (2016). Integer-forcing source coding: Successive cancellation and source-channel duality. In *Proceedings of the IEEE International Symposium on Information Theory (ISIT 2016)*, Barcelona, Spain.
- He, W., Nazer, B., and Shamai Shitz, S. (2018). Uplink-downlink duality for integer-forcing. *IEEE Transactions on Information Theory*, 64(3):1992–2011.
- Hong, S.-N. and Caire, G. (2011). Quantized compute and forward: A low-complexity architecture for distributed antenna systems. In *Proceedings of the IEEE Information Theory Workshop (ITW 2011)*, Paraty, Brazil.
- Hong, S. N. and Caire, G. (2012). Lattice coding strategies for cooperative distributed antenna systems. *IEEE Transactions on Information Theory*. Available online: <http://arxiv.org/abs/1210.0160>.
- Knopp, R. and Humblet, P. A. (2000). On coding for block fading channels. *IEEE Transactions on Information Theory*, 46(1):189–205.
- Kramer, G., Gastpar, M., and Gupta, P. (2005). Cooperative strategies and capacity theorems for relay networks. *IEEE Transactions on Information Theory*, 51(9):3037–3063.
- Krithivasan, D. and Pradhan, S. S. (2009). Lattices for distributed source coding: Jointly Gaussian sources and reconstruction of a linear function. *IEEE Transactions on Information Theory*, 55(12):5268–5651.
- Lenstra, A. K., Lenstra, H. W., and Lovász, L. (1982). Factoring polynomials with rational coefficients. *Mathematische Annalen*, 261(4):515–534.
- Loeliger, H.-A. (1997). Averaging bounds for lattices and linear codes. *IEEE Transactions on Information Theory*, 43(6):1767–1773.

- Nazer, B., Cadambe, V. R., Ntranos, V., and Caire, G. (2016). Expanding the compute-and-forward framework: Unequal powers, signal levels, and multiple linear combinations. *IEEE Transactions on Information Theory*, 62(9):4879–4909.
- Nazer, B. and Gastpar, M. (2011). Compute-and-forward: Harnessing interference through structured codes. *IEEE Transactions on Information Theory*, 57(10):6463–6486.
- Ntranos, V., Cadambe, V., Nazer, B., and Caire, G. (2013). Integer-forcing interference alignment. In *Proceedings of the IEEE International Symposium on Information Theory (ISIT 2013)*, Istanbul, Turkey.
- Ordentlich, O. and Erez, U. (2013). On the robustness of lattice interference alignment. *IEEE Transactions on Information Theory*, 59(5):2735–2759.
- Ordentlich, O. and Erez, U. (2015). Precoded integer-forcing universally achieves the MIMO capacity to within a constant gap. *IEEE Transactions on Information Theory*, 61(1):323–340.
- Ordentlich, O. and Erez, U. (2016). A simple proof for the existence of "good" pairs of nested lattices. *IEEE Transactions on Information Theory*, 62(8):4439 – 4453.
- Ordentlich, O. and Erez, U. (2017). Integer-forcing source coding. *IEEE Transactions on Information Theory*, 63(2):1253–1269.
- Ordentlich, O., Erez, U., and Nazer, B. (2013). Successive integer-forcing and its sum-rate optimality. In *Proceedings of the 51st Annual Allerton Conference on Communications, Control, and Computing*, Monticello, IL.
- Ordentlich, O., Erez, U., and Nazer, B. (2014). The approximate sum capacity of the symmetric K-user Gaussian interference channel. *IEEE Transactions on Information Theory*, 60(6):3450–3482.
- Park, S. H., Simeone, O., Sahin, O., and Shamai, S. (2013). Joint precoding and multivariate backhaul compression for the downlink of cloud radio access networks. *IEEE Transactions on Signal Processing*, 61(22):5646–5658.
- Park, S.-H., Simeone, O., Sahin, O., and Shitz, S. S. (2014). Fronthaul compression for cloud radio access networks: Signal processing advances inspired by network information theory. *IEEE Signal Processing Magazine*, 31(6):69–79.
- Plemmons, R. (1977). M-matrix characterizations in singular m-matrices. *Linear Algebra and its Applications*, 18(2):175 – 188.
- Pradhan, S. S. and Ramchandran, K. (2003). Distributed source coding using syndromes (DISCUS): Design and construction. *IEEE Transactions on Information Theory*, 49(3):626–643.

- Puri, R., Majumdar, A., and Ramchandran, K. (2007). Prism: A video coding paradigm with motion estimation at the decoder. *IEEE Transactions on Image Processing*, 16(10):2436–2448.
- Sanderovich, A., Somekh, O., Poor, H. V., and Shamai, S. (2009). Uplink macro diversity of limited backhaul cellular network. *IEEE Transactions on Information Theory*, 55(8):3457–3478.
- Simeone, O., Somekh, O., Poor, H. V., and Shamai (Shitz), S. (2009). Downlink multicell processing with limited-backhaul capacity. *EURASIP Journal on Advances in Signal Processing*, 2009(1):840814.
- Tse, D. and Viswanath, P. (2005). *Fundamentals of Wireless Communication*. Cambridge University Press, Cambridge.
- Wagner, A. B., Tavildar, S., and Viswanath, P. (2008). The rate region of the quadratic gaussian two-terminal source-coding problem. *IEEE Transactions on Information Theory*, 54(5):1938 – 1961.
- Wyner, A. D. and Ziv, J. (1976). The rate-distortion function for source coding with side information at the decoder. *IEEE Transactions on Information Theory*, 22(1):1–10.
- Yetis, C., Gou, T., Jafar, S., and Kayran, A. (2010). On feasibility of interference alignment in MIMO interference networks. *IEEE Transactions on Signal Processing*, 58(9):4771–4782.
- Zamir, R. (2014). *Lattice Coding for Signals and Networks*. Cambridge University Press.
- Zamir, R., Shamai (Shitz), S., and Erez, U. (2002). Nested linear/lattice codes for structured multiterminal binning. *IEEE Transactions on Information Theory*, 48(6):1250–1276.
- Zhan, J., Nazer, B., Erez, U., and Gastpar, M. (2014). Integer-forcing linear receivers. *IEEE Transactions on Information Theory*, 60(12):7661–7685.
- Zhou, Y., Xu, Y., Yu, W., and Chen, J. (2016). On the optimal fronthaul compression and decoding strategies for uplink cloud radio access networks. *IEEE Transactions on Information Theory*, 62(12):7402–7418.
- Zhou, Y. and Yu, W. (2014). Optimized backhaul compression for uplink cloud radio access network. *IEEE Journal on Selected Areas in Communications*, 32(6):1295–1307.

Zhou, Y. and Yu, W. (2016). Fronthaul compression and transmit beamforming optimization for multi-antenna uplink C-RAN. *IEEE Transactions on Signal Processing*, 64(16):4138–4151.

# CURRICULUM VITAE

